ROLE OF MISFOLDED - NUCLEAR RECEPTOR CO-REPRESSOR (N-CoR) INDUCED TRANSCRIPTIONAL DE-REGULATION IN THE PATHOGENESIS OF ACUTE MONOCYTIC LEUKEMIA (AML-M5).

NIN SIJIN DAWN
(B.Sc., NUS)

A THESIS SUBMITTED
FOR THE DEGREE OF DOCTOR OF PHILOSOPHY

DEPARTMENT OF MEDICINE
YONG LOO LIN SCHOOL OF MEDICINE

NATIONAL UNIVERSITY OF SINGAPORE
2011

ACKNOWLEDGEMENTS

The past four years had been an enriching and fruitful journey of both scientific and self discovery. I would like to take this opportunity to express my deepest gratitude to the many people who have made this possible.

First of all, I would like to thank my supervisor, Dr Matiullah Khan, for providing me with the opportunity to embark on this journey. Heartfelt thanks for all the mentorship, support and encouragement throughout these years. Thank you for giving me the opportunity to express myself and to defend my ideas.

I would also like to extend my sincere gratitude to our many collaborators, Dr Koichi Okumura for his invaluable input on some of the work done in this thesis and for taking the time to vet my thesis; A/Prof Chng Wee Joo and Prof Norio Asou for their kind assistance with the patient samples and A/Prof Motomi Osato for his assistance with the mouse work. My deepest appreciation also goes to A/Prof Motomi Osato and A/Prof Prakash Hande for kindly agreeing to be members of my Thesis Advisory Committee as well as to Dr Deng Lih Wen for the help she had rendered during the Graduate Studies application process.

I am also immensely grateful to Dr Azhar bin Ali for his guidance and advice about life and research. I truly enjoyed the intellectually stimulating conversations we had in the mornings.

My heartfelt thanks to my wonderful lab mates past and present, Angela, Jek, Chai Peng, Hannah, Norlizan, Angie, Li Feng, Leo, Wai Kay, Su Yin, Jayne, Jess, Fen Yee, Wanqiu, Yan Kun and Meg for their

companionship and assistance during the long hours spent in the lab. It has been a real pleasure working with all of you. Special thanks to Li Feng and Wai Kay for their assistance and advice on the Flt3 project.

I was also fortunate to have had received assistance from the staff from the NUMI Core FACS facility. I am grateful for the wonderful help and expertise rendered by Kok Tee and Ling Yao.

Many thanks to the wonderful people I have met along the way, Bee Keow, Mei Xian, Sandy, Tada-San, Judy, Tomoko, Joan, Li Ren, and many more. Thank you for the friendship. Life in the lab will not be the same without you guys.

Finally, I would like to express my most sincere thanks to my family. I feel truly blessed to have a strong and supportive family network. Thank you for the encouragement, understanding and tolerance shown to me during this journey.

Thank you.

Nin Sijin Dawn

September 2011

TABLE OF CONTENTS

CHAPTER 2 MATERIALS AND EXPERIMENTAL PROCEDURES

SUMMARY

The Nuclear Receptor Co-repressor (N-CoR) is a key component of the generic multi-protein co-repressor complex involved in transcriptional control mediated by various transcription factors. Our laboratory previously demonstrated an important role of the misfolded conformational dependent loss (MCDL) of N-CoR in Acute Promyelocytic Leukemia (APL). Encouraged by the results in APL, we analyzed the status of N-CoR in other AML subtypes and identified an APL-like MCDL of N-CoR in primary patient specimens and secondary leukemic cell lines derived from Acute Monocytic Leukemia (AML designated as M5 in the FAB-classification-AML-M5). Here we report the in depth analysis of the molecular mechanism underlying the MCDL of N-CoR and its implication in the malignant growth and transformation of AML-M5 leukemic cells. We also explored the potential of the MCDL of N-CoR as a therapeutic target in AML-M5.

The MCDL of N-CoR was found in AML-M5 derived cell lines and an APL-like N-CoR cleaving activity was observed in both AML-M5 primary patient specimens and secondary leukemic cell lines. Activation of Akt inversely correlated with the status of MCDL of N-CoR in a comparative protein kinase array analysis. These observations implied a possible role of Akt in the MCDL of N-CoR in AML-M5. Akt is an important regulator of cell survival and initiates tumourigenesis by its aberrant serine/threonine kinase activity. A constitutively active Akt promoted N-CoR misfolding while therapeutic and genetic inhibition of Akt activity blocked the misfolding of N-CoR in AML-M5. Moreover, N-CoR misfolding was found to be triggered by Akt induced phosphorylation at Serine 1450 of N-CoR. These observations clearly indicated the importance of Akt

dependent phosphorylation in the misfolding and subsequent loss of N-CoR protein.

Given N-CoR's documented roles in hematopoiesis and as a transcriptional co-repressor, the functional consequence of Akt mediated MCDL of N-CoR in AML-M5 was next studied. Expression analysis of genes involved in hematopoiesis led to the identification of Flt3 as a transcriptional target of N-CoR. N-CoR status in various AML deived cell lines was found to be inversely related to Flt3 expression. N-CoR effectively repressed the activity the Flt3 promoter driven luciferase reporter and was found to be associated with the Flt3 promoter in ChIP assay. N-CoR loss facilitated the IL3-independent growth of BA/F3 cells through the de-repression of the Flt3 gene, and N-CoR loss was augmented by Flt3 ligand stimulation. Enforced N-CoR expression in immature hematopoietic cells inhibited their growth and promoted myeloid lineage commitment, while blocking the N-CoR loss with Genistein; an inhibitor of N-CoR misfolding, significantly down regulated Flt3 level and promoted differentiation of AML-M5 derived cell lines. These findings indicated that aberrant expression of Flt3 in AML-M5 was a consequence of the loss of N-CoR repressive function due to its MCDL. This suggested that N-CoR may have a potential tumour suppressive role in AML-M5 pathogenesis through unmasking the growth promoting potential of Flt3.

In this study, we identified and characterized the importance of the MCDL of N-CoR in the growth of AML-M5 leukemic cells through the in depth analysis of its mechanism and functional consequence. We also demonstrated that therapeutic inhibition of the N-CoR MCDL pathway in AML-M5 leukemic cells led to growth arrest. Together, these findings illustrate the potential of targeting the N-CoR MCDL pathway as an effective therapeutic strategy in AML-M5.

LIST OF PUBLICATIONS

Publications from this thesis

1. **Nin DS**, Kok WK, Li F *et al*. Role of misfolded N-CoR mediated transcriptional deregulation of Flt3 in Acute Monocytic Leukemia (AML)-M5 subtype. *PLoS One.* 2012:7(4): e34501.

2. **Nin DS**, Ali AB, Okumura K *et al*. Akt induced N-CoR phosphorylation is linked to its misfolded conformational loss in Acute Monocytic Leukemia.--- *Submited Manuscript.*

Other Publications

1. Ali AB, **Nin DS**, et al. Role of chaperone mediated autophagy (CMA) in the degradation of misfolded N-CoR protein in non-small cell lung cancer (NSCLC) cells .*PLoS One.* 2011:6(9):e25268

2. Ng PPA, **Nin DS**, Fong JH, *et al*. Therapeutic targeting of nuclear receptor co-repressor (N-CoR) mis-folding in acute promyelocytic leukemia (APL) cells with Genistein. *Mol Can Ther*. 2007;6(8):2240-2248.

3. Ng PPA, Fong JH, **Nin DS**, *et al*. Cleavage of mis-folded nuclear receptor co-repressor confers resistance to unfolded protein response-induced apoptosis. *Cancer Res.* 2006;66(20):9903-9912. (Fong JH and Nin DS contributed equally to this work)

LIST OF TABLES

LIST OF FIGURES

LIST OF ABBREVATIONS

A	Alanine
AML	acute myeloid leukaemia
APL	acute promyelocytic leukaemia
BSA	bovine serum albumin
DAPI	4,6-diamidino-2-phenylindole
DMSO	dimethyl sulfoxide
DNA	deoxyribonucleic acid
E	Glutamic acid
ER	endoplasmic reticulum
ERAD	ER-associated degradation
FAB	French-American-British
Flt3	FMS-like tyrosine kinase
HDAC3	histone deacetylase 3
HMW	high molecular weight
HSC	hematopoietic stem cells
kb	kilo base
kDa	kilo Dalton
MCDL	Misfolded Conformation Dependent Loss.
mRNA	messenger RNA
mTOR	mammalian target of rapamycin
N-CoR	nuclear receptor co-repressor
NR	nuclear receptors
OSGEP endopeptidase	O-Sialoglycoprotein
PBS	phosphate buffered saline
PI	propidium iodide
PI3K	phosphatidyl-inositol 3 kinase

PML	promyelocytic leukaemia
PtdIns	phosphatidyl inositol
PtdIns(3,4,5) P_3	phosphatidylinositol-3,4,5-triphosphate
PVDF	polyvinylidene difluoride
qRT-PCR	real time polymerase chain reaction
RA	retinoic acid
RARα	retinoic acid receptor α
RT-PCR	reverse transcription polymerase chain reaction
SDS	sodium dodecyl sulphate
SDS-PAGE	SDS-Polyacrylamide gel electrophoresis
siRNA	small interfering RNA
UPR	unfolded protein response
WHO	World Health Organization

CHAPTER 1

Introduction

1. INTRODUCTION

1.1 Acute Myeloid Leukemia

The term Acute Myeloid Leukemia (AML) is used to describe a cluster of neoplastic disorders characterized by the clonal expansion of immature blood cells of the myeloid lineage in the bone marrow (BM), blood or in other tissue [1,2]. This accumulation is a result of increased cell proliferation and survival coupled with a block in the ability of the hematopoietic progenitor cells to differentiate[3]. These progenitor cells include cells of the granulocytic, monocyte/macrophage, erythroid and megakaryocytic lineages.

Diagnosis and classification of AML is made primarily on the basis of morphology and cytochemical analysis. Using the widely adopted French-American-British (FAB) classification system[4], AML can be broadly classified into 8 subtypes as determined based on morphology, cellularity, blast percentage and cytochemistry. These subtypes are distinguished based on both the degree of differentiation and cell lineage. Cytochemical stains, including myeloperoxidase, nonspecific esterase and Sudan black B are used in conjunction with morphology in the identification of the subtypes[5,6]. Table 1.1 depicts the various AML subtypes as classified under the FAB system and their associated morphological and cytochemical presentations.

Although the FAB classification has been widely used in AML classification in the past three decades, the discovery that many AMLs are associated with recurring genetic aberrations prompted the World Health Organization (WHO) to come up with a new classification of AML. This new classification system stratifies AMLs based on the recurring molecular parameters associated to the various AMLs as diagnosed by cytogenetics,

molecular genetics and immnophenotyping in addition to their morphological presentations[2]. The different classes of AML and the criteria associated to each subclass as first defined by WHO in 2001 is listed in Table 1.2. This classification was published with the knowledge that it will be constantly modified with increasing information about the various genetic anomalies associated with AML pathogenesis. A revised classification was published by WHO in 2009 with the genetic information acculmulated after the first publication[205].

Although each subtype of AML may differ vastly in their genetic backgrounds regardless of the classification system used, a hallmark of all AMLs is the severe block of myeloid differentiation. Thus it is thought that aberrations involving key transcription factors and its associated co-activators and co-repressors which are essential for the differentiation process is a major driving force for AML pathogenesis.

Table 1.1: The French-American Classification of Acute Myeloid Leukemia.

FAB Subtype	Common Name (% of Cases)	Results of Staining			Associated Translocations and Rearrangements (% of Cases)	Genes Involved
		Myeloperoxidase	Sudan Black	Nonspecific Esterase		
M0	Acute myeloblastic leukemia with minimal differentiation (3%)	−	−	−*	inv(3q26) and t(3;3) (1%)	*EVI1*
M1	Acute myeloblastic leukemia without maturation (15–20%)	+	+	−		
M2	Acute myeloblastic leukemia with maturation (25–30%)	+	+	−	t(8;21) (40%), t(6;9) (1%)	*AML1-ETO, DEK-CAN*
M3	Acute promyelocytic leukemia (5–10%)	+	+	−	t(15;17) (98%), t(11;17) (1%), t(5;17) (1%)	*PML-RARα, PLZF-RARα, NPM RARα*
M4	Acute myelomonocytic leukemia (20%)	+	+	+	11q23 (20%), inv(3q26) and t(3;3) (3%), t(6;9) (1%)	*MLL, DEK-CAN, EVI1*
M4Eo	Acute myelomonocytic leukemia with abnormal eosinophils (5–10%)	+	+	+	inv(16), t(16;16) (80%)	*CBFβ-MYH11*
M5	Acute monocytic leukemia (2–9%)	−	−	+	11q23 (20%), t(8;16) (2%)	*MLL, MOZ-CBP*
M6	Erythroleukemia (3–5%)	+	+	−		
M7	Acute megakaryocytic leukemia (3–12%)	−	−	+†	t(1;22) (5%)	Unknown

*Cells are positive for myeloid antigen (e.g., CD13 and CD33).

†Cells are positive for α-naphthylacetate and platelet glycoprotein IIb/IIIa or factor VIII–related antigen and negative for naphthylbutyrate.

[Reproduced with permission from LÖwenberg, et al., Acute Myeloid Leukemia. *NEJM* **341**(14): 1051-1062 (1999)]

Table 1.2: The World Health Organization (WHO) classification of Acute Myeloid Leukemia

Classification	Description
AML with characteristic genetic abnormalities	This category includes: 1) Acute myeloid leukemia with t(8;21)(q22;q22), (*AML1/ETO*) 2) Acute myeloid leukemia with abnormal bone marrow eosinophils and inv(16)(p13q22) or t(16;16)(p13;q22), (*CBFβ/MYH11*) 3) Acute promyelocytic leukemia with t(15;17)(q22;q12), (*PML/RARα*) 4) variants of Acute myeloid leukemia with 11q23 (*MLL*) abnormalities
AML with multilineage dysplasia	Following MDS or MDS/MPD. Without antecedent MDS or MDS/MPD, but with dysplasia in at least 50% of cells in 2 or more myeloid lineages.
AML and MDS, therapy-related	This category includes: 1) Alkylating agent/radiation–related type 2) Topoisomerase II inhibitor–related type (some may be lymphoid)
AML not otherwise categorized	Classify as: 1) Acute myeloid leukemia, minimally differentiated 2) Acute myeloid leukemia without maturation 3) Acute myeloid leukemia with maturation 4) Acute myelomonocytic leukemia 5) Acute monoblastic/acute monocytic leukemia 6) Acute erythroid leukemia (erythroid/myeloid and pure erythroleukemia) 7) Acute megakaryoblastic leukemia 8) Acute basophilic leukemia 9) Acute panmyelosis with myelofibrosis Myeloid sarcoma

[adapted from Vardiman et al, The World Health Organization (WHO) classification of myeloid neoplasms. *Blood* **100**, 2292-2302 (2002)].

1.1.1. Acute Monoblastic/Monocytic Leukemia

Acute Monoblastic/Monocytic leukemia (AML-M5) is a class of AML classified under the M5 subtype in the FAB classification. It is one of the most common subclass of AML found in young children, representing 18 percent of all pediatric AML; and in children below 2 years the proportion rate of AML-M5 is about 40 to 50 percent[7]. In adults, AML-M5 makes up about 5 to 10 percent of all AML cases and AML-M5 with *MLL1* abnormalities is also a common secondary AML developed after chemotherapy treatment.

AML-M5 is classified as a group of malignant disorder characterized by an abnormal accumulation of immature cells of myelo-monocytic lineage in the bone marrow and peripheral blood[8,9] . It can be further sub classified in to two classes, AML-M5a (also known as Acute Monoblastic Leukemia) where greater than 80 percent of the monocytic cells are monoblasts and AML-M5b where less than 80 percent of monocytic cells are monoblasts with the rest showing (pro) monocytic differentiation. Under the newer World Health Organization (WHO) classification of AML, AML-M5 was classified under Acute Myeloid Leukemia with 11q23 (*MLL1*) abnormalities with the presence of the fusion product between the *MLL1* and *AF9* genes [t(9;11)(p22;q23)], *MLL1-AF9* presenting the highest occurrence rates in the disease[10,11]. Although *MLL1-AF9* is mainly associated with AML-M5, it is not the only genetic anomaly present. Other diverse genetic aberrations have also been reported in the disease[12]. However, despite the varied genetic background of the disease, the phenotypic presentation is almost identical, characterized by the differentiation arrest at the monoblast and/or promonocytic stage coupled with increased survival and proliferation capacities.

1.1.2. Current treatment strategies for AML-M5.

To date, AML-M5 and AMLs in general remain a difficult disease to treat and the most common therapeutic strategies in current clinical practice include aggressive multi-drug chemotherapy using anthracyclins, cytarabine and etoposide. However these current strategies have severe side effects with non negligible mortality and morbidity rates. Although the availability of other treatment options such as allogenic bone marrow transplantation and radiotherapy have greatly improved the outcome of patients, these options remain highly specialized with a treatment related mortality and morbidity rate of approximately 10 to 15 percent[13].

Despite the difficulties in treatment, some small progress has been made in the recent decade which improved the outcome of AMLs and AML-M5. Identification of new therapeutics such as new nucleoside analogues (Fludarabine, Cladribine, Cyclopentenyl, Cytosine and Clofarabine) and monoclonal antibodies against CD33 labeled with radionuclide or toxic compounds; as well as targeted therapies such as imatinib meslyate (Glivec®), Flt-3 inhibitors and farneysal transferase inhibitors which target tumor specific cellular pathways with less cytotoxicity can hopefully increase anti-tumor activity with less toxicity compared to conventional chemotherapy[14].

The mechanisms underlying AML-M5 pathogenesis and the difficulties in treating patients with AML-M5 have only been partially unraveled. Various mechanisms regarding the transformation event and drug resistance play a role in the moderation of disease outcome in patients with AML-M5. Thus it is prudent that more knowledge regarding the molecular

pathology be collected so as to better devise targeted therapeutic approaches to hopefully improve the outcome of patients with AML-M5.

1.2. The Nuclear Receptor Co-repressor (N-CoR), a component of the transcriptional repression machinery and its role in AML pathogenesis.

1.2.1. The importance of the transcription machinery in the regulation of hematopoiesis.

The transcription machinery plays a critical role in the control of normal hematopoiesis by having a major influence on the differentiation of the hematopoietic stem cell (HSC) to cells of the various hematopoietic lineages[15-18]. In normal hematopoiesis, the hematopoietic precursor/stem cell (HSC) matures into more committed multi-potential progenitors and finally to specific cell types of the different lineages. This process of growth and maturation of hematopoietic cells is regulated during normal hematopoiesis through a balance between its capacity to self renew and proliferate versus lineage commitment and differentiation. Regulation is achieved via the controlled expression or repression of certain genes that are involved in self renewal, proliferation and differentiation as well as cell survival. This control is exerted via the cell's transcription machinery and its associated cofactors which include the various co-activator and co-repressor proteins. Figure 1.1 summarizes the role of the transcriptional machinery in the control of hematopoiesis.

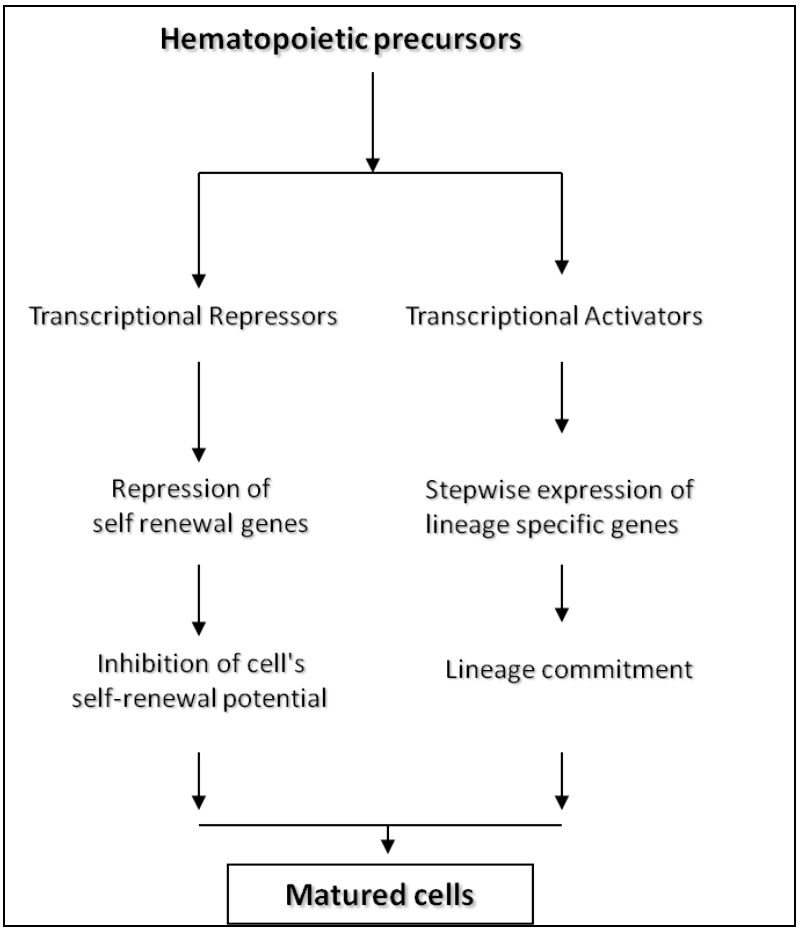

Figure 1.1. Role of the transcription machinery in the control of hematopoiesis. As the hematopoietic precursor/stem cells progress towards the more mature phenotype, there is a stepwise co-operation between the transcription repressors which represses the expression of self-renewal genes and the transcriptional activators which activates the expression of the lineage specific genes.

A number of members of the transcription machinery (mainly transcriptional activators) have been identified to be crucial in the commitment of HSCs to the specific lineages. While factors such as RUNX1/AML1[19-21] have been reported to be important for the proper development for all lineages, the role of other transcription factors are more specific to particular lineages. These include Ikaros[22], tal-1/SCL[23] and Pax5/BSAP[24] which are essential for the development of lymphoid lineage cells as well as GATA-1[25] and LMO2[26] which are critical for erythropoiesis.

In the recent years, transcription factors critical for the development of myeloid lineage cells have also been identified and studied. The importance of the various members of the CCAAT/enhancer binding protein (CEBP) family such as CEBPα/β/ε in myeloid development have been suggested in mice models where various abnormalities in myeloid lineage development have been observed in CEBPα/β/ε knockouts[27-30]. Another transcription factor reported to be essential in myeloid lineage cell commitment is the ETS-domain transcription factor PU.1/SPI1which activates gene expression during myeloid and B-cell development. It is thought that PU.1 and CEBPα work in tandem to regulate the myelopoiesis pathway, determining the final phenotypic fates of the common myeloid progenitors[31]. Recent studies conducted in normal hematopoiesis and leukemogenesis have emphasized that these factors which are involved in transcription, have a major influence on these two processes[32-34]; especially when mutated or dysregulated, these factors become key initiators of AML pathogenesis.

1.2.2. The Nuclear Receptor Co-Repressor (N-CoR).

The nuclear receptor co-repressor N-CoR is a 270 kDa protein which is a key component of the multi-protein co-repressor complex involved in transcriptional control mediated by various transcriptional factors. It mediates gene repression by binding to unliganded nuclear receptors (NR) such as the retinoic acid and thyroid hormone receptors[35] (Fig 1.2) and consists of both the nuclear receptor binding domains as well as multiple repressor domains (Fig 1.3).

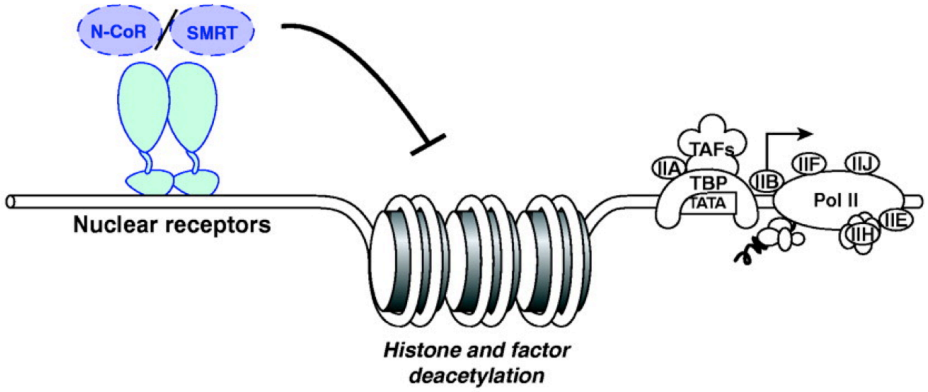

Figure 1.2. Transcriptional repression by N-CoR is mediated by binding of N-CoR to nuclear receptors. Transcriptional repression is brought about by the recruitment of N-CoR/SMRT to the gene promoter region by nuclear receptors. (Reproduced with permission from Jepsen K, Rosenfeld M G J Cell Sci 2002;115:689-698)

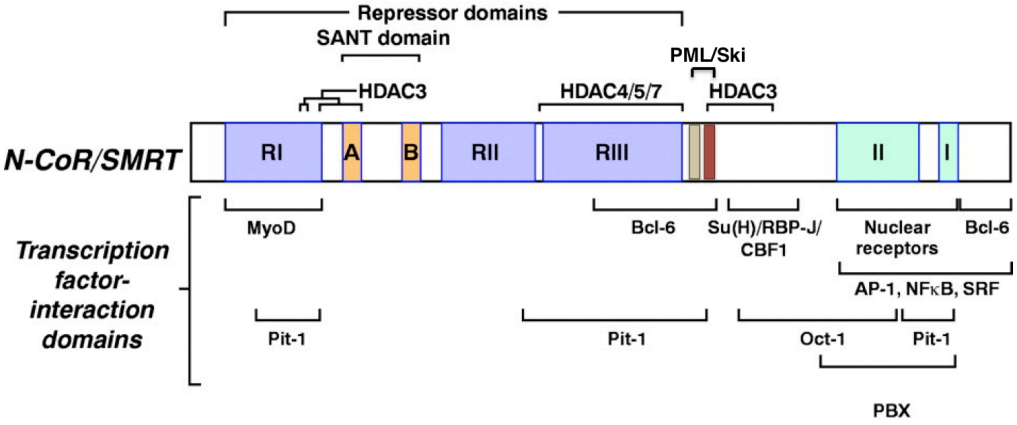

Figure 1.3. The domains of N-CoR/SMRT. Repression domains (RI, RII, RIII) and SANT domains (A and B) are indicated, as are interaction domains for HDACs, nuclear receptors (I and II), PML and Ski and other transcription factors. (Reproduced with permission from Jepsen K, Rosenfeld M G J Cell Sci 2002;115:689-698)

N-CoR mediates gene repression by recruiting histone deacetylases (HDACs) to the promoter region of genes which utilizes it for repression. When associated to the promoter region, the N-CoR/HDAC complex promotes the deacetylation of histones at these regions, changing the conformation of

the chromatin. This makes the chromatin less accessible to transcription activators resulting in gene silencing [36-39] (Fig 1.4).

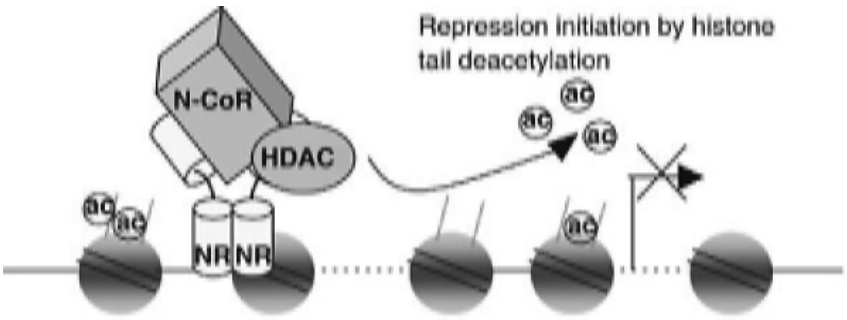

Figure 1.4. Mode of action of N-CoR mediated gene repression. Recruitment of the N-CoR/HDAC complex to the promoter region of genes by nuclear receptors (NR), results in a change in the conformation of the chromatin by deacetylation of the histone tails in these regions. (Reproduced with permission from T Alenghat, J Yu & M A Lazar EMBO J 2006; 25:3966-3974).

Other than HDAC, N-CoR also recruits other factors such as Transducin B-Like 1 (TBL1), the TBL1-related protein (TBLR1)[40] and G Protein Pathway Suppressor 2 (GPS-2)[41] which together mediates the repression by multiple nuclear receptors such as the unliganded thyroid hormone receptor(TR)[42] as well as the retinoic acid receptor (RAR), the peroxisome-proliferator-activated receptors (PPARs) PPARα, PPARβ (also known as PPARδ) and PPARγ, and the liver X receptors (LXRs) LXRα and LXRβ2[43,44]. Other than the nuclear receptors, N-CoR was also found to interact with the mammalian switch-independent 3 protein (mSin3)[45-47]. It was suggested that the interaction between N-CoR and mSin3 is involved in the repression of several non-receptor transcription factors such as Mad/Max[47].

1.2.2.1. N-CoR in normal development.

Physiologically, N-CoR is important in many developmental processes such as proliferation, differentiation and apoptosis. Its importance was underscored by the fact that N-CoR -/- knockout mouse models produced an embryonically lethal phenotype with severe anemia due to defects in definitive erythropoiesis as well as defects in thymocyte and neural development[36]. N-CoR had been reported to be important in neural stem cell differentiation to astrocytes where the PI3K/Akt mediated cytosolic export of N-CoR via its phosphorylation resulted in the concomitant loss of N-CoR nuclear function[48], promoting differentiation. Recently, N-CoR's role in erythroid differentiation was also established with it being important in the regulation of the heme biosynthesis enzyme 5-aminolevulinate synthase (ALA-S2) in K562 cells[49]. A role for N-CoR in the differentiation of pituitary cells[50] as well as in myogenesis[51] had also been cited, highlighting the critical role of N-CoR in regulating differentiation of multiple cell types.

Other than the regulation of differentiation, a novel role for N-CoR in the regulation of circadian metabolic physiology was recently published. Genetic disruption of the N-CoR/HDAC3 interaction in mice resulted in the aberrant regulation of clock genes. This caused the mice to exhibit abnormal circadian behavior. The loss of the functional N-CoR/HDAC3 complex altered the oscillatory patterns of several metabolic genes. This indicated that activation of HDAC3 by N-CoR was critical in the epigenetic regulation of circadian and metabolic physiology[52].

1.2.2.2. N-CoR in Carcinogenesis.

N-CoR being a key component of the transcriptional repression machinery; its expression and function is tightly regulated in normal development. Deregulations of N-CoR function due to changes in expression or aberrant nuclear export have been reported to contribute to carcinogenesis. For example, N-CoR had been shown to be important in the repression of the PI3K/Akt signaling pathway in thyrocytes and its observable loss of expression in thyroid cancer cells was thought to enhance the survival of these cells by activating the PI3K/Akt kinase signaling pathway[53]. N-CoR's role in the transcriptional control of POZ/zinc finger transcription factor BCL-6 was also reported to be essential for the survival of tumor cells in diffuse large B-cell lymphomas[54]. In glioblastoma multiforme (GBM), tumor cells with nuclear localization of N-CoR demonstrate an undifferentiated phenotype. However upon exposure of these cells to agents which promoted N-CoR phosphorylation and subsequent cytosolic translocation, astroglial differentiation was observed[55]. It was also observed that in colorectal cancer primary patient specimens, N-CoR displayed aberrant cytosolic localization. This was due to its phosphorylation by IKKα and this was thought to result in the de-repression of genes which promote the proliferation and survival of these cancer cells[56].

1.2.2.3. N-CoR in AML Pathogenesis.

Although N-CoR has been reported to contribute to the pathogenesis of various types of cancers, it is most widely implicated in the pathogenesis of AML, especially in AMLs involving the AML1-ETO fusion protein and in Acute Promyelocytic Leukemia (APL/ AML-M3).

In AML1-ETO positive myeloid leukemia, it was observed that aberrant recruitment of the N-CoR/HDAC3 complex to ETO in the fusion oncogene repressed gene transcription and inhibited differentiation in hematopoietic precursors[57].

In APL, N-CoR's role in the pathogenesis of the disease has been extensively studied. It is believed that in APL, N-CoR recruited by the fusion oncogene PML-RARα acts as a repressor for the genes that respond to Retinoic Acid (RA). These RA responsive genes are also the genes that are essential for myeloid cell maturation. By dissociating N-CoR from PML-RARα in RA and Genistein treatment, the repression for these genes is lifted which leads to myeloid cell maturation and differentiation[58-61]. Recently a different role for N-CoR in the pathogenesis of APL was proposed. It was shown that PML-RARα mediated the accumulation of a non-functional, misfolded and insoluble form of N-CoR in the endoplasmic reticulum (ER)[62]. In APL, this misfolded N-CoR was subsequently modified in the golgi through glycosylation and was selectively cleaved by an aberrant protease activity induced or activated by the Unfolded Protein Response (UPR)[63].

With these new findings, a bi-functional model for the role of the association between PML-RARα and N-CoR in the pathogenesis of APL was proposed. It was suggested that in APL cells, there exists two forms of N-CoR, a natively folded and stable nuclear residing form and a misfolded and unstable form preferentially localized to the cytosol[62,63]. Similarly, nuclear and cytosolic forms of PML-RARα were thought to exist and it was proposed that each form of PML-RARα engaged the respective form of N-CoR to regulate the two different arms of the transcriptional mechanism, eventually leading to

the dysregulation of both transcriptional activation and repression in APL[64] (Fig 1.5). Based on this new model, the mode of action for RA and Genistein had been redefined to include its effects on the non-functional form of N-CoR and the proposed mechanism of action is summarized in Figure 1.6[64].

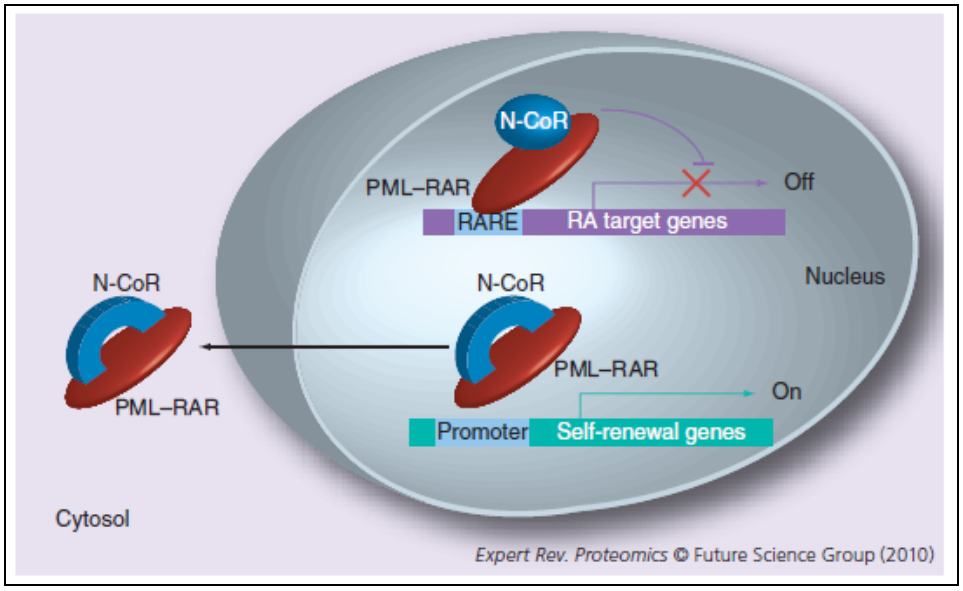

Figure 1.5. Mode of action of bi-functional role of N-CoR in APL pathogenesis. The nuclear and cytosolic forms of PML-RARα possibly engage N-CoR protein in a bi-functional manner with two opposing outcomes. Nuclear PML-RARα represses RA target genes by recruiting native nuclear N-CoR to the promoter regions of RA responsive genes thus repressing the expression of these genes. On the other hand, the self-renewal genes which were originally repressed by N-CoR could be re-expressed due to the loss of functional N-CoR as a result of PML-RARα induced misfolding and cytosolic export. (Reproduced with permission from M Khan Expert Rev. Proteomics 2010; 7(4):501-600).

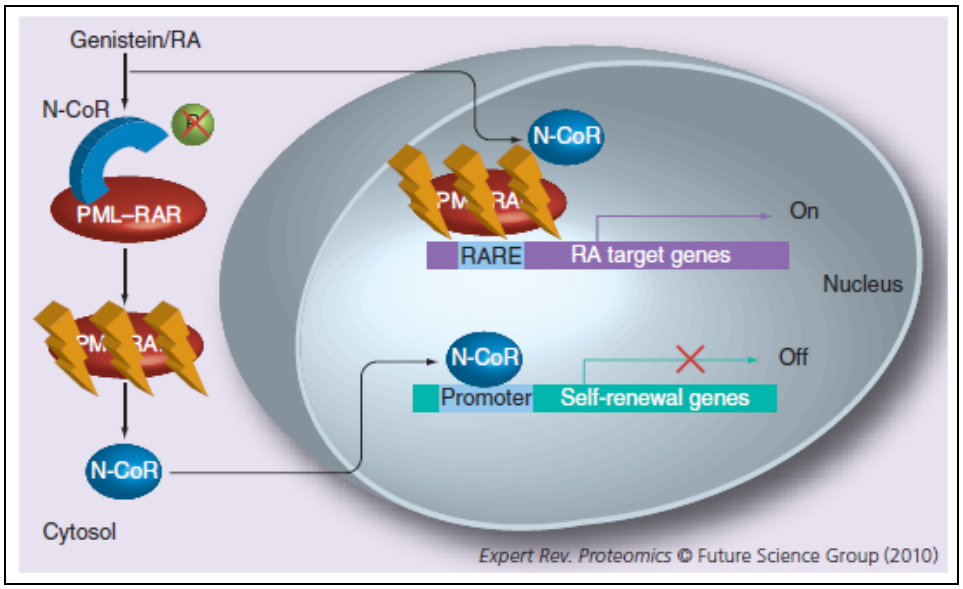

Figure 1.6. Mode of action of Retinoic Acid (RA) and Genistein. RA and Genistein inhibit the association of PML-RARα and N-CoR by inhibiting the aberrant phosphorylation of N-CoR at the N-CoR box. This releases and refolds N-CoR resulting in the restoration of N-CoR function. This dissociation is accompanied by the concurrent degradation of the PML-RARα fusion oncogene. (Reproduced with permission from M Khan Expert Rev. Proteomics 2010; 7(4):501-600).

1.3. Protein Misfolding and its role in AML pathogenesis.

1.3.1. Protein folding and the Unfolded Protein Response (UPR).

The normal function of proteins is determined by its three dimensional structure which is acquired through the folding of the polypeptide chain encoded by the genome. Any changes in the polypeptide chain either via abnormal amino acid modifications or aberrant post-translational modifications may result in changes of the folding process causing protein misfolding[65].

In a normal mammalian cell system, the amino acid sequence in the polypeptide chain contains all the necessary information to determine the conformation of the protein it encodes. However, there are a vast number of

permutations for the way the polypeptide can be folded, thus creating the possibility of the formation of proteins which have a misfolded conformation. Therefore, mammalian cells have evolved a robust protein quality control (PQC) system which utilizes the aid of molecular chaperones to facilitate this folding process and prevent misfolding[66,67]. This system also comprises the Unfolded Protein Response (UPR) which acts to eliminate misfolded or damaged proteins. This UPR is initiated when there is an accumulation of unfolded or misfolded proteins in the endoplasmic reticulum (ER).

The UPR consist of two arms, the first arm known as cytoprotective UPR is the cell's first response to misfolded proteins. This arm utilizes molecular chaperones to first attempt to correct the conformation of the damaged proteins or activate the ubiquitin-proteasome system to eliminate these misfolded proteins before they can exert their cytotoxic effects. In the event where the load of misfolded protein is too high to be cleared by the cytoprotective arm which usually occurs under conditions of disease, the second arm known as cytotoxic UPR is activated. This results in the accumulation of cytotoxic protein aggregates which ultimately eliminates the cells through programmed cell death. A simplified schematic of the dynamic protein folding/misfolding process is represented in Figure 1.7.

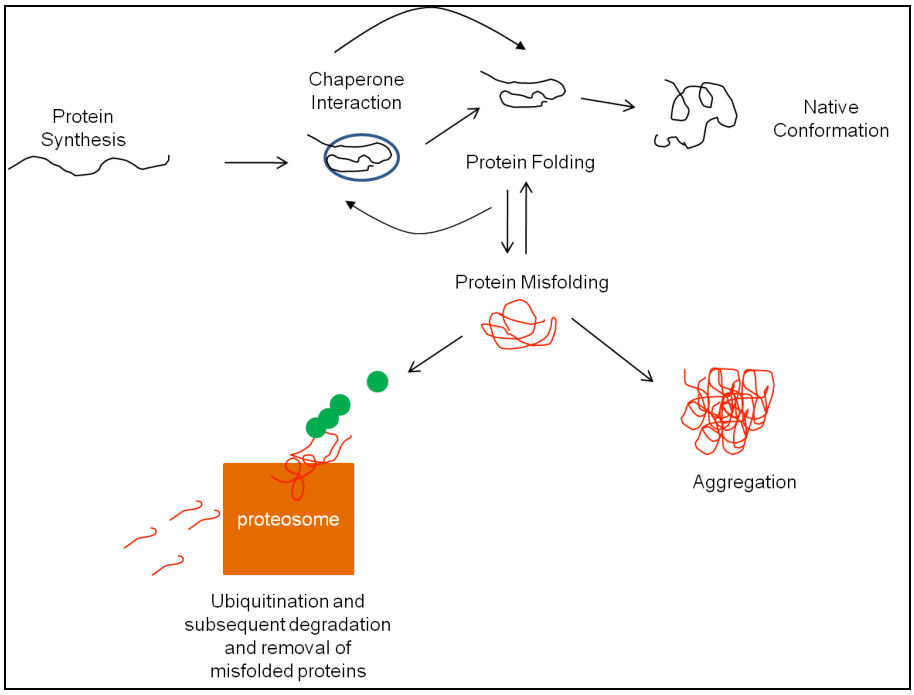

Figure 1.7. A simplified schematic of the dynamic protein folding/misfolding process. After synthesis, the polypeptide chain mediated by molecular chaperones is modified to fold to its final functional native conformation. In the process, misfolding of the polypeptide chain may occur and this may be refolded, degraded or they may form toxic aggregates. (Adapted from Bross & Gregerson Protein Misfolding and Disease, Methods in Molecular Biology Vol 232, Humana Press 2003)

1.3.2. Protein Misfolding and Disease.

Traditionally, protein misfolding has been linked to the pathogenesis of neurological diseases such as Alzheimer's disease and Parkinson's disease[68-70], however recent studies are beginning to reveal new evidences of the involvement of protein misfolding in a multitude of other diseases such as in lung diseases[71,72], ophthalmic tissue diseases[73-78], skeletal muscle diseases[79-83], connective tissue diseases[84-86], Atherosclerosis[87-89] as well as in cancers.

The basis for pathogenesis of most of these conformational diseases is the cellular inability to degrade these misfolded proteins resulting in the formation of cytotoxic aggregates. In these diseases, pathology is predominantly determined by cell damage associated with protein aggregation

thus exhibiting what is considered a 'gain-of-function' pathology[90]. This group of disease includes the neurological disorders Alzheimer's, Parkinson's and Huntington's disease[91-93]. In another group of disease, which includes cystic fibrosis[94], phenylketonuria[95] and fatty acid oxidation defects[96], the misfolded proteins are highly unstable and degraded rapidly resulting in what is termed a 'loss-of-function' pathology related to the decrease in the steady amount of the protein[92,97].

1.3.2.1. Protein Misfolding in Carcinogenesis

In normal conditions, tumor suppressors play a critical role in the regulation of cell division and survival. Tumourigenesis often arises due to the inhibition of the proper function of these proteins as a result of genetic or post-translational aberrations. In some cases, these misfolded tumor suppressors are inactivated resulting in a subsequent loss of function, while in certain cases, these mutated proteins may adopt an aberrant conformation which is regulated differently from its wild-type counterparts.

p53 is a good example of a protein that links the loss of function phenotype due to a misfolded protein conformation to carcinogenesis. p53 is a tumor suppressor protein which is commonly found to be deregulated in multiple cancers due to genetic aberrations. It has been demonstrated that mutations involving the core domain (p53C), which are found in more than 50% of all cancers contributes to p53 misfolding[98,99]. This misfolded variant of p53 was found to be inactive and observed to have a dominant negative effect on normal wild type p53[100]. The loss of functional p53 resulted in the accumulation of mutations in the genome due to the inability of the cell to effectively repair DNA lesions. This inactive conformational variant of p53

had been described to be aggregated in the nucleus and cytoplasm of multiple cancers such as neuroblastomas, retinoblastomas, breast cancers and colon cancers[99,100].

In recent years, more proteins where the loss of function due to a misfolded conformation resulted in the cancer phenotype had been identified. These include proteins such as the WT1 zinc-finger transcription factor where the tumourigenic WT1 inactivation mutation (WT/AR) (a result of improper splicing) was thought to have a role in the development of Wilms' Tumour a pediatric cancer of the kidney[101-103]. Mutations in the von Hippel Lindau (VHL) tumor suppressor, a 213 amino acid protein which assembles with elongins B and C to form the VBC complex[104], triggered misfolding (as observed in multiple tumourigenic mutants of this protein)[105], hence compromising its ability to form the VBC complex and resulted in the development of tumors associated with VHL syndrome. Merlin is another example of a protein where misfolding had been reported to result in a loss of function phenotype that led to the development of tumors associated with Neurofibromatosis type II. A missense point mutation in the N-terminus of this 65 kDa protein disrupts the native conformation of Merlin, thus affecting its ability to dimerize for proper function[106].

1.3.2.2. Protein Misfolding in AML.

Acute Promyelocytic Leukemia (APL) or AML of the M3 subtype under the FAB classification is regarded as a model disease where a definitive link between protein misfolding and leukemogenesis has been established.

PML-RARα, the fusion oncogene associated with more than 95 percent of the known cases of APL was traditionally thought to induce

differentiation arrest through the induction of transcription inhibition of RA target genes[61], via the recruitment of the transcriptional co-repressor N-CoR. However recent studies have revealed a novel mechanism in PML-RARα-induced APL pathogenesis. These new studies have demonstrated the direct role of PML-RARα in the misfolding of N-CoR. These studies suggested that when expressed with PML-RARα, N-CoR displayed several characteristics of misfolding, including its accumulation in the ER as insoluble protein aggregates, aberrant post-translational modifications and destabilization[62-64] . PML-RARα which is a *de novo* misfolded protein by itself, apparently acted as a nucleating event to trigger the conformational re-arrangement of N-CoR resulting in its misfolding. The misfolded N-CoR in the APL was highly unstable and was rapidly degraded by a non-regulated protease activity selectively activated in APL cells. This resulted in the loss of N-CoR protein and thus created a loss of function effect, contributing to the pathogenesis of APL by abrogating the repression of N-CoR target genes[62-64].

Other than abrogating N-CoR's repression on its target genes through N-CoR degradation, the non-regulated protease activity contributed to APL pathogenesis by allowing these cells to escape UPR induced cell death triggered by the accumulation of misfolded N-CoR[63] . It was reported that in the normal cellular environment, PML-RARα induced aggregation of misfolded N-CoR resulted in the amplification of ER stress to a level which ultimately triggered cell death. However in APL, the cells evolved a 'late' cytoprotective arm of UPR via the activation of a non-regulated, protease-mediated clearance of this misfolded N-CoR. This kept the ER stress level below the threshold required to initiate cell death and conferred a survival

advantage to APL cells which contributed to disease pathogenesis[58,62-64] (Fig 1.8).

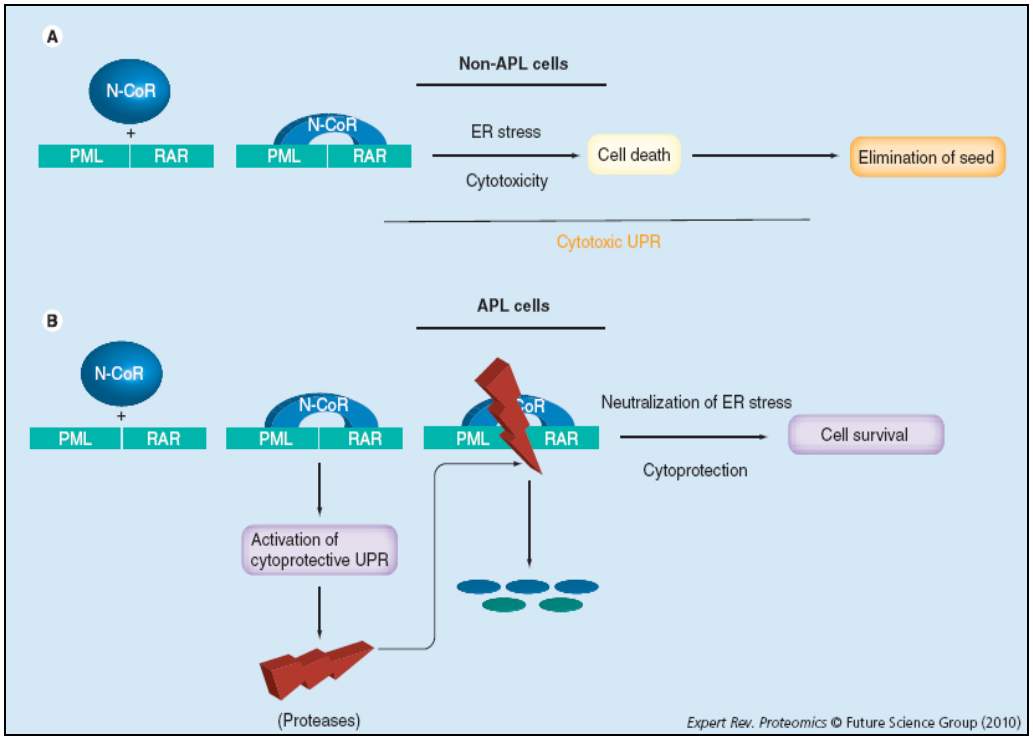

Figure 1.8. The activation of a third proposed cytoprotective arm of UPR in APL promotes cell survival. In the normal cellular environment, misfolded N-CoR is accumulated and ultimately results in cell death (A). However in APL, the activation of cytoprotective UPR negated the effects of misfolded N-CoR accumulation leading to cell survival (B). (Reproduced with permission from M Khan Expert Rev. Proteomics 2010; 7(4):501-600).

1.4. Akt and its role in transcription factor mediated carcinogenesis.

1.4.1 Akt

Akt is a serine/threonine kinase which has major roles in the regulation of multiple cellular processes. These processes include glucose metabolism, apoptosis, cell proliferation, transcription and cell migration. Currently, three mammalian Akt family members have been identified. They are Akt1[107,108], Akt2[109,110] and Akt3[111-113]. These members of the Akt family are reported to be differentially expressed at both the protein and mRNA levels[114-116]. Members of the Akt family of proteins are structurally similar with all members containing a pleckstrin homology (PH) domain in the N-terminus and a proline rich hydrophobic region in the C-terminal end[117,118]. Members of this family also contain a central kinase domain with specificity for serine or threonine residues in the substrate[109,119] (Fig 1.9).

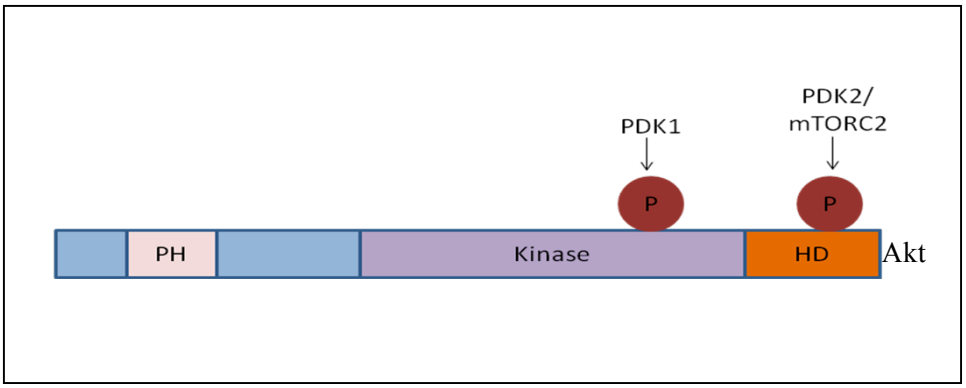

Figure 1.9. Schematic representation of various domains in the Akt family of proteins. All Akt family members contain three distinct functional domains namely the PH (Pleckstrin Homology) domain at the N-terminus, a centrally located kinase domain and the C-terminal regulatory/ hydrophobic domain (HD). The key phosphorylation sites necessary for full Akt activity have been depicted.

1.4.2. Akt activation.

The activation of Akt kinase activity is a multistep process which involves membrane translocation and phosphorylation[120]. Upon the stimulation of growth factors, growth factor receptor tyrosine kinases signal the production of 3'-phosphorylated phosphoinositides 3,4,5-triphosphate (PI-3,4,5-P_3) and PI-3,4-P_2 produced by phosphatidylinoditol 3-kinase (PI3K). The binding of these phospholipids to the PH domain of Akt triggers the translocation of Akt to the plasma membrane where it is phosphorylated. Akt is phosphorylated by the PI-3,4,5-P_3-dependent protein kinase (PDK1) at Threonine 308/309/305 (for Akt1/2/3 respectively) located in the kinase activation loop and at Serine 473/474/472 (for Akt1/2/3 respectively) which is located in the carboxy-terminal tail by the once elusive PDK2. The identity of PDK2 has recently been identified to be the mammalian Target Of Rapamycin Complex 2 (mTORC2) comprising of mTOR, rapamycin-insensitive companion of mTOR (Rictor), GβL, and mammalian stress-activated protein kinase interacting protein 1 (mSIN1)[121,122]. Phosphorylation of Akt at the Serine 473/474/472 residue occurs before and facilitates the phosphorylation at Threonine 308/309/305. The phosphorylation at Threonine 308/309/305 is thought to be essential for the activation of Akt while Serine 473/474/472 is required for maximal activity of Akt kinase[123]. Figure 1.10 represents a simplified schematic of the activation pathway of Akt by its upstream regulators.

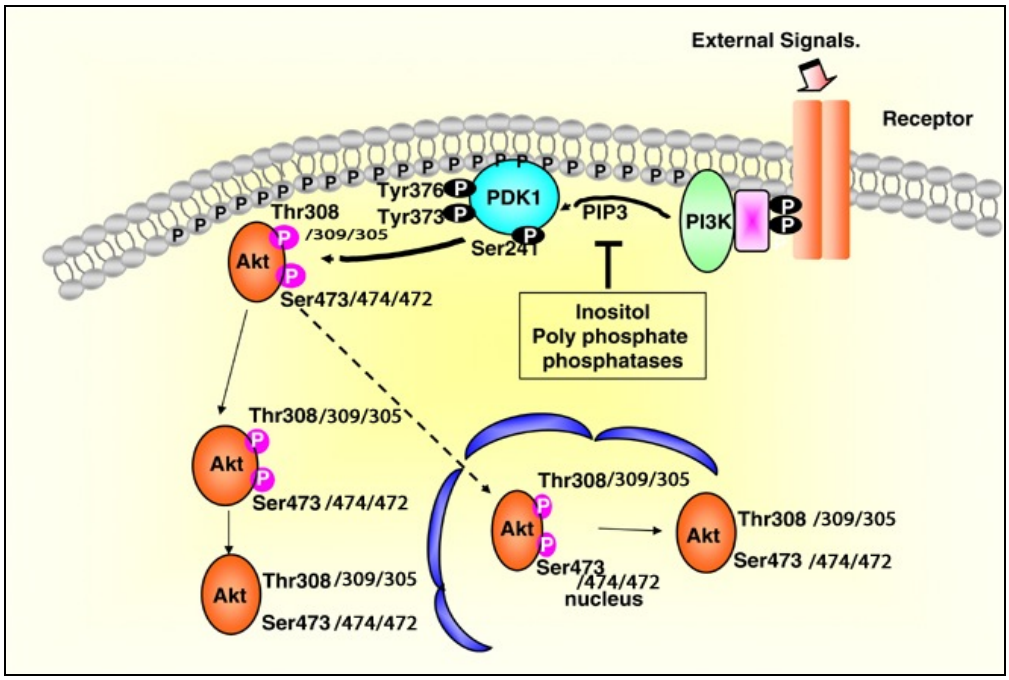

Figure 1.10. The pathway of Akt activation. PI3K is activated by extracellular stimulus. This results in the synthesis of PI-3,4,5-P_3 and PI-3,4-P_2. Binding of these phospholipids to the PH domain of Akt triggers the translocation of Akt to the plasma membrane where it is phosphorylated by PDK1 at Thr 308/309/305 and PDK2/ mTORC2 at Ser 473/474/472. Akt is first phosphorylated at Ser473/474/472 and this in turn facilitates the phosphorylation of the Thr308/309/305 residue for complete activation of Akt. Activated Akt translocates from the plasma membrane to the cytosol or to the nucleus, where it phosphorylates a wide array of downstream effector proteins. Signal termination is mediated by several inositol polyphosphate phosphatases, including PTEN, SHIP, and SHIP2. The activation cycle ends with dephosphorylation of Akt by protein phosphatases. (Adapted from K Du and P N Tsichlis Oncogene 2005; 24:7401-7409).

After activation, Akt translocates from the membrane to the cytosol or the nucleus where it phosphorylates its multitude of substrates. Termination of the signaling cascade occurs with the dephosphorylation of PI-3,4,5-P_3 and PI-3,4-P_2 by the inositol polyphosphate phosphatases which include PTEN, SHIP, and SHIP2. The activation cycle ends with dephosphorylation of Akt by protein phosphatases[124].

1.4.3. Identification and regulation of Akt substrates

The importance of Akt as a key regulator of multiple cellular events has fuelled the search for its substrates to better understand the plethora of roles it plays in normal cell survival as well as in disease. This search for substrates of Akt relevant to its survival promoting effects had been significantly aided by the identification of the preferred phosphorylation consensus motif RxRxx S/T-bulky hydrophobic *in vitro*[125,126]. This consensus RxRxx S/T-bulky hydrophobic sequence where Akt preferentially phosphorylates the serine or threonine residue exists in a large number of mammalian proteins including transcription factors and components of the apoptotic machinery[127]. The identification of the Akt consensus phosphorylation motif in proteins which participate in the apoptotic pathway emphasized the importance of Akt in the regulation of survival in cells via its direct phosphorylation of components of the cell death apparatus. Due to the particular focus of our work on transcription factors and the vast amount of information available with regards to the mammalian cell death machinery and their relationship with Akt, only the regulation of transcription factors via phosphorylation by Akt will be discussed here.

1.4.3.1. Regulation of transcription factors by Akt

The possible involvement of Akt in the regulation of transcription factors was first suggested by the observation that within 30 minutes of their activation by growth factors, both Akt1 and Akt2 detach from the cell surface membrane and translocates to the nucleus[128,129]. Subsequent work performed by various groups identified that the Forkhead family of transcription factors interacted with the insulin-response sequence (IRS)[130,131] which had been

identified in the promoter of genes such as the IGF-binding protein (IGFBP1)[132], phosphoenol pyruvate kinase (PEPCK)[133], apoplipoprotein CIII[134] and glucose-6-phosphatase[135]. Various reports also demonstrated Foxhead family of transcription factors mediated Akt-dependent transcriptional repression of these genes[135-138]. Concurrent work performed on DAF-16 (a Foxhead family member) and the discovery of Akt in the *C.elegans* model revealed that the PI3K/Akt pathway was a key regulator of *nematode* DAF-16 function[139-141]. In mammalian cells, 3 members of the Foxhead family of transcription factors were identified as likely DAF-16 orthologs (FKHR, FKHRL1/AF6q21 and AFX)[142-144]. Analysis of the amino acid sequence of all 3 orthologs and DAF-16 revealed that in all the sequences, there exist 3 sites corresponding to the Akt phosphorylation consensus sequence[127]. Evolutionary conservation of these sequences suggested the importance of these sequences in the function of the transcription factors. It was also reported that all 3 orthologs as well as DAF-16 could be effectively phosphorylated by Akt *in vitro*[145-148].

Akt was thought to mediate the function of these transcription factors by regulating their subcellular localization[145,146]. In the absence of Akt activity, FKHR and FKHRL1 translocates to the nucleus. However when Akt is activated, phosphorylation of these factors at the Akt consensus motif promotes their cytoplasmic retention, thus sequestering them from their nuclear targets. Recent work by Menghini and colleagues also reported a similar mechanism of functional inhibition of the transcription factor GATA2 in adipocytes[149]. Here it was reported that Akt phosphorylation of GATA2 at the Serine 401 residue located within the Akt phosphorylation consensus motif retained GATA2 in the cytoplasm of preadipocytes, modulating its DNA

binding activity and aided preadipocyte differentiation preventing its ability to exert inflammatory function. Another transcription factor which function was reported to be regulated by Akt phosphorylation is the transcriptional activator CREB[150]. It was reported that phosphorylation of CREB at Serine 133 by Akt enhanced the binding of CREB to CBP thus facilitating CREB-mediated transcription.

In carcinogenesis, deregulations in Akt activity have been widely reported and many tumours have been reported to display Akt hyper-activity. Given Akt's role in the regulation of the survival signalling pathway, Akt hyper-activity have been widely associated with the enhanced survival advantage of tumour cells. There is increasing evidence from multiple protein databases suggesting that a large number of transcription factors contain the putative Akt phosphorylation consensus motifs in their amino acid sequences. This suggests that transcription factors could be potential substrates of Akt and any deregulation in Akt activity could possibly contribute to cancer progression by affecting the normal function of these factors, leading to differentiation arrest, the hallmark of cancer.

1.5. The FMS-Like Tyrosine Kinase 3 receptor (Flt3)

1.5.1. Receptor Structure

Flt3 is a membrane bound receptor tyrosine kinase (RTK) essential for normal haematopoiesis and mutations in the FLT3 gene is one of the most frequent genetic aberration found in haematological malignancies.

Located on chromosome13q12, the human Flt3 has an 85% amino acid homology to its mouse counterpart[151]. It belongs to the RTK subclass III family which also includes other members such as the macrophage colony-stimulating factor (M-CSF) receptor, Steel Factor Receptor (KIT) and the

receptor for platelet-derived growth factors A and B (PDGFRA and PDGFRB)[152]. Two forms of the human Flt3 have been identified- the 160 kDa membrane bound N-glycosylated form and the intracellular non-glycosylated 130 kDa form[153,154]. The mature membrane bound form of the Flt3 receptor consist of a extracellular binding domain which have 5 immunoglobulin loops, a juxtamembrane domain, an ATP-binding pocket, an activation loop and a Kinase insert[155] (Fig 1.11).

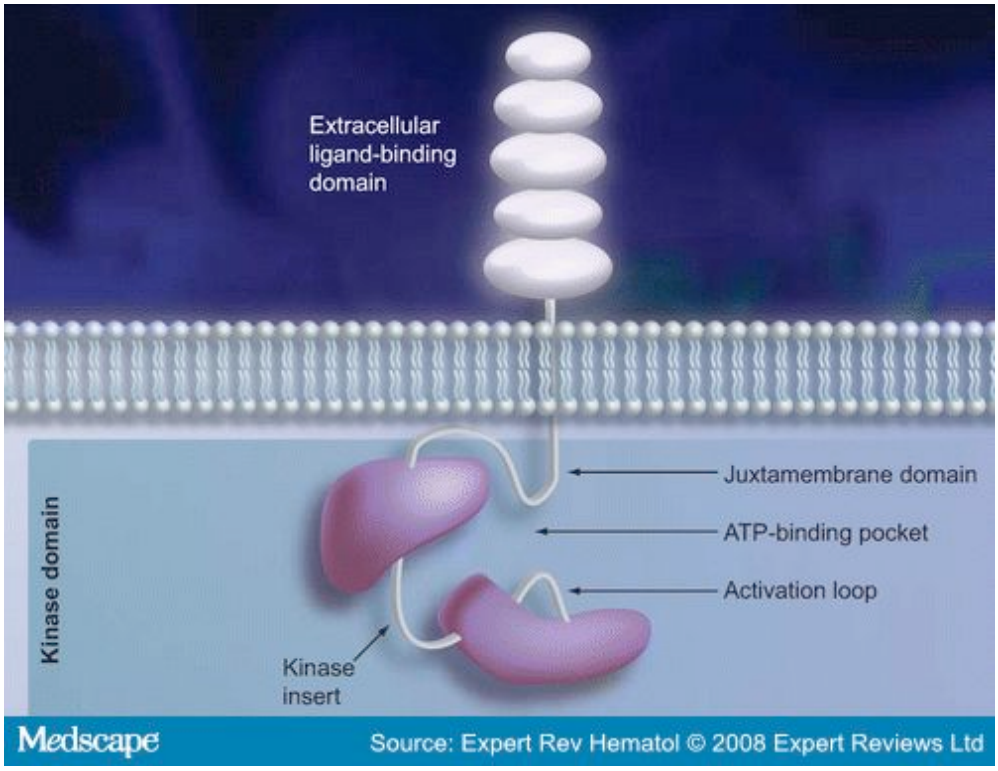

Figure 1.11. A simplified schematic of the Flt3 receptor. The Flt3 receptor monomer consist of multiple domains including the extracellular binding domain which have 5 immunoglobulin loops, a juxtamembrane domain, an ATP-binding pocket, an activation loop and a Kinase insert (Reproduced with permission from K Shami et al, Expert Rev Hematol 2008; 1: 153-160)

1.5.2. Role of Flt3 in normal haematopoiesis.

Flt3 is expressed mainly in the early myeloid and lymphoid progenitors[156] but not in the more matured erthyroid cells[157],

megakaryocytes[158] or mast cells[159]. Expression of the Flt3 receptor in normal haematopoiesis is depicted in Figure 1.12.

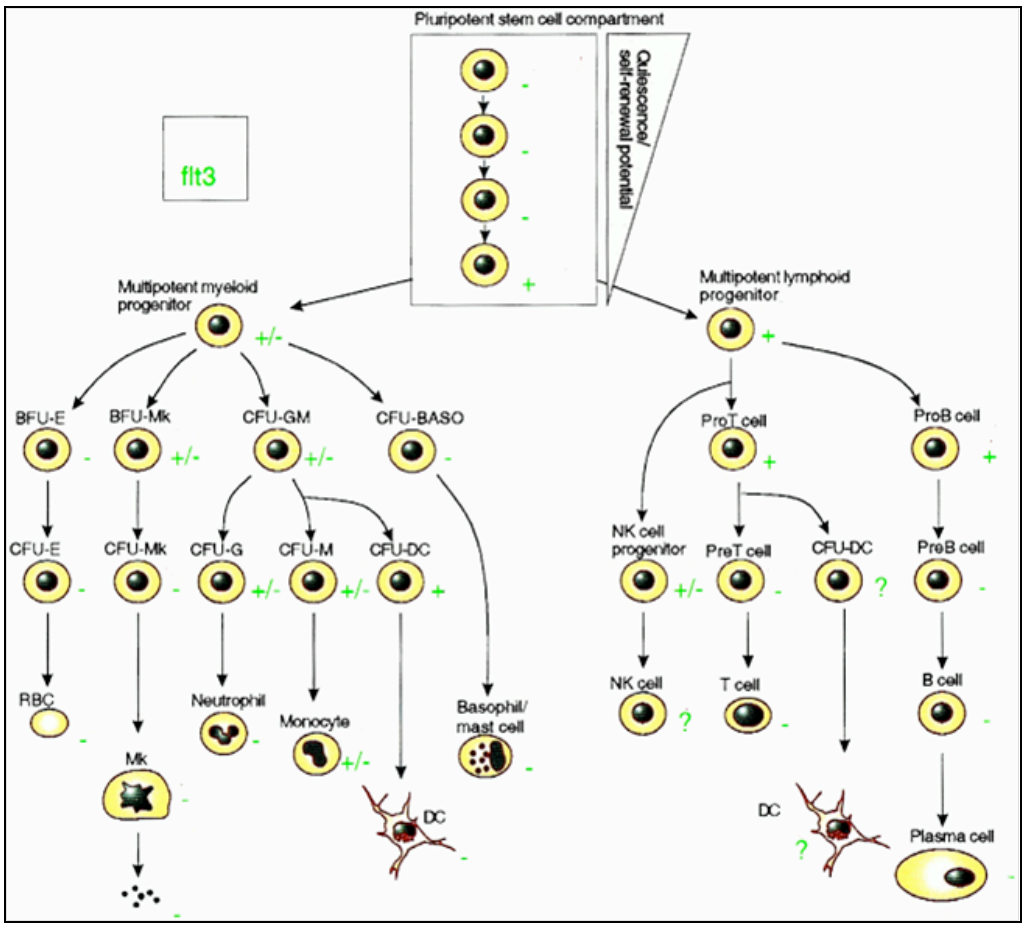

Figure 1.12. Expression of Flt3 in normal haematopoiesis. The figure indicates expression of Flt3 (green) in various classes of hematopoietic stem and progenitor cells as well as mature blood cells. Symbols: (−) most/all cells appear to lack Flt3 expression; (+) most/all cells appear to express Flt3; (+/−) the cell type appears to consist of significant receptor-positive as well as receptor-negative populations; (?) sufficient expression or functional data not available. Abbreviations: BFU, burst-forming units; CFU, colony-forming units; E, erythroid; Mk, megakaryocyte; G, neutrophilic progenitor; M, monocyte/macrophage; DC, dendritic cell; Baso, basophil; RBC, red blood cell; NK, natural killer cell. (Reproduced with permission from Lyman S D et al, Blood 1998; 91: 1101-1134)

In normal cells, binding of the Flt3 ligand to the Flt3 receptor activates the Flt3 signal transduction pathway which promotes the growth of early progenitor cells. Flt3-mediated responses differ greatly for various cell types

and specific responses are dependent on the combination of other growth factors. For example, Flt3 receptor activity stimulated by the Flt3 ligand in the absence of other growth factors promoted the monocytic differentiation of early progenitors without any marked differences in proliferative response[160] while in the presence of other growth stimulating cytokines such as interleukin-3 (IL-3), G-CSF, CSF1, GM-CSF, EPO and KIT ligands the cells showed an enhanced proliferative response and increased the development of granulocytic-monocytic colony formation units[157,160,161]. However, Flt3 stimulation via the Flt3 ligand had no marked effect on erythropoiesis and megakaryopoiesis as these cell lineages do not express Flt3[157].

Preferential expression of Flt3 in primitive hematopoietic cells suggested a role of Flt3 in the regulation of differentiation. It was reported that Flt3 ligand activation of the wild-type Flt3 transfected 32D cells inhibited their progression towards neutrophils, however a complete block of differentiation was not observed[162]. Although Flt3 expression is widespread in the hematopoietic system, it was surprising to observe that the Flt3-/- knockout mouse had relatively normal haematopoiesis with the only defect being a small decrease in the size of the pro-B and pre-B cell compartments[163]. Transplantation experiments in mice with either non-functioning Flt3 or wide-type Flt3 led to the reconstitution of the bone marrow containing mostly cells which expressed the wide-type receptor suggesting a selective growth advantage of these cells. The selective advantage was found in all cell lineages indicating a global effect of Flt3 disruption in the hematopoietic system[163]. Additionally, the lethal phenotype was only observed when Flt3 was knocked out in combination with Kit. Thus it was suggested that Flt3 is important but

not absolutely required for normal haematopoiesis and works together with other growth factors to enhance proliferation and differentiation of myeloid and lymphoid cells. Recent studies by Kikushige et al also reported that Flt3 expression in human HSCs, Granulocyte/Macrophage Progenitor stages promoted and maintained cell survival in these cells. In their experiments, it was observed that activation of the Flt3 signalling pathway in the HSCs and progenitors prevented spontaneous apoptotic cell death via the up regulation of the important pro survival protein MCL-1. This suggested that the human Flt3 signalling pathway has a critical role in the survival of the stem and progenitor cells and present as important targets for AML transformation[164].

1.5.3. Flt3 in leukemogenesis

It was previously suggested that leukemia arise from LSCs which have re-acquired or retained the abilities of self-renewal and unlimited growth and proliferation. Involvement of Flt3 in the proliferation of HSCs and early progenitor cells suggested that Flt3 expression and activation of the Flt3 signaling pathway had possible oncogenic potentials. Evidence from clinical studies had indicated that Flt3 had the capacity to enhance the survival and proliferation of leukemic blasts, with 70% to 100% of AMLs expressing wild-type Flt3[165-167]. Aberrant activation of the Flt3 signaling pathway via tyrosine kinase gain-of-function mutations of the Flt3 receptor are also observed in about 30% of patients with AML. Patients who present with Flt3 receptor activating mutations are reported to have a worse prognosis compared to patients with the wild-type receptor[168,169]. Two types of activating mutations have been identified to contribute to the deregulation of the Flt3 receptor.

The first and most common mutation is the in-frame internal tandem duplication (ITD) in the juxtamembrane (JM) domain of the Flt3 receptor. This FLT3-ITD mutation has been reported in 17 to 26 percent of known AML cases[170,171]. The mutation is an insertional mutation within exon 14 and can vary in length from 3 to more than 400 base pairs[172]. Current knowledge of the cause of this mutation is still vague although it was proposed that the cause could be a failure in the slippage or mismatched pair repair mechanism during the DNA replication process[173,174]. The ITD mutation results in the constitutive activation of Flt3 kinase as it disrupts the JM domain mediated regulation of kinase catalytic activity[175]. The FLT3-ITD mutation has been observed in all subtypes of AML but has been reported to appear most frequently in AML of the M3 and M5 subtypes and has the lowest frequency of occurrence in the M2 subtypes[176-182].

The second type of genetic defect is the single-amino acid mutation in the Flt3 sequence. These are usually missense point mutations in the kinase domain of the Flt3 RTK which can also confer constitutive activity to Flt3. The most reported point mutation is the substitution of tyrosine for aspartic acid at position 835 within the activation loop of the Flt3 kinase domain. Other point mutations at positions 836 and 841 which also result in the constitutive activity of the Flt3 receptor have also been reported[183-185]. The FLT3-D835 mutation is found in 7 percent of AML cases and it is thought that the mechanism of RTK activation is most likely similar to that of other members of the RTK family where the substitution stabilizes the 'open' ATP-binding conformation of the activation loop[186].

Despite the involvement of Flt3 in proliferation, self-renewal and anti-apoptosis, over expression of Flt3 and its mutants alone are not able to induce the complete leukemic phenotype *in vivo*[187]. The FLT3-ITD mutant was observed to induce myeloproliferative phenotype in transduced mouse models but lacked induction of the necessary block in differentiation, a hallmark of AML. Thus the Knudson 2 hit hypothesis of cancer progression seemed to be supported by this observation where a second oncogenic event may be needed to work in tandem with Flt3 deregulation to bring about complete transformation. This was later supported in a study where the transduction of FLT3-ITD into the bone marrow cells of PML-RARα transgenic mice displayed the complete penetrance and rapid progression of APL[162]. This indicated that although aberrant Flt3 signaling may affect differentiation, a more potent mechanism must work in tandem to effect transformation.

Nevertheless, the importance of Flt3 in the maintenance of the survival and proliferative capabilities of the leukemic blasts cannot be denied and aberrant or enhanced Flt3 signaling due to activating mutations or over expression of the receptor may be crucial in providing the leukemic blasts with a survival and proliferative advantage critical for tumor maintenance and progression.

1.6. Hypotheses and Aims of this project.

Recently, our laboratory reported the role of misfolded conformation dependent loss (MCDL) of N-CoR protein in the pathogenesis of APL[58,62,63]. In APL, we reported that the fusion oncoprotein PML-RARα induced misfolding of N-CoR as characterized by N-CoR's detergent insolubility and aberrant cytosolic location. The accumulation of misfolded N-CoR in the endoplasmic reticulum (ER) resulted in the induction of ER stress[62]. This misfolded N-CoR was subsequently found to be cleaved by O-sialoglycoprotein endopeptidase (OSGEP) a heat liable protease[63] which selectively cleaves O-sialyated proteins. This cleavage contributed to the survival of APL cells by preventing the ER stress levels from reaching the threshold where ER stress induced cell death is initiated. We also reported that Genistein, a kinase inhibitor isolated from soy was able to restore native N-CoR function leading to the differentiation and proliferation block in APL[58].

The transcriptional control imparted by N-CoR have been reported to be important for the growth suppressive functions of several tumor suppressor proteins including Mad and Rb[188,189]. Also, N-CoR being a key component of the generic multi-protein co-repressor complex involved in the transcriptional control mediated by various transcription factors has also been suggested to be important in the normal development and maturation of the hematopoietic system, with reports indicating that N-CoR knockout mice are embryonically lethal and appear to die from anemia due to defects in definitive erythropoiesis[36]. Loss of N-CoR protein via MCDL could thus be a key event

in malignant transformation not only in APL but in other AML subtypes as well.

In light of the findings from our laboratory based on the APL model and the essential role of N-CoR in the normal maturation and development of the hematopoietic system, this project was conceived to investigate if MCDL of N-CoR could also contribute to the malignant growth and transformation of other FAB subclasses of AML such as in Acute Monocytic Leukemia (AML designated as M5 in the FAB classification system-AML-M5). Specifically, our aim was to (1) identify the molecular mechanism behind the misfolding of N-CoR in AML-M5, (2) elucidate the physiological and functional consequences of N-CoR MCDL in the pathogenesis of AML-M5 and (3) devise new therapeutic strategies for AML-M5 through targeting the N-CoR MCDL pathway.

CHAPTER 2

Materials

&

Experimental

Procedures

2. MATERIALS AND EXPERIMENTAL PROCEDURES

2.1. Materials

2.1.1. General Reagents

Table 2.1: List of Chemicals, Reagents and Kits

Chemicals/Reagents/Kits	Company	Country
2-Mercaptoethanol	Bio-Rad	CA, USA
4-(2-Aminoethyl) benzenesulfonyl fluoride hydrochloride (AEBSF)	Merck	Darmstadt, Germany
4',6-diamidino-2-phenylindole (DAPI)	Sigma Aldrich	MO,USA
1 kb DNA ladder	Promega	WI,USA
30% Acrylamide-Bis Solution	Bio-Rad	CA, USA
Accuprime Taq Polymerase System	Invitrogen	CA,USA
Agarose	Bio-Rad	CA,USA
Akti-X	Merck	Darmstadt, Germany
Ammonium Persulfate	Bio-Rad	CA,USA
Ampicillin	Sigma Aldrich	MO,USA
Annexin V-FITC Apoptosis Detection Kit	BD Pharmingen	CA,USA
Bovine Serum Albumin (BSA)	Sigma Aldrich	MO,USA
Cell Proliferation Kit I [3-(4,5-dimethylthiazol-2-yl)-2,5-diphenyltetrazolium bromide; (MTT)	Roche	Germany
ChIP-IT Kit	Active Motif	CA,USA
Diethylpyrocarbonate (DEPC)	Sigma Aldrich	MO,USA
Dimethyl sulfoxide (DMSO)	Sigma Aldrich	MO,USA
Dulbucco's Modified Eagle's Medium (DMEM)	Sigma Aldrich	MO,USA
Ethanol	Merck	Darmstadt, Germany
Fetal Bovine Serum (FBS)	Hyclone	Logan, UT
Fugene 6	Roche	Germany
GeneTailor™ Site-Directed Mutagenesis System	Invitrogen	CA,USA
Giemsa Azur Eosin Methylene Blue Solution	Merck	Darmstadt, Germany
Glacial Acetic Acid	Merck	Darmstadt, Germany
Glycine	Bio-Rad	CA,USA
Human Phospho-kinase Array Kit (Proteome Profiler-Antibody Array)	R&D Systems	MN, USA

Chemicals/Reagents/Kits	Company	Country
Isocove's Modified Dulbocco's Medium (IMDM)	Life Technologies	Gaithersburg, MD
Isopropanol	Merck	Darmstadt, Germany
Kanamycin	Sigma Aldrich	MO,USA
Lipofectamine 2000	Invitrogen	CA,USA
Luciferase Assay System (Dual)	Promega	WI,USA
May-Grunwald Solution	Roche	Germany
Methanol	Sigma Aldrich	MO,USA
Murine Reverse Transcriptase, MMLV	Promega	WI,USA
Normal Goat IgG	Santa Cruz Biotechnologies	CA,USA
Normal Mouse IgG	Santa Cruz Biotechnologies	CA,USA
Normal Rabbit IgG	Santa Cruz Biotechnologies	CA,USA
Nucleofector Kit V	Amaxa, Lonza	Cologne, Germany
One Shot® DH5ά™-T1 Competent Cells	Invitrogen	CA,USA
Paraformaldehyde	Sigma Aldrich	MO,USA
Phosphatase Inhibitor Cocktails 1 and 2	Sigma Aldrich	MO,USA
Precision Dual Color Standard Protein Marker	Bio-Rad	CA,USA
Prolong Gold Antifade Reagent	Invitrogen	CA,USA
Protein G Sepharose Breads	Roche	Germany
PVDF Membrane	Bio-Rad	CA,USA
Qiagen plasmid DNA purification Kit (maxi and miniprep kit)	Qiagen GmBH	Hilden, Germany
Qiagen Gel Extraction Kit	Qiagen GmBH	Hilden, Germany
Qiagen RNasey RNA extraction Kit (RNA miniprep kit)	Qiagen GmBH	Hilden, Germany
Recombinant Mouse EPO	R&D systems	MN,USA
Recombinant Mouse Flt3 Ligand	R&D systems	MN,USA
Recombinant Mouse G-CSF	R&D systems	MN,USA
Recombinant Mouse IL-3	R&D systems	MN,USA
Recombinant Mouse SCF	R&D systems	MN,USA
Recombinant Human Flt3 Ligand	R&D systems	MN,USA
Recombinant Human IL-3	R&D systems	MN,USA

Chemicals/Reagents/Kits	Company	Country
RPMI 1640	Life Technologies	Gaithersburg, MD
Skim Milk powder	Sigma Aldrich	MO,USA
SMART-PCR cDNA Synthesis Kit	Clontech	CA,USA
Sodium Dodecyl Sulfate (SDS)	Bio-Rad	CA,USA
Sodium Fluoride	Sigma Aldrich	MO,USA
SuperScript II RT First-Strand kit	Invitrogen	CA,USA
TaqMan Gene Expression Assay (Real time PCR)	ABI systems	CA,USA
Tetramethylethylenediamine (TEMED)	Bio-Rad	CA,USA
Tris-Base	Bio-Rad	CA,USA
Trizol	Sigma Aldrich	CA,USA
Tween 20	Sigma Aldrich	MO,USA

2.1.2. Antisera

2.1.2.1. Western Blotting (WB)

Table 2.2: List of Primary Antibodies (WB)

Target	Company	Description	Dilution	Incubation Conditions
β-Actin	Sigma Aldrich	Mouse Monoclonal	1:10000	Overnight at 4^0C
Akt	Cell Signaling Technologies	Rabbit Polyclonal	1:5000	Overnight at 4^0C
Flag	Sigma Aldrich	Mouse Monoclonal	1:10000	Overnight at 4^0C
Flt3	Santa Cruz Biotechnologies	Rabbit Polyclonal	1:1000	Overnight at 4^0C
GRP 78	Santa Cruz Biotechnologies	Goat Polyclonal	1:1000	Overnight at 4^0C
N-CoR	Santa Cruz Biotechnologies	Goat Polyclonal	1:500	Overnight at 4^0C
N-CoR	Upstate Technologies	Rabbit Polyclonal	1:1000	Overnight at 4^0C
PDI	Santa Cruz Biotechnologies	Rabbit Polyclonal	1:1000	Overnight at 4^0C
Phospho-Akt (Ser473)	Cell Signaling Technologies	Rabbit Polyclonal	1:1000	Overnight at 4^0C
Phospho-Akt substrate (RXXRS/T)	Cell Signaling Technologies	Rabbit Polyclonal	1:1000	Overnight at 4^0C

Table 2.3 : List of Secondary Antibodies (WB)

Description	Company	Dilution	Incubation Conditions
HRP-Goat anti-Rabbit	Zymed Laboratories	1:10000	1 hr, Room Temperature
HRP-Goat anti-Mouse	Zymed Laboratories	1:10000	1 hr, Room Temperature
HRP-Rabbit anti-Goat	Zymed Laboratories	1:10000	1 hr, Room Temperature

2.1.2.2. Immnofluorescence Staining (IF)

Table 2.4: List of Primary Antibodies (IF)

Target	Company	Description	Dilution	Incubation Conditions
Akt	Cell Signaling Technologies	Rabbit Polyclonal	1:200	Overnight, 4^0C
Flag	Sigma Aldrich	Mouse Monoclonal	1:1000	2 hr, Room Temp
GRP 78	Santa Cruz Biotechnologies	Goat Polyclonal	1:100	2 hr, Room Temp
N-CoR	Santa Cruz Biotechnologies	Goat Polyclonal	1:100	2 hr, Room Temp
N-CoR	Santa Cruz Biotechnologies	Rabbit Polyclonal	1:100	2 hr, Room Temp
PDI	Santa Cruz Biotechnologies	Rabbit Polyclonal	1:100	2 hr, Room Temp
Phospho-Akt (Ser473)	Cell Signaling Technologies	Rabbit Polyclonal	1:20	Overnight, 4^0C

Table 2.5: List of Secondary Antibodies (IF)

Description	Company	Dilution	Incubation Conditions
Alexa Flour Chicken Anti-Goat 488	Invitrogen	1:200	1 hr, Room Temperature
Alexa Flour Chicken Anti-Goat 594	Invitrogen	1:200	1 hr, Room Temperature
Alexa Flour Chicken Anti-Mouse 488	Invitrogen	1:200	1 hr, Room Temperature
Alexa Flour Chicken Anti-Mouse 594	Invitrogen	1:200	1 hr, Room Temperature
Alexa Flour Chicken Anti-Rabbit 488	Invitrogen	1:200	1 hr, Room Temperature
Alexa Flour Chicken Anti-Rabbit 594	Invitrogen	1:200	1 hr, Room Temperature

2.1.2.3 Flow Cytometry Analysis

Table 2.6: List of antibodies used in Flow Cytometry Analysis

Target	Company	Conjugation	Incubation Conditions
CD14	BD Pharmingen	FITC	1 hr, Room Temperature
Annexin V	BD Pharmingen	FITC	15 mins, 4^0C

2.1.3. Primer Sequences

2.1.3.1. Semi-Quantitative RT-PCR primers

Table 2.7: List of semi-quantitative RT-PCR primers

Gene	Sequence	Annealing Temperature (^{0}C)	Cycles
GATA-1	Forward: 5'-ATATGCCGGCTGGGCCTACG-3' Reverse: 5'-GGTGGTCGTCTGGCAGTTGG-3'	60	30
GATA-2	Forward: 5'-TCATCTTCCGCGGGGGGTAG-3' Reverse: 5'-GGACATCTTCCGGTTCCGAGTC-3'	60	30
C/EBPα	Forward: 5'-CAAGCGGGTGGAACAGCTGAG-3' Reverse: 5'-TGCTCCCCTCCTTCTCTCATGG-3'	60	30
PU.1	Forward: 5'-CGTGCACAGCGAGTTCGAGAG-3' Reverse: 5'-GCGCGCCATCTTCTGGTAGG-3'	60	30
IL5Rα	Forward: 5'-CCTGCAGAACGACCACTCACTAC-3' Reverse: 5'-CACTCTCTCAAGGGCTTGTGTTC-3'	60	30
MBP	Forward: 5'-GCGCTCAACCAGGGTCAAGTC-3' Reverse: 5'-AAGAGAACTAGCTGAGCCCATTCC-3'	60	30
MCP-5	Forward: 5'-GCCTACCTGGAAATTGTAACTTCC-3' Reverse: 5'-CAGCTGAAGATTGTGGTCAAAGTC-3'	60	35
EoPO	Forward: 5'-TATGGCAGTGAGGTCTCCCTCTC-3' Reverse: 5'-GGTACTGACTGTCCAAGCGGAAC-3'	60	30
FCεRIα	Forward: 5'-GTGTTAGCAGTCCCTCAGAAACC-3' Reverse:5'-TACAGTAATGTTGAGGGGCTCAG-3'	60	35
Notch-1	Forward: 5'-TACTACGGCCGCGAGGAGGA-3' Reverse: 5'-TGGCAGACATGCGCAGGTCA-3'	60	30
FOG-1	Forward: 5'-CCTCCCAGCGCAGATGTTAACTC-3' Reverse: 5'-GGTCTCTTTGGGCTTCTCGTCTG-3'	60	35
PAX-5	Forward: 5'-AGAGCGGGTGTGTGACAATGAC-3' Reverse: 5'-GCACACTGCTCCCGATGTCAG-3'	60	35
EBF	Forward: 5'-TGGCCCGGGCTCACTTTGAG-3' Reverse: 5'-GAGCAAGACTCGGCACATTTCTG-3'	60	35
HoxA9	Forward: 5'-ATCCCAATAACCCAGCAGCCAAC-3' Reverse: 5'-ACACACAGCTATCAGCACTAATGC-3'	60	30
HoxA10	Forward: 5'-GATTCCCTGGGCAATTCCAAAGG-3' Reverse: 5'-CCCAGGAGATGGCGAGTGTG-3'	60	30/40
β-catenin	Forward: 5'-GTAGAAGCTGGTGGAATGCAAGC-3' Reverse: 5'-ATAGTGAAGGCGAACTGCATTCTGG-3'	60	30/40
Flt3	Forward: 5'-TCAGGGGCAATGCCCGTCTG-3' Reverse: 5'-CTGCATCTGCCAGCTGACATCC-3'	60	30/40

JunB	Forward: 5'-GCCTCCACCTTCAAGGAGGAAC-3' Reverse: 5'-GGGCAGGGGACGTTCAGAAG-3'	60	30
Plakoglobin	Forward: 5'-ACGAGGGCACTGCCACCTAC-3' Reverse: 5'-AGGCCGTCGCTGTAGGTGTC-3'	60	30
Scl/Tal1	Forward: 5'-CTCGGCAGCGGGTTCTTTGG-3' Reverse: 5'-CATTGAGCAGCTTGGCCAAGAAG-3'	60	30
Stat5A	Forward: 5'-GGAAGTTTGACTCCCCGGAACG-3' Reverse: 5'-CTGGCCACATCCATGGTCTCATC-3'	60	30
N-CoR1	Forward: 5'-GACTCTGATATGGCAGCTGCTCAG-3' Reverse: 5'-GCTGAGCATCCGCATAGTCAGAG-3'	60	30
HPRT	Forward: 5'-GAAGGAGATGGGAGGCCATCAC-3' Reverse: 5'-CAACAATCCGCCCAAAGGGAAC-3'	60	30

2.1.3.2. Real Time PCR Primer Assays (Taqman)

Table 2.8: List of Taqman Assays used in Real Time PCR Analysis

Gene	Taqman Gene expression array ID
GATA1	HS01085821_g1
GATA2	HS00231119_m1
C/EBP alpha	HS02915002_s1
C/EBP gamma	HS00156454_m1
PU.1	HS02786711_m1
ILR5 alpha	HS00236871_m1
MBP	HS00921945_m1
EPO	HS01071098_g1
HoxA9	HS00365956_m1
HoxA10	HS00538183_m1
beta Catenin	HS00994404_g1
Flt3	HS00975659_m1
JunB	HS00957891_s1
Plakoglobin	HS00158408_m1
Scl/Tal1	HS01097987_m1
Stat5A	HS00559643_m1
FCεRI alpha	HS01090133_g1
Notch1	HS01062014_m1
FOG1	HS00419119_m1
Pax5	HS00277134_m1
EBF	HS03045361_m1

2.1.3.3. ChIP Assay Primers

Table 2.9: List of Primers used in ChIP assay

Gene Promoter	Sequence	Annealing Temperature (^{0}C)	Cycles
CD36	Forward: 5'-AAGACAGGAAAACCTGAGCCTTCC-3' Reverse: 5'-CTCACTCATTTTGGGCCTCAGTTG-3'	60	25
Flt3	Forward: 5'-ACCTCCCTAATTGCCTTGGTTGAC-3' Reverse: 5'-GGATCTTTGAGGCCCTGAGAAAGG-3'	60	25
Scl/Tal1	Forward: 5'-AAAAGAGGTCTTCGCTCCCTTTCC-3' Reverse: 5'-ATCCCACCGCATGCACACAAC-3'	60	25

2.1.3.4. siRNA sequences

Table 2.10: List of siRNA sequences used in siRNA mediated gene knockdown

Target	Sequence
Akt	5'-ATA CCG GCA AAG AAG CGA TGC TGC A-3'
N-CoR	5'-AATGCTACTTCTCGAGGAAACA-3'
Luciferase	5'-CGTACGCGGAATACTTCGA-3'

2.1.3.5 Site directed mutagenesis sequences

Table 2.11: List of primers used in Site Directed Mutagenesis

	Forward primer	Reverse Primer
Ser1450-Ala	5'-TGCGAGCCCGGCACACG GCAGTGGTGAGCT-3'	
Ser1450-Apa	5'-TGCGAGCCCGGCACACG GATGTGGTGAGCTCT-3'	5'-CGTGTGCCGGGCTCG CACTGGCTCGCCTG-3'
Ser1450-Glu	5'-TGCGAGCCCGGCACACG GAAGTGGTGAGCTCT-3'	

Table 2.12: Primers used for analysis of base pair mutations

	Forward primer	Reverse Primer
N-CoR MutA	5'-GACAACAACTC AGGTTCAATCAG -3'	5'-CTCTGGATATGG TGTTCTGGTAG -3'

2.1.4. Plasmids

2.1.4.1. pACT –N-CoR-Flag

The non-viral mammalian expression vector, carrying the ampicillin bacterial resistant gene and the CMV promoter, pACT was purchased from Promega, USA. The pACT-N-CoR-Flag consist of 2 tandem repeats of the Flag sequence, linked to the C-terminal end of the mouse N-CoR sequence. It was cloned into the vector site at the *Nco1* and *Xba1* restriction sites.

2.1.4.2. pEGFP-MLL1-AF9

The non-viral mammalian expression vector, carrying the kanamycin bacterial resistant gene, the gene encoding the Enhanced Green Fluorescent protein (GFP) variant of the *Aequorea victoria* and the CMV promoter, pEGFP-C1 was purchased from Clontech, USA. The MSCV-MLL1-AF9-MIG plasmid was a kind gift from Dr Scott. A. Armstrong from the Harvard Medical School, Boston, Massachusetts, USA. The MLL1-AF9 sequence was excised via *Eco1* blunt end restriction digestion and cloned into the pEGFP-C1 vector. The pEGFP-MLL1-AF9 plasmid contains the GFP tagged at the N-terminus of the MLL1-AF9 sequence.

2.1.4.3. pECFP-myr-Akt

The pECFP-myr-Akt plasmid was a kind gift from Dr Koichi Okumura from the Cancer Science Institute, National University of Singapore. pECFP-C1 plasmid encodes an Enhanced Cyan Fluorescent (CFP) variant of the *Aequorea victoria* Green Fluorescent Protein (GFP) gene. It is a non-viral

mammalian expression vector carrying the kanamycin bacterial resistant gene and the CMV promoter.

2.1.4.4. Luciferase reporter plasmids.

The Flt3 (-901)-luciferase reporter plasmids were kind gifts from Dr Shinichiro Takahashi from the Division of Hematology, Kitasato University School of Allied Health Science, Kanagawa, Japan. The Flt3 promoter region (up to 901 basepairs upstream of the Flt3 transcriptional start site) was cloned into the pGL3 Luciferase reporter Vector from Promega, USA. The pGL3 vector contains a modified coding region for the firefly (*Photinus pyralisi)* luciferase gene. It carries an ampicillin bacterial resistant gene and lacks the eukaryotic promoter and enhancer sequences to allow for the cloning of putative regulatory sequences.

2.1.5. Cell Lines

2.1.5.1. AML-M5 cell lines

The AML-M5 cell lines, THP-1, SigM5 and Mono-Mac-1 were obtained from DSMZ - Deutsche Sammlung von Mikroorganismen und Zellkulturen GmbH (German Collection of Microorganisms and Cell Cultures). The AML-M5 cell lines Nomo-1 and MV-4-11 were kind gifts from Dr Motomi Osato from the Cancer Science Institute of Singapore and Dr Chien Shing Chen from Loma Linda University, California, USA. The cell lines THP-1, Mono-Mac-1 and Nomo-1 carry the t (9:11) (p22; q23) translocation resulting in the expression of the fusion protein MLL1-AF9. While both THP-1and Nomo-1 are known to express the wild type Flt3 receptor, Mono-Mac-1 is known to carry a constitutively active Flt3 receptor due to an activating point mutation at tyr594 in the kinase domain of the Flt3 receptor. The cell line MV-4-11

carries a t (4:11) (q21; q23) translocation resulting in the expression of the fusion protein MLL-AF4 and is known to carry the Flt3-ITD mutant receptor. The cell line SigM5 has no reported chromosomal translocations and no known Flt3 receptor status.

2.1.5.2. AML cell lines from other FAB subtypes

The AML-M2 cell line HL60 was purchased from the American type Culture Collection.

2.1.5.3. Non AML cell lines

The non-AML cell lines U937 (Histiocytic Lymphoma), K562 (Chronic Myelogenous Leukemia) and HEK 293T (Human Embryonic Kidney) cells were obtained from the American type Culture Collection. The mouse pro B-cell line BA/F3 was obtained from DSMZ - Deutsche Sammlung von Mikroorganismen und Zellkulturen GmbH (German Collection of Microorganisms and Cell Cultures).

2.1.6. AML primary patient specimens.

A total of 12 AML primary patient specimens and were used in this study. Primary leukemic specimens used in this study were obtained at the time of diagnosis. Diagnoses of AML were made from the morphology and cytochemistry according to the French–American–British (FAB) classification as well as immunophenotypic and cytogenetic analyses. Mononuclear cells were isolated from peripheral blood or bone marrow samples. This study was approved by the Institutional Review Boards and informed consent was obtained from the patients in accordance with the Declaration of Helsinki. The samples were obtained from Dr Norio Asou from Kumamoto University,

Japan, as well as from Dr Chng Wee Joo from the Department of Hematology-Oncology, National Cancer Institute of Singapore.

2.2. Experimental Procedures

2.2.1. Tissue Culture and Techniques

2.2.1.1. Mammalian cell culture maintenance.

All Cells were cultured in either RPMI 1640, IMDM, α-MEM or DMEM supplemented with heat in-activated Fetal Bovine Serum (FBS), in a humidified atmosphere of 5% CO_2 at 37^0C. Detailed culture conditions and cytokine requirements of the various cell lines are listed in Table 2.13. Cells were split at a ratio of 1:10 every 2 to 3 days.

Table 2.13: List of cell lines and culture medium composition.

Cell Line	Description/ Species	Culture Medium Composition
HL60	FAB-M2/Human	RPMI1640 + 10%FBS
NB4	FAB-M3/Human	RPMI1640 + 10%FBS
Mono-Mac-1	FAB-M5/Human	RPMI1640 + 10%FBS
MV-4-11	FAB-M5/Human	RPMI1640 + 10%FBS
Nomo-1	FAB-M5/Human	RPMI1640 + 10%FBS
SigM5	FAB-M5/Human	IMDM + 20%FBS
THP-1	FAB-M5/Human	RPMI1640 + 10%FBS
BA/F3	Pro-B/ Mouse	RPMI1640 + 10%FBS+10ng/ml rmIL-3
HEK293T	Embryonic Kidney/ Human	DMEM + 10% FBS
K562	CML/Human	RPMI1640 + 10%FBS
U937	Histiocystic Lymphoma/ Human	RPMI1640 + 10%FBS

2.2.1.2. Storage of cells.

Suspension cells were pelleted directly at 200 g for 5 minutes while adherent cells were first trypsinized before pelleting. Cell pellets were resuspended in freezing medium (10% DMSO v/v in FBS) at a density of 1 X

10^6 cells/ml of freezing medium. 1 ml aliquots were stored in polypropylene cryovials and tubes were frozen slowly at 1^0C per minute in -80^0C overnight. Vials were then transferred and stored in -80^0C for short-term storage or in liquid nitrogen for long term storage.

2.2.1.3. Revival of frozen cells.

Frozen cell stocks were thawed rapidly in a 37^0C water bath and transferred to an appropriate volume of culture media (pre-warmed to 37^0C). Cells were pellet at 200 g for 5 minutes and resuspended in fresh culture media to remove traces of DMSO. The cells were then transferred to a sterile culture flask and incubated at 37^0C in a humidified atmosphere of 5% CO_2.

2.2.1.4. Treatment of cells with drug compounds, cytokines and antibodies.

2.2.1.4.1. Treatment of THP-1 cells with AEBSF.

THP-1 cells were seeded at a density of 2 x 10^5 cells/ml and appropriate amounts of either vehicle or AEBSF (to final concentrations of 50, 100, 200 and 400 μM) were added and incubated at 37^0C in a humidified atmosphere of 5% CO_2 for 48 hours before harvesting for protein expression analysis.

2.2.1.4.2. Treatment of THP-1 cells with Genistein.

THP-1 cells were seeded at a density of 2 x 10^5 cells/ml and appropriate amounts of either vehicle or Genistein (to final concentrations of 12.5, 25, 50 and 100 μM) were added and incubated at 37^0C in a humidified atmosphere of 5% CO_2 for 48 hours before harvesting for protein and gene expression analysis.

2.2.1.4.3. Treatment of THP-1 cells with Akti-X.

THP-1 cells were seeded at a density of 2 x 10^5 cells/ml and appropriate amounts of either vehicle or Akti-X (to final concentrations of 1, 2.5, 5 and 10 μM) were added and incubated at 37^0C in a humidified atmosphere of 5% CO_2 for 24 hours before harvesting for protein expression analysis.

2.2.1.4.4. Treatment of THP-1 cells with Kaletra.

THP-1 cells were seeded at a density of 2 x 10^5 cells/ml and appropriate amounts of either vehicle or Kaletra (to final concentrations of 1, 2.5, 5 and 10 μM) were added and incubated at 37^0C in a humidified atmosphere of 5 % CO_2 for 24 hours before harvesting for protein expression analysis.

2.2.1.4.5. Treatment of THP-1 cells with anti-Flt3 antibody.

THP-1 cells were serum starved overnight and seeded at a density of 4 x 10^5 cells/ml in 3 mls of serum free media in a 6-well plate. Anti-Flt3 antibody or control IgG was added in various amounts (1, 0.5, 2.5,5 μg) and cells were incubated for 60 minutes at 37^0C in a humidified atmosphere of 5 % CO_2. Cells were then stimulated with 30 ng/ml of rh-Flt3 ligand for 4 hours before harvesting for protein expression analysis.

2.2.1.4.6. Treatment of BA/F3 cells with rm-Flt3 ligand.

BA/F3 cells which were electroporated with either 2 μg of N-CoR siRNA or 2 μg of control siRNA were allowed to recover in IL-3 containing growth medium for 48 hours to allow for Flt3 receptor expression. Cells were then washed once in 1X PBS, resuspended in IL-3 free culture medium or Flt3

ligand (100 ng/ml) supplemented media and seeded at 2000 cells/100 µl in 96-well plate. Cells were assayed for growth proliferation over duration of 4 days.

2.2.1.4.7. Treatment of HEK293T cells with rh-Flt3 ligand

HEK293T cells were transfected with either 6 µg of MSCV-GFP-Flt3 (WT) expression vector or 6 µg MSCV-GFP-Empty vector and incubated for 24 hours. After which cells were serum starved overnight and stimulated with 30 ng/ml of rh-Flt3 ligand for 4 hours before cells are assayed for SDS-PAGE and Western Blotting Analysis.

2.2.1.5. Transfection of cells.

2.2.1.5.1. Transfection in HEK293T cells using Fugene 6.

HEK293T cells were transfected using the lipid base transfection reagent Fugene 6 (Roche, Germany) according to the manufacturer's instructions. Briefly cells were seeded at 1 x 10^5 cells/ml in a sterile 10 cm TC dish and incubated for 18-22 hours at 37^0C in a humidified atmosphere of 5% CO_2. On the day of transfection, 18 µl of Fugene 6 was mixed in 150 µl of serum free-DMEM and incubated for 5 minutes. 6 µg of DNA was then added and incubated for 15 minutes. The transfection mix was then added drop wise to the cells. Cells were grown for 48 hours before being assayed.

2.2.1.5.2. Transfection in HEK293T cells using Lipofectamine 2000.

HEK293T cells were transfected with Lipofectamine 2000 reagent (Invitrogen, US) according to the manufacturer's protocol. Briefly, cells were seeded into at 1 x 10^5 cells/ml in 3 mls of DMEM in a 6-well plate and grown overnight (until 80-90% confluency).

On the day of transfection, DNA/siRNA and Lipofectamine 2000 were prepared separately in 250 µl of serum free-DMEM and incubated for 5

minutes at room temperature. Diluted DNA was combined with the Lipofectamine 2000 and the mix was incubated for 20 minutes at room temperature. The transfection complexes were added drop wise to the cells and incubated for 4 hours at 37ºC before replacing the medium with fresh DMEM. Cells were then grown for 48 hours before being assayed.

2.2.1.5.3. Transfection in AML cell lines and BA/F3.

The AML cell lines THP-1 and HL60 were transfected via electroporation using the Amaxa Cell line Nucleofector Kit (Amaxa, Cologne, Germany) and the Nucleofector II system. Briefly, cells were pelleted at 90 g for 10 minutes and resuspended in 100 µl of Nucleofector solution. Cells were then electroporated using the Nucleofector II system set to cell line specific programs. Cells were then immediately added to pre-warmed culture media and transferred to a sterile TC dish and grown for 48 hours before being assayed. Cell line specific Nucleofector solution and program requirements can be accessed at the Amaxa website.

2.2.1.5.4. siRNA mediated gene knockdown

All siRNA (Qiagen, Hilden, Germany) were synthesized as fully annealed oligonucleotide duplexes. The lyophilized siRNA were reconstituted in 1ml of sterile water as suggested by the manufacturer. For siRNA-mediated knockdown of N-CoR in HL60 and BA/F3 cells and siRNA mediated Akt knockdown in THP-1 cells, 2 µg of siRNA was transfected by electroporation using the Cell Line Nucleofector kit V (Amaxa, Cologne, Germany) according to the manufacturer's optimized protocol. In case of HEK293T cells, siRNA was transfected using Lipofectamine 2000 (Invitrogen, Carlsbad, CA, USA). A mock siRNA targeting the luciferase sequence, which is not found in the

mammalian genome, was used as control. All siRNA sequences used are depicted in Table 2.10 in section 2.1.3.4.

2.2.2. Protein Assays.

2.2.2.1. Direct Lysis of cells.

Cell lysates were prepared by pelleting cells at 200 g for 5 minutes. Cell pellets were washed using ice cold 1X PBS and was lysed directly with 5X pellet volume of 1X SDS sample buffer (50 mM Tris pH 6.8, 10% Glycerol, 2% SDS, 0.1% Bromophenol Blue, 5% β-mercaptoethanol). Lysates were sonicated briefly at 5W for 10 seconds using the Branson Sonifier150 and this was repeated twice. Cell lysates were then heat inactivated at 50^0C for 10 minutes. Lysates were stored at -80^0C for analysis by SDS-PAGE and Western Blotting.

For primary patient specimens that arrived as frozen cell pellets, the pellets were lysed directly with 2X SDS sample buffer and prepared and stored as mentioned above.

2.2.2.2. *In Vitro* Cleavage Assay

Crude cellular extracts of cell lines and primary patient specimens were prepared in RSB buffer (10 mM Tris pH 8.0, 10 mM NaCl, 3 mM MgCl2, 0.1% NP-40) incubated on ice for 15 minutes and nuclei were removed by centrifugation at 800 g for 5 minutes. N-CoR substrate was prepared from HEK293T cells transfected with N-CoR and PML-RARα expression plasmids in 2X NT buffer (40 mM Tris pH 8.0, 1.2 M NaCl). Optimized cleavage assays were performed at 37^0C in buffer containing 300 mM NaCl, 50 mM Tris pH 8.0. The reaction was stopped by heating the samples at 50^0C in SDS

sample buffer and proteins were resolved with SDS-PAGE and transferred to PVDF membranes for western blotting.

2.2.2.3. Protein Solubility Assay

Cellular extracts were prepared in NET buffer (20 mM Tris pH 8.0, 300 mM NaCl, 1 mM EDTA, 0.5% NP-40, 1 tablet/10 ml Complete Mini protease inhibitor tablet [Roche, Germany]) and rotated at 4^0C for 45 minutes. The insoluble fraction was separated from the soluble fraction by centrifugation at 20000 g for 10 minutes. SDS sample buffer was then added to the fractions and fractions were heat inactivated at 50^0C for 10 minutes. Proteins were resolved with SDS-PAGE and transferred to PVDF membranes for western blotting.

2.2.2.4. Immunoprecipitation

For Immunoprecipitation (IP), 4 X 10^8 cells were pelleted at 200 g for 5 minutes, washed once in ice cold PBS and lysed in 1 ml of IP buffer (20 mM Tris pH 7.4, 300 mM NaCl, 0.5% NP-40, 1 mM EDTA, 200 µM AEBSF, 1 tablet/50 ml Complete protease inhibitor tablet [Roche, Germany], 1 mM NaF, 20 mM β-Glycerolphosphate, 10 ul/ml Phosphatase Inhibitor Cocktail I [Sigma, USA], 10 µl/ml Phosphatase Inhibitor Cocktail II [Sigma, USA]). The lysate was sonicated at 5 W for 10 seconds twice using the Branson Sonifier150. Lysate was then centrifuged at 850 g for 5 minutes and a fraction of the supernatant was taken and inactivated by adding 4X SDS sample buffer to a final concentration of 1X and heated at 50^0C for 10 minutes this will be analyzed by SDS-PAGE and Western Blotting as input controls. The remaining supernatant was then subjected to immunoprecipitation by rotating with 10 µg of anti-N-CoR antibody or 10 µg of normal goat IgG for 2.5 hours

at 4^0C. 50 µl of Protein G sepharose beads (Roche, Germany) resuspended in IP buffer was then added to each reaction and rotated for another 1.5 hours. Protein bound to the Protein G beads were then pelleted at 850 g for 5 minutes. The supernatant was carefully removed and protein bound beads were washed 4 times with IP buffer. Bound protein was released from the beads by addition of 2 X SDS sample buffer and supernatant was collected after centrifugation at 850 g for 5 minutes. The supernatant consisting of mainly immunoprecipitated protein was heat inactivated at 50^0C for 10 minutes and stored at -80^0C for analysis by SDS-PAGE and Western Blotting.

2.2.2.5. *In Vitro* Phosphorylation Assay

HEK293T cells were transfected with pAct-N-CoR-Flag and incubated for 48 hours. Flag-tagged N-CoR was immunoprecipitated from HEK293T cells using the Affinity Flag M2 resin (Sigma Aldrich, MO, USA). Purified flag-tagged N-CoR was eluted from the resin using 3X flag peptide (Sigma Aldrich, MO, USA).

Active Akt kinase was purified from pCFP-Myr-Akt transfected HEK293T cells and immunoprecipitated using anti-pAkt (Ser473) immobilized beads (Cell Signaling Technologies, CA, USA).

In vitro phosphorylation assay was performed using the non-radioactive Akt kinase assay kit (Cell Signaling Technologies, CA, USA) as describe by the manufacturer. Briefly, purified active Akt kinase was resuspended in 50 µl of 1X kinase buffer supplemented with 1 µl of 10 mM and 4 µg purified flag-tagged N-CoR. The mixture was incubated at 30^0C for 30 minutes for the phosphorylation to take place. The reaction was then terminated with 3X SDS sample buffer.

In vitro phosphorylation of N-CoR was analyzed via western blotting assay with anti-phospho Akt substrate (RxRxx pS/pT) antibody. Amount of N-CoR added to the reaction was detected using anti-Flag antibody while Akt kinase was detected using the pAkt (Ser 473) antibody.

2.2.3. Protein expression analysis

2.2.3.1. SDS-PAGE

Cell lysates were resolved on SDS-PAGE. Denaturing polyacrylamide gels of 6, 8 or 10% acrylamide (Components are listed in 2.14) were cast using a mini-Protean gel caster (BioRad). Gels were poured into the caster, overlaid with water and allowed to set for 1 hour. Once set, water was removed and stacking gel (5% acrylamide mix, 125 mM Tris [pH 6.8], 1% SDS, 4 mM EDTA) was poured. Both reservoirs were then filled with 1x SDS-PAGE running buffer (25 mM Tris-Base, 192 mM glycine, 0.1% SDS w/v). Protein samples (Concentration dependent on protein to be visualized) were loaded and run through the stacking gel at 10 mA before separating at 17 mA at 4^0C. Gels were then either stained with Coomassiee Blue staining solution for 30 minutes and destained overnight to visualize total protein or subjected to western blotting.

Table 2.14: Components of Gels used in SDS-PAGE

COMPONENTS	GEL PERCENTAGE (%)		
	6	**8**	**10**
Water (ml)	5.3	4.6	4.0
30% acrylamide mix (ml)	2.0	2.7	3.3
1.5 M Tris-pH 8.8 (ml)	2.5	2.5	2.5
10% APS (µl)	100	100	100
10% SDS (µl)	100	100	100
TEMED (µl)	8	6	4
Total Volume (ml)	10	10	10

2.2.3.2. Western Blotting

Resolved proteins were transferred onto PVDF membrane using the wet transfer system (Bio-Rad, US) in cold 1X transfer buffer (48 mM Tris-base, 37 mM Glycine, 0.037% SDS w/v) with 10% methanol. Transfer was carried out at a constant current of 60 mA for 2.5hrs at 4^0C. Membrane was then blocked for non-specific interactions with 5% skimmed milk powder (Sigma Aldrich, MO, USA) in PBS 0.01% Tween-20 at room temperature for 1 hour. The membrane was then incubated with the primary antibody (*see* Table 2.2 in section 2.1.2.1 for dilution and incubation times). Following 3 washes of 10 minutes each in PBS; 0.01% Tween-20, the appropriate peroxidase-conjugated secondary antibody was added to the membrane for 1 hour at room temperature (concentration specified in Table 2.3 in section 2.1.2.1). Membranes were again washed 5 times for 10 minutes each in PBS 0.01% Tween-20 and finally visualized by using enhanced chemiluminescent reagents (Amersham) and exposure to Fuji X-Ray film. To reprobe the membrane with another primary antibody, antibodies were stripped by

incubating the membrane for 15 to 45 minutes (depending on the antibody) at room temperature in stripping buffer (200 mM glycine, 1% SDS, pH 2.5). The membrane was then re-blocked in 5% skimmed milk before being incubated with a new primary antibody.

2.2.4. Cell Based Assays

2.2.4.1. May-Grunwald-Giemsa Staining

Cells were cytospun onto glass slides at 1000 rpm for 5 minutes. Fixing was then performed using May-Grunwald solution (Merck, Germany) for 5 minutes at room temperature and stained with Giemsa stain diluted in 1XPBS for 30 minutes. Slides were washed with distilled water and cell morphology was observed using light microscopy.

2.2.4.2. Immnofluorescence Staining

Cells were cytospun onto glass slides and fixed with 3% paraformaldehyde at 37^0C and permeabilized with 0.2% Triton-X-100 in PBS for 5 minutes at 4^0C. After blocking with 5% Bovine Serum Albumin (BSA), the cells were stained with primary antibody at 1:100 dilution in 5% BSA for 2 hours followed by fluorescence labeled secondary antibodies at 1:200 dilution in 2.5% BSA for 1 hour. The cell nuclei were then stained with 4', 6-diamidino-2-phenylindole (DAPI) at 1:3000 dilution in 5% BSA for 10 minutes. Slides were visualized using confocal microscopy.

2.2.4.3. Cell Proliferation Assay

The cell proliferation assay was carried out using the Cell Proliferation Kit I [3-(4,5-dimethylthiazol-2-yl)-2,5-diphenyltetrazolium bromide; (MTT)] (Roche, Germany) as described by the manufacturer. Briefly, cells were seeded into 96-well plates at 8 x 10^3 cells per well in 100 µl of culture medium

containing various concentrations of AEBSF, Genistein, Kaletra or Akti-X. The plates were then incubated at 37^0C at 5% CO_2 for the durations stated. After the incubation period, MTT labeling reagent was added and incubated at 37^0C for 4 hours. This was followed by the addition of the solubilization solution and the reaction was then allowed to stand overnight at 37^0C. The spectrophotometric absorbance was measured using a microplate reader (Ultramark, Biorad) at wavelength 595 nm with a reference wavelength of 655 nm. For statistical analysis, the results of the proliferation assays were reported as mean ± SD. Statistical analysis was performed using unpaired t-test. P value less than 0.05 was considered to be statistically significant.

2.2.4.4. Apoptosis Assay

Detection of phosphatidylserine (PS) on the outer leaflet of apoptotic cells was performed using FITC conjugated Annexin V (Pharmingen, San Diego, CA) and Propidium Iodide (Pharmingen, San Diego, CA) according to the manufacturer's recommendations. Briefly, cells were pellet and washed once with ice cold 1X PBS. Cell pellets were then resuspended in 1X Annexin V binding buffer and FITC conjugated anti-Annexin V antibody and Propidium Iodide were added at 1:20 dilution. Mixture was then allowed to incubate for 15 minutes in the dark at room temperature. Flow cytometry was performed using fluorescence activated cell sorting (NUMI core facility and CSI flow Cytometry Unit, National University of Singapore).

2.2.4.5. Determination of Cell Differentiation

THP-1 cells were grown with various concentrations of Genistein or vehicle and incubated for 72 hours at 37^0C at 5% CO_2. Cells were then collected, washed twice with PBS + 0.5% bovine serum albumin and

incubated for 60 minutes on ice in 500 µl of PBS + 0.5% bovine serum albumin with PE conjugated monoclonal mouse anti-human CD14 antibody or control IgG ((Pharmingen, San Diego, CA). Antibody conjugated cells were washed with PBS + 0.5% bovine serum albumin and analyzed using fluorescence activated cell sorting (NUMI core facility and CSI Flow Cytometry Unit, National University of Singapore).

2.2.4.6. Colony Assay

1×10^4 GFP and c-Kit positive cells purified from bone marrow (BM) cells infected with MSCV-IRES-GFP-N-CoR or empty vector were cultured in 35-mm plates in 1 ml Methocult M3131 methylcellulose medium (StemCell Tec., Canada) containing 1% antibiotic-antimycotic supplemented with 10 ng/ml recombinant murine IL-3, 10 ng/ml SCF, 100 ng/ml G-CSF and 10 ng/ml EPO. Morphology of MSCV-IRES-GFP-N-CoR or vector infected cells was determined by May-Grunwald-geimsa staining.

2.2.4.7. Long-Term Culture-Initiating Cell (LTC-IC) Assay

1×10^4 GFP and c-Kit positive cells were cultured for 18 days in a 6-well plate on an OP9 stromal cell layer in 2 ml αMEM medium supplemented with 10% FBS, 1% antibiotic-antimycotic and 10 ng/ml recombinant murine IL-3, 100 ng/ml G-CSF, 10 ng/ml SCF and 10 ng/ml EPO (Pepro Tech EC Ltd). Hematopoietic cells were then harvested and subjected to Wright-Giemsa staining for morphological analysis.

2.2.5. *In vivo* Transplantation Assay in Mice

5 x 10^5 transfected BM cells were transplanted intravenously into sub lethally irradiated C57BL/6 mice (8 Gy). The recipient mice were examined at week 3,6 and 10 for blood cell counts and GFP positivity in peripheral blood.

Phoenix-Eco packaging cell line was kindly provided by A/Prof Motomi Osato (Cancer Science Institute, Singapore).

2.2.6. Gene expression analysis

2.2.6.1. Reverse Transcription PCR (RT-PCR) analysis

Total RNA was isolated using the RNeasy® Mini Kit protocol for isolation from mammalian cells using a table top centrifuge (Qiagen GmBH, Hilden, Germany). Briefly, Cells were lysed using 350 µl of Buffer RLT which is a highly denaturing guanidine-thiocynate containing buffer (which inactivates RNases) supplemented with 0.01% 2-mercaptoethanol using gentle syringing (5 times through a blunt 20-guage needle). Next 350 µl of 70% ethanol was added and sample was mixed by gentle pipetting. The sample was then applied to the RNeasy spin column for binding of the RNA to the resin. The resin was washed with DNase1 containing buffer RW1 to remove protein and DNA contaminants. The resin was again washed with ethanol containing buffer RPE and RNA was eluted from the resin using 30 µl of DEPC treated water.

From each sample, 2 µg of RNA was aliquoted into a sterile microcentrifuge tube with 3 pmoles of oligo-dT (18-mer) and DEPC-treated water added to a final volume of 21 µl. The mixture was incubated at 65°C for 15 minutes and immediately quenched on ice. A mastermix of 10 µl of 5 X RT buffer, 1 µl of 25 mM dNTPs, 0.5 µl of RNasin Inhibitor, 1 µl of murine reverse transcriptase and sterile water was prepared to a total volume of 29 µl for each sample. The mastermix was added to the RNA and mixed. The sample was incubated at 42°C for 1 hour for the generation of cDNA. PCR amplification was carried out in 50 µl volumes (1 µl of 10 X or 100 X diluted

template, 1X PCR reaction buffer, 200 nM of each dNTP, 0.8 μM of each primer and 1.5 units of DNA polymerase were used for each reaction). List of genes and their corresponding primers used are listed in Table 2.7 in section 2.1.3.1.

Gene expression analysis was carried by agarose gel electrophoresis where PCR products were resolved in 1% w/v agarose gel (1 g of electrophoretic grade agarose powder in 100 ml 1X TAE buffer [40 mM Tris-acetate (pH 7.8), 1 mM EDTA]) stained with Gel Red (Life Technologies, Delhi, India) at a 1:10000 dilution and expression levels visualized using Trans UV on the Gel Doc System (Bio-Rad, CA, USA).

2.2.6.2. Real time PCR (qRT-PCR) analysis

For cell lines, total RNA was isolated using the RNeasy Mini Kit (Qiagen GmBH, Hilden, Germany). From each sample, 2 μg of RNA was converted into cDNA as described in section 2.2.6.1.

For analysis of gene expression normal mouse hematopoietic cells, each type of hematopoietic cells was purified from mouse bone marrow cells by FACS using cell specific antibodies. About 5000 cells from each population were lysed using Trizol, and total RNA was purified according to the manufacturer's instructions (Life Technologies, Rockville, MD). First-strand cDNA was synthesized using SMART-PCR cDNA Synthesis Kit (Clontech).

qRT-PCR analysis was carried out using the Taqman® Gene Expression Assay System (Applied Biosystems, CA,USA) and C_t values were recorded using the ABI Prism 7300 Real Time PCR system (Applied

Biosystems, CA, USA). The PCR reaction and PCR conditions were as follows,

Table 2.15: qRT- PCR Reaction set up using the Taqman® Gene Expression Assay System.

Component	Volume used per reaction (µl)
2X Taqman Universal PCR master mix	12.5
20X Primer Mix	1.25
Nuclease Free Water	10.25
cDNA	1
Total Volume	25

Table 2.16: qRT-PCR conditions using the ABI Prism 7300 system.

Step	Temperature (^{0}C)	Time	Number of Cycles
Initial denaturation	95	10 min	1
Denaturing	94	15 secs	40
Annealing	60	1 min	
Elongation	60	10 mins	1

For gene expression analysis in human leukemic cell lines, list of genes and assay used are listed in Table 2.8 in section 2.1.3.2. Expression of the housekeeping gene HPRT was used as the endogenous control.

For gene N-CoR and Flt3 gene expression analysis in mouse hematopoietic cells, the Taqman® Gene expression Assays (Mm 00448681_m1 for N-CoR and Mm00439016_m1 for Flt3) were used and expression of housekeeping gene GAPDH was used as an endogenous control.

Analysis of the data was carried out as follows.

For gene expression in cell lines, data was analyzed using the comparative C_t method where the cell line HL60 was used as the reference sample and the HPRT gene was used as the endogenous gene control.

For gene expression in mouse hematopoietic cells, the same comparative C_t method was applied with the expression levels in the total

bone marrow fraction used as the reference sample and the expression of the GAPDH gene used as the endogenous gene control.

Briefly, in qRT-PCR the cycle number at which the increase in fluorescence (and there for the amount of cDNA) is logarithmic. The point at which the fluorescence crosses the preset threshold is called the C_t. In the comparative C_t method, relative gene expression is compared based on an assumption that the primer efficiencies are relatively similar. In this method the need to generate a standard curve is omitted. The Comparative C_t method involves comparing the C_t values of the samples of interest with a reference sample or calibrator .The C_t values of both the reference sample and the samples of interest are normalized to an endogenous housekeeping gene. The comparative C_t method is also known as the $2^{-\Delta\Delta Ct}$ method, where

$$\Delta\Delta C_t = \Delta C_{t,sample} - \Delta C_{t,reference}$$

Here, $\Delta C_{T,sample}$ is the C_t value for any sample normalized to the endogenous housekeeping gene and $\Delta C_{t,\ reference}$ is the C_t value for the reference sample also normalized to the endogenous housekeeping gene. Data representation is in the form of a bar graph plotted on a log scale with a base of 10, where expression level in the reference sample for all genes will be set to 0 while genes which are up-regulated relative to expression levels in the reference sample will be given a positive value and those which are repressed relative to expression levels in the reference sample will be given a negative value.

Raw Ct values which were undetermined were set to 40. Data represented is the average obtained from 3 independent experiments.

2.2.7. Promoter Studies

2.2.7.1. Dual Luciferase Reporter Assay

For analysis of N-CoR repression of the Flt3 promoter, suspension leukaemia cell lines HL60, THP-1, K562 and U937 were co-transfected with 1 μg of Flt3 full-length promoter / firefly luciferase reporter plasmid or promoter-less pGL3-basic vector and 5 ng of CMV / renilla luciferase plasmid (as internal control to normalize firefly luciferase signal) by electroporation, using the Cell Line Nucleofector kit (Amaxa, Cologne, Germany). The cells were harvested for luciferase assay, 48 hours post-electroporation, as described by the Dual Luciferase Assay kit (Promega, WI, USA).

In this Assay system, the activities of firefly (*Photinus pyralis*) and *Renilla* (*Renilla reniformis* or sea pansy) luciferases are measured sequentially from a single sample. The firefly luciferase reporter is measured first by adding 20 μl of Luciferase Assay Reagent II (LARII) to 20 μl of cell lysate to generate a signal which lasts for at least 1min. After quantification of the firefly luminescence using the luminometer, this reaction is quenched via the addition of 100 μl of the Stop & Glo® Reagent to the same sample and a second reading which records the *Renilla* luciferase activity is then taken. For data analysis, the ratio between the readings for the firefly luciferase activity and the *Renilla* activity is taken and normalised to the readings obtained from the corresponding control samples expressing the promoter-less pGL3-basic vector.

Adherent HEK293T cell line was co-transfected with 50 pmol of N-CoR-targeting siRNA, 1 μg of Flt3 full-length promoter / firefly luciferase reporter plasmid or promoter-less pGL3-basic vector, 5 ng of CMV / renilla

luciferase plasmid and various dosages of pAct-Flag / N-CoR or its empty vector, using Lipofectamine 2000 (Invitrogen, Carlsbad, CA, USA). The cells were harvested and reporter activity determined 72 hours post-transfection, as specified by the Dual Luciferase Assay kit.

2.2.7.2. ChIP Assay

Chromatin Immunoprecipitation (ChIP) was carried out with the commercially available ChIP-IT kit (Active Motif, Carlsbad, CA, USA) according to the manufacturer's instructions. In this method, intact cells are fixed using formaldehyde, which cross links and preserves protein-DNA interactions. The DNA is then sheared into small uniform fragments via sonication at 5 W using the Sonifier150. Prior to precipitation, an aliquot of the chromatin isolated from HL60 was taken as input DNA control. Chromatin linked to N-CoR was precipitated with either 3 μg of ChIP-grade N-CoR C-20 antibody (Santa Cruz Biotechnology, CA, USA) or 3 μg of non-specific goat IgG (Santa Cruz Biotechnology, CA, USA).

Following immunoprecipitation, cross-linking is reversed and the proteins are removed by Proteinase K treatment and the DNA is purified as described by the kit's manual. The purified immunoprecipitated chromatin was subject to RT-PCR analysis, using the Accuprime Taq polymerase system (Invitrogen, Carlsbad, CA, USA). The sequences of the primers used in ChIP assay are presented in Table 2.9 in section 2.1.3.3. The priming site for the ChIP primers is highlighted in Figure 2.1.

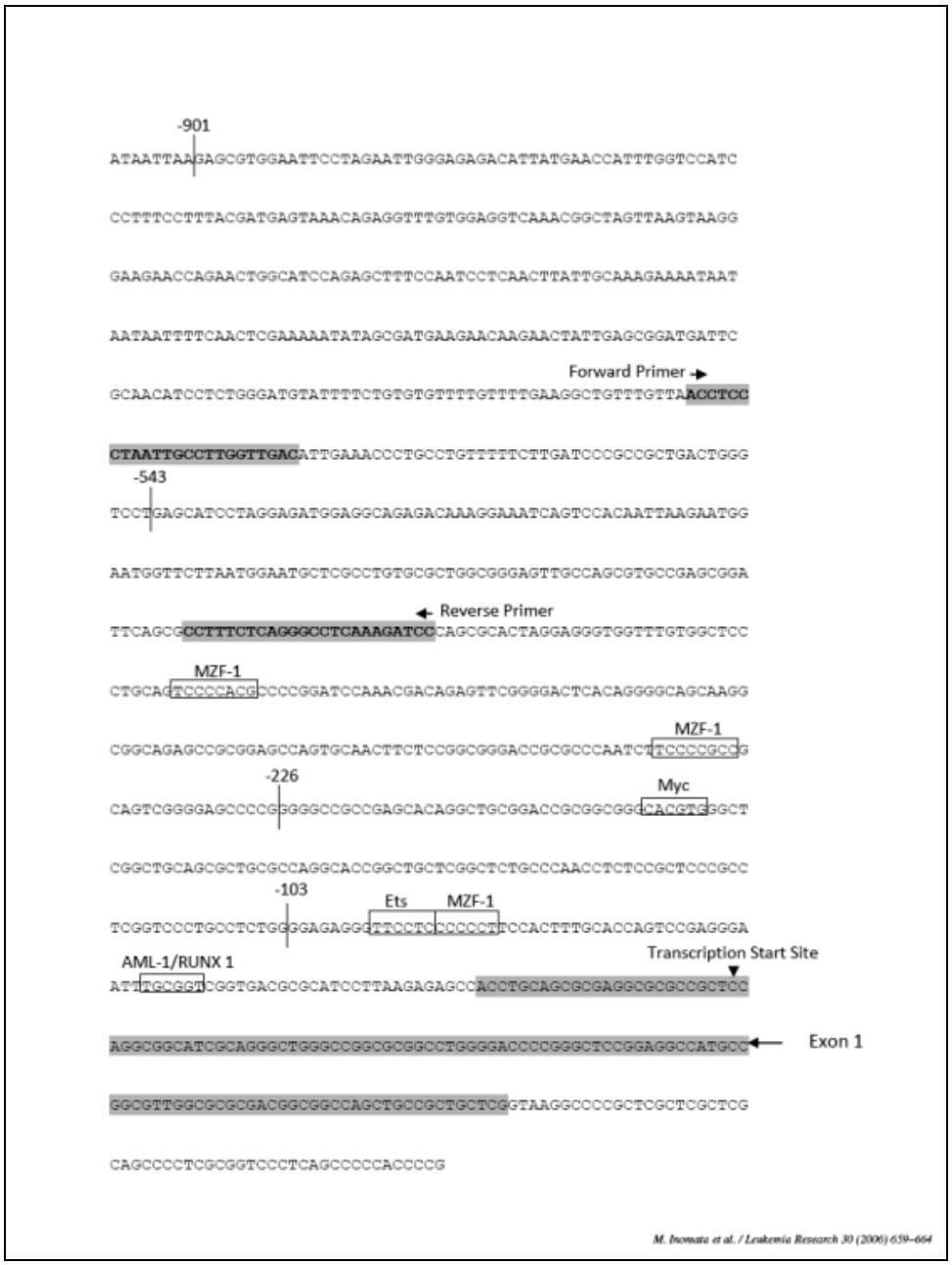

Figure 2.1: Flt3 promoter sequence and ChIP primers priming sites. The Flt3 promoter sequence up to -901 base pairs upstream of the transcriptional start site in exon 1(highlighted). The forward and reverse primers are indicated in bold font and grey highlights. The primers prime in a region upstream of known transcription factor binding sites which are indicated in boxes.

2.2.8. Creation of N-CoR mutants.

2.2.8.1. Site Directed mutagenesis

Identification of Akt phosphorylation consensus site RxRxx S/T- bulky hydrophobic in the human N-CoR sequence was identified using the online motif identification software Human Protein Kinase Database.

Site directed mutagenesis of pAct-N-CoR-Flag to generate the mutant which cannot be phosphorylated and the phosphomimetic mutants were carried out using the GeneTailor™ Site-Directed Mutagenesis System (Invitrogen, CA, USA) using the primers listed in Table 2.11 in section 2.1.3.5. A brief workflow of the GeneTailor™ Site-Directed Mutagenesis System is outlined in figure 2.2.

Briefly, the plasmid was first methylated using 100 ng of plasmid DNA, 1.6 µl of Methylation buffer, 1.6 µl of 10 X Sadenosylmethionine (SAM), 1.0 µl of DNA methylase (4 U/ul) and sterile water at 37^0C for 1 hour. Next the mutagenesis reaction was carried out using 2.5 µl of methylated plasmid, 5 µl of 10X High Fidelity PCR buffer, 0.3 mM of dNTP, 50 mM Magnesium Sulphate, 0.3 µM each of the mutagenic forward and corresponding complementary reverse primer and 0.3 µl of Platinum® *Taq* High Fidelity polymerase (5 U/µl) and sterile water added to a final volume of 50 µl. The amplification reaction was carried out as depicted Table 2.17.

Table 2.17: PCR conditions for mutagenesis reaction.

Step	Temperature (^{0}C)	Time	Number of Cycles
Initial denaturation	94	2 min	1
Denaturing	94	30 secs	30
Annealing	55	30 secs	
Extension	68	12 min (1min/Kb)	

Final Extension	68	10 mins	1

After the reaction, 10 µl of the product was analyzed using 0.8% agarose gel to check of mutagenesis efficiency.

2.2.8.2. Gel Extraction

To improve on transformation efficiency, mutagenesis product was resolved in 0.8% agarose gel and the DNA band of interest was excised under UV light with a clean scalpel. This was followed by the removal of excess gel to reduce gel size and purified using the QIAGEN QIAquick®Gel Extraction Kit.

The gel slice was weighed and 3 volumes of buffer QG was added to 1 volume of gel and solubilized at 50^0C for 10 minutes. 1 volume of isopropanol was then added to the solubilized DNA. The mixture was then added to the QIAquick spin column. After binding to the resin, the resin was washed with ethanol containing wash buffer PE. Bound DNA was eluted with 15µl of sterile water and used for transformation.

2.2.8.3. Transformation.

One vial of DH5ά™-T1® *E. Coli* competent cells (provided with the mutagenesis system) for each reaction was thawed on ice for 5 minutes. Purified DNA was pipetted into the competent cells and mixed by tapping gently. The vial was incubated on ice for 7 minutes and further incubated for exactly 30 seconds at 42°C. The vial was immediately placed on ice for 1 minute before the addition of 200 µl of pre-warmed SOC medium (2% bacto-tryptone, 0.5% bacto-yeast extract, 0.05% sodium chloride and 20 mM glucose) to each vial. The vial was placed in a shaking incubator at 30°C for 1 hour at 225 rpm. 100 µl from each transformation

vial was then spread onto separately labeled LB agar plates with 50 μg/ml of ampicillin. The agar plates were inverted and incubated at 37°C overnight. The following day, a single and well-isolated colony was picked and inoculated into 5 ml of LB broth (1% bacto-tryptone, 0.5% bacto-yeast extract and 1% sodium chloride) with 50 μg/ml of ampicillin in 14 ml bacterial culture tubes. The inoculated culture was then incubated for 14 to 16 hours at 37 °C. 0.5 ml of overnight culture was used to prepare glycerol stock by addition of 0.5 ml of 80% glycerol (v/v) and stored at -80^{0}C while the remaining culture was used for plasmid purification.

2.2.8.4. Plasmid purification

Plasmid purification from 5 ml overnight cultures was carried out using the QIAprep® Miniprep Kit. Bacterial cells were pelleted at 6800 g for 3 minutes at room temperature. Pelleted bacterial cells were then resuspended in 250 μl of RNase A containing buffer P1. 250 μl of the lysis buffer P2 was then added to lyse the bacterial cells. 350 μl of the pre-chilled neutralizing buffer N3 was than mixed immediately and the mixture centrifuged for 10 minutes at 17900 g. The supernatant was then applied to the QIAprep spin column to allow for plasmid DNA binding to the resin. The resin was then washed with 0.5 ml of buffer PB to remove trace nuclease activity. The resin was washed again with 0.75 ml of ethanol containing buffer PE. Plasmid DNA was eluted with 30 μl of sterile water and subjected to analysis by restriction enzyme digestion.

2.2.8.5. Determination of successful mutants.

Purified plasmid DNA was then subjected to restriction enzyme digestion by XbaI at 37^{0}C for 2 hours to identify clones which display the

correct fragment sizes after digestion (one 11.3 kbp fragment and one 750 bp fragment). Clones with the correct digestion pattern were then sent for DNA sequencing using the primers in Table 2.12, section 2.1.3.5. (Sequencing was done at the DNA sequencing service provided by AIT Biotech Singapore).

2.2.8.6. Large Scale Plasmid purification.

For large-scale plasmid purification, glycerol stock prepared from colonies which carried successful mutants was first streaked onto LB agar plates with 50 μg/ml of ampicillin and incubated at 37^0C overnight. The following day, a single and well-isolated colony was picked and inoculated into 5 ml of LB broth (1% bacto-tryptone, 0.5% bacto-yeast extract and 1% sodium chloride) with 50 μg/ml of ampicillin in 14 ml bacterial culture tubes. The inoculated culture was then incubated for 4 to 6 hours at 37°C with agitation at 225 rpm after which 0.5 ml of the culture was added to 200 ml of LB broth containing 50 μg/ml of ampicillin in a large conical flask. The culture was then incubated overnight at 37°C with agitation at 225 rpm.

Plasmid DNA was then prepared from the large culture using the QIAGEN® Plasmid Purification Maxi Kit. Bacterial cells were pelleted at 6000 g for 15 minutes at 4^0C. The bacterial pellet was then resuspended in 10 ml of RNase A containing buffer P1. Cells are then lysed by adding 10 ml of the lysis buffer P2. 10 ml of pre chilled buffer P3 was then added and the reaction incubated on ice for 20 minutes to allow genomic DNA, proteins and cell debris to precipitate. Precipitated contaminants were then removed by centrifugation at 20000 g for 30 minutes at 4^0C. The

supernatant was collected and centrifuged again at 20000 g for 15 minutes at 4^0C. The supernatant was then applied to the QIAGEN-tip column to allow the plasmid DNA to bind to the resin. The column was then washed with buffer QC to remove the trace contaminants. The DNA was then eluted from the resin using 15 ml of the elution buffer QF and precipitated by adding 10.5 ml (0.7 volumes) of room temperature isopropanol mixed and centrifuged immediately at 15000 g for 30 minutes at 4^0C. The DNA pellet was then washed with 5 ml of 70% ethanol and centrifuged at 15000 g for 10 minutes at 4^0C. The supernatant was then carefully decanted and the pellet was air dried for 5 to 10 mins and redissolved in 500 µl of sterile water. Quality and quantity of the DNA was determined using the photo spectrometer and DNA aliquoted and stored in -20^0C for further use.

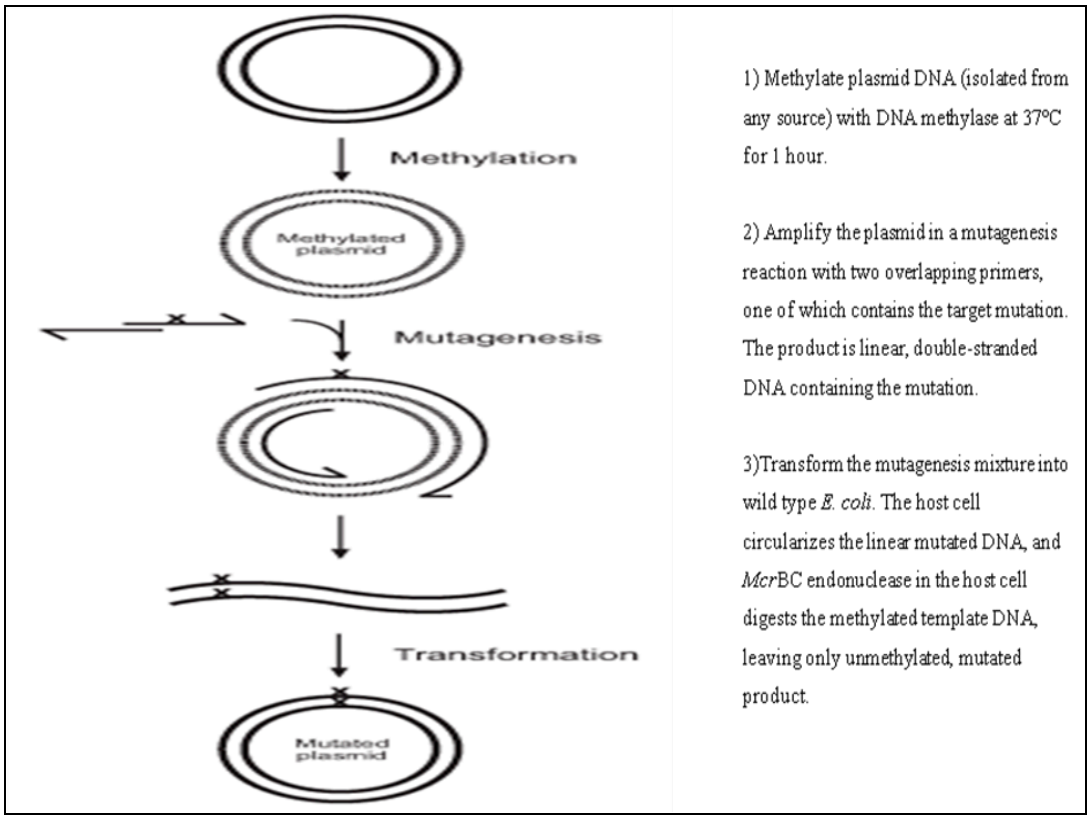

Figure 2.2: Workflow of the GeneTailor™ Site Directed Mutagenesis System. (Reproduced with permission from Invitrogen Singapore Pte Ltd.)

CHAPTER 3

Results

3. RESULTS

3.1. Akt induced N-CoR Phosphorylation is linked to its misfolded conformation dependent loss in Acute Monocytic Leukemia (AML)-M5 subtype.

3.1.1. N-CoR is processed by an APL-like aberrant protease activity in AML-M5 cells.

Recently our laboratory reported a role for the misfolded conformation dependent loss (MCDL) of N-CoR protein in the malignant growth and transformation of APL cells[58,62,63]. However the molecular mechanisms underlying the misfolding of N-CoR and its implications in other AML subtypes are still unclear. Thus in an attempt to investigate if a similar mechanism contributed to the malignant growth and transformation of leukemic cells in other AML subtypes, the status of N-CoR protein in selected commercially available AML derived human leukemia cell lines was first determined.

In this initial screening, an APL-like loss of N-CoR was observed in multiple leukemic cell lines derived from Acute Monocytic Leukemia, an AML subtype designated as AML-M5 in the FAB (French American and British) classification. As previously observed in the APL derived NB4 cell line, multiple AML-M5 derived leukemic cell lines contained a cleaved N-CoR fragment of approximately 100kDa. This fragment was most likely generated from the proteolytic processing of full length N-CoR protein as no intact full length protein was detected in any of these AML-M5 cells (Fig. 3.1). In contrast, an intact N-CoR protein of about 270 kDa was observed in U937, a monocytic cell line derived from histiocytic lymphoma; and in HL60,

an AML-M2 derived cell line (Fig. 3.1). This absence of full length N-CoR in AML-M5 derived cells was not a result of N-CoR mRNA down regulation as levels of N-CoR transcript in the AML-M5 derived cells was not significantly lower compared to the levels found in HL60 cells (Fig. 3.2A and B), suggesting that the lack of N-CoR expression in AML-M5 was due to post-translational processing.

Next, to determine if an APL-like aberrant protease activity was also involved in the processing of N-CoR protein in these AML-M5 cells, an optimized N-CoR cleavage assay was performed. In this assay, cytosolic extracts of AML-M5 (THP-1 and Nomo-1) or non-AML-M5 (U937) cells was incubated with flag-tagged N-CoR protein ectopically expressed in HEK293T cells. The processing of N-CoR protein was thereafter determined using the anti-Flag antibody in western blotting assay. As shown in figure 3.3, incubation of flag-tagged N-CoR protein with the extract of THP-1 cells generated a cleaved 100kDa N-CoR fragment which was identical in size to the cleaved N-CoR fragment found in the endogenous N-CoR protein profile of THP-1 cells (Fig. 3.3A, lane 2). Similarly, Nomo-1 cell extract contained an activity which completely digested full length N-CoR protein, however in this instance no cleaved N-CoR fragment was generated (Fig. 3.3A, lane 4). This was consistent with the endogenous N-CoR protein profile observed in Nomo-1 cells, where the 100kDa cleaved N-CoR band was not detected. In contrast, flag-tagged N-CoR incubated with the extract of U937 cells under identical assay conditions was not digested. This suggested that U937 cells lacked the N-CoR cleaving activity found in THP-1 or Nomo-1 cells (Fig. 3.3, lane 6). The N-CoR cleaving activity detected in the extracts of THP-1 and Nomo-1

cells was found to be completely deactivated by boiling, indicating the probable involvement of a heat-labile protease (Fig. 3.3A, lanes 3 and 5). A THP-1-like N-CoR cleaving activity was also found in three other AML-M5 derived cells namely MM1, MV-4-11 and SigM5 (Fig. 3.3B). As observed in the AML-M5 derived cell lines, leukemic cells obtained from four out of five histologically confirmed primary human AML-M5 specimens contained an N-CoR cleaving activity similar to that of either THP-1 or Nomo-1 cells (Fig. 3.3C). In contrast, no N-CoR cleaving activity was detected in primary human leukemia cells derived from the AML-M1 subtype (Fig. 3.3C, third panel). The N-CoR loss in THP-1 cells was also observed to be effectively blocked by AEBSF, a broad spectrum protease inhibitor, and Kaletra, a clinical grade HIV protease inhibitor, resulting in the stabilization of full length N-CoR protein (Fig. 3.4A), while no N-CoR stabilization was observed with the proteasome inhibitor MG132 (Fig 3.4B). This suggested that N-CoR cleaving activity present in AML-M5 cells was most likely due to an aberrant protease activity.

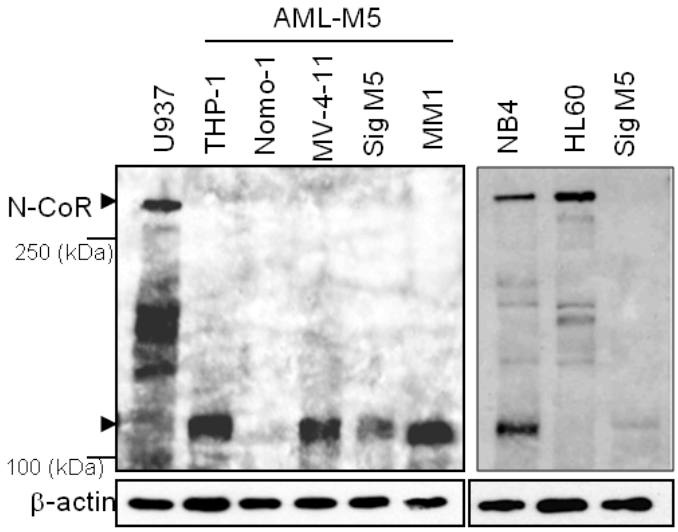

Figure 3.1. Selective loss of N-CoR protein in AML-M5 derived cell lines. An aliquot of whole cell extract prepared from various AML derived cell lines as mentioned on the top of each lane was resolved in SDS-PAGE and stained with anti-N-CoR antibody. N-CoR was found to be selectively loss in multiple cell lines derived from AML-M5.

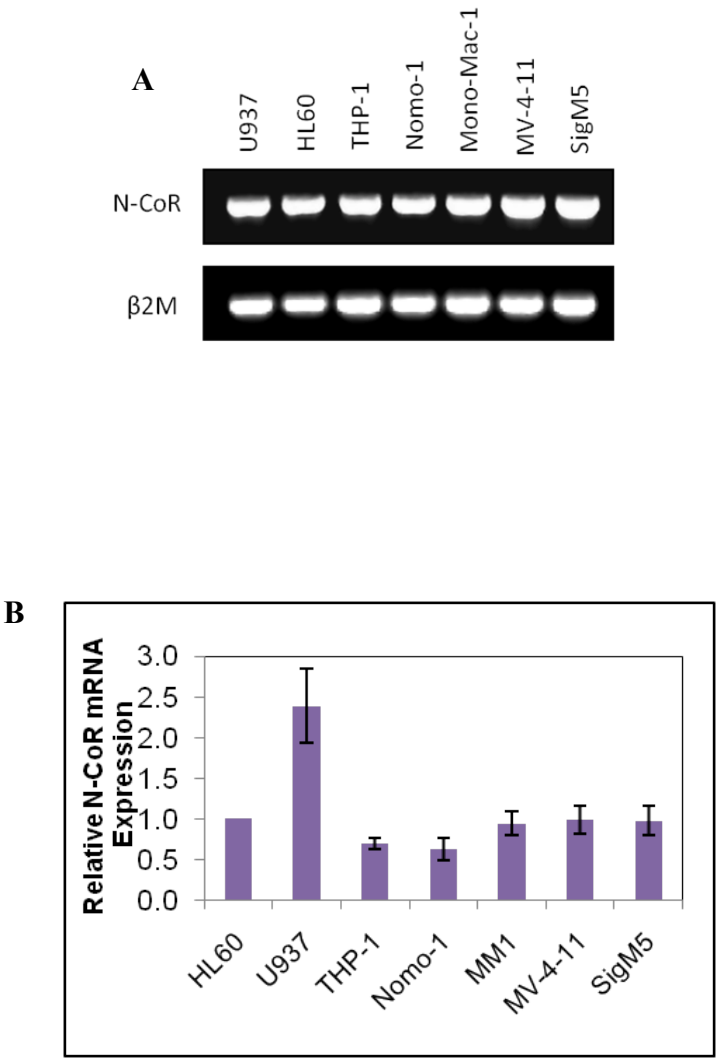

Figure 3.2. Loss of N-CoR protein in AML-M5 cells was a post transcriptional event. N-CoR loss in AML-M5 is not due to any significant down-regulation of N-CoR transcript levels as determined via semi-quantitative PCR (A) and real time PCR analysis (B).

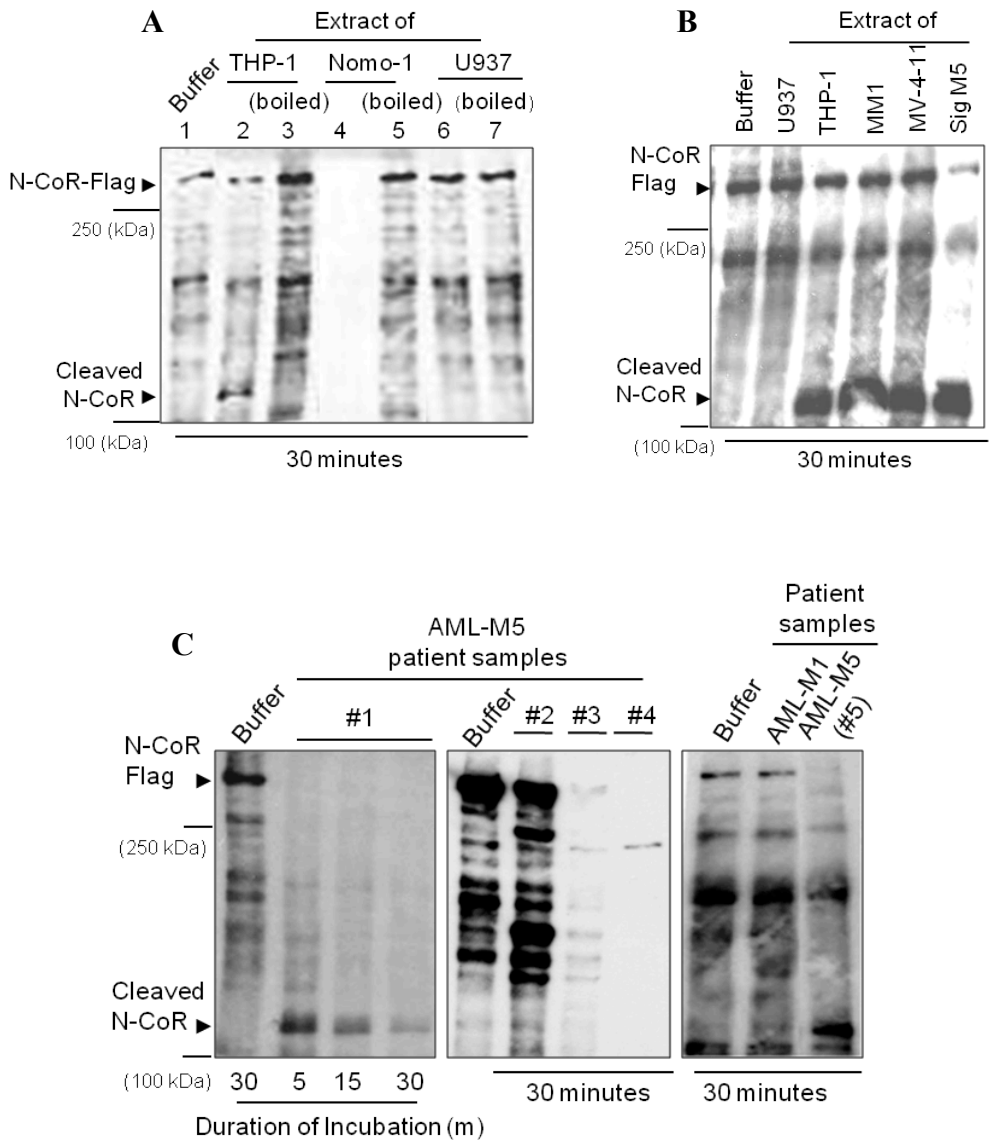

Figure 3.3. AML-M5 contained a heat-labile N-CoR cleaving activity. (A) AML-M5 cells contain a N-CoR cleaving activity. An aliquot of flag-tagged N-CoR protein was incubated with the extract of THP-1 (lanes 2, 3), Nomo-1 (lanes 4, 5), or U937 (lanes 6, 7) cells, and presence of N-CoR cleaving activity in the respective extract was determined by the generation of a 100 kDa cleaved N-CoR fragment (THP-1 cells) or cleavage of full length N-CoR protein (Nomo-1 cells) in western blotting assay with anti-Flag antibody. Cellular extract in lanes (3, 5 and 7) marked as "boiled" were pre-heated at 100^0C for 10 minutes. In the lanes labeled as "buffer", equal volume of buffer lacking cell extract was used. (B) AML-M5 cells of varied genetic background harbor identical N-CoR cleaving activity. N-CoR cleavage assay was performed using an aliquot of whole cell extract of various AML-M5 cells as mentioned on the top each lane. (C) Primary human AML-M5 specimens contain N-CoR cleaving activity. Flag-tagged N-CoR protein was incubated with the extract of five independent primary AML-M5 specimens for the duration as mentioned at the bottom of each panel, and level of N-CoR digestion was determined in western blotting assay with anti-Flag antibody. In lane labeled as "buffer", equal volume of buffer lacking cell extract was used. Extract of a primary AML-M1 specimen was used as control (2nd lane of third panel).

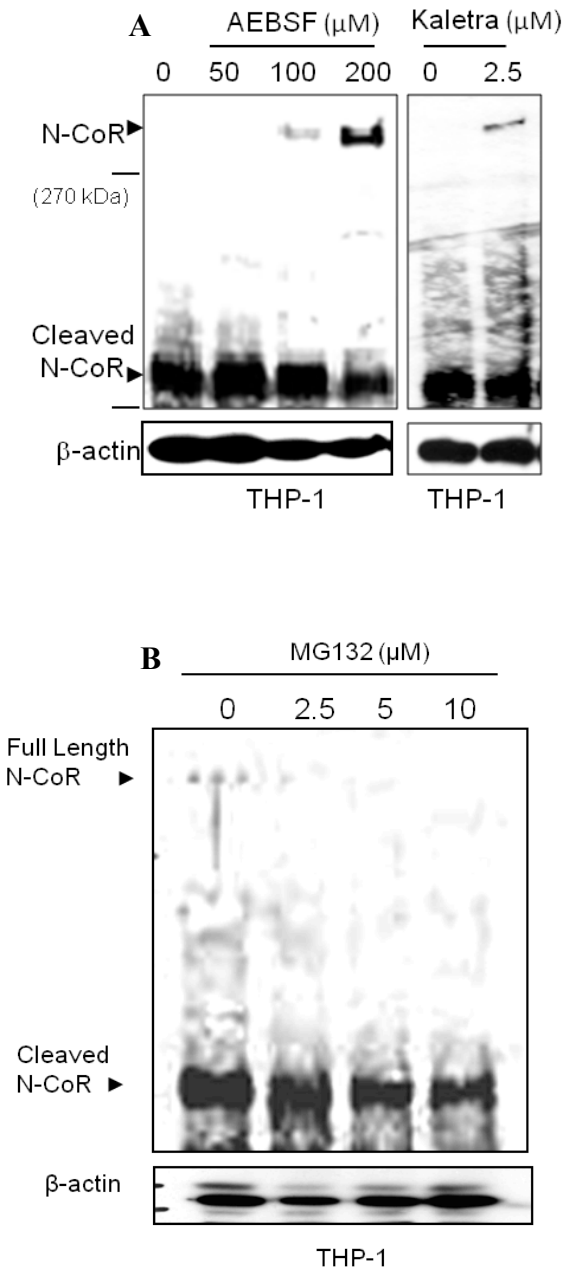

Figure 3.4. Cleaving activity found in AML-M5 was mainly protease mediated. (A) AEBSF and Kaletra abrogated N-CoR cleaving activity in AML-M5. Level of full length endogenous N-CoR protein in THP-1 cells after treatment with the broad spectrum protease inhibitor AEBSF or Kaletra for a duration of 48hours, as determined by western blotting assay. The doses of AEBSF used are indicated at the top of each lane. AEBSF stabilized endogenous full length N-CoR in a dose dependent manner. (B) No stabilization of endogenous full length N-CoR was observed in THP-1 cells after treatment with the proteasome inhibitor MG132 in a similar fashion.

3.1.2. AML-M5 cells harbor the misfolded N-CoR protein.

The N-CoR loss observed in AML-M5 cells was thought to be triggered by the misfolding of N-CoR protein as reported previously in APL derived cells[58,63]. In its native conformation, N-CoR is a detergent soluble protein which preferentially localizes to the nucleus in a majority of mammalian cells. In contrast, misfolded and unstable N-CoR protein found in APL cells was detergent insoluble, largely localized to the ER (endoplasmic reticulum) and linked to the amplification of ER stress [58,62,63]. The misfolding of N-CoR protein was significantly inhibited by Genistein, a tyrosine kinase inhibitor from soy, but not by AEBSF, although both of these agents could block its loss in APL derived cells with equal efficiency [58]. Given these findings, experiments were designed and carried out to explore if N-CoR degradation in AML-M5 cells was also due to a misfolded conformation.

First, to determine if Genistein was able to block N-CoR loss in AML-M5, THP-1 cells was treated in the same manner as described previously in APL[58]. Here, it was observed that, Genistein stabilized N-CoR protein in a dose dependent manner (Fig. 3.5A). In THP-1 cells, the Genistein-stabilized N-CoR was mostly detergent soluble (S), suggesting a return of misfolded N-CoR to its native conformation after treatment (Fig. 3.5B, lane 5). In contrast, a significant portion of N-CoR stabilized by AEBSF appeared as a high molecular weight (HMW) N-CoR protein band which was detergent insoluble (I) (Fig. 3.5B, lane 4), suggesting that AEBSF stabilized N-CoR was largely misfolded. The HMW detergent resistant N-CoR band observed in AEBSF treated THP-1 cells was most likely resulted from post-translational modifications and covalent linkages of other cellular proteins to the misfolded

N-CoR. Under identical assay conditions, the relative solubility or insolubility of beta actin, a reference protein, was hardly affected (Fig. 3.5B, middle panel). Consistent with the findings of the solubility assay, a significant portion of N-CoR in the AML-M5 derived cell lines THP-1, MV-4-11 and MM1 was found to be localized in the cytosol; while in U937 and HL60 cells, N-CoR was mostly confined to the nucleus (Fig. 3.6A). Flag-tagged N-CoR, which was preferentially localized to the nucleus of HEK293T cells when expressed alone, was found to be translocated to the cytosol when co-expressed with MLL1-AF9, the fusion oncogene linked to the transformation of THP-1 and MM1 cells (Fig. 3.6B). After Genistein treatment, the cytosolic N-CoR was observed to be re-localized to the nucleus of THP-1 cells (Fig. 3.6C). These data indicate that in AML-M5 cells, N-CoR displayed distinctive signs of misfolding.

Next to investigate if this misfolded N-CoR resulted in the amplification of ER stress in AML-M5, ER localization and the effect of misfolded N-CoR on the expression level of the ER stress marker PDI was analyzed. It was observed that in the cytosol of THP-1 cells, a significant portion of N-CoR protein co-localized with the ER resident proteins PDI and GRP78/BiP (Fig. 3.7), and the level of ER stress in AML-M5 cells was also significantly higher as indicated by the higher levels of PDI expressions across all AML-M5 cell lines when compared to non-AML-M5 derived cell lines (Fig. 3.8A). These observations indicated a role of ER localized misfolded N-CoR in the amplification of ER stress. Moreover, AEBSF effectively increased HMW PDI levels, indicating an amplification of ER stress after AEBSF

treatment. In contrast, Genistein treatment caused a noticeable reduction in ER stress levels (Fig. 3.8B).

Taken together, these findings suggested that N-CoR degradation in AML-M5 leukemic cells was most likely due to a misfolded protein conformation which was linked to the selective amplification of ER stress in these cells.

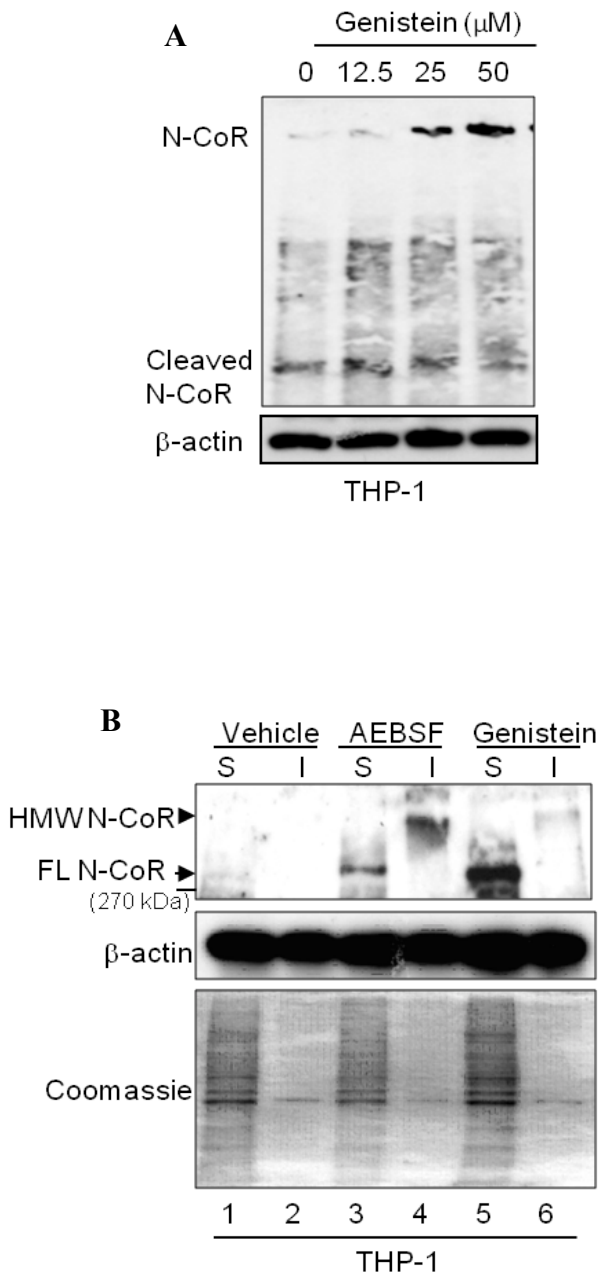

Figure 3.5. Native N-CoR conformation could be rescued by Genistein but not by AEBSF. (A) Level of full length and cleaved N-CoR protein in THP-1 cells treated with Genistein in a dose dependent manner was determined in western blotting assay using N-CoR antibody. (B) Relative solubility/insolubility of N-CoR protein in AEBSF or Genistein treated THP-1 cells was determined by protein solubility assay. Soluble (S) and insoluble (I) fractions of AEBSF- or Genistein-treated THP-1 cells were separated by high speed centrifugation and N-CoR level in each fraction was determined by western blotting assay using anti-N-CoR antibody. A HMW (high molecular weight) variant of N-CoR protein, which was part of insoluble fraction, was detected only in AEBSF treated cells. The relative solubility/insolubility of β-actin in each fraction was used as control. The level of total of protein in each fraction was determined by coomassiee blue staining.

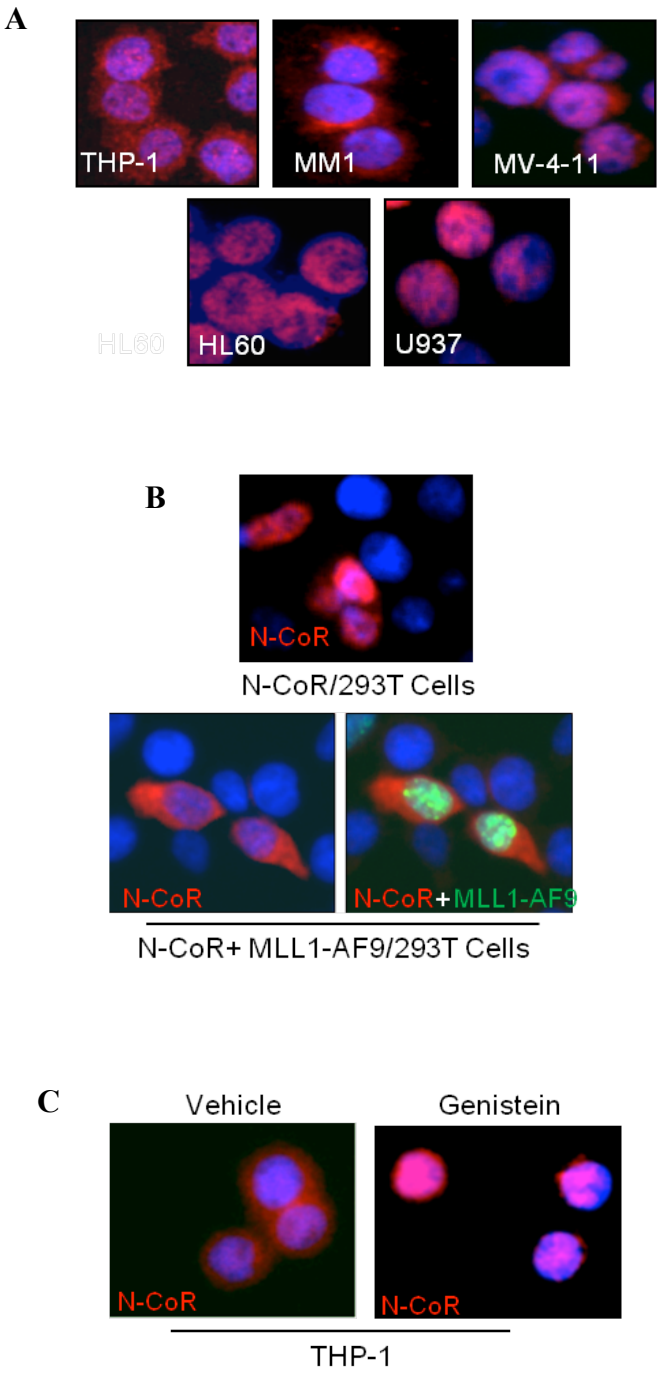

Figure 3.6. N-CoR localization was mainly cytosolic in AML-M5 cells and nuclear localization was restored by Genistein. (A) Subcellular distribution of N-CoR (red signals) in AML-M5 derived cell lines (THP-1, MV4-11 and MM1) and non-AML-M5 derived cell lines HL60 and U937 was determined by staining the cells with anti-N-CoR antibody and florescence labeled secondary antibody. Nucleus was stained with DAPI (blue signals). The signals were analyzed by confocal microscopy. (B) Subcellular distribution of Flag-tagged N-CoR (red signal) expressed alone (upper panel) or with MLL1-AF9 (green, lower panel) in HEK293T cells was determined by confocal microscopy. DNA was stained with DAPI (blue signal). (C) Subcellular distribution of N-CoR (red signal) in THP-1 cells treated with vehicle or Genistein at 50 µM concentration was determined by confocal microscopy.

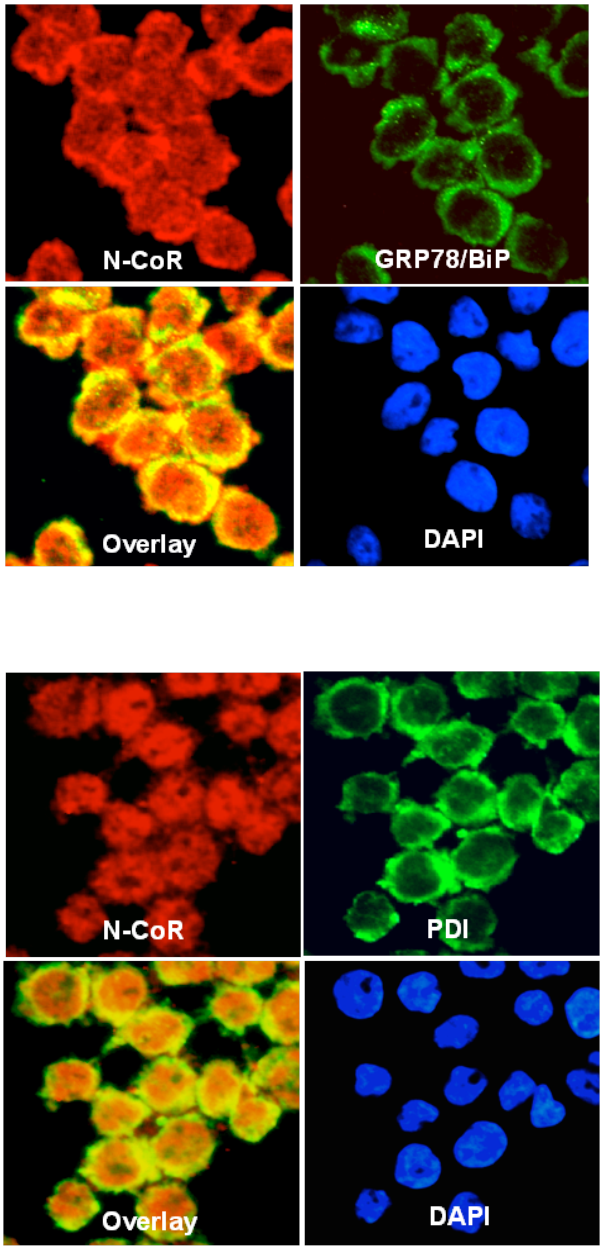

Figure 3.7. N-CoR in AML-M5 was preferentially localized to the ER. Localization of N-CoR in THP-1 cells were evaluated by confocal microscopy after staining with Anti-N-CoR antibody (Red Signal) and the ER resident proteins GRP78 /BiP (top panel) or PDI (bottom panel) (both Green Signals). Yellow signal in Overlay indicate almost complete N-CoR co-localization with the ER resident proteins GRP78/BiP and PDI. DNA was stained with DAPI to indicate the nucleus.

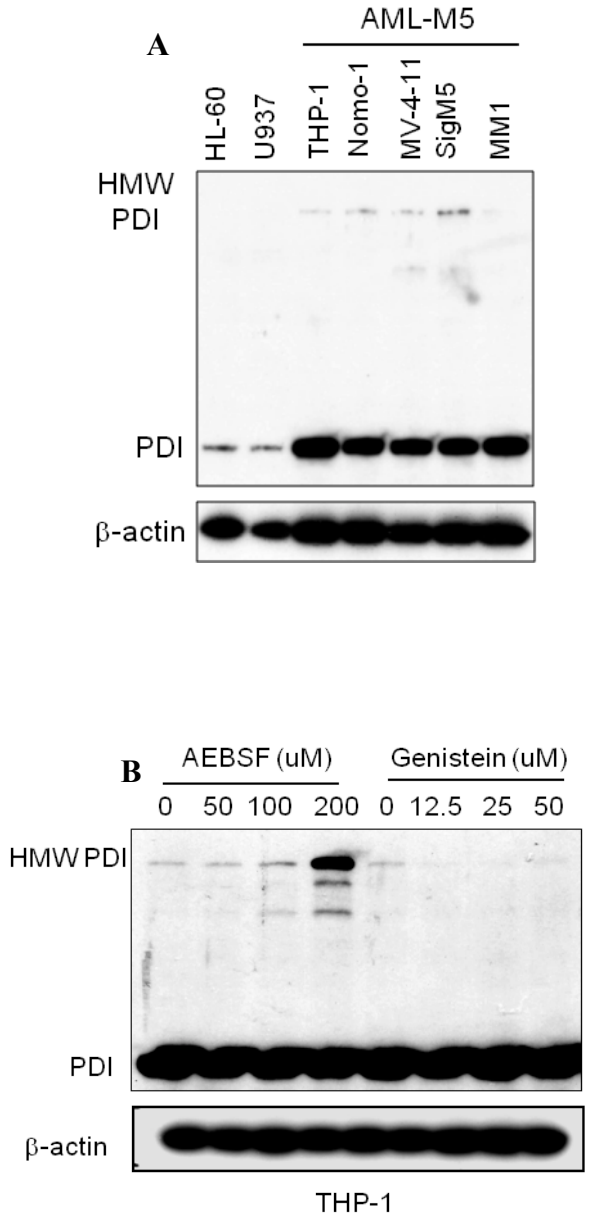

Figure 3.8. Misfolded N-CoR in AML-M5 led to the accumulation of ER stress. (A) Selective **a**ccumulation of ER stress was observed in AML-M5 derived cell lines. Relative level of ER stress in AML-M5 derived cell lines was compared to that of non-AML-M5 derived cell lines (HL60 and U597) by determining the level of native and HMW (high molecular weight) PDI protein. (B) AEBSF amplifies ER stress in THP-1 cells while Genistein reduces HMW PDI levels. Relative level of ER stress in THP-1 cells treated with AEBSF or Genistein in a dose dependent manner was determined by the level of HMW (high molecular weight) PDI protein.

3.1.3. Misfolded N-CoR exhibits aberrant serine/ threonine phosphorylation.

The conformation of a protein is defined by the free energy of its amino acid residues and minor alterations in the amino acid sequence can significantly alter the folding landscape of whole polypeptide sequences promoting misfolding [64,90]. Besides genetic modifications, the natural folding landscape of the polypeptide sequence can also be altered by aberrant post-translational modifications.

Previously, our laboratory reported a role for aberrant serine/threonine phosphorylation in PML-RARα induced misfolding of N-CoR protein in APL[58]. To investigate if N-CoR misfolding was also caused by a similar aberrant post-translational modification in AML-M5, the relative level of serine/threonine phosphorylated N-CoR in the total N-CoR protein stabilized by AEBSF or Genistein in THP-1 cells was first determined. N-CoR immunoprecipitated from the whole cell extract of AEBSF or Genistein treated THP-1 cells was resolved, transferred onto PVDF membrane and probed with a generic phospho-serine/threonine antibody. To quantify the amount of immunoprecipitated N-CoR protein, the membrane was reprobed with N-CoR antibody. Here, it was observed that N-CoR immunoprecipitated (IP) from AEBSF treated THP-1 cells displayed significantly higher levels of serine/threonine phosphorylation when compared to N-CoR immunoprecipitated from Genistein treated cells (Fig. 3.9, left top panel), with the total amount of N-CoR immunoprecipitated from both types of cells almost identical (Fig. 3.9, left lower panel).

After AEBSF treatment, the level of phosphorylated N-CoR protein increased most likely due to the inhibition of the protease responsible for its degradation. Genistein, on the other hand, may block the loss of N-CoR indirectly by inhibiting its aberrant phosphorylation. Although more commonly known for its strong anti-tyrosine kinase activity, Genistein's potent inhibitory effect on serine/threonine kinase activity was not entirely unexpected given its recently documented role as a serine/threonine kinase inhibitor [58]. Hence, with the data obtained thus far, it was hypothesized that there could be a role for kinases in the observed misfolding of N-CoR in AML-M5.

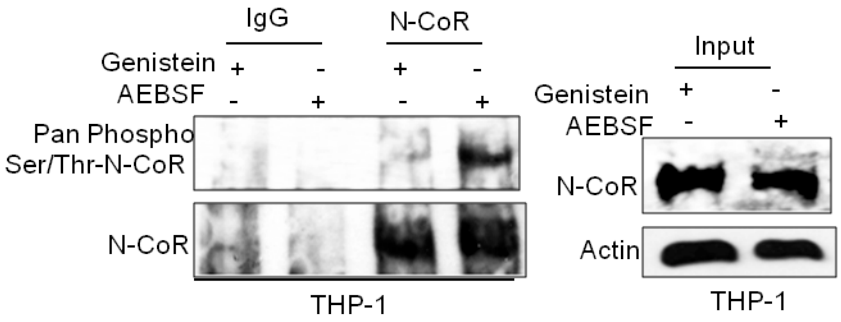

Figure 3.9. Misfolded N-CoR in AML-M5 displayed aberrant serine/threonine phosphorylation. Levels of serine/threonine phosphorylated N-CoR in THP-1 cells treated with AEBSF or Genistein was determined by staining the immunoprecipitated N-CoR protein with a generic phospho serine/threonine antibody (upper left panel). An aliquot of immunoprecipitated N-CoR was also stained with N-CoR antibody (lower left panel). Moreover, level of total N-CoR protein in each treated sample was determined by western blotting (right panel).

3.1.4 Identification of Akt as a mediator of N-CoR misfolding in AML-M5 cells.

In order to validate the hypothesis, identification of potential kinases which may be hyper-activated in AML-M5 was carried out by employing the proteome Profiler^{TM} Human Phospho-kinase antibody array system from R&D Systems. Complete analysis of all kinases available in the array was performed using cell lysates prepared from the N-CoR intact U937, HL60 and K562 (reported to contain full length native N-CoR[63]) cell lines and the five N-CoR negative AML-M5 cell lines. Expression analysis via densitometric quantification of all spots on the array blots (the list of kinases and their positions on the array is appended in Appendix 1) revealed that only Akt phosphorylated at the Serine 473 residue was preferentially up-regulated in all the five AML-M5 derived cell lines when compared to the other non AML-M5 derived cell lines (Fig. 3.10). The phosphorylation event by mTORC2 at this site facilitates the activating phosphorylation of Threonine 308 in Akt resulting in the full activation of Akt kinase activity. To validate the results of the array, western blotting assay was performed on lysates prepared from the cell lines used in the array as well as on multiple AML-M5 patient specimens to determine the levels of phospho-Akt (Ser473). The western blotting analysis corroborated with that of the array indicating that phospho-Akt (Ser473) levels were indeed higher in the AML-M5 cell lines (Fig. 3.11A) as well as in multiple AML-M5 patient specimens where N-CoR was loss (Fig. 311B), suggesting Akt kinase activity was indeed preferentially up regulated in AML-M5.

Next, in order to identify if Akt kinase was indeed involved in the accumulation of misfolded N-CoR in AML-M5, the ability to stabilized N-CoR in THP-1 cells after loss of Akt kinase activity was accessed. Two approaches were taken, one via siRNA mediated knockdown of Akt in THP-1 cells and two, via the inhibition of Akt kinase activity by inhibiting its activating phosphorylation using the commercial Akt kinase specific inhibitor Akti-X which inhibits the phosphorylation of Akt (Merck, Darmstadt, Germany)[190,191]. Both siRNA mediated Akt knockdown and inhibition of Akt kinase activity by Akti-X were able to stabilize full length N-CoR in THP-1 cells (Fig. 3.12A and B). Since inhibition of Akt kinase activity by both siRNA mediated Akt knockdown and Akti-X treatment were able to stabilize N-CoR in THP-1 cells, the detergent solubility of this stabilized N-CoR was next accessed. Solubility assay as previously described was performed and it was observed that the N-CoR stabilized by both methods was found mainly in the soluble fraction (Fig. 3.13A). When N-CoR localization was analyzed via immunofluorescence assay, it was observed that N-CoR displayed a predominantly nuclear localization after Akt inhibition by both methods in THP-1 cells (Fig 3.13 B). This indicated that by blocking the activity of Akt in THP-1 cells, native properties of N-CoR were restored (a phenomenon similar to that observed when THP-1 cells were treated with Genistein) strongly implicating the involvement of Akt kinase activity in the misfolding of N-CoR found in AML-M5 cells.

To prove the concept that Akt activation was crucial in the induction of N-CoR misfolding, a constitutively activated, NH2-terminally myristoylation signal-attached Akt (myr-Akt) mutant was co-expressed with flag-tagged N-

CoR in HEK293T cells. This ectopically expressed N-CoR was then similarly tested for detergent solubility. In this assay, it was observed that only in the presence of the myr-Akt mutant was N-CoR found to accumulate in the insoluble fraction (Fig. 3.14A). Another indication that Akt kinase activity was indeed important in the misfolding of N-CoR was its ability to induce N-CoR cytosolic localization. Immunofluorescence assay performed in HEK293T cells revealed that in the presence of the mry-Akt mutant, N-CoR displayed a predominantly cytosolic localization (Fig. 3.14B, lower panel) while in the absence of the mutant N-CoR localization was predominantly nuclear (Fig. 3.14B, upper panel).

Taken together these data indicated that Akt kinase activity was indeed important in the misfolding of N-CoR and could be the common factor that initiated N-CoR MCDL in AML-M5.

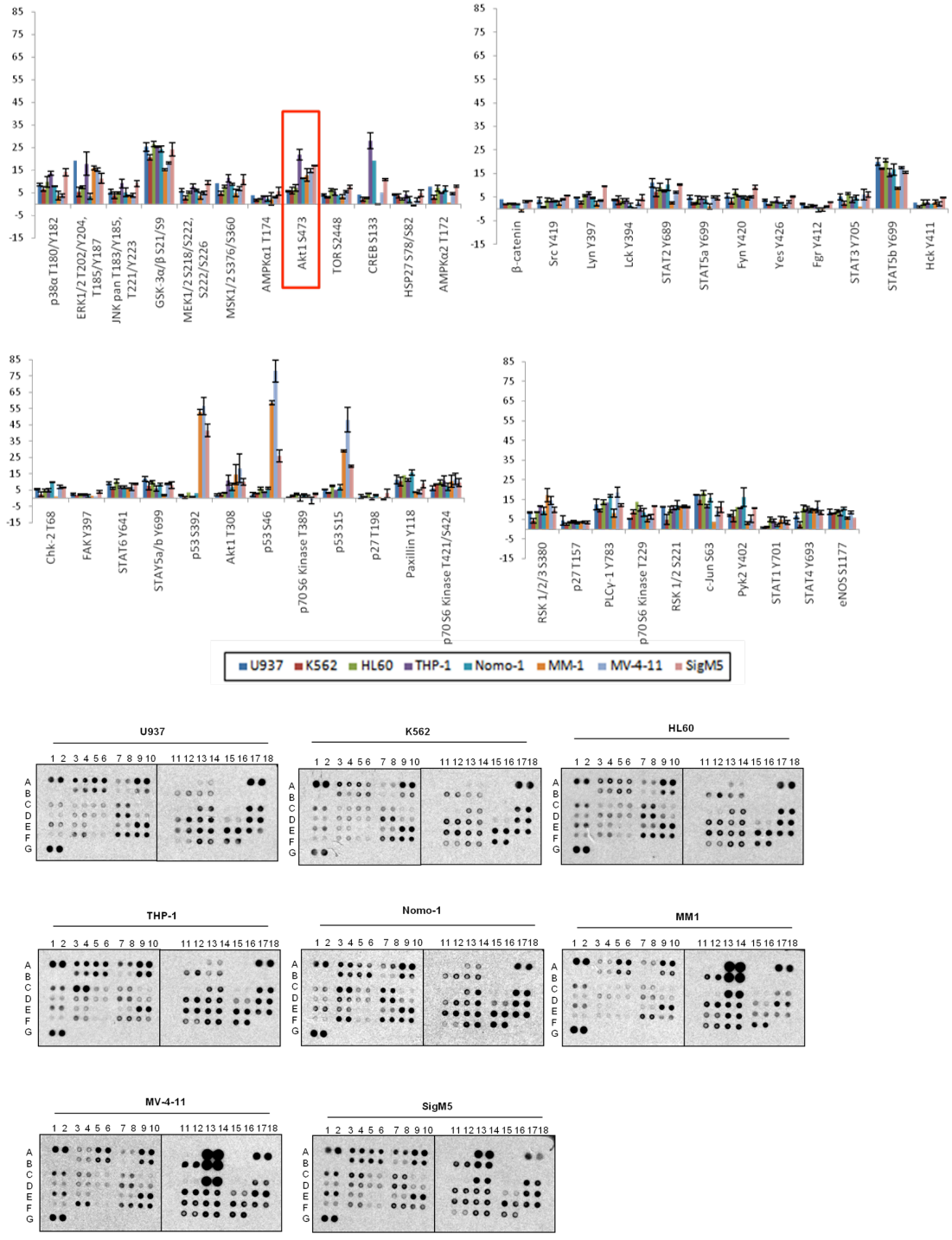

Figure 3.10. pAkt at serine 473 was selectively up-regulated in AML-M5. Level of activated kinases in five AML-M5 and three non-AML-M5 (HL60, U937 and K562) derived cell lines were determined by the Proteome Profiler™ Human Phospho-kinase antibody array system. The level of activity of each kinase in these two subsets of cells was quantified and presented as bar graphs. Results presented are the averages of 3 independent experiments (upper panel). Raw blots used in the quantification and coordinate markers for each spot on the blot are annotated. The list of kinases and their respective location on the blots are appended in Appendix 1 (lower panel)

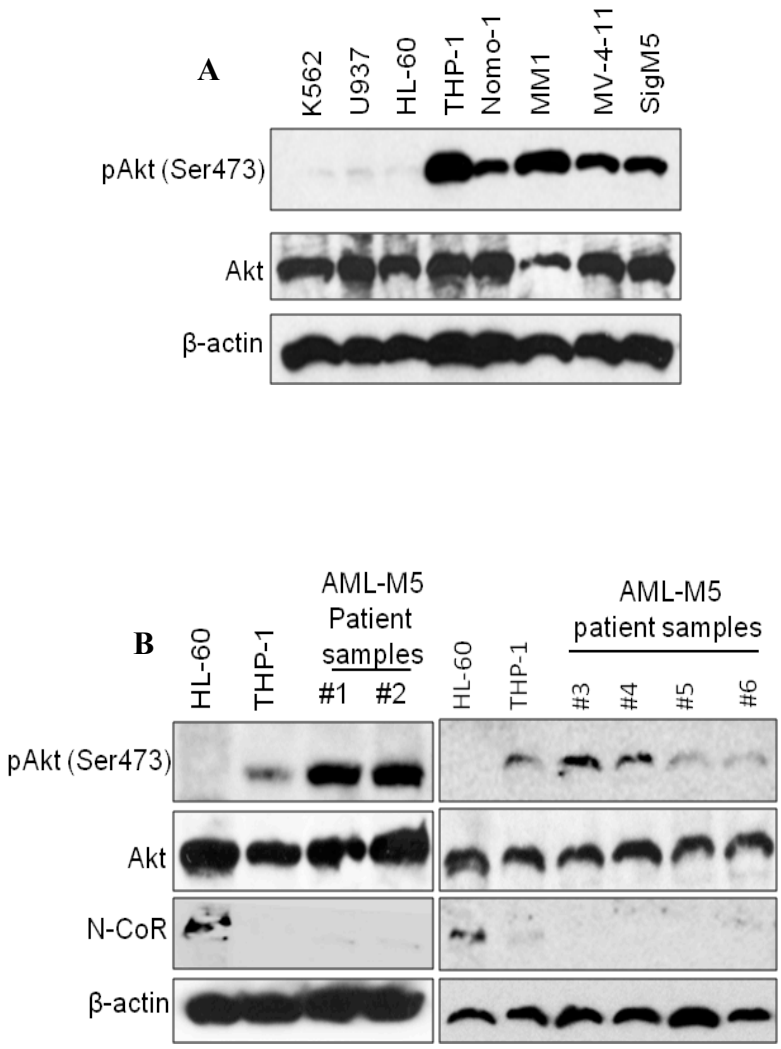

Figure 3.11. Akt activity was selectively up regulated in AML-M5 derived cell lines and primary specimens. (A) Level of activated Akt (pAkt (Ser473)) in various AML-M5 and non-AML-M5 cell lines was determined by western blotting. (B) Level of activated Akt (pAkt (Ser473)) and N-CoR protein in six primary human AML-M5 specimens were determined by western blotting.

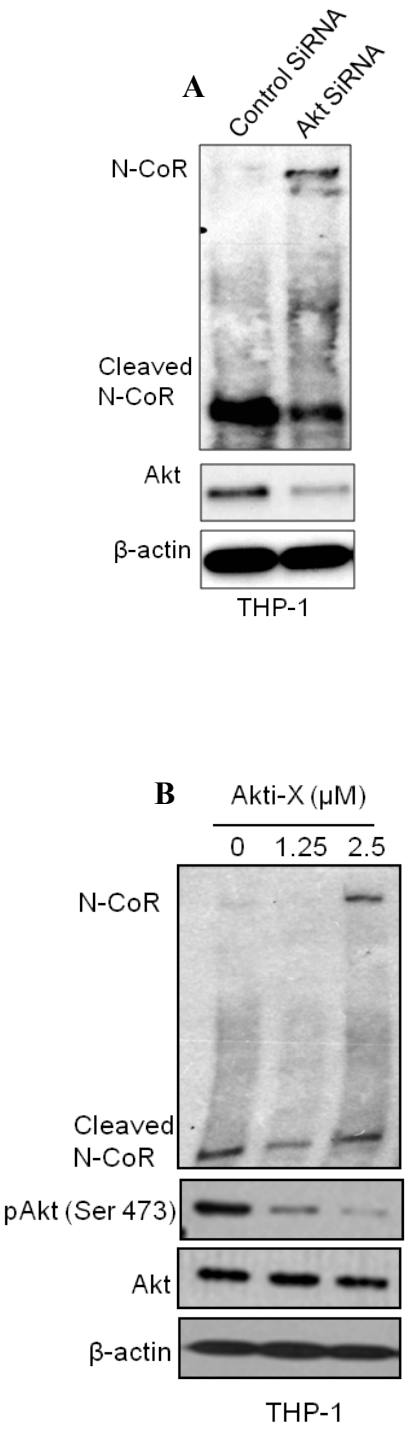

Figure 3.12. Loss of Akt activity resulted in the stabilization of N-CoR in THP-1. (A) N-CoR was stabilized after siRNA mediated Akt knockdown as determined via western blotting assay with anti-N-CoR antibody. Level of knockdown was determined by western blotting assay with anti-Akt antibody. (B) The specific inhibitor of Akt kinase activity Akti-X was able to stabilize N-CoR at 2.5 μM concentration as determined via western blotting with anti-N-CoR antibody. Inhibition of Akt kinase activity was determined by examining the levels of pAkt (Ser473) using pAkt (Ser473) specific antibody.

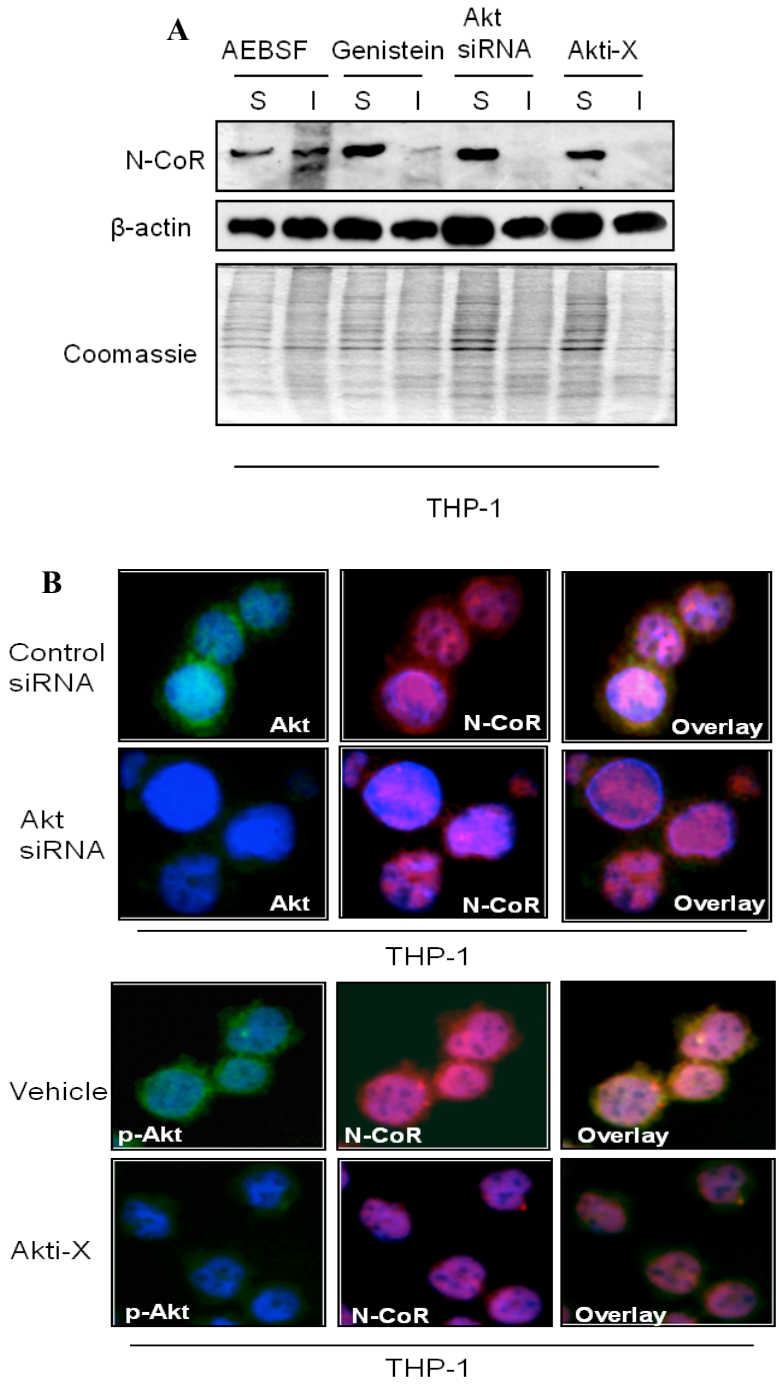

Figure 3.13. Native N-CoR conformation was rescued by loss of Akt kinase activity. (A) Relative solubility/insolubility of N-CoR protein in Akt silenced or Akti-X (a specific inhibitor of Akt kinase activating phosphorylation) treated THP-1 cells was determined by protein solubility assay. Soluble (S) and insoluble (I) fractions of treated THP-1 cells were separated by high speed centrifugation and N-CoR level in each fraction was determined by western blotting assay using an anti-N-CoR antibody. N-CoR stabilized by AEBSF and Genistein in THP-1 cells was used as controls for N-CoR solubility/insolubility. The relative solubility/insolubility of β-actin in each fraction was determined as control. The level of total of protein in each fraction was determined by coomassiee blue staining. (B) Subcellular distribution of N-CoR (red signal) in THP-1 cells treated with Control or Akt siRNA (upper panel) or with vehicle or Akti-X at 2.5 μM concentration (lower panel) was determined by confocal microscopy.

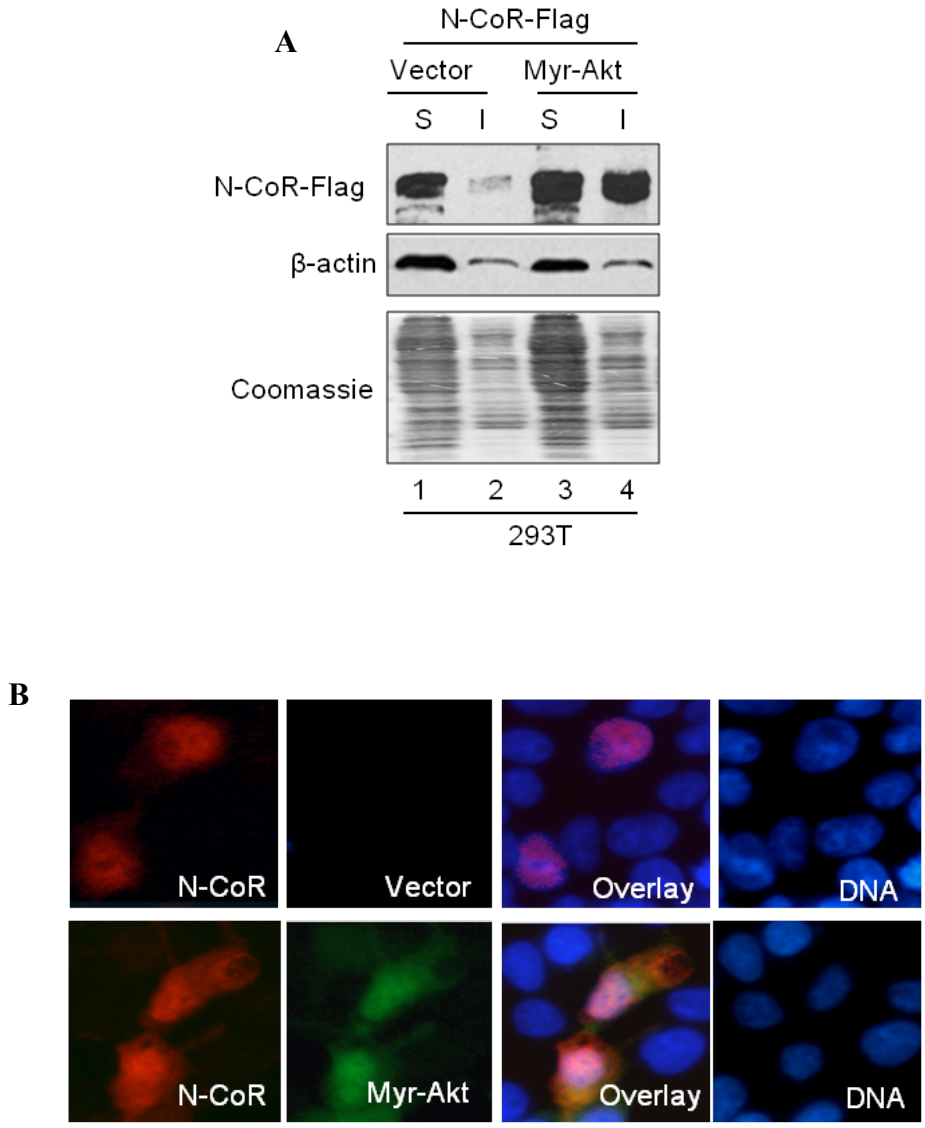

Figure 3.14. Constitutively active Akt can induce N-CoR misfolding in HEK293T cells. (A) Relative solubility/insolubility of flag-tagged N-CoR protein in HEK293T cells when expressed with a constitutively active Akt kinase (myr-Akt) was determined by protein solubility assay. Soluble (S) and insoluble (I) fractions were separated by high speed centrifugation and N-CoR level in each fraction was determined by western blotting assay using an anti-Flag antibody insoluble N-CoR was detected only in the presence of a constitutively active Akt kinase. The relative solubility/insolubility of β-actin in each fraction was determined as control. The level of total of protein in each fraction was determined by coomassiee blue staining. (B) Subcellular distribution of N-CoR (Red Fluorescence) protein in HEK293T cells after co-expression with the constitutively active Akt mutant, myr-Akt (Green Fluorescence) as determined using the anti-Flag anti-body followed by a red fluorescence tagged antibody. Preferential localization of N-CoR to the cytosol was observed after co-expression with myr-Akt while N-CoR was localized mainly in the nucleus in the absence of the myr-Akt.

3.1.5. N-CoR is a direct substrate of Akt.

Data obtained thus far suggested that Akt kinase activity was essential for the accumulation of misfolded N-CoR in THP-1 cells. However it was still unclear as to whether N-CoR was directly phosphorylated by Akt kinase or was the effect indirect. Thus, to establish if N-CoR was a direct substrate of Akt and if this phosphorylation event was indeed critical in the initiation of N-CoR misfolding in AML-M5, the following series of experiments were carried out.

It had been established that Akt kinase preferentially phosphorylates serine/threonine residues after the Akt kinase recognition motif RxRxx **S/T**-bulky hydrophobic (where X represents any amino acid). Thus the first step was to identify if there were any potential sites in the N-CoR sequence which fit this consensus motif. Using the Human Protein Reference database website, two putative Akt phosphorylation sites in the human N-CoR sequence was identified at moderate stringency. In the scan, a Serine residue at position 1450 and a Threonine residue at position 1925 in the human N-CoR amino acid sequence were found after the putative Akt consensus motif (Fig. 3.15A upper panel). Multiple sequence alignment performed using ClustalW revealed that these two Akt substrate consensus motifs and its surrounding regions were highly conserved in both the mouse and human sequence (Fig. 3.15B lower panel).

Next to identify if the inhibition of Akt kinase activity was able to abrogate serine/threonine phosphorylation in the Akt kinase consensus motif of N-CoR, THP-1 cells was treated with AEBSF or Akt siRNA and full length N-CoR was immunoprecipitated. The immunoprecipitated N-CoR obtained

from each treatment was accessed for Akt mediated serine/threonine phosphorylation via western blotting with a phospho-Akt substrate (RxRxx pS/pT) antibody which specifically recognizes serine/threonine residues phosphorylated at the RxRxx S/T motif in western blotting assay. In this assay it was observed that in AEBSF stabilized N-CoR, the serine/threonine residue at the Akt consensus motif site was phosphorylated. In contrast, N-CoR stabilized via siRNA-mediated loss of Akt activity did not display RxRxx pS/pT phosphorylation (Fig. 3.16). Similarly, when flag-tagged N-CoR was ectopically expressed in HEK293T cells in combination with the constitutively active myr-Akt mutant and subjected to the same immunoprecipitation assay, it was also noted that only in the presence of Akt kinase activity was the N-CoR phosphorylated at the Akt substrate motif (Fig. 3.17A). *In vitro* phosphorylation performed using purified flag-tagged N-CoR and Akt kinase also revealed that Akt kinase was able to directly phosphorylate N-CoR at the RxRxx S/T motif (Fig 3.17B). These data clearly showed that N-CoR was indeed a direct substrate of Akt.

Next, it was hypothesized that the loss of phosphorylation in native N-CoR stabilized by Genistein observed previously was most likely due to the drug's activity on Akt. Thus to validate this thought, the status of Akt activity after AEBSF and Genistein treatments in THP-1 cells were compared. Here, it was observed that while Genistein treatment resulted in a dose dependent loss of Akt kinase activity as indicated by the dose dependent loss of phosphorylation at the Serine 473 residue essential for full activation of Akt kinase activity, AEBSF treatment did have any significant effect on Akt kinase activity (Figure 3.18A). Thereafter, phosphorylation assay as performed

previously was carried out on AEBSF and Genistein treated cells and immunoprecipitated N-CoR was probed with the Akt substrate RxRxx pS/pT specific antibody. In Genistein treated cells, a loss of RxRxx pS/pT phosphorylation was observed implying that the loss of phosphorylation of native N-CoR stabilized by Genistein observed previously was partly due to the loss of Akt kinase activity in these cells (Figure 3.18B).

Taken together, these observations indicated that in AML-M5, N-CoR misfolding was due to its direct phosphorylation by Akt at the RxRxx S/T motif.

A

803	1443 - 1446	TVRS	[pS/pT]XX[E/D/pS*/pY*]	Casein Kinase II substrate motif	PubMed
804	**1445 - 1450**	**RSRHTS**	**RXRXX[pS/pT]**	**Akt kinase substrate motif**	PubMed
805	1445 - 1450	RSRHTS	X[pS/pT]XXX[A/P/S/T]	G protein-coupled receptor kinase 1 substrate motif	PubMed

1102	1919 - 1921	LRT	LRpT	LKB1 Kinase substrate motif	PubMed
1103	**1920 - 1925**	**RTRGKT**	**RXRXX[pS/pT]**	**Akt kinase substrate motif**	PubMed
1104	1920 - 1925	RTRGKT	X[pS/pT]XXX[A/P/S/T]	G protein-coupled receptor kinase 1 substrate motif	PubMed

B

Akt consensus sequence : RXRXXS/T

Akt substrate site 1
Human : KYEDVKAGETVRSRHTSVVSS
Mouse : KYEDVKAGEPVRARHTSVVSS

Akt substrate site 2
Human : PPPKSRYEEELRTRGKTTITA
Mouse : PPPKSRYEEELRTRGKTTITA

Figure 3.15. Two putative Akt substrate motifs were identified in the human N-CoR sequence. (A) Screen captures of results obtained during the motif scan searching for kinase substrate motifs using the Human Protein reference database where only the sites which showed up as putative Akt kinase substrate motifs are shown. (B) The Akt substrate consensus sequence and it surrounding sequences are highly conserved in both the human and mouse N-CoR sequences.

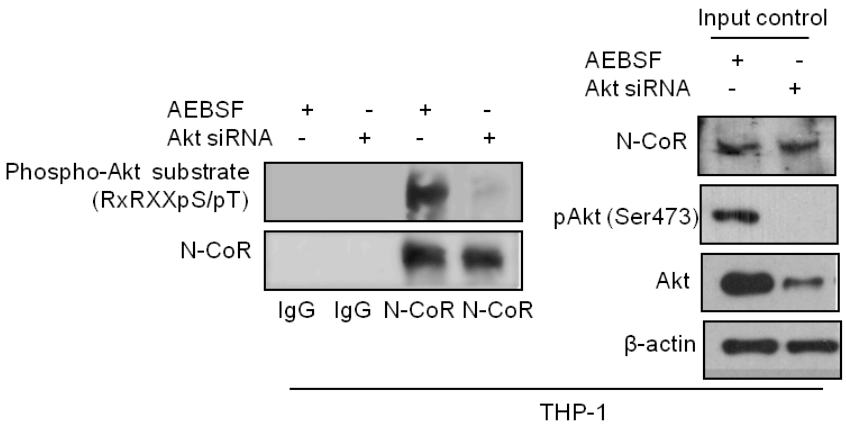

Figure 3.16. Inhibition of Akt kinase activity inhibited the phosphorylation of N-CoR in THP-1. Phosphorylation of immunoprecipitated full length N-CoR at the Akt consensus site in AEBSF treated cells versus that of Akt siRNA treated cells as determined by western blotting using a Phospho-Akt substrate (RxRxx pS/pT) specific antibody (left panel). Crude amounts of N-CoR loaded for immunoprecipitation as determined via western blotting using anti-N-CoR antibody (right panel).

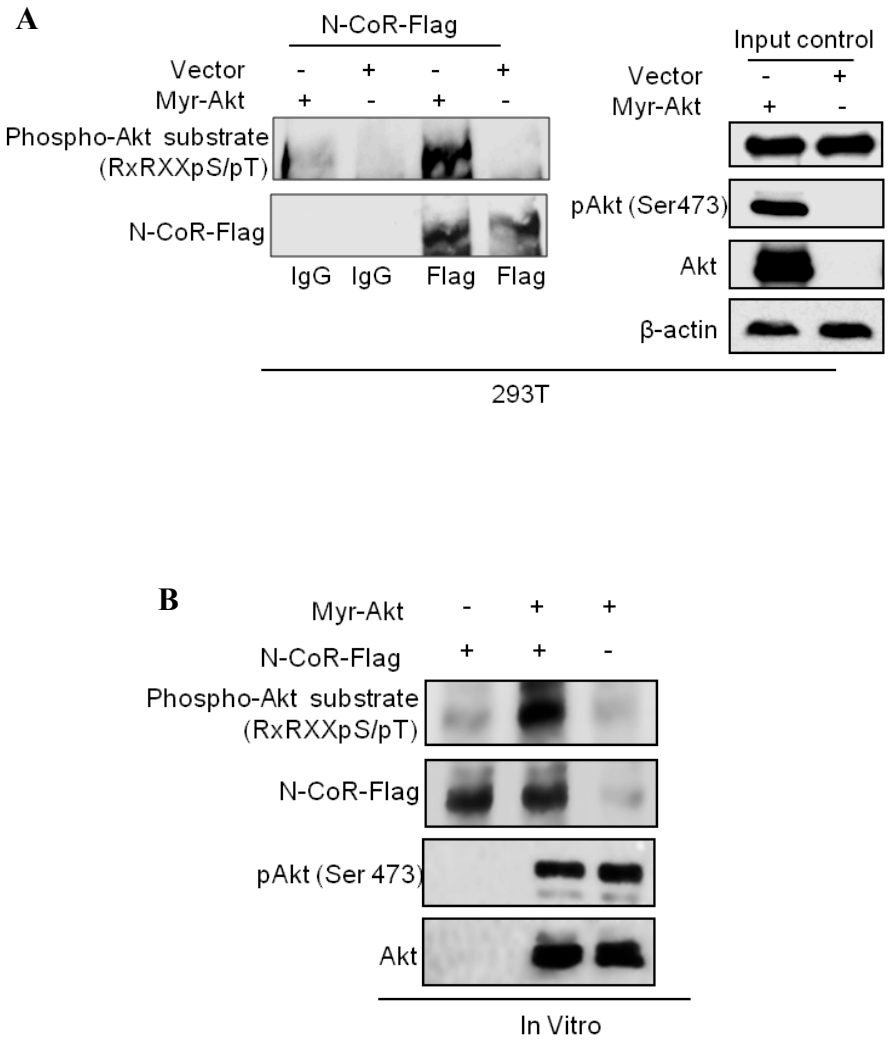

Figure 3.17. Akt kinase activity directly phosphorylates of N-CoR at the RxRxx S/T site. (A) Phosphorylation of immunoprecipitated flag tagged N-CoR at the Akt consensus site in HEK293T cells as determined via western blotting assay using a Phospho-Akt substrate (RxRxx pS/pT) specific antibody (left panel). Crude amounts of N-CoR loaded for immunoprecipitation as determined via western blotting using anti-Flag antibody (right panel). (B) Active Akt Kinase directly phosphorylates N-CoR *in vitro*. Active Akt Kinase directly phosphorylates N-CoR *in vitro*. Purified flag-tagged N-CoR was subjected to *in vitro* kinase assay with purified active Akt kinase and subjected to western blotting assay with phospho-Akt substrate (RxRxx pS/pT) specific antibody.

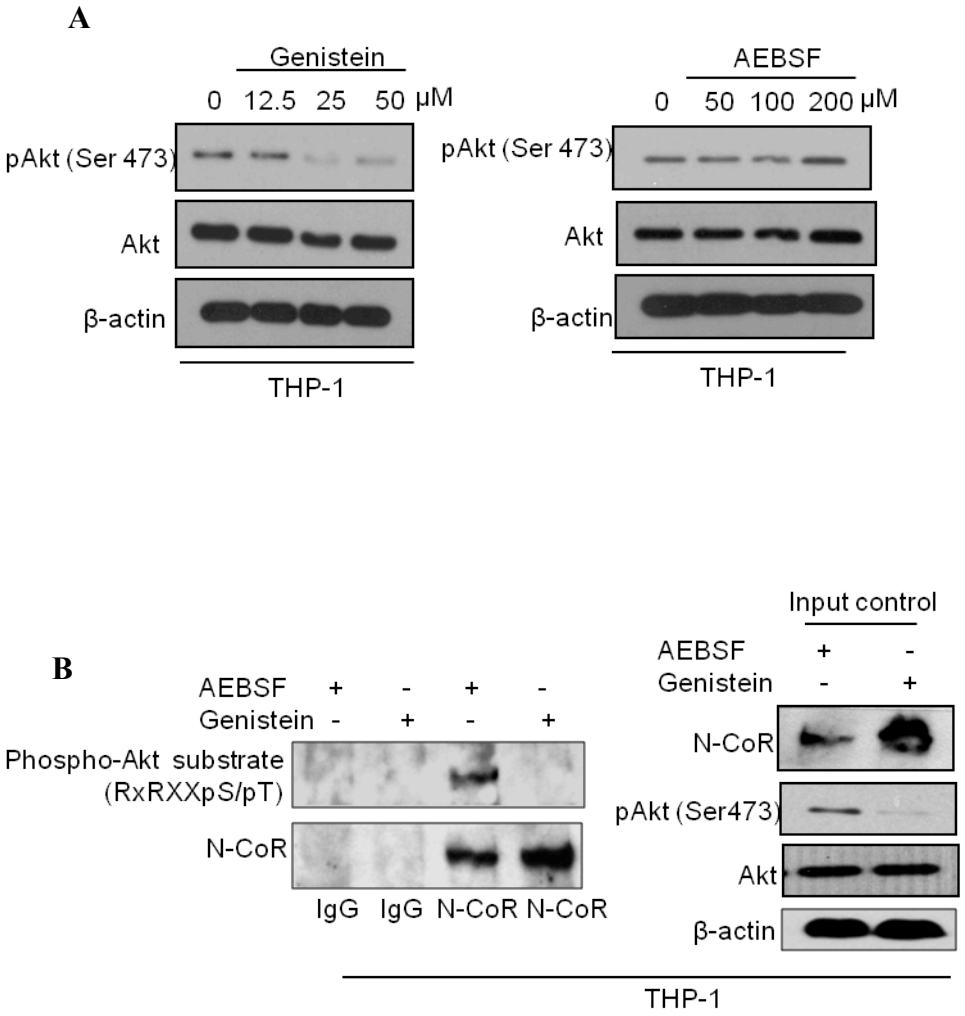

Figure 3.18. Loss of N-CoR phosphorylation after Genistein treatment was due to the loss of Akt kinase activity in THP-1. (A) Genistein treatment resulted in the dose dependent loss of Akt kinas activity as indicated by the loss of pAkt (Ser473) expression after treatment (left panel). AEBSF treatment did not have a significant effect on Akt kinase activity (right panel). (B) Phosphorylation of immunoprecipitated N-CoR at the Akt consensus site in THP-1 cells after AEBSF and Genistein treatment as determined via western blotting assay using a Phospho-Akt substrate (RxRxx pS/pT) specific antibody (left panel). Crude amounts of N-CoR loaded for immunoprecipitation as determined via western blotting using anti-Flag antibody (right panel).

3.1.6. Phosphorylation at the Serine 1450 residue by Akt was essential for the misfolding of N-CoR protein.

The data obtained in the above sets of experiments strongly suggested the importance of Akt mediated phosphorylation in the induction of the misfolded conformation of N-CoR. Thus in a proof of concept approach, mutagenesis of the Akt kinase consensus motifs in N-CoR to a non-phosphorable Alanine residue was performed to access the ability of Akt kinase activity to induce the accumulation of misfolded N-CoR in these mutants. Based on the data obtained in figure 3.15, two mutants of N-CoR were created, one single mutant for each of the identified Akt substrate consensus sites. The location of the mutated sites on N-CoR and sequencing results of the two successful mutants and are shown in figure 3.19A and B. The mutants were next tested for their ability to be phosphorylated by Akt via ectopic expression with the myr-Akt mutant in HEK293T cells followed by immunoprecipitation assay as carried out previously to identify the true Akt substrate site in the N-CoR sequence. As observed in figure 3.20, only the single S1450A mutant showed a loss of phosphorylation in the presence of Akt kinase activity while the ability of the single T1950A mutant to become phosphorylated by Akt activity was not affected. This suggested that the Serine 1450 residue after the Akt substrate consensus motif in the N-CoR sequence was the actual Akt substrate site subjected to phosphorylation in Akt mediated misfolding of N-CoR.

Next to validate that this phosphorylation at Serine 1450 was indeed crucial for the induction of N-CoR misfolding, the HEK293T system was utilized and solubility assay was performed as described previously. As

depicted in figure 3.21, only the S1450A mutant was unable to accumulate in the insoluble fraction in the presence Akt kinase activity. Under the same assay conditions, the ability of myr-Akt to induce N-CoR misfolding of the T1950A mutant and wild-type N-CoR in HEK293T cells was not affected. This suggested the importance of the phosphorylation event by Akt at Serine 1450 in N-CoR in the initiation of N-CoR misfolding in AML-M5.

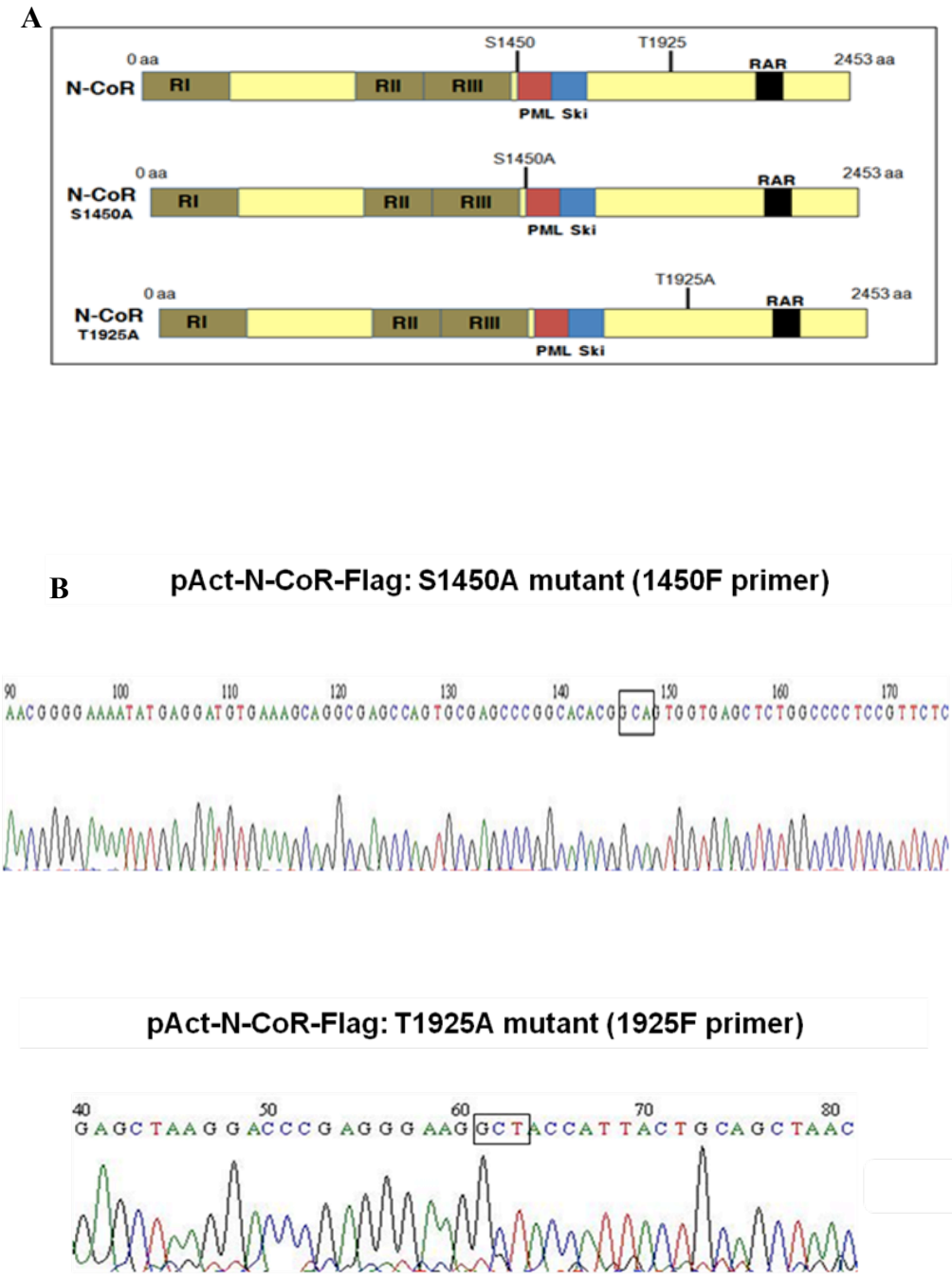

Figure 3.19. Site directed mutagenesis of Serine 1450 and Threonine 1925 in the N-CoR sequence to a non-phosphorable Alanine residue. (A) Successful Serine to Alanine mutation was created at position 1450 and 1925 of pAct-N-CoR-Flag. Locations of these mutations in N-CoR are depicted. (B) Successful mutants were determined via sequencing analysis and the chromatograms of the successful mutants are shown. Mutations are indicated by a black box.

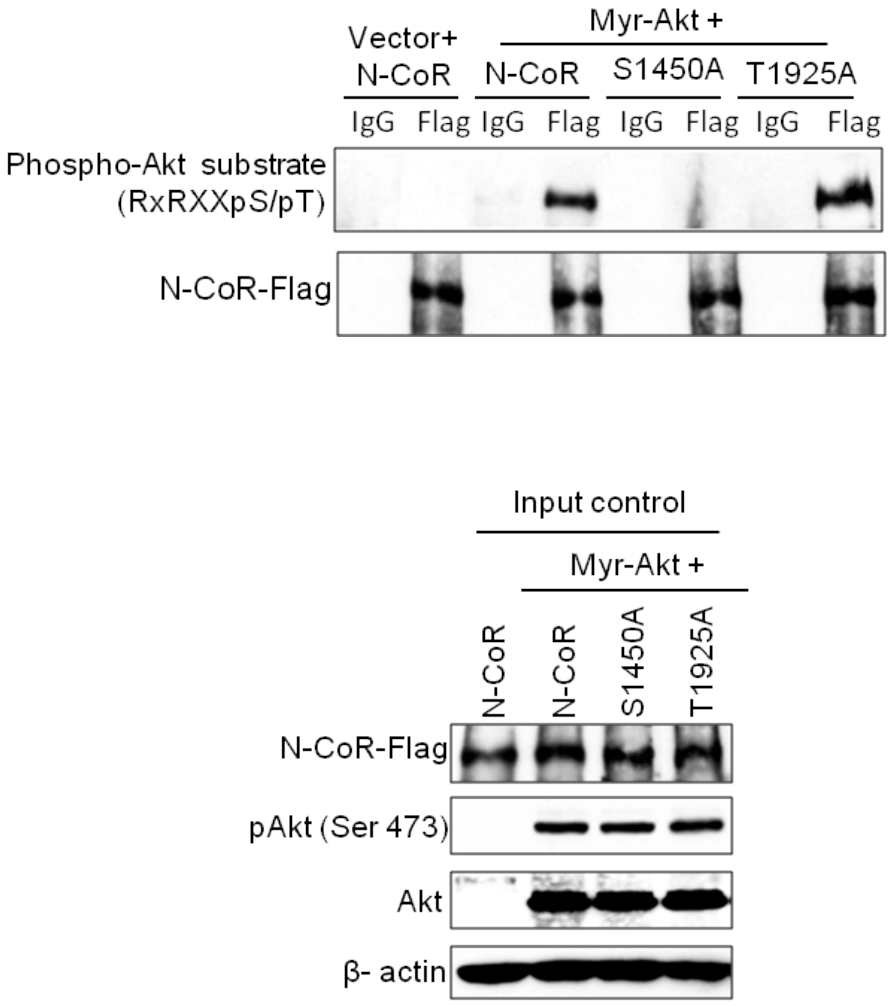

Figure 3.20. Serine 1450 after the Akt consensus motif was the true phospho-acceptor site in the N-CoR sequence. (A) Serine to Alanine mutagenesis at position1450 in the Akt consensus site in N-CoR resulted in the inability of Akt kinase to phosphorylate immunoprecipitated N-CoR as determined via the a Phospho-Akt substrate specific antibody while the Threonine to Alanine mutation at position 1925 did not affect N-CoR phosphorylation by Akt kinase (top panel). Crude amounts of N-CoR loaded for immunoprecipitation as determined via western blotting using anti-Flag antibody (bottom panel).

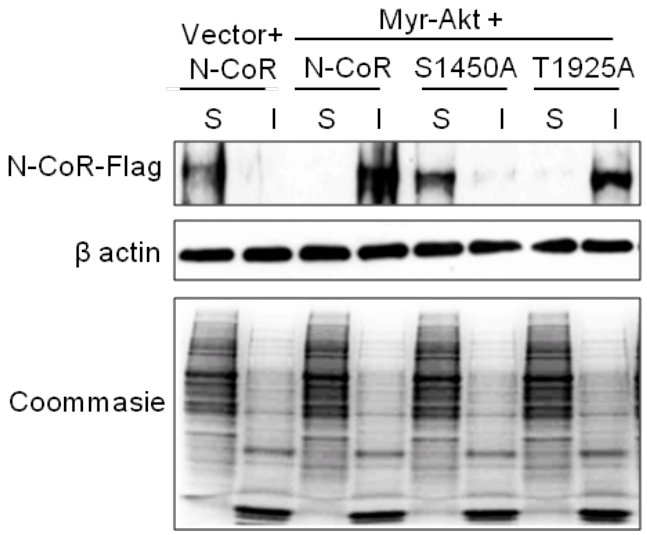

Figure 3.21. Phosphorylation of N-CoR by Akt at Serine 1450 was essential for the induction of N-CoR misfolding. Relative solubility/insolubility of flag tagged N-CoR protein (WT or mutants, S1450A or T1925A) in HEK293T cells when expressed with a constitutively active myr-Akt was determined by protein solubility assay. Soluble (S) and insoluble (I) fractions were separated by high speed centrifugation and N-CoR level in each fraction was determined by western blotting assay using an anti-Flag antibody. Insoluble N-CoR was detected only when Serine1450 in N-CoR was mutated. The relative solubility/insolubility of β-actin in each fraction was determined as control. The level of total of protein in each fraction was determined by coomassiee blue staining.

3.1.7. The negative charge conferred by the phosphorylation event initiates N-CoR misfolding in AML-M5.

A phosphorylation event results in a change in protein conformation by conferring a negative charge to the residue it phosphorylates. Thus to determine if by conferring a negative charge at position 1450 in N-CoR, misfolding could be induced, a phosphomimetic mutant was created by mutating the Serine at position 1450 to a Glutamic acid residue which carries a native negative charge due to the -COOH group. Successful site directed mutagenesis was determined via DNA sequencing (Fig 3.22). Detection of protein misfolding in this mutant (designated S1450E) was accessed using protein solubility assay and immunofluorescence assay. When ectopically expressed in HEK293T cells in the absence of any Akt kinase activity, the phosphomimetic mutant S1450E was observed to accumulate in the insoluble fraction when compared to the wild type N-CoR which only accumulated in the soluble fraction (Fig. 3.23A). The mutant was also observed to preferentially localize to the cytosol (Fig. 3.23B) in contrast to the predominantly nuclear localization of wild-type N-CoR in immunofluorescence assay. These results showed that the S1450E mutant displayed hallmark signs of misfolding.

Next, to determine if cytosolic localization of the mutant N-CoR induced ER stress (a key feature of misfolded proteins) in the cells which are expressing it, immunofluorescence assay was performed to look for the up-regulation of the ER stress marker GRP78/BiP in these cells. As observed in figure 3.24, HEK293T cells which expressed the mutant N-CoR S1450E had

elevated GRP78/BiP levels while surrounding cells which were not transfected with the mutant expressed basal GRP78/BiP levels.

Collectively, the observations indicated that a negative charge conferred by the phosphorylation event mediated by Akt kinase activity at position 1450 in the N-CoR protein was critical for the initiation of its loss through misfolding in AML-M5.

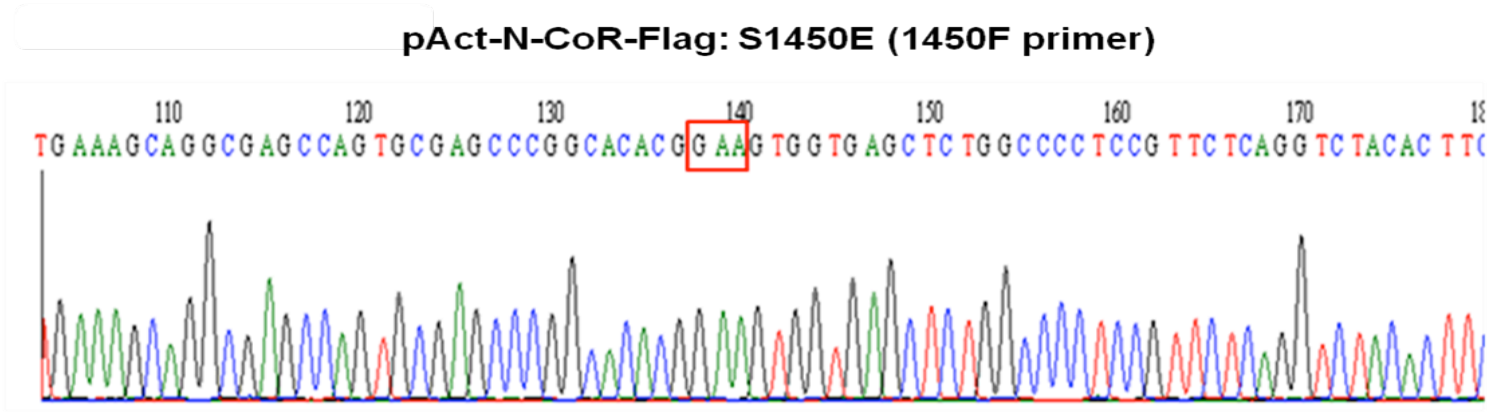

Figure 3.22. Successful Serine to Glutamic acid mutation was determined via sequencing. Sequencing chromatogram of successful Serine to Glutamic Acid 1450 (S1450E) mutant. Desired mutation is indicated by a box on the sequence.

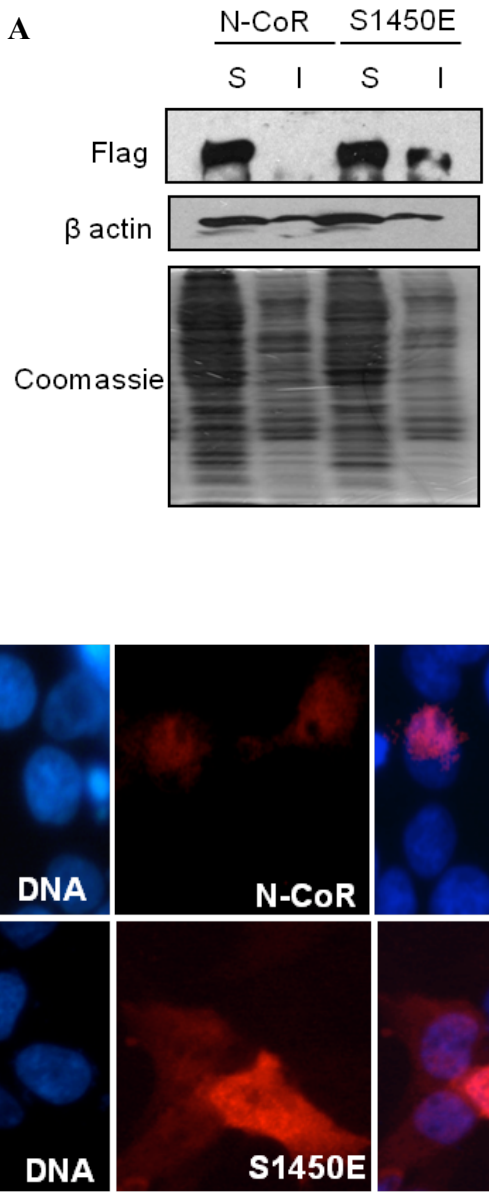

Figure 3.23.The phosphomimetic N-CoR S1450E displayed properties of misfolded N-CoR. (A) N-CoR phosphomimetic mutant S1450E accumulates in the insoluble fraction. Relative solubility/insolubility of flag tagged N-CoR protein (WT or mutant S1450E) in HEK293T cells was determined by protein solubility assay. Soluble (S) and insoluble (I) fractions were separated by high speed centrifugation and N-CoR level in each fraction was determined by western blotting assay using an anti-Flag antibody. S1450E was found to accumulate in the insoluble fraction while under the same conditions N-CoR (WT) accumulated only in the soluble fraction. The relative solubility/insolubility of β-actin in each fraction was determined as control. The level of total of protein in each fraction was determined by coomassiee blue staining. (B) Subcellular distribution of N-CoR (WT) and S1450E (Red Fluorescence) protein in HEK293T cells was determined using the anti-Flag antibody followed by a red fluorescence tagged antibody. Preferential localization of S1450E to the cytosol was observed.

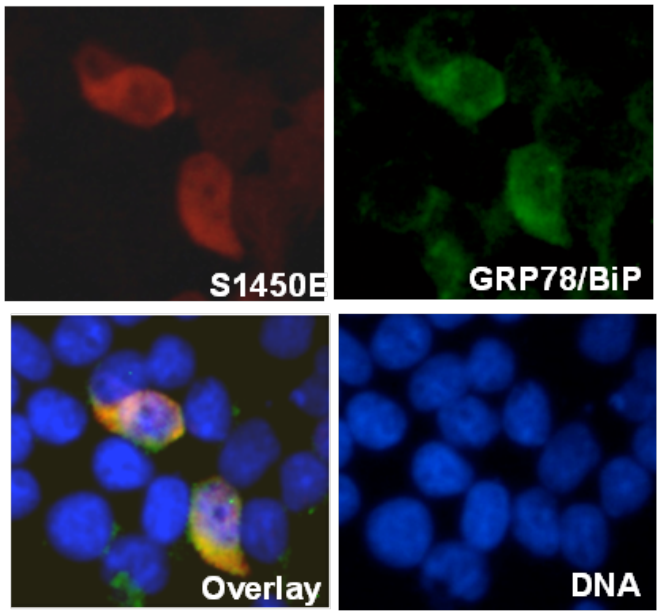

Figure 3.24. Expression of the phosphomimetic N-CoR S1450E resulted in the accumulation of ER stress. Accumulation of ER stress levels in cells transfected with S1450E (Red Fluorescence) protein in HEK293T cells was determined using the anti-Flag anti-body followed by a red fluorescence tagged antibody. Elevated GRP78/BiP levels as indicated by the increase in GRP78/BiP immunofluorescence (Green Fluorescence) as detected after staining with anti- GRP78/BiP antibody followed by a green fluorescence tagged antibody indicated the accumulation of ER stress in transfected cells.

3.2. Role of misfolded N-CoR mediated transcriptional deregulation of Flt3 in the pathogenesis of Acute Monocytic Leukemia (AML)-M5 subtype.

3.2.1. N-CoR loss correlates with the up-regulation of Flt3 expression.

N-CoR being a generic transcriptional co-repressor had been documented to be essential in the repression of many developmental genes. Thus, the most critical effect of Akt mediated N-CoR MCDL in AML-M5 cells would be the transcriptional deregulation of genes which were normally repressed by N-CoR. This was particularly so for genes which are associated with the normal growth and development of hematopoietic cells. Therefore, in an attempt to identify hematopoietic genes which expressions were deregulated owing to the MCDL of N-CoR protein, the levels of selected hematopoietic genes in N-CoR negative AML-M5 derived cell lines and cell lines which contained intact N-CoR were analyzed. The goal was to identify genes which expressions would reflect an inverse correlation to the N-CoR status of these two groups of AML derived cell lines.

RT-PCR and qRT- PCR analysis of 21 genes reported to be important in normal hematopoiesis and lineage commitment [192] using the previously characterized N-CoR positive cell lines, HL60 (a AML-M2 derived cell line) ,U937 (a monocytic cell line derived from histocystic lymphoma) and N-CoR null AML-M5 derived cell lines THP-1, Nomo-1, Mono-Mac-1 (MM1), MV-4-11 and SigM5 revealed that only the Flt3 gene was observed to be highly up regulated in the N-CoR negative cell lines when compared to those expressing N-CoR (Fig. 3.25 and Fig. 3.26). Further analysis of more N-CoR positive and negative cell lines revealed that this inverse relationship between N-CoR and

Flt3 expression seemed to hold true (Fig. 3.27). The inverse relationship between N-CoR and Flt3 expressions was also found to be translated to the protein level in the all the AML-M5 cell lines (Fig 3.28A) as well as in multiple histologically confirmed primary AML-M5 patient specimens (Fig 3.28B), with both the 130 kDa intracellular non–glycosylated and the 160 kDa membrane bound glycosylated forms observed to be highly expressed. Furthermore, siRNA mediated N-CoR knockdown performed on N-CoR positive HL60 revealed that after N-CoR ablation, Flt3 transcript levels was significantly up-regulated while the levels of two other genes which did not have a correlation with N-CoR status was not altered (Fig. 3.29 left panel). Successful N-CoR knockdown in HL60 cells was determined via western blotting and RT-PCR (Fig. 3.29 middle and right panel). Conversely, over-expression of flag- tagged N-CoR in THP-1 cells brought about a down regulation of Flt3 levels (Fig. 3.30). This inverse correlation between N-CoR loss and Flt3 expression suggested that N-CoR might have role in the regulation of Flt3 expression in AML-M5 cells.

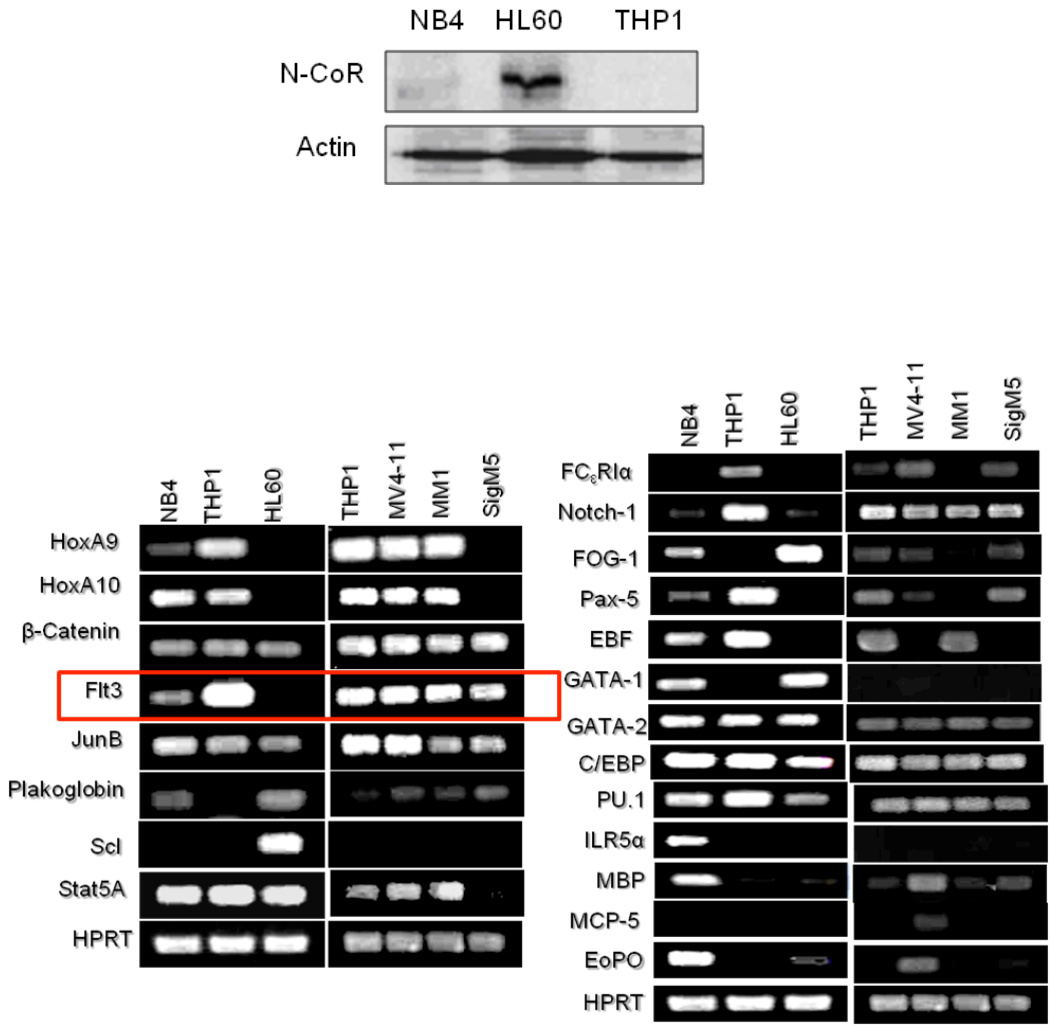

Figure 3.25. N-CoR loss was associated with Flt3 up-regulation in semi-quantitative PCR analysis. Relative expression of N-CoR protein in HL60, NB4 and THP-1 as determined via western blotting assay using anti-N-CoR antibody (top panel). RT-PCR analysis of selected hematopoietic genes in AML-M5, APL and N-CoR expressing HL60 cells. Only the Flt3 gene expression showed an inverse relationship to N-CoR protein status in the cell lines used (bottom panel).

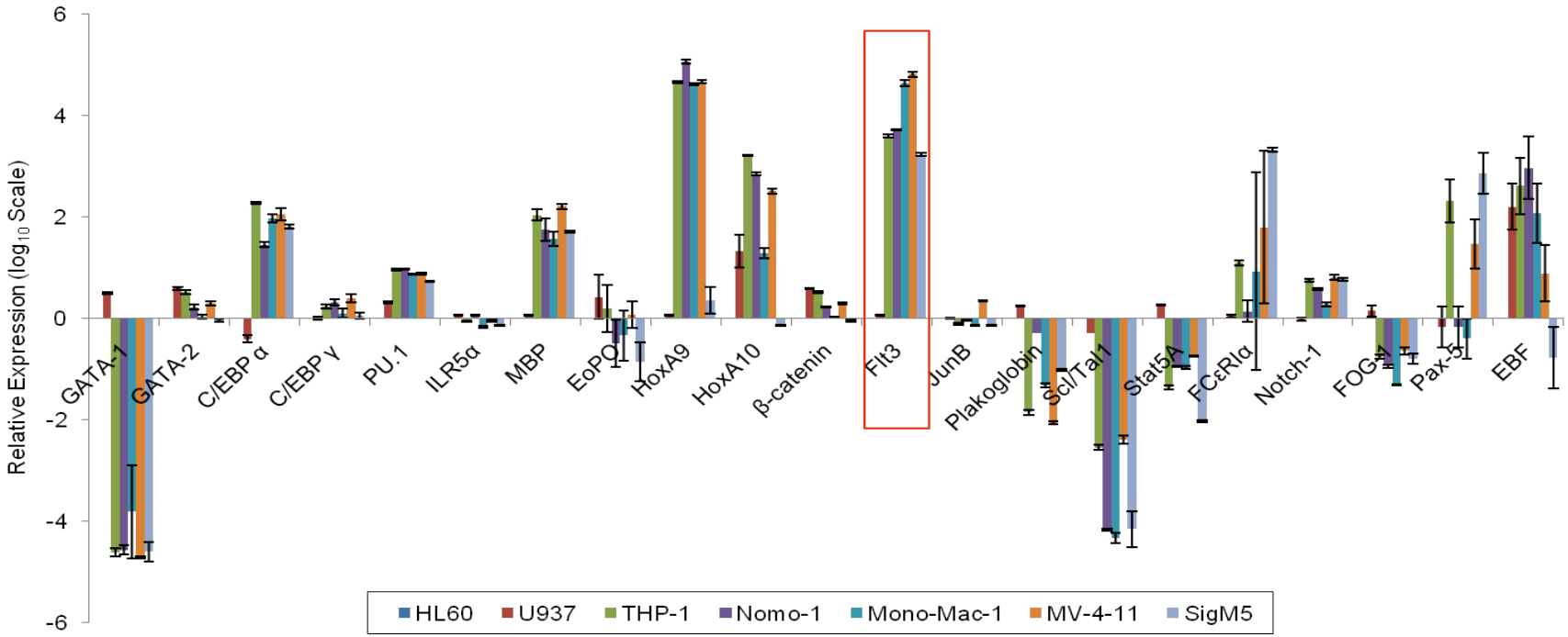

Figure 3.26. N-CoR loss was associated with up regulation of Flt3 in qRT-PCR analysis. Relative expression of selected hematopoietic genes in AML-M5 and non-AML-M5 (HL60 and U937) cells were determined by qRT-PCR analysis. Data was analyzed using the comparative C_t method using the expression level of each gene in HL60 cells as the reference value, and the level of expression of the HPRT gene was used as control. The graph was plotted on a log scale with a base of 10. Expression levels in HL60 cells for all genes were set to 0 while genes which were up-regulated relative to their expression levels in HL60 cells were given positive values, and those which were down-regulated relative to expression level in HL60 cells were given negative values. Raw C_t values which registered as undetermined were set to 40. (Results presented are the averages of 3 independent experiments.)

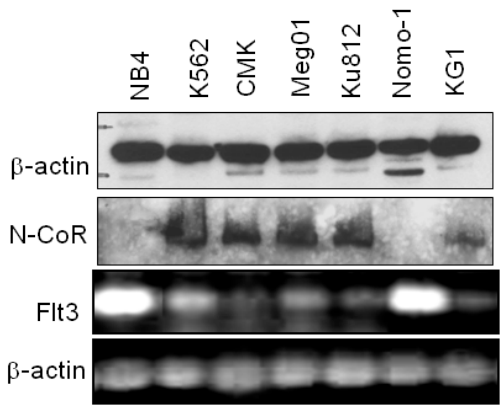

Figure 3.27. Flt3 expression was inversely related to N-CoR protein status. N-CoR and Flt3 levels in various human leukemic cell lines were determined in western blotting and RT-PCR analysis respectively.

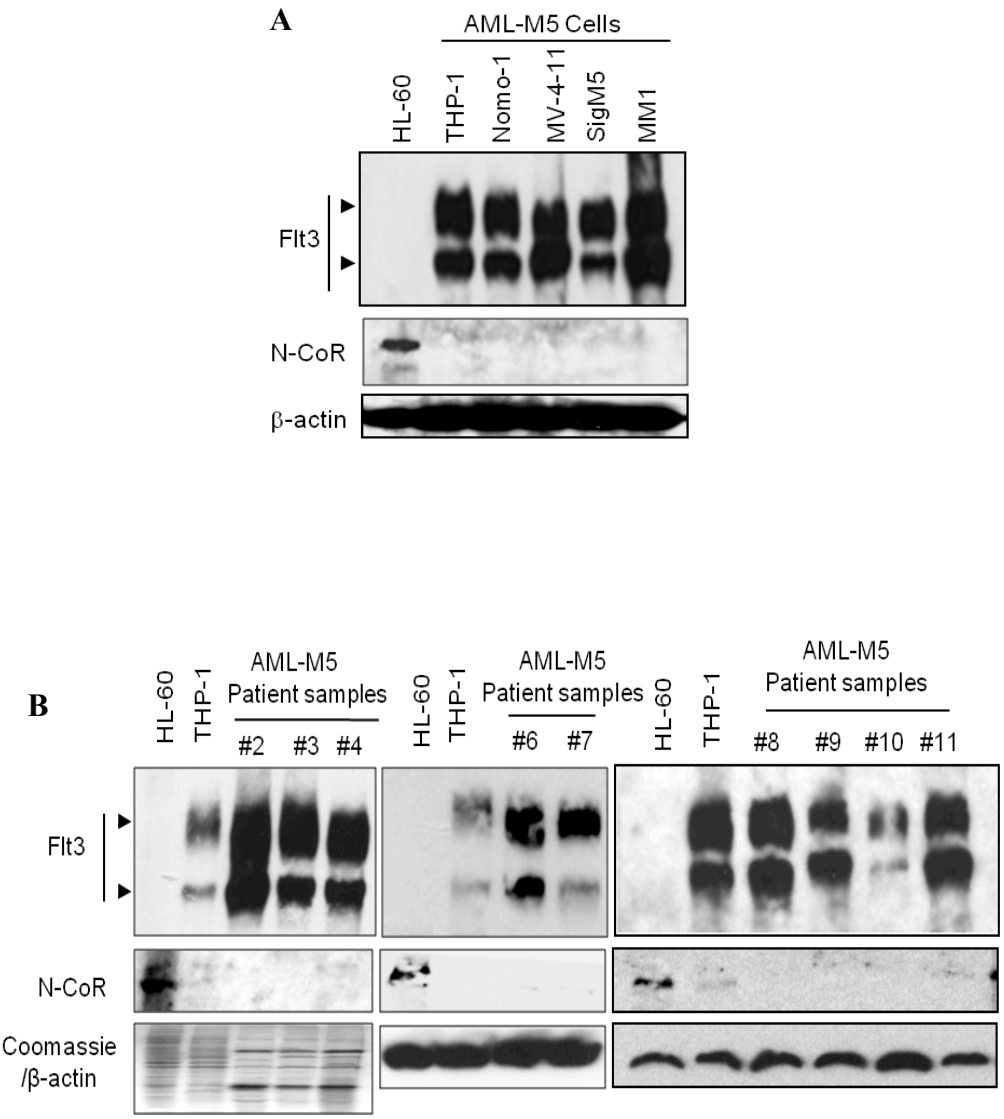

Figure 3.28. The inverse relationship between N-CoR and Flt3 was translated to the protein level. Flt3 and N-CoR levels in AML-M5 derived cell lines (A) and in multiple histologically confirmed human primary AML-M5 specimens (B) were determined through western blotting assay using the respective antibodies. Levels of N-CoR and Flt3 in HL60 cells were used as a reference.

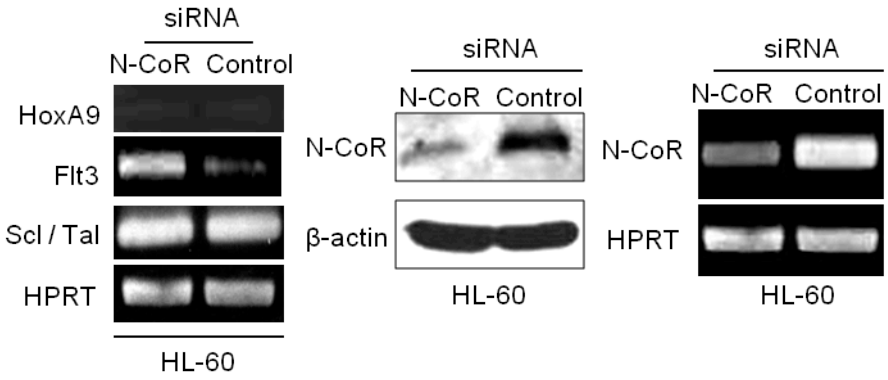

Figure 3.29. siRNA mediated N-CoR knockdown in HL60 up regulated Flt3 levels. Levels of Flt3, HoxA9 and Scl/Tal in HL60 cells transfected with N-CoR or control siRNA were determined by RT-PCR analysis (left panel). N-CoR knock down efficiency at protein (middle panel) and transcript level (right panel) in HL60 cells transfected with anti-N-CoR or control siRNA was determined through western blotting assay and RT-PCR analysis.

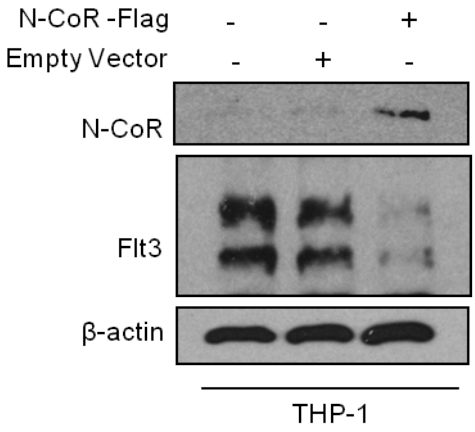

Figure 3.30. Over-expression of flag-tagged N-CoR in N-CoR null THP-1 cells resulted in the down-regulation of Flt3 levels. Ectopic expression of flag-tagged N-CoR in THP-1 cells resulted in the loss of Flt3 expression as determine via western blotting assay with anti-Flt3 antibody. Levels of ectopic N-CoR expression were determined via western blotting assay with anti-Flag antibody.

3.2.2. Flt3 is a transcriptional target of N-CoR.

The observation of reduced Flt3 levels in cells which expressed N-CoR suggested that this could be due to a direct repression of the Flt3 gene by N-CoR. Therefore, to show that N-CoR was actually involved in the repression of Flt3, the activity of a luciferase reporter driven by the full length Flt3 promoter (up to 901 base pairs upstream of the transcriptional start site) was compared in N-CoR positive and negative leukemic cell lines. The Flt3-luciferase reporter [Flt3 (-901)] activity was significantly lower in N-CoR intact HL60, K562 and U937 cells; whereas in THP-1 cells which lacked an intact N-CoR protein, reporter activity was significantly higher (Fig. 3.31). Introduction of ectopic N-CoR in THP-1 cells (Fig. 3.32A) resulted in a dose dependent reduction of Flt3 promoter activity (Fig. 3.32B).

To further prove that the Flt3 promoter was repressed by N-CoR, the effect of ectopic N-CoR expression on Flt3 promoter activity was determined via luciferase assay performed in HEK293T cells. In the initial experiments, it was noted that despite repeated attempts, no significant reduction in the Flt3 reporter activity by ectopic N-CoR was observed in HEK293T cells (data not shown). Thinking that this lack of reduction in the Flt3 reporter activity by ectopic N-CoR could be a result of the high levels of endogenous N-CoR protein present in HEK293T cells, the experiment was next repeated using N-CoR ablated HEK293T cells. N-CoR ablation by N-CoR siRNA increased the basal Flt3 reporter activity in HEK293T cells when compared to its activity in non-ablated cells (Fig. 3.33). Moreover, ectopic restoration of N-CoR in N-CoR ablated HEK293T cells down regulated this augmented Flt3 promoter activity in a dose dependent manner, and its value came down to a level which

was lower than the basal value (Fig. 3.33). The degree of Flt3 promoter inhibition by ectopic N-CoR was only two fold in N-CoR intact HEK293T cells irrespective of dose; while in N-CoR ablated cells, a seven fold reduction was observed when N-CoR was introduced at a maximum concentration of 1μg (Fig. 3.34). All these observations strongly indicated a role for N-CoR in the direct regulation of the Flt3 promoter.

In AML-M5, N-CoR repressive function was thought to be loss due to Akt mediated N-CoR misfolding. Thus to test the effect of misfolded N-CoR conformation on N-CoR mediated repression of the Flt3 promoter, the S1450E phosphomimetic mutant of N-CoR was utilized. It was observed that while wild-type N-CoR induced a 8 fold increase in the repression of Flt3 promoter activity, the phosphomimetic S1450E displayed a significant loss of N-CoR repressive effect on the Flt3 promoter (Fig. 3.35). These observations further suggested the active role of functional N-CoR in the repression of the Flt3 promoter.

To identify the region in the Flt3 promoter which was essential for N-CoR mediated repression, the luciferase reporter driven by various fragments of the Flt3 promoter region were utilized. The various constructs driven by the various fragments of the Flt3 promoter are depicted in figure 3.36A. Ectopic expression of N-CoR in HEK293T cells with the luciferase reporter constructs driven by the different Flt3 promoter regions revealed that the region more than 226 base pairs (bps) upstream of the Flt3 transcriptional start site was required for optimal N-CoR mediated Flt3 expression repression (Fig. 3.36B). This suggested that N-CoR and its associated co-repressor complex may bind somewhere in this region to repress Flt3 gene expression. Thus, to validate

that N-CoR suppression of Flt3 expression was via its binding to the Flt3 promoter region, association of N-CoR protein with the promoter of Flt3 was analyzed by chromatin immunoprecipitation (ChIP) assay. To better map the region of the Flt3 promoter specifically associated with N-CoR, chromatin extracts of HL60 or NB4 cells were immunoprecipitated with anti-N-CoR antibody. The DNA co-precipitated with N-CoR was amplified with primers flanking various regions of the Flt3 promoter. Primers were designed to amplify DNA in each of the following regions within the Flt3 promoter sequence, between 614 bps to 814 bps and between 75 bps to 272 bps, upstream of the transcriptional start site. Only the primers located in the 614 bps to 814 bps region upstream of the transcriptional start site in the Flt3 promoter region (Chapter 2, Fig. 2.1) was able to amplify the DNA co-precipitated with N-CoR antibody (Fig. 3.37), while the primers which amplify the 75 bps to 272 bps upstream region failed to do so (data not shown). This further suggested that N-CoR and its associated repressor complex may have bound to the Flt3 promoter through a region located in the 614 bps to 814 bps upstream region of the promoter sequence. CD36, a known N-CoR target gene, was used as a positive control in this assay.

Taken together, the data obtained thus far indicated that Flt3 repression may be brought about by the recruitment of the N-CoR repressor complex to its promoter region and loss of N-CoR in AML-M5 results in the subsequent loss of Flt3 gene repression in these cells.

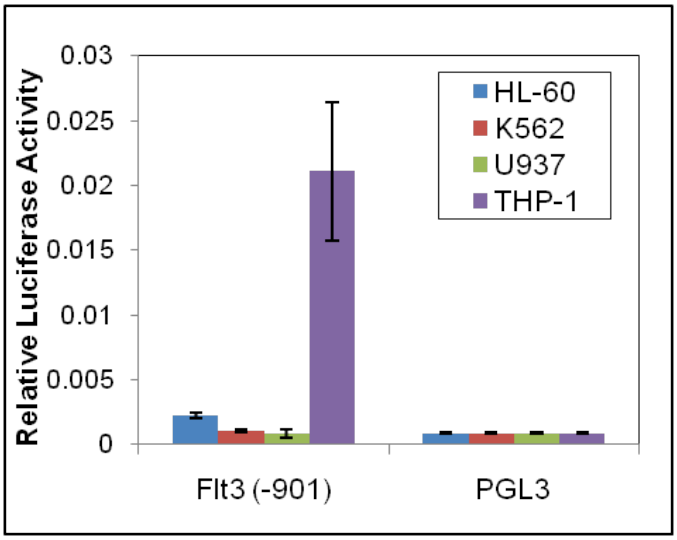

Figure 3.31. Flt3 promoter activity was up regulated in N-CoR negative cells. Relative activity of a luciferase reporter driven by the Flt3 promoter was determined in various leukemic cell lines. The cells were transfected with reporter and reference plasmids using electroporation. The values presented in each bar represent the average of three independent experiments.

A

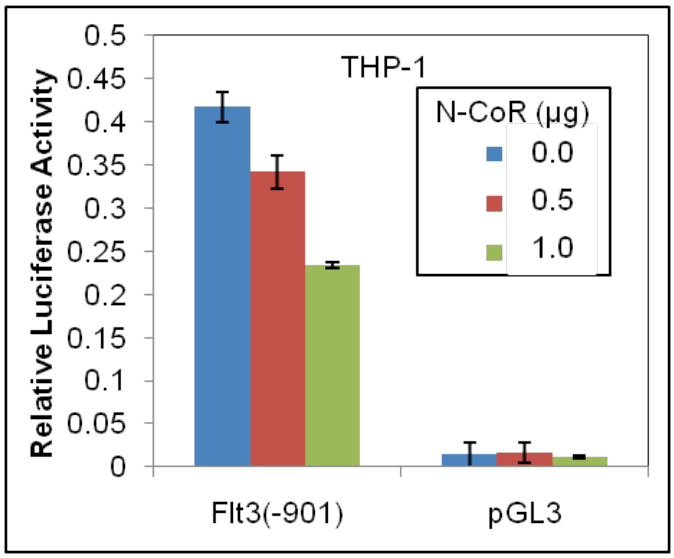

B

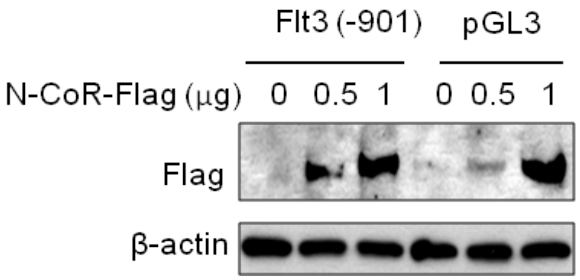

Figure 3.32. Ectopic expression of N-CoR in THP-1 cells down regulated Flt3 promoter activity in a dose dependent manner. (A) Effect of ectopic N-CoR on the activity of the Flt3 promoter in THP-1 cells electroporated with flag-tagged N-CoR plasmid in a dose dependent manner was determined via luciferase assay. The values presented in each bar represent the average of three independent experiments. (B) In parallel, levels of ectopic N-CoR protein in THP-1 cells used in the luciferase assay were determined in western blotting assay with anti-Flag antibody.

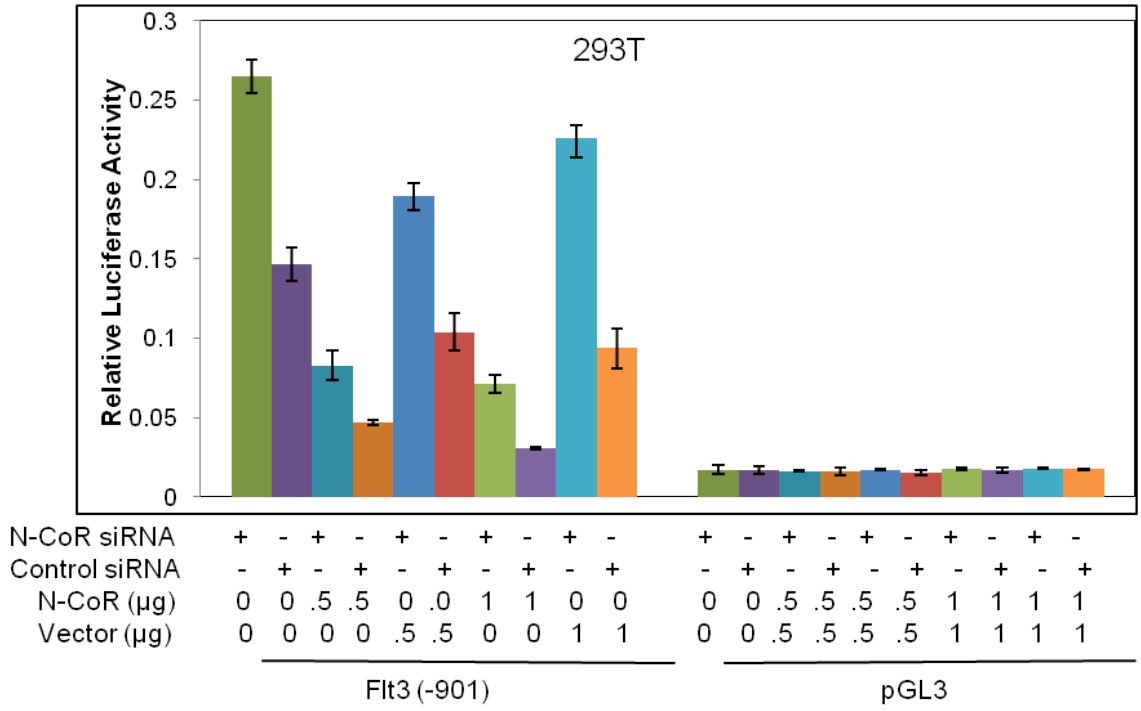

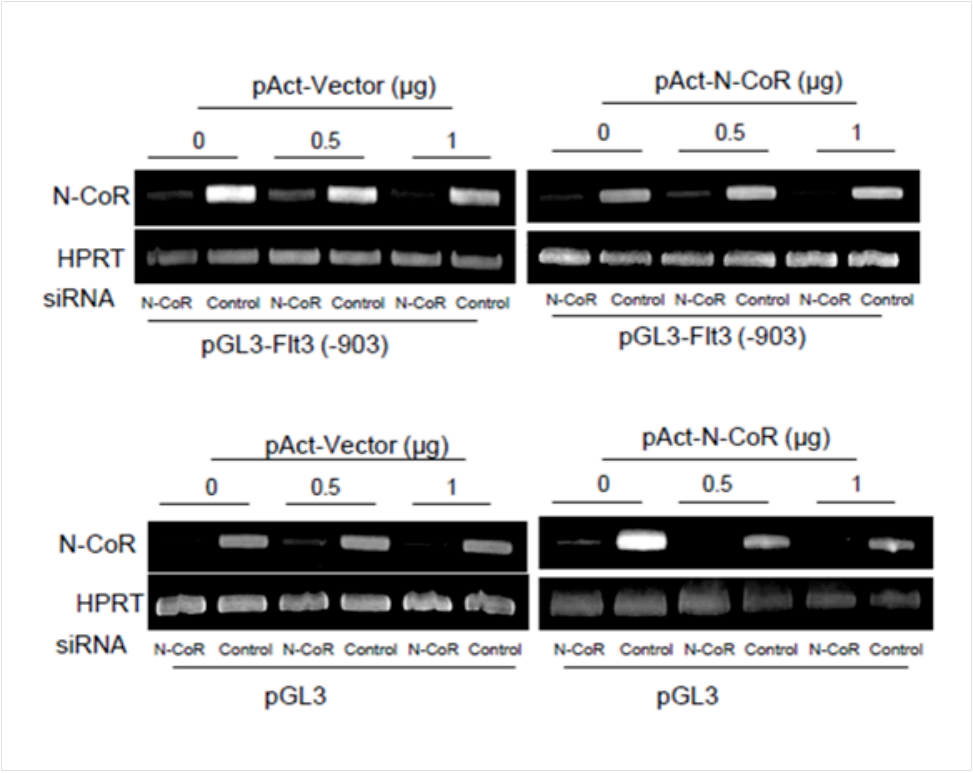

Figure 3.33. Ectopic expression of N-CoR in N-CoR ablated HEK293T cells down regulated Flt3 promoter activity in a dose dependent manner. Effect of ectopic N-CoR on the activity of the Flt3 promoter in HEK293T cells transfected with N-CoR or control siRNA was determined using luciferase assay. In pGL3-Flt3 (-901) reporter plasmid, luciferase reporter was placed under the control of the full length Flt3 promoter. The values presented in each bar represent the average of three independent experiments (upper panel). N-CoR knockdown efficiency in experiments performed was determined by RT-PCR (lower panel).

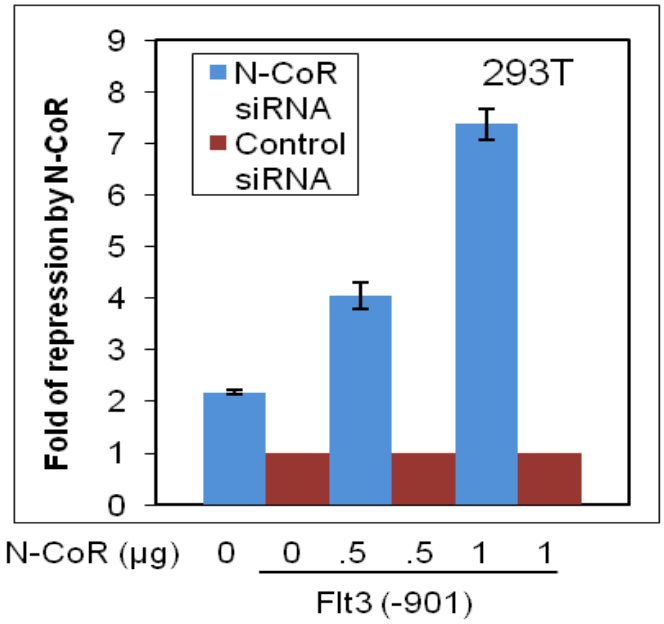

Figure 3.34. Dose dependent fold of repression of Flt3 promoter activity by ectopic N-CoR in N-CoR ablated or non-ablated cells. The dose dependent fold repression by ectopic N-CoR in N-CoR ablated or non-ablated HEK293T cells was calculated by dividing the mean relative luciferase activity in N-CoR siRNA transfected cells with that of control siRNA transfected cells of Figure 3.31.

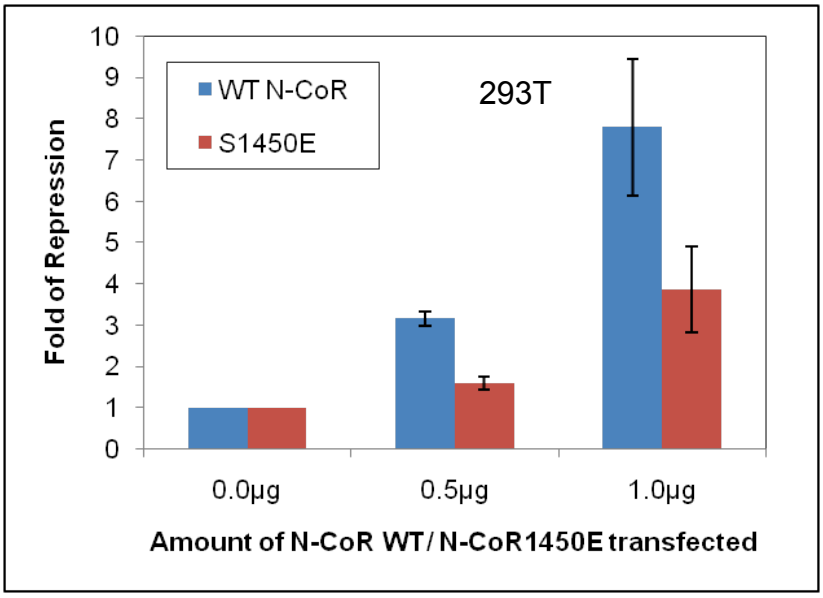

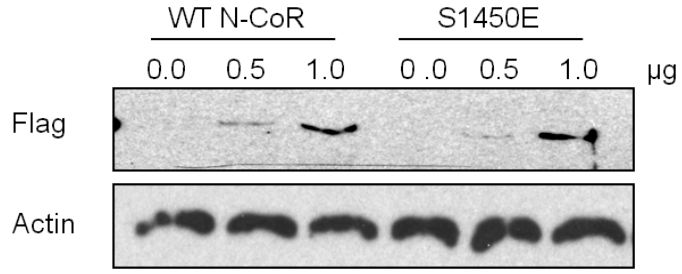

Figure 3.35. Loss of N-CoR repressive function on the Flt3 promoter due to a misfolded conformation. The dose dependent fold repression by ectopic wild type N-CoR (WT) or the N-CoR phosphomimetic S1450E on the Flt3 promoter as determined by luciferase assay (top panel). The amount of N-CoR transfected as determined by western blotting assay with anti-flag antibody (bottom panel).

A

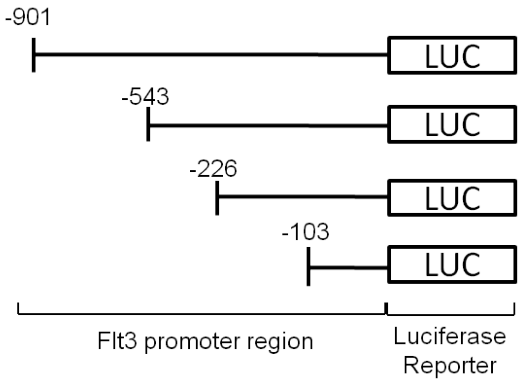

B

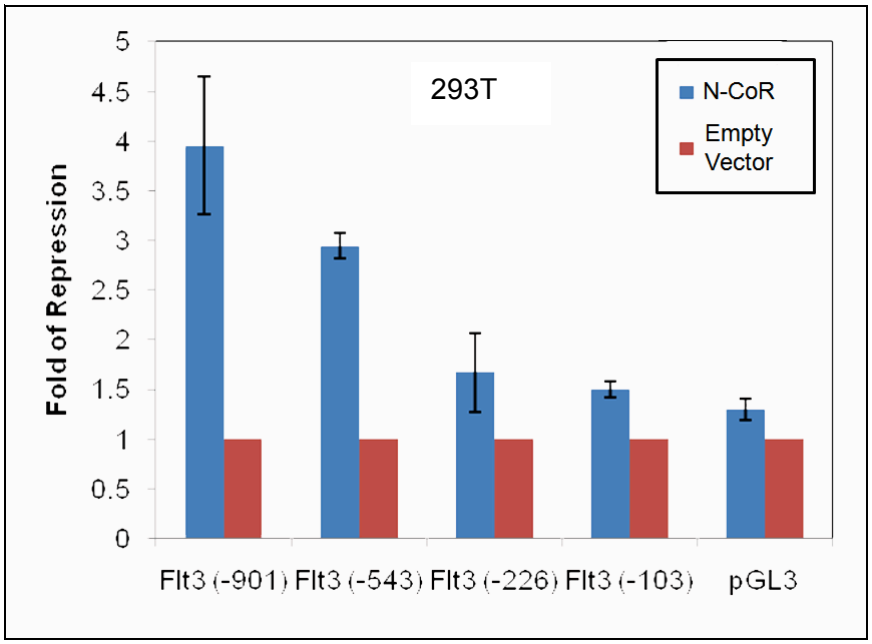

Figure 3.36. The region more than 226bps upstream of the transcriptional start site in the Flt3 promoter was required for optimal repression of the promoter activity by N-CoR. The various luciferase constructs driven by the different regions in the Flt3 promoter (A). Fold of repression of luciferase activity of the various constructs by N-CoR in HEK293T cells. The values presented in each bar represent the average of three independent experiments (B).

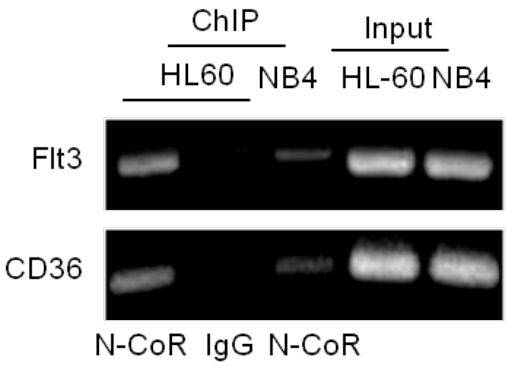

Figure 3.37. N-CoR was associated with the Flt3 promoter. Relative amounts of Flt3 promoter sequence associated with N-CoR protein in HL60 or NB4 cells were determined through ChIP assay. The antibody used in the ChIP assay is mentioned at the bottom. N-CoR association with CD36 promoter, a known N-CoR target gene, was determined as positive control.

3.2.3. N-CoR loss promoted IL-3 independent growth potential of BA/F3 cells via the up-regulation of Flt3.

Given the importance of Flt3 in the maintenance of survival and proliferative capabilities of HSCs as well as leukemic blasts, it was hypothesized that aberrant expression of the receptor due to N-CoR loss may be crucial in providing AML-M5 cells with a survival and proliferative advantage. Thus in a proof of concept approach, BA/F3 cells, an IL-3 dependent murine bone marrow-derived cell line which expressed undetectable levels of the Flt3 receptor and a high level of endogenous N-CoR was utilized in an attempt to analyze the effects of N-CoR loss and Flt3 expression, on the IL-3 independent growth properties of these cells.

First N-CoR level was ablated in BA/F3 cells via siRNA mediated gene knockdown and the level of Flt3 protein expression accessed via western blotting with an antibody which was capable of detecting the murine form of the Flt3 receptor. It was observed that in N-CoR ablated BA/F3 cells; there was an increase in the level of expression of the Flt3 protein (Fig. 3.38A). Next, the IL-3 independent growth properties of this N-CoR intact and N-CoR ablated BA/F3 cells was accessed, in the presence and absence of Flt3 ligand stimulation. It was observed that in the absence of IL-3 stimulation, N-CoR ablated BA/F3 cells had a slight proliferative advantage over non-ablated cells, with a proliferative index of about 2 times that of the non-ablated cells. When stimulated with the Flt3 ligand, this proliferative advantage was greatly enhanced to about 4 fold. This suggested that N-CoR loss promoted the IL-3 independent growth potential of BA/F3 cells and this growth capacity was

greatly potentiated by the activation of the Flt3 signaling pathway via Flt3 ligand simulation (Fig. 3.38B).

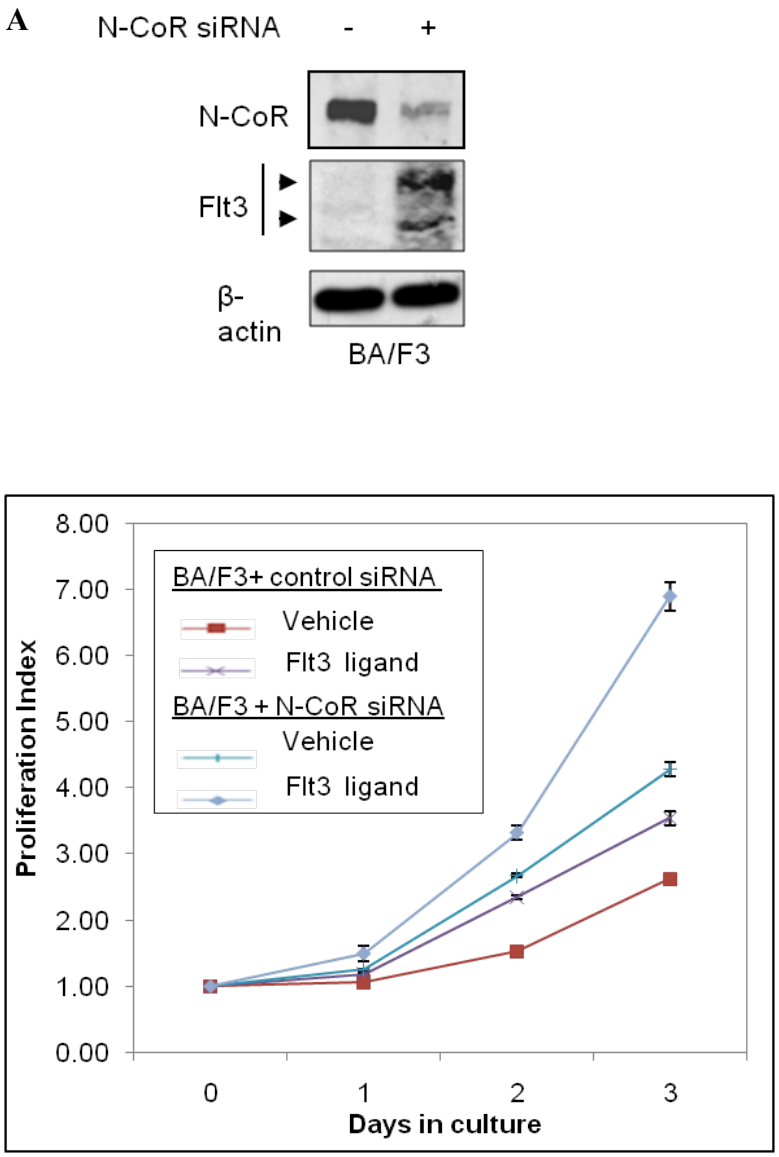

Figure 3.38. N-CoR loss promoted IL-3 independent growth potential of BA/F3 cells, potentiated by Flt3 ligand stimulation. (A) Levels of N-CoR and Flt3 protein in Ba/F3 cells transfected with control or anti-N-CoR siRNA were determined via western blotting assay with an anti-Flt3 antibody which recognizes the murine form of the receptor and N-CoR (C-20) antibody. (B) N-CoR loss mediated Flt3 expression enhanced the IL-3 independent growth potential of BA/F3 cells. Effect of IL-3 independent growth of Ba/F3 cells transfected with control or N-CoR siRNA (population from A) with and without Flt3 ligand stimulation were determined by cell proliferation assay. The Y-axis of the graph represents the proliferation index of viable cells, and the duration of culture is plotted on the X-axis. The symbols used in the graph are as follows: Control siRNA transfected cells treated with vehicle (—■—), Control siRNA transfected cells stimulated with Flt3 ligand (—×—), N-CoR siRNA transfected cells treated with vehicle (—|—) and N-CoR siRNA transfected cells stimulated with Flt3 ligand (—◆—). The values presented in each graph are average of three independent experiments.

3.2.4. N-CoR loss was potentiated by Flt3 signaling activation.

With the observations in BA/F3 cells and findings which linked Akt activity to misfolded conformation dependent N-CoR loss, it was thought that Flt3 signaling activation by the Flt3 ligand might have resulted in the potentiation of N-CoR loss. This may result in the amplification of the growth advantage mediated by N-CoR loss in AML-M5. Therefore, to test this hypothesis, the effect of Flt3 ligand stimulation on the level of N-CoR protein in HEK293T cells in the presence or absence of the Flt3 receptor was accessed. As shown in figure 3.39A, Flt3 ligand stimulation down-regulated N-CoR protein levels in HEK293T cells in a Flt3 receptor dependent manner. Down regulation of the 160 kDa membrane bound form of the Flt3 receptor due to receptor internalization after ligand binding was used to access for Flt3 signaling induction by the Flt3 ligand.

To investigate whether N-CoR loss in AML-M5 cells was potentiated by Flt3 activation, it was hypothesized that the blockade of Flt3 ligand binding to the Flt3 receptor would result in some stabilization of the N-CoR protein in THP-1 cells. Thus, selective blockade of Flt3 receptor with Flt3 antibody in THP-1 cells followed by Flt3 ligand stimulation was conducted. In this experiment it was observed that the inability of the Flt3 ligand to bind to the Flt3 receptor as indicated by the loss of receptor internalization resulted in the stabilization N-CoR protein in THP-1 cells in a dose dependent manner (Fig. 3.39B). These data suggested that an oncogenic stimulus which promotes cellular growth through Flt3 activation could amplify Flt3 mediated survival by further inducing N-CoR loss and receptor expression up regulation.

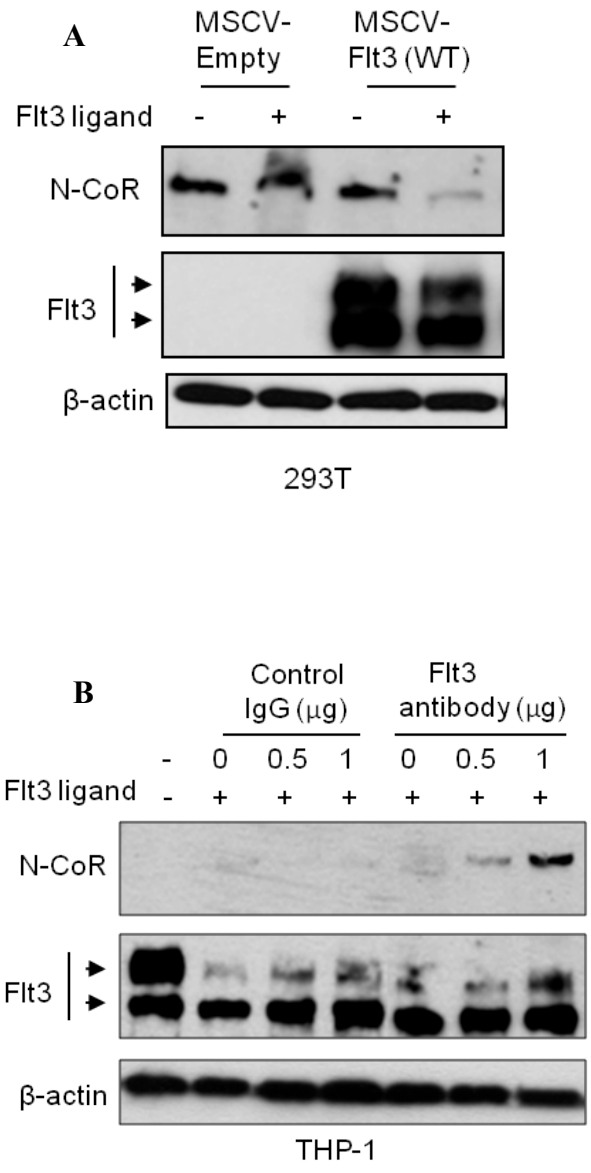

Figure 3.39. N-CoR loss promoted growth potential which was amplified by Flt3 signaling activation. (A) Flt3 stimulation leads to N-CoR loss. Levels of N-CoR and Flt3 proteins in HEK293T cells treated with vehicle or Flt3 ligand (30 ng/ml) was determined by western blotting assay. (B) Blocking Flt3 stimulation leads to N-CoR stabilization in THP-1 cells. Effect of Flt3 antibody on the levels of N-CoR and Flt3 proteins in THP-1 cells treated with vehicle or Flt3 ligand (30 ng/ml) was determined by western blotting assay.

3.2.5. A potential tumor suppressive role for N-CoR via Flt3 expression regulation.

The data collected thus far suggested that N-CoR may have a tumor suppressive role in normal hematopoiesis by restricting the proliferative capabilities of HSCs and its multi-potential progenitors via its regulation of pro-survival signaling receptors such as Flt3. Its resulting loss of function due to MCDL of N-CoR protein may contribute to the acquisition of tumorigenicity in AML-M5 by enhancing the survival and growth potentials of the leukemic cells. Therefore, in an attempt to validate this hypothesis, the expression levels of N-CoR and Flt3 during the progression of normal hematopoiesis was first accessed. qRT-PCR analysis of N-CoR and Flt3 transcript levels in mouse HSCs/progenitor cells and committed cells of various lineages purified using multi-parametric Flow Cytometry was conducted. Here, N-CoR transcript levels was observed to be up-regulated in a progressive manner as the fractions were purified for the more matured myeloid cell phenotype when compared to levels expressed in total bone marrow. The lowest expression levels were found in the c-kit^{+} stem cell/progenitor cell population and the highest in the mature monocyte/ granulocyte and erythrocyte populations. This observed N-CoR transcript up-regulation was accompanied by the concurrent down-regulation of Flt3 mRNA expression in these populations (Fig. 3.40).

Next, to investigate the effects of this increased N-CoR expression on the commitment of HSCs/ progenitor cells towards the myeloid lineage, the effect of enforced N-CoR expression on the growth and maturation of c-Kit^{+} HSC/progenitor cells was determined. Mouse bone marrow (BM) cells were

first transduced with either the MSCV-IRES-GFP-N-CoR or control vector MSCV-IRES-GFP and FACS purified GFP positive c-Kit$^+$ cells were isolated and accessed for their growth and differentiation properties. In methylcellulose colony formation assay, it was observed that MSCV-IRES-GFP-N-CoR infected c-Kit$^+$ cells made significantly fewer colonies when compared to MSCV-IRES-GFP infected cells (Fig. 3.41, right upper panel). Moreover, when the morphology of cells present in these colonies was analyzed by Wright-Giemsa staining, cells derived from the MSCV-IRES-GFP-N-CoR infected colonies displayed morphological feature of matured myeloid cells (Fig. 3.41, right lower panel). To better identify the phenotypes of cells after enforced N-CoR expression, long-term culture initiating cell assay (LTC-IC) was employed. In this assay it was observed that a relatively higher percentage of granulocyte (G), macrophage (M), and granulocyte-macrophage (GM) colonies were found in MSCV-IRES-GFP-N-CoR infected cells compared to cells infected with MSCV-IRES-GFP (Fig. 3.42A and B). This suggested that enforced N-CoR expression in immature hematopoietic cells led to their maturation towards the myeloid lineage.

To access the effect of N-CoR on the re-populating capacity of HSCs *in vivo*, around 5x10^5 BM MNCs infected with MSCV-IRES-GFP-N-CoR or control vector were implanted intravenously into sub-lethally irradiated recipient mice and the number of GFP positive cells in the peripheral blood of the recipient mice was analyzed by FACS 3, 6 and 10 weeks after implantation. At all time points, the percentage of GFP positive cells in the peripheral blood of MSCV-IRES-GFP-N-CoR transplanted mice was significantly lower when compared to those of mice transplanted with the

control vector (Fig. 3.43) indicating that N-CoR expression in the HSCs inhibited their re-populating capacity.

These findings collectively suggested a role for N-CoR in the suppression of growth and survival potentials required for the maturation and commitment of HSCs/ progenitor cells toward the myeloid lineage probably through the loss of expression of pro-survival receptors such as Flt3. Thus it was hypothesized that N-CoR loss in AML-M5 possibly disrupts this tumor suppressive function resulting in subsequent disease pathogenesis.

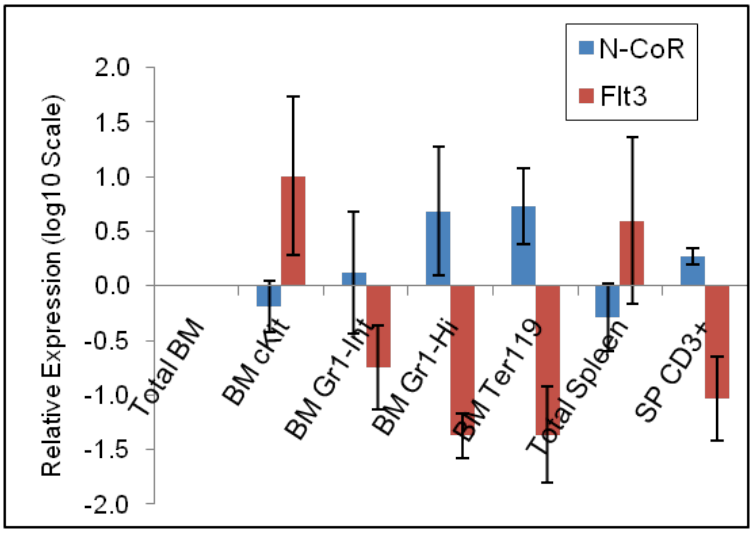

Figure 3.40. Stepwise up-regulation of N-CoR transcript levels as HSCs mature towards the myeloid lineage, accompanied by the concurrent down regulation of Flt3 transcript levels. Levels of N-CoR and Flt3 transcripts in purified mouse hematopoietic cells were determined by qRT-PCR analysis. The values presented in the graph are average of three independent experiments**.**

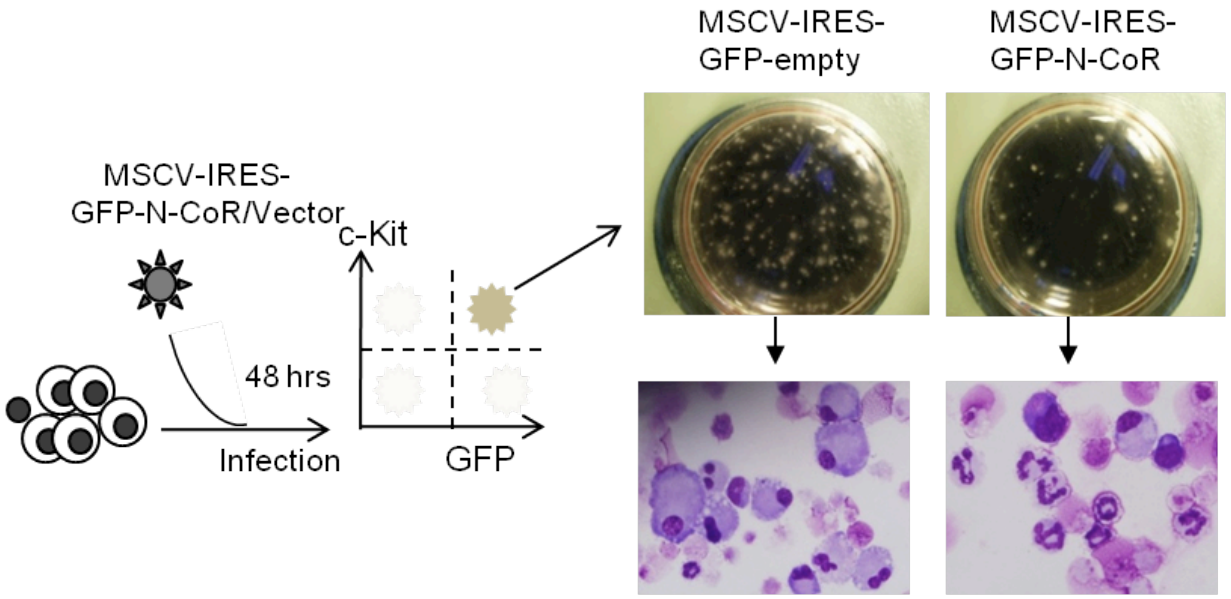

Figure 3.41. Enforced N-CoR expression in c-Kit$^+$ stem cell/progenitor cells inhibits their self-renewal potential. Growth and self-renewal potentials of purified mouse stem cells transduced with MSCV-IRES-GFP-N-CoR or empty vector were determined in colony formation assay and Wright-Giemsa staining.

A

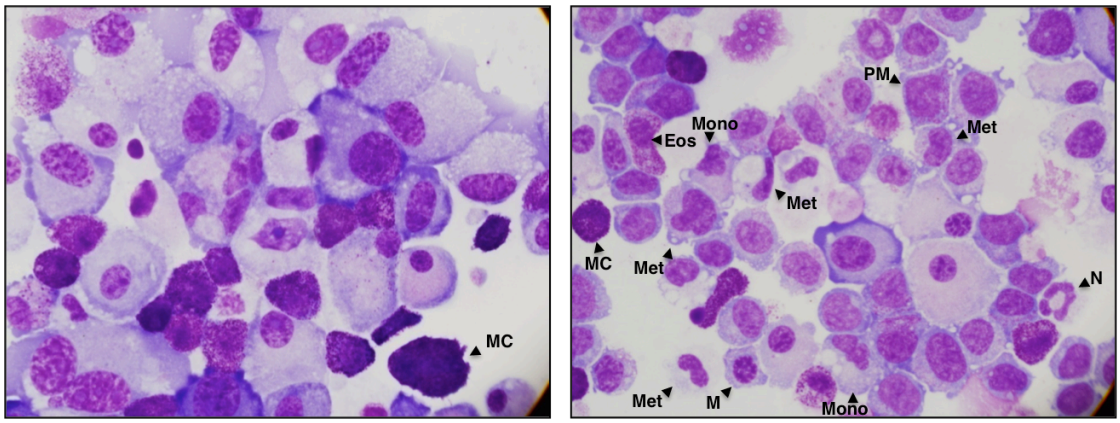

B

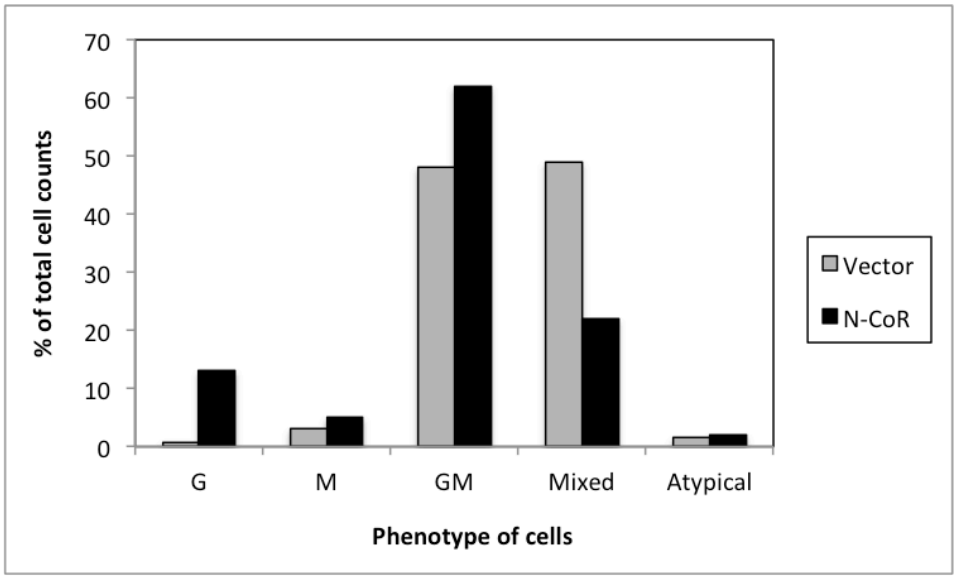

Figure 3.42. Enforced N-CoR expression in c-Kit$^+$ stem cell/progenitor cells induced myeloid lineage differentiation. Morphology of purified mouse bone marrow cells transduced with MSCV-IRES-GFP-N-CoR or control vector was determined with Wright-Geimsa staining where Eosinophils (Eos), mast cells (MC), meta-myelocytes (Met), monocytes (Mono), Myelocytes (M), neutrophils (N) and promyelocytes (PM) are labeled (A). The phenotype of cells scored against total cell count and represented as a histogram (B).

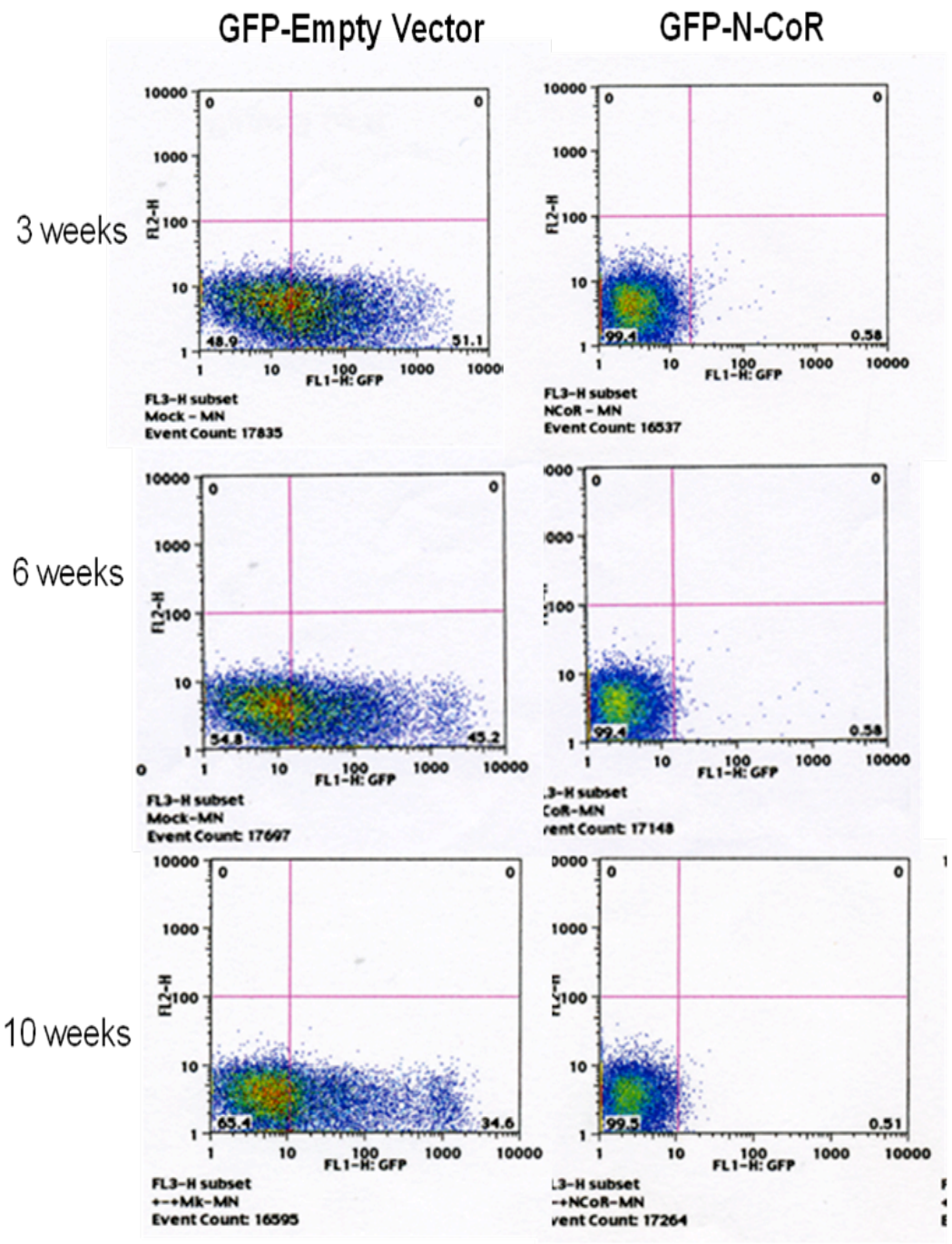

Figure 3.43. Enforced N-CoR expression inhibited the growth and repopulating potential of c-Kit$^+$ stem cell/progenitor cells *In* vivo. 5 x 10^5 transfected BM cells were transplanted intravenously into sub lethally irradiated C57BL/6 mice (8 Gy). The recipient mice were examined at week 3, 6 and 10 for blood cell counts and GFP positivity in peripheral blood.

3.2.6. Restoration of N-CoR tumor suppressive function down-regulated Flt3 expression and induced terminal differentiation of AML-M5 cells.

To validate the hypothesis, the effects of N-CoR function restoration in the AML-M5 cell line THP-1 on the growth and proliferative properties of the cells were tested. Utilizing Genistein, a drug which our laboratory had previously shown to restore N-CoR native properties in AML-M5 cells, the effect of Genistein induced restoration of N-CoR function on Flt3 expression in THP-1 was first accessed. It was observed that in THP-1 cells, Genistein down-regulated Flt3 expression at both the transcript and protein levels with maximum loss of expression occurring at 50 μM, the dose which most effectively restored N-CoR expression (Fig. 3.44).

Next the effect of N-CoR restoration and Flt3 down regulation on the proliferative properties of THP-1 cells was tested via MTT assay. Here, a dose dependent inhibition of the growth capacity of treated cells was observed. This inhibition was most pronounced again at the dose of 50 μM (Fig. 3.45). Morphological analysis via Wright-Giemsa Staining of treated cells, revealed that this growth inhibition was likely due to the relieve of differentiation arrest as a significant number of Genistein-treated THP-1 cells displayed characteristics of matured monocytic cells such as horseshoe-shaped nuclei (Fig. 3.46A). Genistein induced differentiation progression was further supported by the ability of Genistein to up-regulate the level of CD14, a marker for myeloid/monocytic lineage maturation in THP-1 cells in a dose dependent manner when analyzed by FACS and RT-PCR analysis (Fig. 3.46B and C). This suggested that Genistein induced growth arrest in THP-1 cells

was likely a due to the restoration of the ability of these cells to progress in myeloid/ monocytic lineage differentiation.

Next, in order to determine if the restoration of N-CoR function had a role in this progression in differentiation, siRNA mediated N-CoR knockdown in THP-1 cells was performed and the ability of these cells to differentiate after Genistein treatment was investigated. The expression level of the monocytic cell maturation marker CD14 at the transcript level was used as an indicator for progression of differentiation. It was observed that in the cells where N-CoR was knocked down, there was no restoration of N-CoR protein expression and Flt3 levels were not reduced compared to the non-ablated cells. CD14 transcript levels after Genistein treatment was also not significantly induced in the N-CoR ablated cells (Fig. 3.47), indicating that N-CoR function was necessary in Genistein induced Flt3 down regulation and the subsequent growth inhibition and differentiation progression of THP-1 cells.

Collectively, these observations suggested that N-CoR may have an essential role in the progression of myeloid cell maturation in normal hematopoiesis and its aberrant loss in AML-M5, contributes to disease pathogenesis by augmenting the survival and proliferative capacities of these cells via the aberrant re-expression of pro-survival receptors such as Flt3.

The dynamic role of natively folded and misfolded N-CoR protein in the growth promoting function of Flt3 has been presented schematically in figure 3.48. In the absence of N-CoR protein, Flt3 levels are maintained at a relatively higher level during the growth and self-renewal of immature hematopoietic cells. However, as these cells proceed towards maturation, N-CoR levels are gradually up regulated, leading to the down regulation of Flt3

levels and suppression of cellular growth and self-renewal potentials (Fig. 3.48, top panel). In AML-M5 cells, loss of N-CoR function due to Akt mediated misfolding abolishes its repressive control on the Flt3 gene, leading to the restoration of Flt3 expression and ectopic re-activation of cellular self-renewal and growth potentials (Fig. 3.48, lower panel).

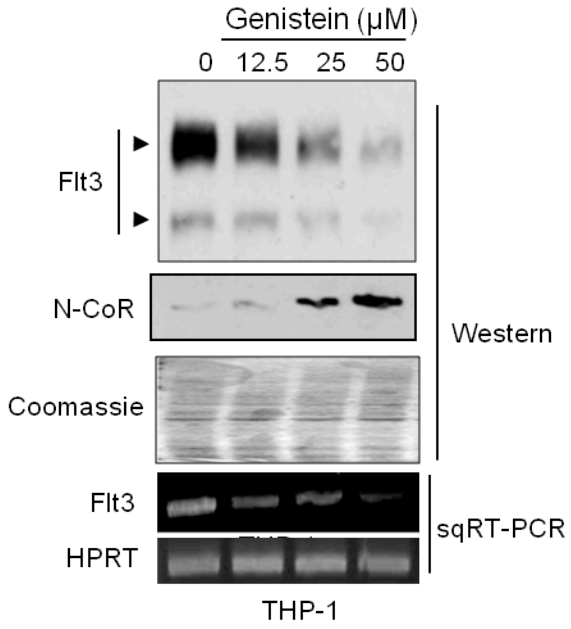

Figure 3.44. Flt3 levels were down regulated at both the protein and mRNA levels after Genistein treatment. Level of Flt3 expression was determined via western blotting and semi-quantitative RT-PCR analysis.

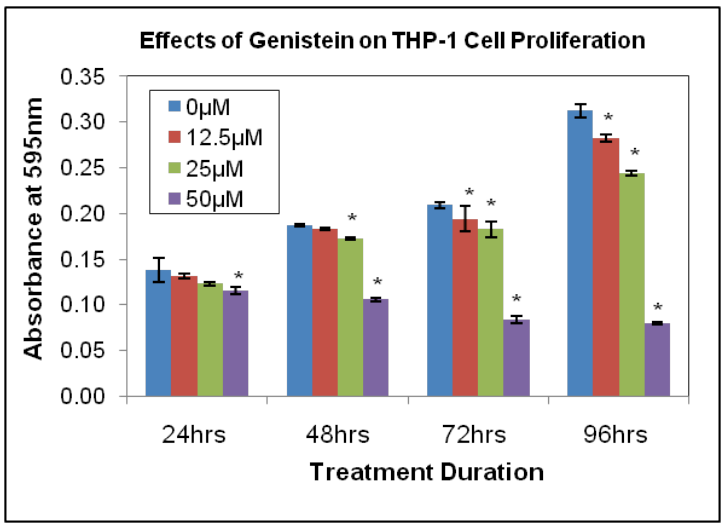

Figure 3.45. Genistein inhibited the proliferation of THP-1 cells. Genistein inhibited the proliferation of THP-1 cells in a dose dependent manner when determined via growth proliferation assay (MTT). Results are representative of 3 independent experiments and asterisks represent $p<0.05$ as determined by unpaired student-t test.

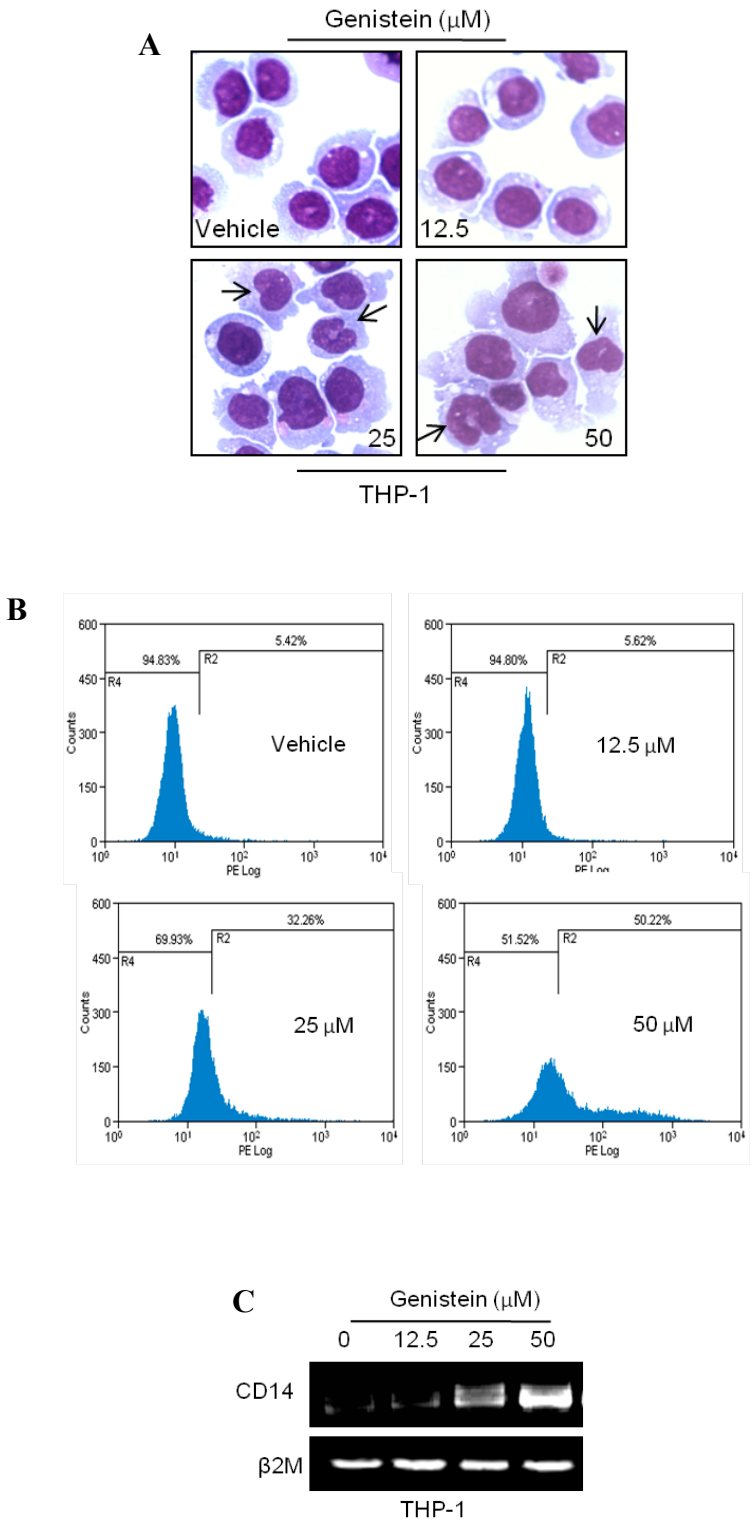

Figure 3.46. Genistein induced THP-1 differentiation progression. (A) Nuclear morphology of THP-1 cells treated with Genistein for the duration of 72 hours in a dose dependent manner was determined in Wright–Giemsa assay. The arrowheads mark the indented-shaped nucleus of differentiated cells. (B) & (C) CD14 levels in THP-1 cells treated with Genistein for 72 hours in a dose dependent manner was determined by FACS (B) and semi-quantitative RT-PCR (C) analysis.

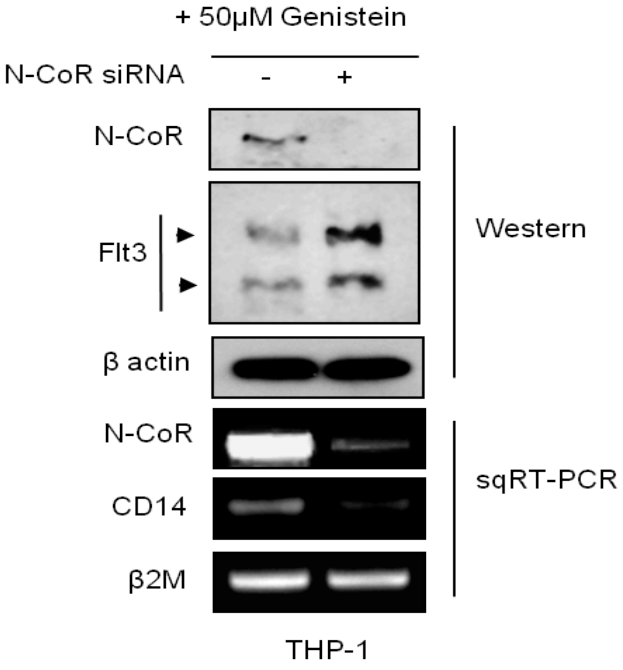

Figure 3.47. N-CoR was required for Genistein induced THP-1 differentiation progression. N-CoR, Flt3 and CD14 levels in THP-1 cells transfected with N-CoR siRNA and treated with 50 μM Genistein for 72 hours was determined by western blotting assay and RT-PCR analysis.

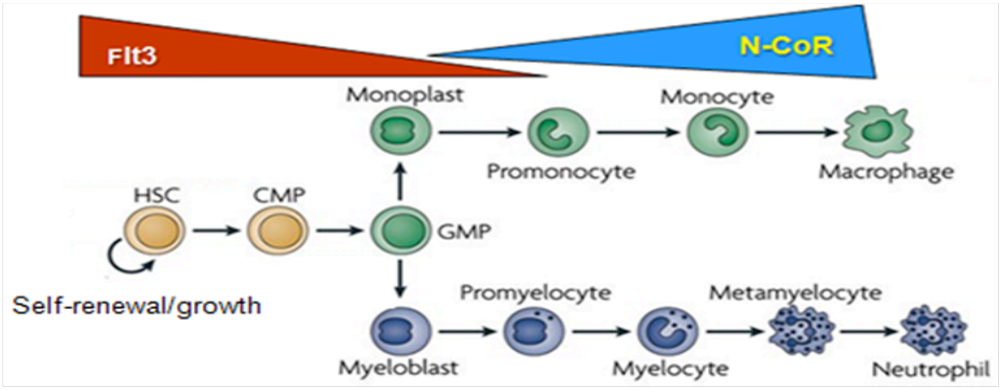

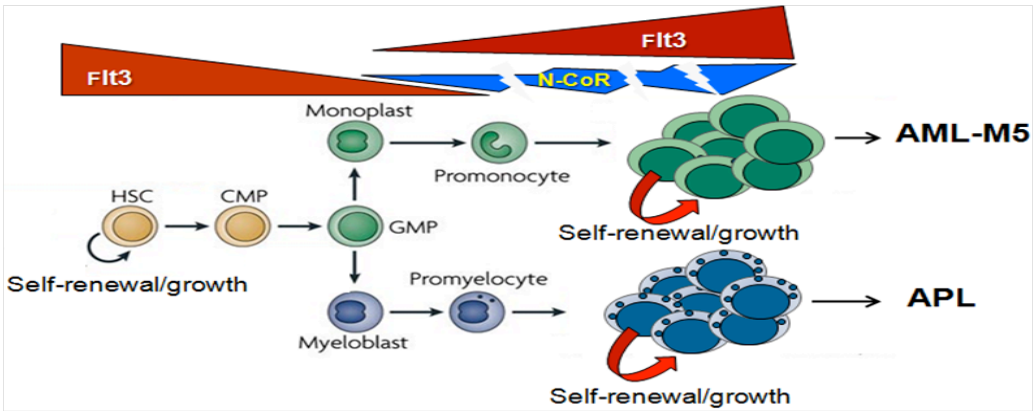

Figure 3.48. Schematic representation of N-CoR-induced suppression of Flt3 in normal and leukemic cells. In the absence of N-CoR, Flt3 level is maintained at relatively higher level in immature hematopoietic cells, contributing to their increased growth and self-renewal potentials. However, as these cells proceed towards maturation, N-CoR level is gradually up regulated resulting in the suppression of Flt3 level and down-regulation of cellular growth and self-renewal potentials. Due to the loss of misfolded N-CoR protein in AML-M5 cells, Flt3 level is up regulated and AML-M5 cells regain the growth and self-renewal advantages (lower panel).

3.3. Targeting the N-CoR MCDL pathway as a therapeutic strategy in AML-M5.

3.3.1. Targeting the clearing of misfolded N-CoR.

The data collected in the previous studies conducted in APL and in this thesis, suggested that the misfolded conformational loss of N-CoR was a two-stage process. The first stage in the process of N-CoR loss was the aberrant post translational modification of N-CoR protein brought about by an oncogenic insult such as hyper-activation of Akt in AML-M5 or the expression of the fusion oncogene PML-RARα in APL[62]. This was followed by the activation of the proposed third arm of the unfolded protein response (UPR) - the 'late' cytoprotective UPR arm resulting in the subsequent proteolytic clearing of this misfolded N-CoR in the leukemic cells.

The clearing of misfolded N-CoR during the activation of 'late' cytoprotective UPR in APL had been previously shown to prevent the accumulation ER stress brought about by misfolded N-CoR to a level which would trigger cell death[63]. A similar cytoprotective UPR mechanism was also thought to be present in AML-M5, allowing these cells to circumvent ER stress induced cell death due to the accumulation of misfolded N-CoR protein. The involvement of a heat liable protease in the clearing of misfolded N-CoR in AML-M5 was suggested in this thesis. It was shown that the inhibition of this protease activity by protease inhibitors were able to prevent misfolded N-CoR clearing, resulting in the accumulation of ER stress in AML-M5 cells (Fig. 3.4A, 3.5B and Fig. 3.8B). It was thought that this inhibition would result in the accumulation of ER stress beyond the threshold level needed to initiate cell death.

Thus to validate this thought, the effects of AEBSF and Kaletra on the proliferation of THP-1 cells was carried out using MTT assay. In this assay, it was observed that both AEBSF and Kaletra were able to induce a dose dependent inhibition of cell proliferation in THP-1 cells; with the maximum inhibition occurring at the dose which most effectively prevented misfolded N-CoR clearing (Fig. 3.49). After both AEBSF and Kaletra treatment, treated cells displayed a distinct morphology characterized by fragmented nuclei and shrinkage of the cytoplasm, suggesting apoptotic cell death (Fig. 3.48). AEBSF treated THP-1 cells also displayed a clear dose dependent increase in apoptotic cells as indicated by Annexin V and Propidium Iodide (PI) staining. The percentage of apoptotic cells was the highest at the dose which most effectively stabilized N-CoR and displayed the highest ER stress levels (Fig. 3.50). This indicated that the protease inhibitors blocked the clearing of misfolded N-CoR resulting in the accumulation of ER stress to levels beyond the survival threshold leading to cell death.

The selectivity of protease inhibitors for APL was previously reported and similarly, both the protease inhibitors tested showed a selective sensitivity to AML-M5 derived cell liines when cell proliferation after treatment was accessed in both AML-M5 and non-AML-M5 derived cell lines (Fig 3.52A and B).

A

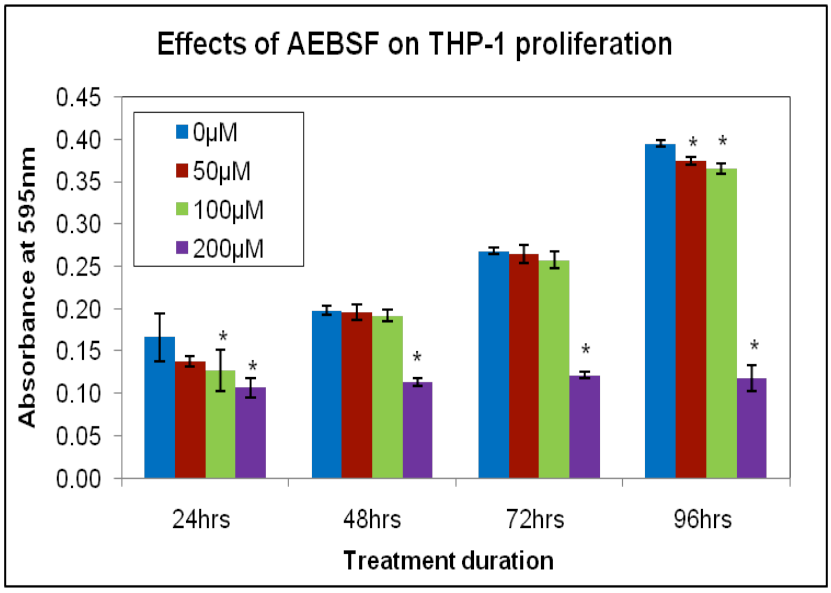

B

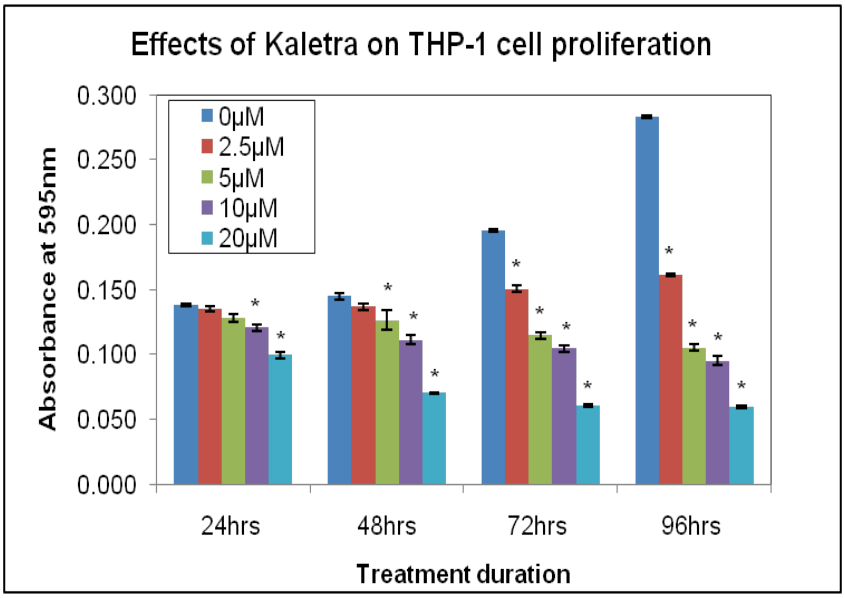

Figure 3.49. Protease Inhibitors, AEBSF and Kaletra inhibited the proliferation of THP-1 cells. AEBSF (A) and Kaletra (B) inhibited the proliferation of THP-1 cells in a dose dependent manner when determined via growth proliferation assay (MTT). Results are representative of 3 independent experiments and asterisks represent $p<0.05$ as determined by unpaired student-t test.

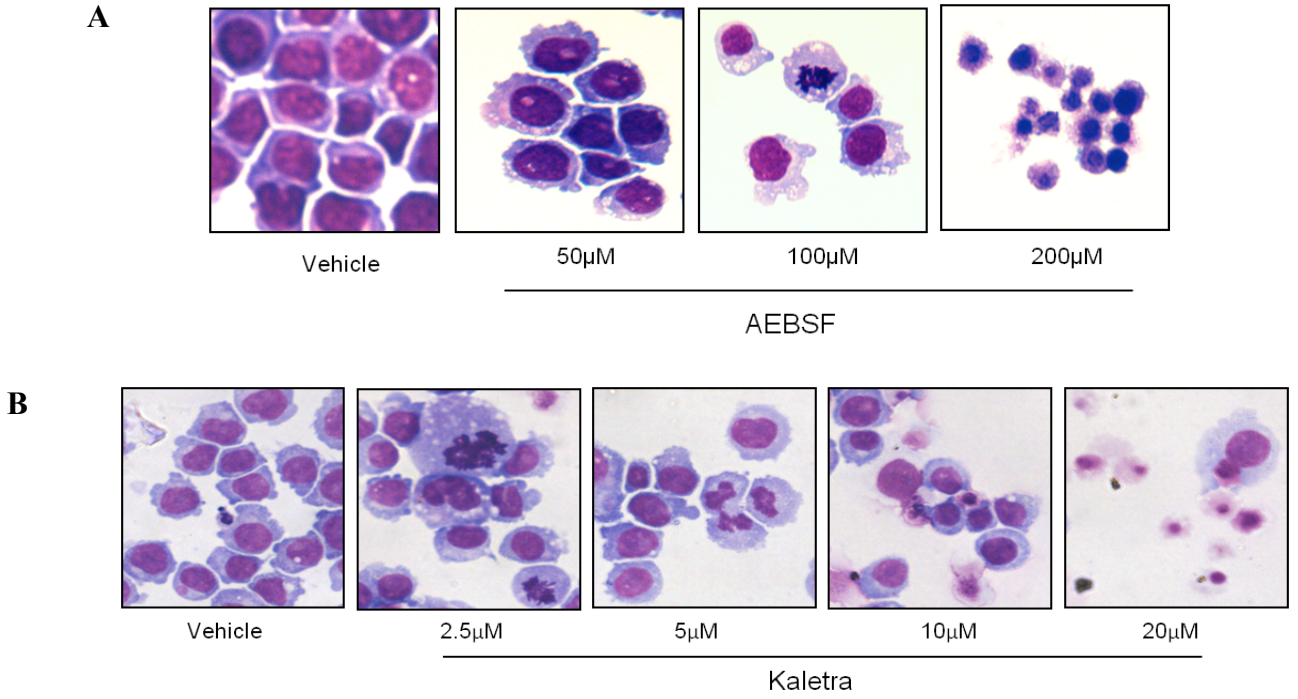

Figure 3.50. Both AEBSF and Kaletra treated cells displayed morphological characteristics of apoptotic cell death. The morphology of THP-1 cells treated with AEBSF (A) or Kaletra (B) in a dose dependent manner for a total duration of 72 hours was determined by Wright-Giemsa staining.

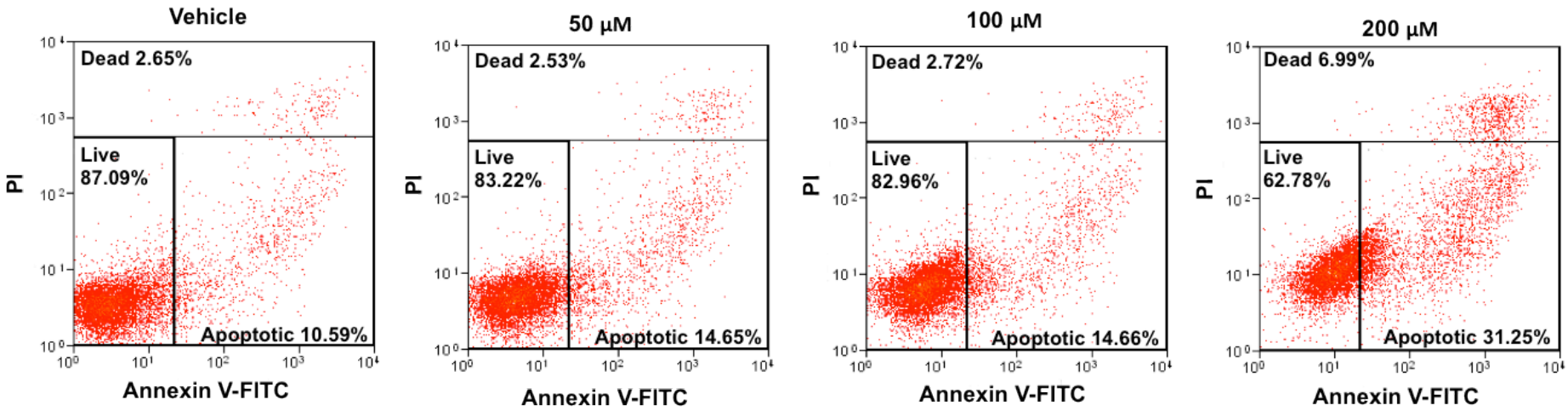

Figure 3.51. AEBSF treated cells displayed characteristics of apoptotic cell death. Annexin V and PI staining of THP-1 cells treated with AEBSF in a dose dependent manner for a total duration of 72 hours was determined by Flow cytometric analysis. There was a dose dependent increase in the percentage of apoptotic cells after AEBSF treatment.

A

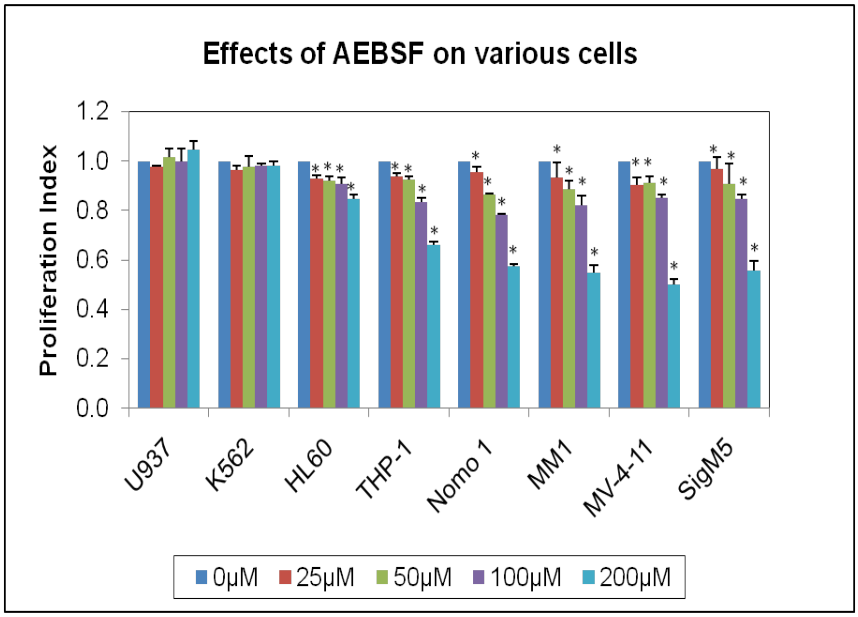

B

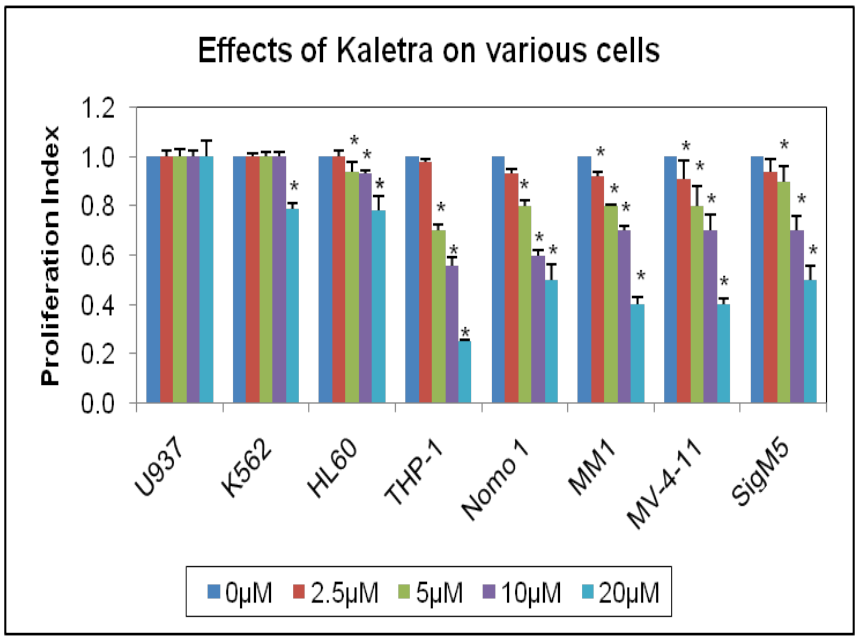

Figure 3.52. Protease Inhibitors AEBSF and Kaletra promote selective growth arrest of AML-M5 derived cell lines. Growth of AML-M5 (THP-1, Nomo-1, MM1, MV-4-11 and SigM5) and non-AML-M5 (U937, K562 and HL60) derived cell lines treated with AEBSF (A) or Kaletra (B) in a dose-dependent manner for a total duration of 72 hours was determined though MTT based cell proliferation assay. The value presented in each bar graph is average of three independent experiments asterisks represent $p<0.05$, as determine by unpaired student-t test.

3.3.2. Targeting the misfolding of N-CoR.

In APL, N-CoR misfolding was brought about by its association with the fusion oncogene PML-RARα. Compounds which target this association such as All-Trans-Retinoic acid and Genistein disrupts the association thus resulting in the return of N-CoR native conformation and function[58,62] which eventually results in terminal differentiation and cell death.

In AML-M5, it was observed that N-CoR misfolded conformation was initiated by the phosphorylation of N-CoR by Akt activity. Thus, drugs which inhibit this phosphorylation event would pose as good candidates for AML-M5 therapy. Previously, it was observed that Genistein, a kinase inhibitor was able to restore N-CoR native properties (Fig. 3.5A and Fig 3.6C) and relieve the differentiation block in AML-M5 (Fig. 3.43 and Fig. 3.45). The blockade of N-CoR misfolding was thought to be through the inhibition of Akt kinase activity in AML-M5 and this was validated by western blotting assay. In THP-1 cells, it was observed that Akt kinase activity was inhibited in a dose dependent manner as indicated by the dose dependent reduction of phospho-Akt (Ser473) after Genistein treatment (Fig. 3.18A). Similarly, inhibition of Akt activity by the Akt specific inhibitor Akti-X was also observed to bring about the restoration of N-CoR native conformation (Fig. 3.13). Akti-X was observed to inhibit THP-1 cell proliferation in a dose dependent manner when its effect on cell growth was accessed via MTT assay (Fig. 3.53). After Akti-X treatment, treated cells displayed a distinct morphology characterized by fragmented nuclei and shrinkage of the cytoplasm, suggesting apoptotic cell death (Fig. 3.54). This growth inhibition by Genistein and Akti-X was also

found to be selective to AML-M5 derived cell lines when compared to their effects on non-AML-M5 derived cell lines (Fig. 3.55).

The selectivity of protease inhibitors and agents which prevent Akt mediated N-CoR misfolding indicate a possible role of MCDL of N-CoR in the selective growth inhibition of AML-M5 leukemic cells. This illustrates the promise of targeting the N-CoR MCDL pathway as a therapeutic strategy in AML-M5.

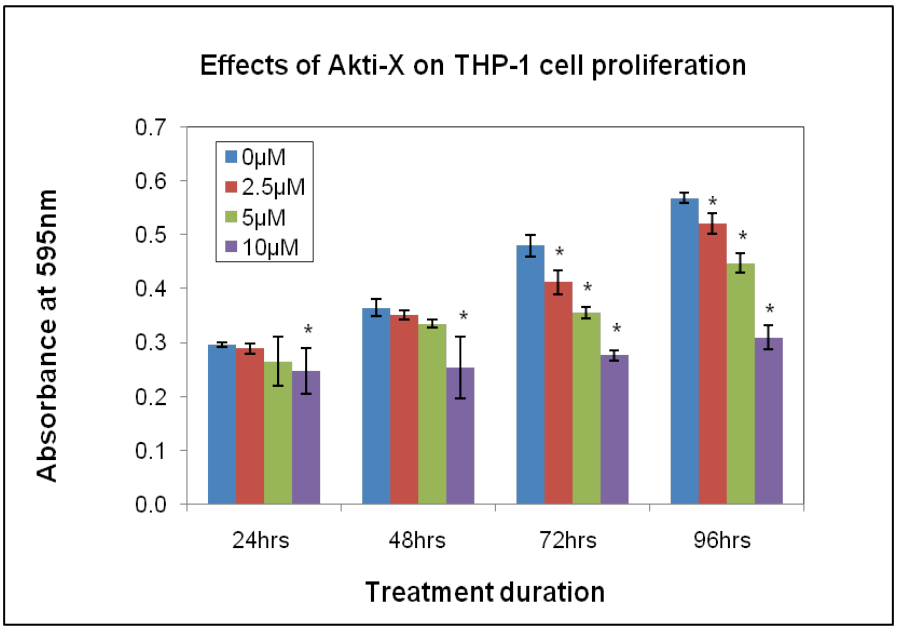

Figure 3.53. Akti-X inhibited the proliferation of THP-1 cells. Akti-X inhibited the proliferation of THP-1 cells in a dose dependent manner when determined via growth proliferation assay (MTT). Results are representative of 3 independent experiments and asterisks represent $p<0.05$ as determined by unpaired student-t test.

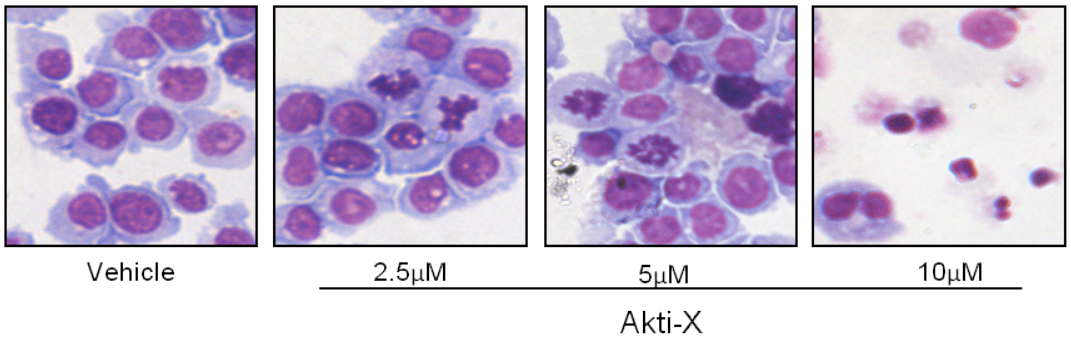

Figure 3.54. Akti-X treated cells displayed morphological characteristics of apoptotic cell death. The morphology of THP-1 cells treated with Akti-X in a dose dependent manner for a total duration of 72 hours was determined by Wright-Giemsa staining.

A

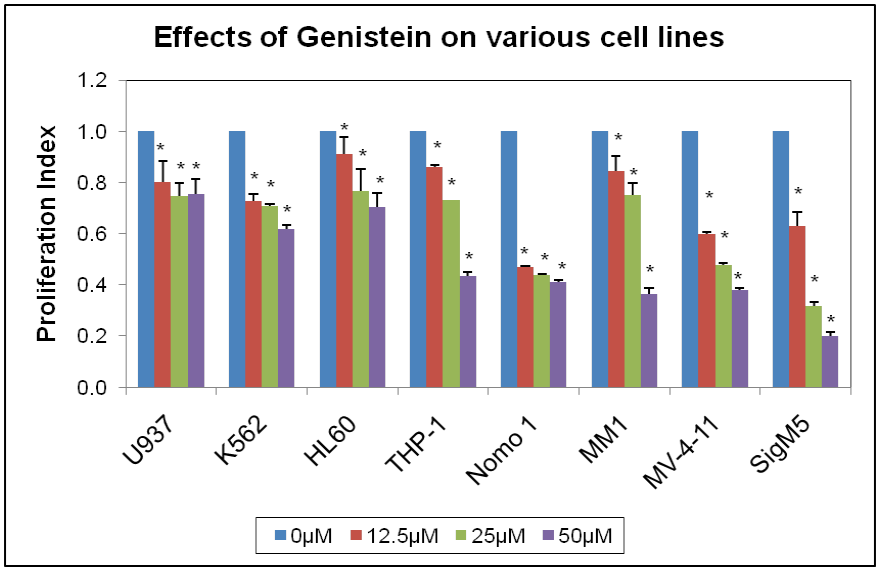

B

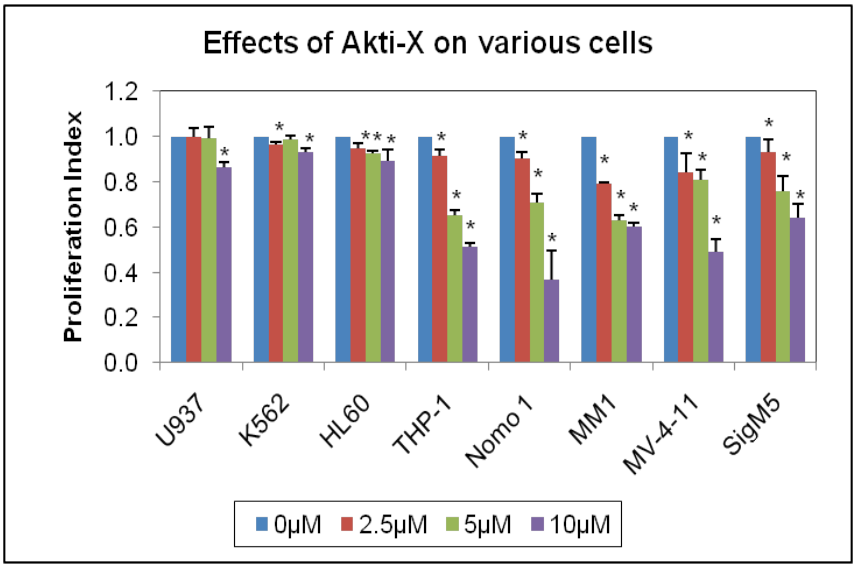

Figure 3.55. Kinase Inhibitors Genistein and Akti-X promote selective growth arrest of AML-M5 derived cell lines. Growth of AML-M5 (THP-1, Nomo-1, MM1, MV-4-11 and SigM5) and non-AML-M5 (U937, K562 and HL60) derived cell lines treated with Genistein (A) or Akti-X (B) in a dose-dependent manner for a total duration of 72 hours was determined though MTT based cell proliferation assay. The value presented in each bar graph is average of three independent experiments asterisks represent $p<0.05$, as determine by unpaired student-t test.

CHAPTER 4

Discussion

4. DISCUSSION

4.1 Misfolded Conformational Dependent Loss (MCDL) of N-CoR in AML-M5.

4.1.1 Identification of APL-like N-CoR MCDL in AML-M5.

In our initial screening, we identified APL-like MCDL of N-CoR in multiple cell lines from AML of the M5 subtype, where the presence of the 100 KDa N-CoR band and in vitro cleavage activity was consistant in all the cell lines derived from this subtype of AML. In the cell lines which were derived from the other FAB subclasses of AML (an average of 2 cell lines from each FAB subclass), the protein expression of full length N-CoR was not as uniform across cell lines derived from the each FAB subclass as that observed in AML-M5 (data not shown). Furthermore, the 100 KDa cleaved N-CoR band and in vitro N-CoR cleaving activity was only observed in cell lines derived from the M3 (APL) and M5 subtype (data not shown). As we did not look at the N-CoR transcript levels in all these cell lines, it is unclear if the lack of N-CoR protein expression in some of these cell lines was due to the suppression of N-CoR transcript levels. More cell lines and primary patient specimens derived from the various FAB classes should be study to better identify the specificity of N-CoR MCDL to AML-M5 and APL.

4.1.2. Processing of misfolded N-CoR in AML-M5 by aberrant protease activity.

Previously, it was reported that in APL, N-CoR was in a misfolded conformation as characterized by its detergent insolubility and aberrant cytosolic localization resulting in the amplification of ER stress[62]. This amplification of ER stress was kept below the threshold levels required to

initiate cell death by the processing of this misfolded N-CoR by an aberrant protease activity[63]. In this study, it was reported that N-CoR was observed to display several characteristics of misfolding and was processed by an aberrant protease activity in AML-M5.

In mammalian cells, there exists an efficient protein quality monitoring system known as the Unfolded Protein Response (UPR). UPR is activated in response to the intracellular accumulation of misfolded proteins in the ER[193,194]. There are two arms to this UPR response, one which is cytoprotective and the other which is cytotoxic. The first response to the accumulation of misfolded protein is the activation of molecular chaperones in an attempt to refold these proteins. When this system fails to clear the misfolded proteins, a second defense mechanism, ER-associated degradation or ERAD is activated. This process promotes ubiquitin-proteasome mediated degradation of the misfolded proteins. When this cytoprotective UPR response fails, cytotoxic UPR takes over to eliminate cells which harbor these misfolded proteins.

It was interesting to note that inhibition of proteasome activity in AML-M5 did not seem to have an effect on the clearance of misfolded N-CoR (Fig 3.4B). It is unclear if this was due to an inherent non-functional ubiquitin-proteasome system in these cells or if the ERAD function was directly inhibited by the misfolded N-CoR itself. However, the failure of this system to clear misfolded N-CoR in AML-M5 cells did not seem to have affected the cells' ability to escape the cytotoxicity brought about by the accumulation of misfolded N-CoR. Instead, there seemed to be a selective induction of a third proposed arm of the UPR pathway, the 'late' cytoprotective arm (which was

first suggested in APL cells) in AML-M5 cells[63]. This third arm which was associated with increased aberrant protease activity seemed to negate the negative effects of the accumulation of misfolded N-CoR on cellular growth in AML-M5. The involvement of aberrant protease activity in AML pathogenesis was first reported in APL. Cleavage of PML-RARα by neutrophil elastase was shown to be important for the pathogenesis of APL in mice [195,196]. Subsequently, our laboratory reported the role of aberrant processing of misfolded N-CoR by the protease O-Sialoglycoprotein-Endopeptidase (OSGEP) in APL's resistance to Unfolded Protein Response (UPR) - induced apoptosis[63].

The findings reported in this thesis suggested that a similar aberrant protease activity in the processing of N-CoR in AML-M5. The degree and pattern of N-CoR loss across all AML-M5 derived cells was more or less comparable despite the differences in their genetic backgrounds. Although all AML-M5 derived cells displayed almost complete loss of full length N-CoR protein, the cleaved 100 kDa N-CoR fragment was less pronounced in Nomo-1 cells when compared to other AML-M5 derived cells. Consistent with this finding, incubation of flag-tagged N-CoR with Nomo-1 cell extract did not generate any 100 kDa N-CoR fragment despite complete digestion of full length N-CoR protein (Fig. 3.1 and 3.3). The lack of cleaved N-CoR in Nomo-1 cells could be due to the higher potency of N-CoR cleaving activity in Nomo-1 cells which could have further digested the cleaved N-CoR in addition to digestion of full length N-CoR. It is also likely that Nomo-1 cells posses an N-CoR cleaving activity which is distinct from the activity found in

other AML-M5 derived cell lines, and cleaved N-CoR protein in a distinct manner.

The generation of the 100 kDa N-CoR fragment in most of the AML-M5 derived cell lines which was identical in size to that found in APL suggested that the cleaving activity in AML-M5 could possibly be mediated by OSGEP. However, despite the detection of OSGEP mRNA expression in AML-M5 cell lines, OSGEP was not identified in the N-CoR cleaving fraction of AML-M5 cell lysate after gel filtration chromatography in our attempt to identify the potential proteases involved in N-CoR processing in AML-M5 (data not shown). Furthermore, it was observed that AML-M5 derived cell lines displayed a complete loss of full length N-CoR protein while in the APL cell line NB4, the loss was not complete. Thus, it is possible that some other protease or a combination of proteases may be involved in the processing of N-CoR in AML-M5. Despite this, the data suggested that N-CoR cleavage in all AML-M5 derived cell lines was probably triggered by an identical non-regulated proteolytic mechanism which was selectively activated in AML-M5 leukemic cells to circumvent the cytotoxicity associated with the misfolded N-CoR protein.

Normal mammalian cells possess a robust protein quality control mechanism regulated by the ubiquitin-proteasome system that promptly dispenses non-amenable misfolded proteins to refolding by molecular chaperones. However in protein misfolding diseases, the function of the ubiquitin-proteasome system is severely compromised, resulting in excess accumulation of misfolded proteins in the ER, creating a potentially life threatening situation for the host cells. Furthermore, an excessive

accumulation of misfolded proteins in the subcellular compartment can directly impair proteasome function, resulting in further accumulation of misfolded proteins and amplification of ER stress. This usually leads to cell death, which largely forms the pathogenic basis in various neurological disorders such as Alzheimer and Parkinson's diseases. In tumor cells derived from APL or AML-M5, protease mediated degradation of misfolded N-CoR protein may constitute an alternative mechanism for the disposal of misfolded proteins, leading to the attenuation of ER stress and eventual protection of AML-M5 cells from ER stress-induced apoptosis. Thus, degradation of misfolded N-CoR protein through aberrant protease activity could represent a tumor cell specific adaptive protein quality control mechanism specifically activated to remove misfolded proteins that are non-amenable to traditional protein quality control mechanism.

4.1.3. Involvement of Akt kinase activity in the misfolding of N-CoR.

Unlike APL where the expression of the fusion oncogene PML-RARα is found in almost all cases of the disease (> 95%), the occurrence of fusion oncogenes in AML-M5 is less homogenous. Although the MLL1-AF9 fusion oncogene was found in more than half of the AML-M5 cases, other diverse genetic anomalies were also frequently reported[12]. Thus unlike APL, the misfolding of N-CoR in AML-M5 could not be attributed to the fusion oncogene alone. In APL, misfolded N-CoR which was localized to the cytosol was reported to be aberrantly phosphorylated at the Serine/Threonine residues in the presence of PML-RARα [58,197]. In AML-M5, the misfolded N-CoR was also found to be aberrantly phosphorylated at the Serine/Threonine residue

(Fig 3.9). Thus, the involvement of a common kinase activity in the uniform loss of N-CoR in genetic variants of AML-M5 could not be ruled out.

The involvement of aberrant kinase activity in the loss of N-CoR nuclear function due to cytosolic export was first reported in neuronal cells. In that report, Akt induced phosphorylation of N-CoR was found to be linked to its aberrant cytosolic export in cytokine stimulated neuronal cells, suggesting that N-CoR function could be adversely affected by Akt activity[48]. In a more recent publication, phosphorylation of N-CoR by IKKα was also linked to its aberrant cytosolic export in colorectal cancer cells[56]. These reports suggested that aberrant phosphorylation of N-CoR by kinase hyper-activity could result in the loss of N-CoR nuclear function due to aberrant cytosolic export.

The findings reported in this study identified Akt as the kinase involved in the misfolding of N-CoR in AML-M5. This was not surprising, as Akt phosphorylation of N-CoR had been reported previously. A recent study by Yu et al[198] and the results obtained in figure 3.11 revealed that Akt was hyper-activated in AML-M5 cell lines and multiple AML-M5 patient specimens. This strongly suggests Akt kinase as the common factor which contributed to the misfolding of N-CoR across all AML-M5 variants.

4.1.4. Akt phosphorylation of N-CoR at Serine 1450 was essential in the initiation of the misfolded conformation.

Based on the data obtained, it appeared that N-CoR misfolding in all AML-M5 derived cells was primarily caused by an identical phosphorylation event by Akt kinase activity at the Serine residue at position 1450 triggered by the various forms of oncogenic alterations associated with the transformation of AML-M5 cells. The phosphorylation at Serine 1450 could alter the local

free energy and destabilized the core of N-CoR protein, leading to its conformational change and subsequent degradation in AML-M5 cells. The change in three-dimensional structure due to the phosphorylation at Serine 1450 might have led to the exposure of the hydrophobic residues in the N-CoR protein normally buried in the core. This could result in the facilitation of N-CoR's interaction with molecular chaperones, ultimately targeting the misfolded N-CoR to the ER. The ER targeting of misfolded N-CoR could initially trigger ER stress; however, its subsequent degradation could have attenuated ER stress, eventually protecting AML-M5 cells from ER stress-induced apoptosis. Interestingly, an important role of Akt in protecting cells from ER stress-induced apoptosis by attenuating cellular ER stress has recently been identified [199]. The AEBSF-induced ER stress amplification in THP-1 cells was due to the net ER accumulation of misfolded N-CoR protein as a result of the inhibition of its degradation by proteases. Conversely, Genistein induced N-CoR stabilization could have resulted from the restoration of native N-CoR conformation due to inhibition of Akt activity. This resulted in the inhibition of serine 1450 phosphorylation, thus facilitating its transport back to the nucleus from the ER eventually reducing ER stress levels and restoring N-CoR nuclear function.

4.2 Functional Consequence of MCDL of N-CoR in AML-M5.

4.2.1. Flt3, a transcriptional target of N-CoR.

The main function of N-CoR as a transcriptional co-repressor is achieved in the nucleus. Thus Akt mediated aberrant cytosolic export would result in the loss of N-CoR transcriptional function. Small-scale genetic

screening conducted via comparative real time PCR analysis identified the pro-survival signaling receptor Flt3 as a transcriptional target of N-CoR.

Promoter studies indicated that N-CoR and its associated co-repressor complex exerted its control on Flt3 expression by binding to the promoter region of the Flt3 gene (Fig. 3.31 to 3.37). Although N-CoR acts as a co-repressor for multiple transcription factors, there are no reports of N-CoR itself binding to any known specific DNA sequences. Thus it is unclear if the association of N-CoR with the Flt3 promoter region is direct, or mediated indirectly by other DNA binding transcription factors. Using the luciferase reporter driven by various truncated fragments of the full length Flt3 promoter as well as ChIP assay performed with primers encompassing the truncated and full length Flt3 promoter, the putative region which was associated to N-CoR was identified. This N-CoR binding site on the Flt3 promoter identified through luciferase and ChIP assay was located between 614 to 814 bps upstream of the Flt3 transcriptional start site. This putative N-CoR binding site was upstream of the Flt3 promoter region where most of the transcriptional factor binding sites had been identified.

Computational analysis using the TRANSFAC database (a database about eukaryotic transcription regulating DNA sequence elements and the transcription factors binding to and acting through them) revealed several putative transcription factor binding sites such as PPARα, RXR and RAR, all of which are known to utilize N-CoR for their function as transcriptional repressors. However more work is required to confirm the identity of the transcription factor that tethers N-CoR to the Flt3 promoter. This identification will be crucial for the complete understanding of N-CoR's role in the

regulation of Flt3 expression and its implication in hematopoiesis and leukemogenesis.

4.2.2. Effect of misfolded N-CoR on the regulation of Flt3 expression.

In this study, it was identified that N-CoR misfolding in AML-M5 was due to its phosphorylation at the Serine 1450 residue by Akt kinase activity. This observation was further supported by the spontaneous misfolding of the phosphomimetic N-CoR S1450E (where the serine 1450 residue was replaced with a glutamic acid residue to mimic the phosphorylation event). The phosphomimetic N-CoR was shown to have a weaker repressive action on the Flt3 promoter when compared to wild type N-CoR via luciferase assay (Fig 3.35). To test if the misfolded N-CoR exerts any dominant negative effects on wild-type N-CoR, the same promoter assay was performed with the co-expression of wild-type N-CoR in combination with increasing doses of phosphomimetic N-CoR. In this set of experiments, no dominant negative effect of the phosphomimetic N-CoR was observed over the wild-type N-CoR (data not shown). Previously, it was reported that Akt phosphorylation of the Foxhead family of transcription factors inhibit their nuclear function by sequestering them in the cytosol[145,146]. This prevented the binding of these factors to the promoter regions of the genes they regulate. Thus Akt mediated N-CoR misfolding may have a similar mode of action on N-CoR's transcriptional role in AML-M5. The phosphorylation may have resulted in the re-localization and degradation of N-CoR, preventing the binding of N-CoR to its transcriptional targets ultimately resulting in the loss of repression of these genes.

4.2.3. Tumor suppressive role of N-CoR in AML-M5.

The ultimate goal of the work presented here was to identify how the APL-like post-translational loss of N-CoR contributed to the pathogenesis of AML-M5. To that end, this study revealed that N-CoR mediated transcriptional control of Flt3 might be essential for the control of the cellular self-renewal and growth potentials of hematopoietic cells during normal hematopoiesis. When this control is abolished due to post-translational N-CoR loss, AML-M5 cells could reacquire the capacities of growth and survival, which ultimately led to leukemogenesis in conjunction with other factors involved in differentiation arrest.

Flt3 is involved in the growth of early progenitor cells. Recent studies by Kikushige et al demonstrated that Flt3 expression in human HSCs, Granulocyte/Macrophage Progenitor could prolong their survival. This suggested that Flt3 plays a critical role in the survival of the stem and progenitor cells as well as in AML transformation [164]. The data presented in this study suggested that loss of N-CoR mediated Flt3 repression enhanced the IL-3 independent proliferative capacity of BA/F3 cells and this growth was potentiated by Flt3 ligand stimulation (Fig 3.38). It was also shown that in normal HSCs/ progenitor cells, expression of N-CoR inhibited the growth potential of these cells and induced myeloid lineage commitment (Fig 3.41 to 3.43). It was also observed that as the cells progress towards maturation to the myeloid phenotype, N-CoR expression was up regulated while Flt3 level decrease proportionately (Fig 3.40). Physiologically, N-CoR is important in many developmental processes such as proliferation, differentiation and apoptosis. De-regulations of N-CoR function due to changes in expression or

loss of transcriptional function due to aberrant nuclear export contributed to carcinogenesis[53-56]. As shown in this report, loss of N-CoR function due to misfolding conferred a proliferative advantage to AML-M5 cells via the up-regulation of the pro-survival Flt3 receptor and therapeutic restoration of N-CoR function effectively inhibited this growth capacity and induced terminal differentiation. This observation illustrated the putative tumor suppressive function of N-CoR via its regulation of Flt3 at least in AML-M5.

The tumor suppressive effect of N-CoR might not be limited to its regulation of Flt3. N-CoR being a component of the generic co-repressor complex might also be involved in the repression of other oncogenes which work in combination with Flt3 to elicit the leukemic phenotype. Furthermore, there had been reports suggesting that the expression of Flt3 and its mutants alone were not able to induce the complete leukemic phenotype[162]. This implies that Flt3 has to work with other oncogenic factors for leukemogenesis to occur. Thus a more comprehensive screening using genome wide micro array analysis would give a better picture of the tumor suppressive effect of N-CoR via the genes it regulates and the other factors which work in tandem with Flt3 to bring about the leukemic phenotype.

4.2.4. Akt, N-CoR loss and Flt3 over-expression, a possible positive feedback mechanism in the amplification of survival signals.

The PI3K/Akt survival pathway and its non-regulated activation by cell surface receptors such as EGFR[200] and Flt3[201,202] had been widely implicated in carcinogenesis. Akt had been reported to be a downstream molecule of Flt3 ligand mediated Flt3 signaling[202]. In the data obtained in figure 3.39, Flt3 activation was found to enhance N-CoR loss. This suggested

a possible positive feedback mechanism where the aberrant expression of the Flt3 receptor and its subsequent activation via Flt3 ligand stimulation or activating mutations could result in the enhancement of N-CoR loss through Akt activation. It was also of interest to note that N-CoR was reported to be a negative regulator of PI3K and loss of N-CoR function in thyroid cancer cells contributed to the activation of Akt dependent survival pathway in these cells[53]. This same mechanism may also contribute to the enhancement of the survival advantage of AML-M5 leukemic cells as a consequence of N-CoR loss.

4.3. Targeting the N-CoR MCDL pathway as a therapeutic strategy in AML-M5.

Despite the advances in our knowledge of the mechanisms involved in leukemogenesis and the quest for constant improvements in therapeutic strategies used in the clinics for AML treatment, AML to date remains a difficult disease to treat. This could be attributed to the vast genetic aberrations which play major roles in disease pathogenesis. Although Flt3 activating mutations have been widely associated with the poorer prognosis of AML patients, the fact that more than 70% of AMLs express the wild-type Flt3 receptor implies that the native receptor is also important in the enhancement of survival and proliferation of leukemic blasts[165-167]. Current therapies for AML in clinical practice include aggressive multi-drug chemotherapy, radiotherapy and allogenic bone marrow transplantations. However these current strategies have severe side effects and widespread cytotoxicity.The use of tyrosine kinase inhibitors especially Flt3 kinase

inhibitors in AML treatment has recently gained prominence as an effective non-invasive strategy for disease management. However, most of these agents exhibit positive outcomes only in a subset of patients as their efficacy largely depend on the expression of the Flt3 mutants or the constitutively active forms of the receptor kinases found in the leukemic blasts. For example, most Flt3 kinase inhibitors have been evaluated solely in *in vitro* cell culture systems which express the mutant Flt3 receptors but not the wild-type. It had been reported that wild-type Flt3 signaling affected the efficacy of the Flt3 inhibitors[203]. In many patients, especially in the newly diagnosed AML cases which are heterozygous for both the mutant and wild-type receptors[204], there is a need to find new strategies which are effective against both the wild-type and mutant Flt3 receptor. Furthermore, resistance against these inhibitors is a major drawback that limits the effectiveness of such tyrosine kinase inhibitor based therapy[206]. Thus a stategy, which targets the expression of the receptor regardless of its mutational status and activity, could possibly address these issues.

Based on the results obtained in this study, it was postulated that N-CoR regulates the expression of the Flt3 promoter regardless of its mutational status. N-CoR loss and the reciprocal up-regulation of Flt3 expression were evident across cells which express the wild-type Flt3 receptor (THP-1 and Nomo-1) and those which express the activating mutants (MV-4-11: Flt3-ITD, MM1: Flt3-TDK at position 592). There are no known reports on the mutational status of the Flt3 receptor in SigM5 cells (Fig. 3.28A). This relationship was also observed across all the AML-M5 primary patient specimens used despite the heterozygosity of Flt3 receptor mutational status

across the specimens (Fig. 3.28B). Thus, therapeutic targeting of the N-CoR MCDL pathway could be a useful strategy in AML-M5 therapy irrespective of Flt3 receptor mutational status.

In this study, it was proposed that N-CoR loss in AML-M5 was a two-stage process. The first step was the change in conformation of native N-CoR to the misfolded form by the oncogenic insult. In the case of AML-M5, it was triggered by the hyper-activation of Akt kinase activity followed by the aberrant phosphorylation of N-CoR at the Serine 1450 residue. This misfolded N-CoR then accumulates in the ER. In the normal non-permissive environment of most mammalian cells the accumulation of misfolded N-CoR in the ER leads to apoptotic cell death. However in the permissive environment of AML-M5 leukemic cells where there was the activation of the proposed 'late' cytoprotective arm of UPR, the misfolded N-CoR was processed by a non-regulated proteolytic process. This keeps the ER stress below the threshold levels needed to induce cell death. In our laboratory, we have identified several agents with therapeutic potential which targeted either the mechanism of N-CoR misfolding or blocked the processing of misfolded N-CoR protein. Some of these agents such as the kinase inhibitor Genistein, the Akt specific inhibitor Akti-X and the protease inhibitors AEBSF and Kaletra displayed selective cytotoxic effects against AML-M5 derived cell lines (Fig. 3.52 and Fig. 3.55) and might have the potential to be used as effective therapeutic strategies for targeting the pathway of N-CoR MCDL in AML-M5.

4.4. Concluding Remarks.

In the work presented here, we demonstrated the existence of APL-like misfolded conformational dependent loss (MCDL) of N-CoR in AML-M5. The misfolding of N-CoR in AML-M5 was initiated by the aberrant phosphorylation of N-CoR at Serine 1450 by Akt hyper-activity. This subsequently led to the degradation of misfolded N-CoR by a non-regulated proteolytic mechanism that we termed as the cytoprotective third arm of the Unfolded Protein Response pathway or the 'late' cytoprotective pathway. The dynamics of the N-CoR MCDL pathway and how it may contribute to disease pathogenesis in AML-M5 is depicted on figure 4.1.

The pro-survival receptor Flt3 was identified as a direct target of N-CoR mediated repression. Loss of functional N-CoR in AML-M5 resulted in the aberrant expression of the Flt3 receptor in leukemic blasts, thus conferring a survival advantage to these cells. The proposed action of N-CoR loss on Flt3 expression is summarized in figure 4.2.

Finally, based on the evidence of uniform N-CoR MCDL across AML-M5 derived cell lines of varied genetic backgrounds, blocking N-CoR MCDL with various agents was proposed as a promising therapeutic strategy for AML-M5. Figure 4.3 and figure 4.4 summarizes how this pathway could be blocked at certain stages and its end effect on the survival of AML-M5 leukemic cells.

AML-M5 is defined as a group of malignant disorder characterized by an abnormal accumulation of immature cells of myelo-monocytic lineage in the bone marrow and peripheral blood. Although AML-M5 is caused primarily by a wide array of genetic defects, including chromosomal

translocation involving the *MLL-1* gene, the leukemia cells in all AML-M5 variants display almost identical phenotype characterized by differentiation arrest and increased self-renewal capacity. Despite significant progress in the understanding of diverse genetic anomalies associated with AML-M5, it is still unclear as to how these diverse genetic anomalies could possibly create an indistinguishable and almost uniform cellular and clinical feature in the different variants of AML-M5. Interestingly, Yu and colleagues had recently reported a relevant mouse model for human monocytic leukaemia through Cre/lox controlled myeloid specific deletion of PTEN. In this study, PTEN knockout mice were observed to have Akt hyper-activation and 11 out of 18 of these mice develop leukemia. Analysis of the leukemic blasts confirmed monocytic differentiation in the blasts[198]. Given the relationship between Akt hyper-activity and N-CoR MCDL identified in the work presented in this thesis, it is likely that these uniform phenotypic features could be manifested through the de-regulation of a common factor such as N-CoR, a critical regulatory factor in the normal growth and maturation of early myeloid cells.

Despite all these evidence, more work is required to fully understand the roles of normal and misfolded N-CoR in normal and malignant hematopoiesis. To that end, the creation of myeloid lineage cell specific N-CoR knockout mice and the generation of the phosphomimetic and constitutively misfolded N-CoR knock in mice models are currently underway. Successful creation of these models will greatly enhance our understanding of the role of N-CoR in AML-M5 disease progression.

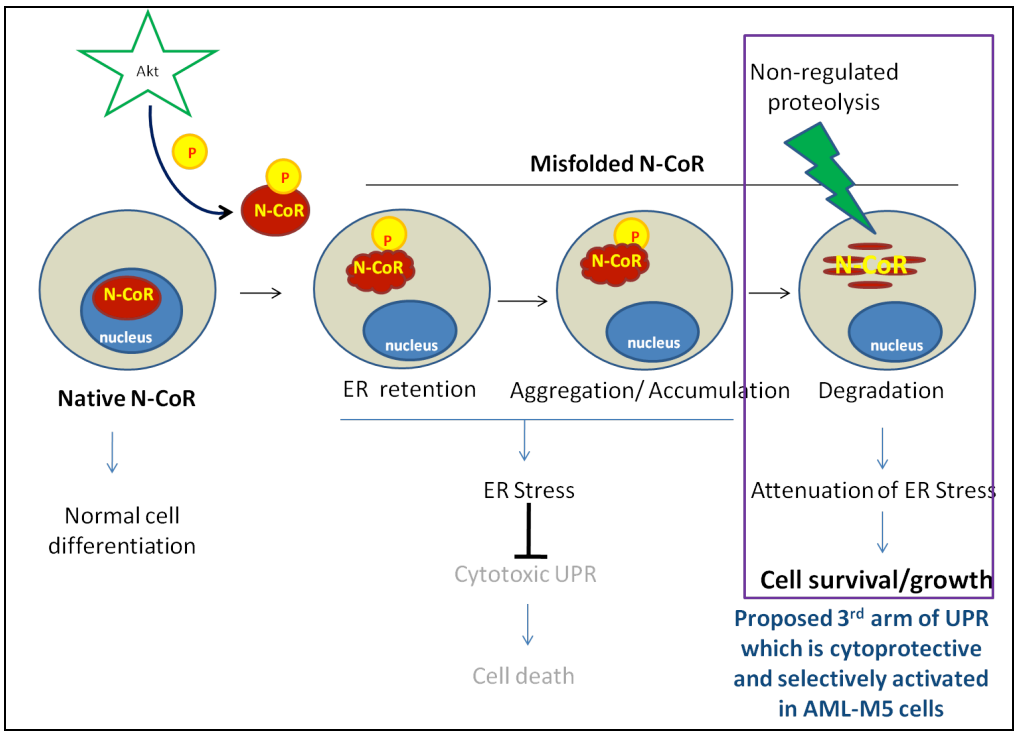

Figure 4.1. Dynamics of the N-CoR MCDL pathway in AML-M5. An oncogenic insult such as Akt hyper-activation in AML-M5 blasts brings about the aberrant phosphorylation of N-CoR. This disrupts the natural folding landscape of N-CoR protein resulting in the production of N-CoR with a misfolded N-CoR. The misfolded N-CoR protein is then transported from the nucleus where it normally exerts it functions to the Endoplasmic Reticulum (ER) where it accumulates. The activation of the Unfolded Protein Response (UPR) first attempts to refold this misfolded protein however due to the high protein load, there is an excessive aggregation and accumulation of misfolded N-CoR protein in these cells. In the permissive environment of the AML-M5 leukemic blasts where there is an activation of non-regulated proteolysis, this misfolded N-CoR is degraded through the proposed cytoprotective 3rd arm of UPR/ 'late' cytoprotective UPR, first identified in APL. This results in the attenuation of ER stress, thus bypassing the effects of the cytotoxic UPR arm. This leads to the continued survival and growth of the AML-M5 leukemic cells, contributing to disease pathogenesis.

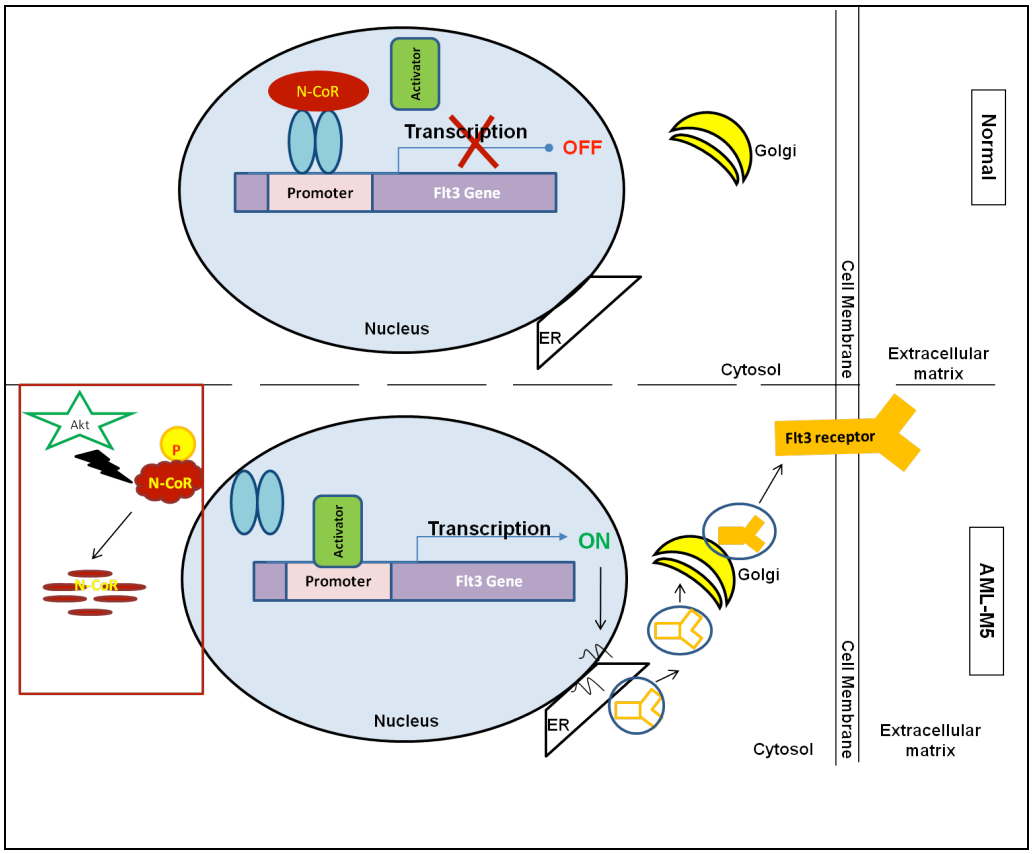

Figure 4.2. Mode of action of N-CoR MCDL on Flt3 receptor expression in AML-M5. In normal monocytes, the expression of functional N-CoR results in the recruitment of the N-CoR co-repressor complex to the Flt3 promoter region. This prevents the binding of the transcriptional activators to the Flt3 promoter thus inhibiting the transcription and expression of the Flt3 receptor (upper panel).
In AML-M5, post-translational loss of functional N-CoR due to Akt mediated phosphorylation results in the dissociation of the co-repressor complex from the Flt3 promoter region. This gives transcriptional activators access to the Flt3 promoter region. Binding of the transcriptional activators activates Flt3 gene transcription and subsequent receptor expression. The re-expression of this pro-survival signaling receptor provides the leukemic blasts with a proliferative advantage contributing to AML-M5 disease pathogenesis (lower panel).

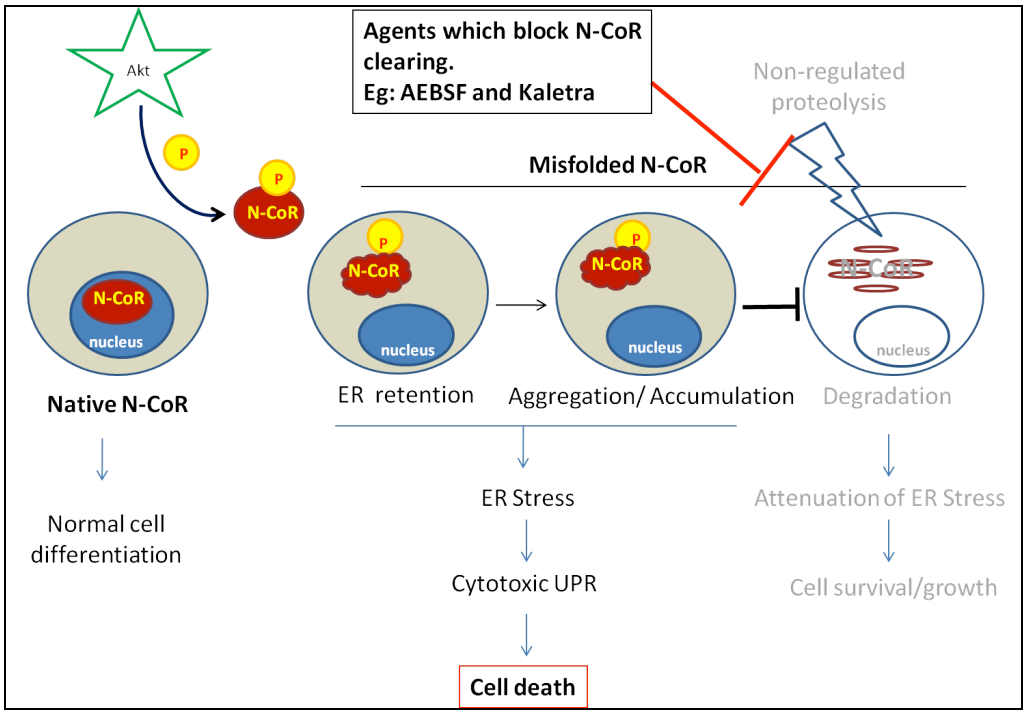

Figure 4.3. Mechanism of action of agents which block the clearing of misfolded N-CoR in AML-M5. Protease inhibitors such as AEBSF and Kaletra inhibit the proteases involved in the non-regulated proteolysis of misfolded N-CoR. This inhibition results in the excessive accumulation of the misfolded N-CoR protein in the Endoplasmic Reticulum (ER) activating the cytotoxic UPR arm in AML-M5 leukemic cells. This will eventually lead to ER stress induced cell death of AML-M5 leukemic cells.

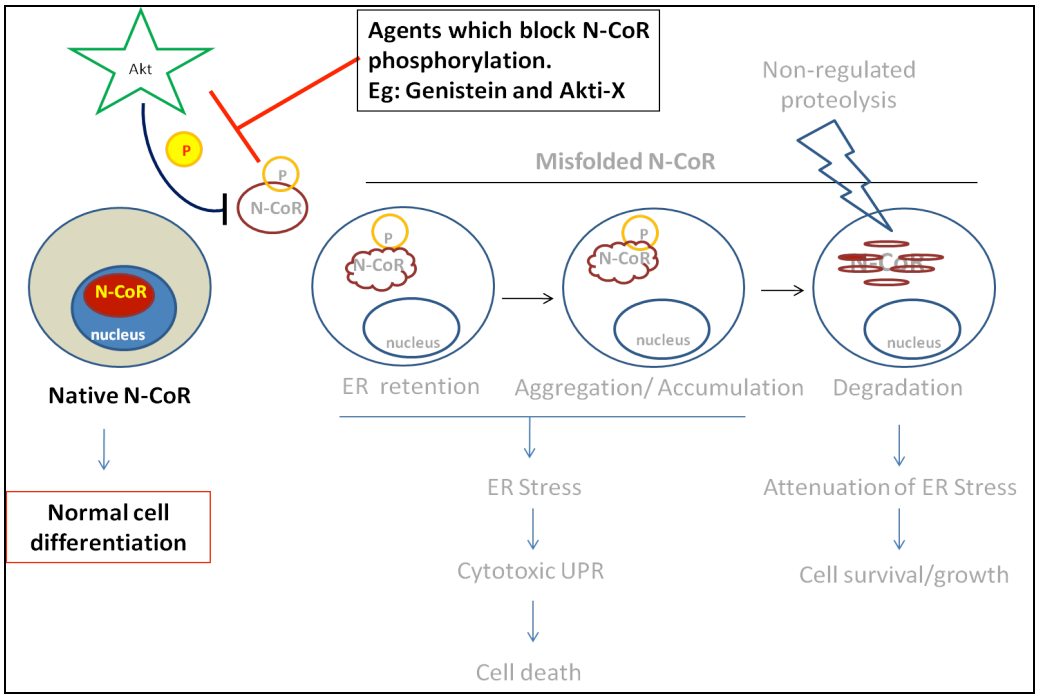

Figure 4.4. Mechanism of action of agents which prevent the misfolding of N-CoR in AML-M5. Agents such as Genistein and Akt inhibitors can prevent the aberrant phosphorylation of N-CoR in AML-M5. This results in the maintenance of N-CoR in its functional native conformation. This restores nuclear functions of N-CoR such as Flt3 repression. Due to the restoration of N-CoR function, the AML-M5 leukemic cells lose the proliferative advantage conferred by the Flt3 receptor and revert to the pathway of normal myeloid cell maturation, in conjunction with cellular signals regulated by native N-CoR.

REFERENCES

1 Jaffe, E. S., Harris, N. L. & Stein, H. *World Health Organization Classification of Tumours: Pathology and genetics of Tumours of Haematopoietic and Lymphoid Tissues.*, (IARC Press, 2001).

2 Vardiman, J. W., Harris, N. L. & Brunning, R. D. The World Health Organization (WHO) classification of the myeloid neoplasms. *Blood* **100**, 2292-2302 (2002).

3 Sekeres, M. A., Kalaycio, M. E. & Bolwell, B. J. *Clinical Malignant Hematology*. (McGraw-Hill, 2007).

4 Bennett, J. M., Catovsky, D. & Daniel, M. T. Proposals for the classification of the acute leukemias. French-American-British (FAB) Cooperative Group. *Br J Hematol* **33**, 451-458 (1976).

5 Bennett, J. M., Catovsky, D. & Daniel, M. T. Criteria for the diagnosis of acute leukemia of megakaryocyte lineage (M7).A report of the French-American-British (FAB) Cooperative Group. *Ann Intern Med* **103**, 460-462 (1985).

6 Bennett, J. M., Catovsky, D. & Daniel, M. T. Proposal for the recognition of minimally differentiated acute myeloid leukemia (AML-M0). *Br J Hematol* **78**, 325-329 (1991).

7 Raimondi, S. C. *et al.* Chromosomal Abnormalities in 478 Children with Acute Myeloid Leukemia: clinical Characteristics and Treatment Outcome in a Cooperative Pediatric oncology Group Study POG8821. *Blood* **94**, 3707-3716 (1999).

8 Haferlach, T. *et al.* Distinct genetic patterns can be identified in acute monoblastic and acute monocytic leukaemia (FAB AML M5a and M5b): a study of 124 patients. . *Br J Haematol* **118**, 426-431 (2002).

9 Villeneuve, P., Kima, D. T., Xub, W., Brandwein, J. & Chang, H. The morphological subcategories of acute monocytic leukemia (M5a and M5b) share similar immunophenotypic and cytogenetic features and clinical outcomes. *Leukemia Res* **32**, 269-273 (2008).

10 Brian V. Balgobind *et al.* Novel prognostic subgroups in childhood 11q23/MLL-rearranged acute myeloid leukemia: results of an international retrospective study. *Blood* **114**, 2489-2496 (2009).

11 Swansbury, G. J., Slater, R., Bain, B. J., Moorman, A. V. & Secker-Walker, L. M. Hematological malignancies with t(9;11)(p21-22;q23): a laboratory and clinical study of 125 cases. European 11q23 Workshop participants. *Leukemia* **12**, 792-800 (1998).

12 Karauzum, S. B. *et al.* Novel Cytogenetic findings revealed by conventional cytogentic and FISH analyses in Leukemia patients. *Exp Oncol* **27**, 229-232 (2005).

13 Stevens, R. F., Hann, I. M., Wheatley, K. & Gray, R. G. Marked improvements in outcome with chemotherapy alone in paediatric acute myeloid leukemia: reslults of the United Kingdom Medical Research

Council's 10th AML Trial. MRC Childhood Leukaemia Working Party. *Br J Haematol* **101**, 130-140 (1998).

14 Verschuur, A. Acute monocytic leukemia. *Orphanet Encyclopedia* (2004).

15 Blau, H. M. & Baltimore, D. Differentiation requires continuous regulation. *J Cell Biol* **112**, 781-783 (1991).

16 Davis, R. L., Weintraub, H. & Lassar, A. B. Expression of a single balanced transfected cDNA converts fibroblasts to myoblasts. *Cell* **51**, 987-1000 (1987).

17 Orkin, S. H. Transcription factors and hematopoietic development. *J Biol Chem* **270**, 4955-4958 (1995).

18 Shivdasani, R. A. & Orkin, S. H. The transcriptional control of hematopoiesis. *Blood* **87**, 4025-4039 (1996).

19 Burel, S. A. *et al.* Dichotomy of AML1-ETO functions: growth arrest versus block of differentiation. *Mol Cell Biol.* **21**, 5577-5590 (2001).

20 Guzman, C. G. d. *et al.* Hematopoietic stem cell expansion and distinct myeloid developmental abnormalities in a murine model of the AML1-ETO translocation. *Mol Cell Biol.* **22**, 5506-5517 (2002).

21 Speck, N. A. & Gilliland, D. G. Core-binding factors in haematopoiesis and leukaemia. *Nat Rev Cancer.* **2**, 502-513 (2002).

22 Georgopoulos, K. *et al.* The Ikaros gene is required for the development of all lymphoid lineages. *Cell* **79**, 143-156 (1994).

23 Shivdasani, R. A., Mayer, E. L. & Orkin, S. H. Absence of blood formation in mice lacking the T-cell leukaemia oncoprotein tal-1/SCL. *Nature* **373**, 432-434 (1995).

24 Urbanek, P., Wang, Z. Q., Fetka, I., Wagner, E. F. & Busslinger, M. Complete block of early B cell differentiation and altered patterning of the posterior midbrain in mice lacking Pax5/BSAP. *Cell* **79**, 901-912 (1994).

25 Pevny, L. *et al.* Erythroid differentiation in chimaeric mice blocked by a targeted mutation in the gene for transcription factor GATA-1. *Nature* **349**, 257-260 (1991).

26 Warren, A. J. *et al.* The oncogenic cysteine-rich LIM domain protein rbtn2 is essential for erythroid development. *Cell* **78**, 45-57 (1994).

27 Zhang, D. E. *et al.* Absence of granulocyte colony-stimulating factor signaling and neutrophil development in CCAAT enhancer binding protein alpha-deficient mice. *Proc Natl Acad Sci U S A* **21**, 569-574 (1997).

28 Wang, X., Scott, E., Sawyers, C. L. & Friedman, A. D. C/EBPalpha bypasses granulocyte colony-stimulating factor signals to rapidly induce PU.1 gene expression, stimulate granulocytic differentiation, and limit proliferation in 32D cl3 myeloblasts. *Blood* **95**, 560-571 (1999).

29 Verbeek, W., Wächter, M., Lekstrom-Himes, J. & Koeffler, H. P. C/EBPepsilon -/- mice: increased rate of myeloid proliferation and apoptosis. *Leukemia* **15**, 103-111 (2001).
30 Sasaki, K. *et al.* Absence of fetal liver hematopoiesis in mice deficient in transcriptional coactivator core binding factor beta. *Proc Natl Acad Sci U S A* **93**, 12359-12363 (1996).
31 Reddy, V. A. *et al.* Granulocyte inducer C/EBPalpha inactivates the myeloid master regulator PU.1: possible role in lineage commitment decisions. *Blood* **100**, 483-490 (2002).
32 Wolff, L. Contribution of oncogenes and tumor suppressor genes to myeloid leukemia. *Biochim Biophys Acta* **1332**, F67-104 (1997).
33 Lubbert, M., Herrmann, F. & Koeffler, H. P. Expression and regulation of myeloid-specific genes in normal and leukemic myeloid cells. *Blood* **77**, 909-924 (1991).
34 Nichols, J. & Nimer, S. D. Transcription factors, translocations, and leukemia. *Blood* **80**, 2953-2963 (1992).
35 Hörlein, A., Näär, A. & Heinzel, T. Ligand-independent repression by the thyroid hormone receptor mediated by a nuclear receptor co-repressor. *Nature* **377**, 397-404 (1995).
36 Jepsen, K. *et al.* Combinatorial roles of the nuclear receptor corepressor in transcription and development. *Cell* **102**, 753-763 (2000).
37 Wen, Y., Perissi, V. & Staszewski, L. The histone deacetylase-3 complex contains nuclear receptor corepressors. . *Proc Natl Acad Sci U S A* **97**, 7202-7207 (2000).
38 Li, J., Lin, Q., Wang, W., Wade, P. & Wong, J. Specific targeting and constitutive association of histone deacetylase complexes during transcriptional repression. *Genes Dev* **16**, 687-692 (2002).
39 Pazin, M. & Kadonaga, J. What's up and down with histone deacetylation and transcription? . *Cell* **89**, 325-328 (1997).
40 Yoon, H. *et al.* Purification and functional characterization of the human N-CoR complex: the roles of HDAC3, TBL1 and TBLR1. *EMBO J* **22**, 1336-1346 (2003).
41 Zhang, J., Kalkum, M., Chait, B. & Roeder, R. The N-CoR-HDAC3 nuclear receptor corepressor complex inhibits the JNK pathway through the integral subunit GPS2. *Mol Cell* **9**, 611-623 (2002).
42 Yoon, H., Choi, Y., Cole, P. & Wong, J. Reading and function of a histone code involved in targeting corepressor complexes for repression. *Mol Cell Biol* **25**, 324-335 (2005).
43 Chawla, A., Repa, J., Evans, E. & Mangelsdorf, D. Nuclear receptors and lipid physiology: opening the X-files. *Science* **294**, 1866-1870 (2001).
44 Glass, C. K. & Ogawa, S. Combinatorial roles of nuclear receptors in inflammation and immunity. *Nat Rev Immunol.* **6**, 44-55 (2006).

45 Alland, L. *et al.* Role for N-CoR and histone deacetylase in Sin3-mediated transcriptional repression. *Nature* **387**, 49-55 (1997).
46 Heinzel, T. *et al.* A complex containing N-CoR, mSin3 and histone deacetylase mediates transcriptional repression. *Nature* **387**, 43-48 (1997).
47 Laherty, C. *et al.* SAP30, a component of the mSin3 corepressor complex involved in N-CoR-mediated repression by specific transcription factors. *Mol Cell* **2**, 33-42 (1998).
48 Hermanson, O., Jepsen, K. & Rosenfeld, M. N-CoR controls differentiation of neural stem cells into astrocytes. *Nature* **419**, 934-939 (2002).
49 Zhang, D., Cho, E. & Wong, J. A critical role for the co-repressor N-CoR in erythroid differentiation and heme synthesis. *Cell Res* **17**, 804-814 (2007).
50 Xu, L. *et al.* Signal-specific co-activator domain requirements for Pit-1 activation. *Nature* **395**, 301-306 (1998).
51 Bailey, P. *et al.* The nuclear receptor corepressor N-CoR regulates differentiation: N-CoR directly interacts with MyoD. *Mol Endocrinol* **13**, 1155-1168 (1999).
52 Alenghat, T. *et al.* Nuclear receptor corepressor and histone deacetylase 3 govern circadian metabolic physiology. *Nature* **456**, 997-1000 (2008).
53 Furuya, F. *et al.* Nuclear receptor corepressor is a novel regulator of phosphatidylinositol 3-kinase signaling. *Mol Cell Biol.* **27**, 6116-6126 (2007).
54 Parekh, S. *et al.* BCL6 programs lymphoma cells for survival and differentiation through distinct biochemical mechanisms. *Blood* **110**, 2067-2074 (2007).
55 Park, D. *et al.* N-CoR pathway targeting induces glioblastoma derived cancer stem cell differentiation. *Cell Cycle* **6**, 467-470 (2007).
56 Fernández-Majada, V. *et al.* Aberrant Cytoplasmic Localization of N-CoR in Colorectal Tumors. *Cell Cycle* **6**, 1748-1752 (2007).
57 Gelmetti, V. *et al.* Aberrant recruitment of the nuclear receptor corepressor-histone deacetylase complex by the acute myeloid leukemia fusion partner ETO. *Mol Cell Biol* **18**, 7185-7191 (1998).
58 Ng, A. P. P. *et al.* Therapeutic targeting of nuclear receptor corepressor misfolding in acute promyelocytic leukemia cells with genistein. *Mol Cancer Ther* **6**, 2240-2248 (2007).
59 Grignani, F. *et al.* Fusion proteins of the retinoic acid receptor-alpha recruit histone deacetylase in promyelocytic leukaemia. *Nature* **391**, 815-818 (1998).
60 Guidez, F. *et al.* Reduced retinoic acid-sensitivities of nuclear receptor corepressor binding to PML- and PLZF-RARalpha underlie molecular

pathogenesis and treatment of acute promyelocytic leukemia. *Blood* **91**, 2634-2642 (1998).

61 Lin, R. J. *et al.* Role of the histone deacetylase complex in acute promyelocytic leukemia. *Nature* **391**, 811-814 (1998).

62 Khan, M. M. *et al.* The fusion oncoprotein PML-RARalpha induces endoplasmic reticulum (ER)-associated degradation of N-CoR and ER stress. *J Biol Chem* **279**, 11814-11824 (2004).

63 Ng, A. P. P. *et al.* Cleavage of misfolded nuclear receptor corepressor confers resistance to unfolded protein response-induced apoptosis. *Cancer Research* **66**, 9903-9912 (2006).

64 Khan, M. Interplay of protein misfolding pathway and unfolded-protein response in acute promyelocytic leukemia. *Expert Rev. Proteomics* **7**, 591-600 (2010).

65 Gergersen, N., Bross, P., Vang, S. & Christensen, J. H. Protien Misfolding and Human Disease. *Annu Rev Genom Human Genet* **7**, 103-124 (2006).

66 Levinthal, C. Are there pathways for protein folding? *J. Chim. Phys.* **65**, 44-45 (1998).

67 Eillis, R. J. The molecular chaperone concept. *Semin. Cell. Biol.* **1**, 1-9 (1990).

68 Kelly, J. Alternative conformation of amyloidogenic proteins amd their multi-step assembly pathways. *Curr. Opin. Struct. Biol* **8**, 101-106 (1998).

69 Dobson, C. M. The structural basis of protein folding and its links with human disease. *Philos Trans R Soc Lond B Biol Sci* **356**, 133-145 (2001).

70 Reilly, M. M. Genetically determined neuropathies. *J. Neurol* **245**, 6-13 (1998).

71 Gustaffson, M., Thyberg, J., N7slund, J., Eliasson, E. & Johansson, J. Amyloid fibril formation by pulmonary surfactant protein C. *FEBS Lett* **464**, 136-142 (1999).

72 Bridges, J. P., Wert, S. E., Nogee, L. M. & Weaver, T. E. Expression of a human SP-C mutation associated with interstitial lung disease disrupts lung development in transgenic mice. *J Biol Chem* **278**, 52739-52746 (2003).

73 Munier, F. L. *et al.* Kerato-epithelin mutations in four 5q31-linked corneal dystrophies. *Nat. Genet* **15**, 247-251 (1997).

74 Clou, N. J. & Hohenester, E. A model of FAS1 domain 4 of the corneal protein hig-h3 gives a clearer view on corneal dystrophies. *Mol. Vis.* **9**, 440-448 (2003).

75 Kintworth, G. K. *et al.* Familial subepithelial corneal amyloidoses-a lactoferrin-related amyloidoses. *Investig. Ophthalmol. Vis. Sci* **38**, 2756-2763 (1997).

76 Nilsson, M. R. & Dobson, C. M. In vitro characterization of lactoferrin aggregation and amyloid formation. *Biochemistry* **42**, 375-382 (2003).
77 Berlau, J. *et al.* Analysis of aqueous humor proteins of eyes with and without pseudoexfoliation syndrome. *Graefes Arch Clin Exp Ophthalmol.* **239**, 743-746 (2001).
78 Bek, T. Ocular changes in heredo-oto-ophthalmo-encephalopathy. *Br. J. Ophthalmol* **84**, 1298-1302 (2000).
79 Askanas, V. & Engel, W. K. Sporadic inclusion-body myositis and its similarities to Alzheimer's disease brain. Recent approaches to diagnosis and pathogenesis and relation to aging. *Scand. J. Rheumatol* **27**, 389-405 (1998).
80 Askanas, V. & Engel, W. K. Proposed pathogenetic cascade of inclusion-body myositis: importance of amyloid-beta, misfolded proteins, predisposing genes, and ageing. *Curr. Opin. Rheumatol* **15**, 737-744 (2003).
81 Calado, A. *et al.* Nuclear inclusions in oculopharyngeal muscular dystrophy consist of poly(A) binding protein 2 aggregates which sequester poly(A) RNA. *Hum. Mol. Genet* **9**, 2321–2328 (2000).
82 Gofrlach, M., Burd, C. G. & Dreyfuss, G. The mRNA poly(A)-binding protein: localization, abundance and RNA-binding specificity. *Exp. Cell Res.* **211**, 400-407 (1994).
83 Rankin, J., Wyttenbach, A. & Rubinsztein, D. C. Intracellular green fluorescent protein-polyalanine aggregates are associated with cell death. *Biochem. J.* **348**, 15-19 (2000).
84 Jonca, N. *et al.* Corneodesmosin, a component of epidermal corneocyte desmosomes, displays homophilic adhesive properties. *J. Biol. Chem* **277**, 5024-5029 (2002).
85 Levy-Nissenbaum, E. *et al.* Hypotrichosis simplex of the scalp is associated with nonsense mutations in CDSN encoding corneodesmosin. *Nat. Genet* **34**, 151-153 (2003).
86 Scaturro, M. *et al.* A missense mutation (G1506E) in the adhesion G domain of laminin-5 causes mild juctional epidermolysis bullosa. *Biochem. Biophys. Res. Commun* **309**, 96-103 (2003).
87 Ursini, F., Davies, K. J. A., Maiorino, M., Parasassi, T. & Sevanian, A. Atherosclerosis: another protein misfolding disease? *Trends Mol. Med.* **8**, 370-374 (2002).
88 Lusis, A. J. Atherosclerosis. *Nature* **407**, 233-241 (2000).
89 Haggqvist, B. *et al.* Medin: an integral fragment of aortic smooth muscle cell-produced lactadherin forms the most common human amyloid. *Proc. Natl. Acad. Sci. U. S. A.* **96**, 8669-8674 (1999).
90 Bross, P. & Gregersen, N. *Methods in Molecular Biology-Protein Misfolding and Disease*. 2003 edn, Vol. 232 (Humana Press, 2003).
91 Carrell, R. W. & Lomas, D. A. Conformational disease. *Lancet* **350**, 134-138 (1997).

92 Carrell, R. W. & Lomas, D. A. Alpha1-antitrypsin deficiency: a model for conformational diseases. *N Engl J Med* **346**, 45-53 (2002).

93 Sørensen, C. B. *et al.* Identification of novel and known mutations in the genes for keratin 5 and 14 in Danish patients with epidermolysis bullosa simplex. *J Invest Dermatol* **112**, 184-190 (1999).

94 Riordan, J. R. Cystic fibrosis as a disease of misprocessing of the cystic fibrosis transmembrane conductance regulator glycoprotein. *Am J Hum Genet* **64**, 1499-1504 (1999).

95 Waters, P. J., Parniak, M. A., Akerman, B. R. & Scriver, C. R. Characterization of phenylketonuria missense substitutions, distant from the phenylalanine hydroxylase active site, illustrates a paradigm for mechanism and potential modulation of phenotype. *Mol Genet Metab* **69**, 101-110 (2000).

96 Gregersen, N. *et al.* Mutation analysis in mitochondrial fatty acid oxidation defects: exemplified by acyl-CoA dehydrogenase deficiencies, with special focus on genotype-phenotype relationship. *Hum Mutat* **18**, 169-189 (2001).

97 Waters, P. J. Degradation of mutant proteins, underlying "loss of function" phenotypes, plays a major role in genetic disease. *Curr. Issues Mol. Biol* **3**, 57-65 (2001).

98 Bullock, A. N. & Fersht, A. R. Rescuing the function of mutant p53. *Nat Rev Cancer* **1**, 68-76 (2001).

99 Ridiger, S., Freund, S. M. V., Veprintsev, D. B. & Fersht, A. R. CRINEPT-TROSY NMR reveals p53 core domain bound in an unfolded form to the chaperone Hsp90. *Proc Natl Acad Sci U S A* **99**, 11085-11090 (2002).

100 Ishimaru, D. *et al.* Conversion of wild- type p53 core domain into a conformation that mimics a hot-spot mutant. *J. Mol. Bio* **333**, 443-451 (2003).

101 Scharnhorst, V., van-der-Eb, A. J. & Jochemsen, A. G. WT1 proteins; functions in growth and differentiation. *Gene* **273**, 141-161 (2001).

102 Dome, J. S. & Coppes, M. J. Recent advances in Wilms tumor genetics. *Curr Opin Pediatr* **14**, 5-11 (2002).

103 Haber, D. A., Timmers, H. T., Pelletier, J., Sharp, P. A. & Housman, D. E. A dominant mutation in the Wilms tumor gene WT1 coooperates with the viral oncogene E1A in transformation of primary kidney cells. *Proc Natl Acad Sci U S A* **89**, 6010-6014 (1992).

104 Duan, D. R. *et al.* Inhibition of transcription elongation by the VHL tumor suppressor protein. *Science* **269**, 1402-1406 (1995).

105 Clifford, S. C. *et al.* Contrasting effects on HIF-1 alpha regulation by disease causing pVHL mutations correlate with patterns of tumorigenesis in von Hippel-Lindau disease. *Hum Mol Genet* **10**, 1029-1038 (2001).

106 Gutmann, D. H., Hirbe, A. C. & Haipek, C. A. Functional analysis of neurofibromatosis 2 (NF2) missense mutations. *Hum Mol Genet* **10**, 1519-1529 (2001).

107 Coffer, P. J. & Woodgate, J. R. Molecular cloning and characterization of a novel putative protein-serine kinase related to the cAMP-dependent and protein kinase C families,. *Eur. J. Biochem* **201**, 475-481 (1991).

108 Jones, P. F., Jakubowicz, T., Pitossi, F. J., Maurer, F. & Hemmings, B. A. Molecular cloning and identification of a serine/threonine protein kinase of the second messenger subfamily. *Proc Natl Acad Sci U S A* **88**, 4171-4175 (1991).

109 Cheng, J. Q. *et al.* Amplification of AKT2 in human pancreatic cells and inhibition of AKT2 expression and tumorigenicity by antisense RNA. *Proc Natl Acad Sci U S A.* **93**, 3636-3641 (1996).

110 Staal, S. P. Molecular cloning of the akt oncogene and its human homologues AKT1 and AKT2: amplification of AKT1 in a primary human gastric adenocarcinoma. *Proc Natl Acad Sci U S A.* **84**, 5034-5037 (1987).

111 Konishi, H. *et al.* Molecular cloning and characterization of a new member of the RAC protein kinase family: association of the pleckstrin homology domain of three types of RAC protein kinase with protein kinase C subspecies and beta gamma subunits of G proteins. *Biochem Biophys Res Commun.* **216**, 526-534 (1995).

112 Brodbeck, D., Cron, P. & Hemmings, B. A. A human protein kinase Bgamma with regulatory phosphorylation sites in the activation loop and in the C-terminal hydrophobic domain. *J Biol Chem.* **274**, 9133-9136 (1999).

113 Nakatani, K., Sakaue, H., Thompson, D. A., Weigel, R. J. & Roth, R. A. Identification of a human Akt3 (protein kinase B gamma) which contains the regulatory serine phosphorylation site. *Biochem Biophys Res Commun.* **257**, 906-910 (1999).

114 Bellacosa, A. *et al.* Structure, expression and chromosomal mapping of c-akt: relationship to v-akt and its implications. *Oncogene* **8**, 745-754 (1993).

115 Altomare, D. A., Lyons, G. E., Mitsuuchi, Y., Cheng, J. Q. & Testa, J. R. Akt2 mRNA is highly expressed in embryonic brown fat and the AKT2 kinase is activated by insulin. *Oncogene* **16**, 2407-2411 (1998).

116 Altomare, D. A. *et al.* Cloning, chromosomal localization and expression analysis of the mouse Akt2 oncogene. *Oncogene* **11**, 1055-1060 (1995).

117 Musacchio, A., Gibson, T., Rice, P., Thompson, J. & Saraste, M. The PH domain: a common piece in the structural patchwork of signalling proteins. *Trends Biochem Sci.* **18**, 343-348 (1993).

118 Datta, K. *et al.* AH/PH domain-mediated interaction between Akt molecules and its potential role in Akt regulation. *Mol Cell Biol.* **15**, 2304-2310. (1995).
119 Bellacosa, A., Testa, J. R., Staal, S. P. & Tsichlis, P. N. A retroviral oncogene, akt, encoding a serine-threonine kinase containing an SH2-like region. *Science* **254**, 274-277 (1991).
120 Bellacosa, A. *et al.* Akt activation by growth factors is a multiple-step process: the role of the PH domain. *Oncogene* **17**, 313-325 (1998).
121 Frias, M. A. *et al.* mSin1 is necessary for Akt/PKB phosphorylation, and its isoforms define three distinct mTORC2s. *Curr Biol.* **16**, 1865-1870 (2006).
122 Sarbassov, D. D. *et al.* Rictor, a novel binding partner of mTOR, defines a rapamycin-insensitive and raptor-independent pathway that regulates the cytoskeleton. *Curr Biol.* **14**, 1296-1302 (2004).
123 Bellacosa, A. & Testa, J. R. AKT plays a central role in tumorigenesis. *Proc Natl Acad Sci U S A* **98**, 10983-10985 (2001).
124 Du, K. & Tsichlis, P. N. Regulation of the Akt kinase by interacting proteins. *Oncogene* **24**, 7401–7409 (2005).
125 Alessi, D. R., Caudwell, F. B., Andjelokvic, M., Hemmings, B. A. & Cohen, P. Molecular basis for the substrate specificity of protein kinase B; comparison with MAPKAP kinase-1 (PDK-1): Structural and functional homology with the *Drosophila* DSTPK61 kinase. *Curr Biol.* **7**, 776-789 (1996b).
126 Walker, K. S. *et al.* Activation of protein kinase B beta and gamma isoforms by insulin in vivo and by 3-phosphoinositide-dependent protein kinase-1 in vitro: comparison with protein kinase B alpha. *Biochem J.* **331**, 299-308 (1998).
127 Datta, S. R., Brunet, A. & Greenberg, M. E. Cellular survival: a play of three Akts. *Genes Dev* **13**, 2905-2927 (1999).
128 Andjelković, M. *et al.* Role of translocation in the activation and function of protein kinase B. *J Biol Chem* **272**, 31515-31524 (1997).
129 Meier, R., Alessi, D. R., Cron, P., Andjelković, M. & Hemmings, B. A. Mitogenic activation, phosphorylation, and nuclear translocation of protein kinase Bbeta. *J Biol Chem* **272**, 30491-30497 (1997).
130 Unterman, T. G. *et al.* Hepatocyte nuclear factor-3 (HNF-3) binds to the insulin response sequence in the IGF binding protein-1 (IGFBP-1) promoter and enhances promoter function. *Biochem. Biophys. Res. Commun.* **203**, 1835–1841 (1994).
131 Powell, D. R. *et al.* Multiple proteins bind the insulin response element in the human IGFBP-1 promoter. . *Prog. Growth Factor Res.* **6**, 93–101 (1995).
132 Suwanickul, A., Morris, S. L. & Powell, D. R. Identification of an insulin-responsive element in the promoter of the human gene for

insulin-like growth factor binding protein-1. *J Biol Chem* **268**, 17063–17068 (1993).

133 O'Brien, R. M., Lucas, P. C., Forest, C. D., Magnuson, M. A. & Granner, D. K. Identification of a sequence in the PEPCK gene that mediates a negative effect of insulin on transcription. *Science* **249**, 533–537 (1990).

134 Li, W. W. *et al.* Common genetic variation in the promoter of the human apo CIII gene abolishes regulation by insulin and may contribute to hypertriglyceridemia. *J. Clin. Invest.* **96**, 2601–2605 (1995).

135 Dickens, M., Svitek, C. A., Culbert, A. A., O'Brien, R. M. & Tavare, J. M. Central role for phosphatidylinositide 3-kinase in the repression of glucose-6-phosphatase gene transcription by insulin. *J Biol Chem* **273**, 20144–20149 (1998).

136 Streeper, R. S. *et al.* A multicomponent insulin response sequence mediates a strong repression of mouse glucose-6-phosphatase gene transcription by insulin. *J Biol Chem* **272**, 11698–11701 (1997).

137 Cichy, S. B. *et al.* Protein kinase B/Akt mediates effects of insulin on hepatic insulin- like growth factor-binding protein-1 gene expression through a conserved insulin response sequence. *J Biol Chem* **273**, 6482–6487 (1998).

138 Liao, J., Barthel, A., Nakatani, K. & Roth, R. A. Activation of protein kinase B/Akt is sufficient to repress the glucocorticoid and cAMP induction of phosphoenolpyruvate carboxykinase gene. *J Biol Chem* **273**, 27320–27324 (1998).

139 Lin, K., Dorman, J. B., Rodan, A. & Kenyon, C. daf-16: An HNF-3/forkhead family member that can function to double the life-span of Caenorhabditis elegans. *Science* **278**, 1319–1322 (1997).

140 Ogg, S. *et al.* The Fork head transcription factor DAF-16 transduces insulin-like metabolic and longevity signals in C. elegans. . *Nature* **389**, 994–999 (1997).

141 Paradis, S. & Ruvkun, G. *Caenorhabditis elegans* Akt/PKB transduces insulin receptor-like sugnals from AGE-1 PI3 kinase to the DAF-16 transcription factor. . *Genes Dev* **12**, 2488–2498 (1998).

142 Davis, R. J. *et al.* Structural characterization of the FKHR gene and its rearrangement in alveolar rhabdomyosarcoma. *Hum. Mol. Genet.* **4**, 2355–2362 (1995).

143 Borkhardt, A. *et al.* Cloning and characterization of AFX, the gene that fuses to MLL in acute leukemias with a t(X;11)(q13;q23). *Oncogene* **14**, 195–202 (1997).

144 Anderson, M. J., Viars, C. S., Czekay, S., Cavenee, W. K. & Arden, K. C. Cloning and characterization of three human forkhead genes that comprise an FKHR-like gene subfamily. *Genomics*, 187–199 (1998b).

145 Biggs, W. H., Meisenhelder, J., Hunter, T., Cavenee, W. K. & Arden, K. C. Protein kinase B/Akt-mediated phosphorylation promotes nuclear exclusion of the winged helix transctiption factor FKHR1. . *Proc Natl Acad Sci U S A* **96**, 7421–7426 (1999).

146 Brunet, A. *et al.* Akt promotes cell survival by phosphorylating and inhibiting a Forkhead transcription factor. *Cell* **96**, 857–868 (1999).

147 Kops, G. J. *et al.* Direct control of the Forkhead transcription factor AFX by protein kinase B. *Nature* **398**, 630–634 (1999).

148 Tang, E. D., Nuñez, G., Barr, F. G. & Guan, K. L. Negative regulation of the Forkhead transcription factor FKHR by Akt. *J Biol Chem* **274**, 16741–16746 (1999).

149 Menghini, R. *et al.* Phosphorylation of GATA2 by Akt Increases Adipose Tissue Differentiation and Reduces Adipose Tissue-Related Inflammation : A Novel Pathway Linking Obesity to Atherosclerosis. *Circulation* **111**, 1946-1953 (2005).

150 Du, K. & Montminy, M. CREB is a regulatory target for the protein kinase Akt/PKB. *J Biol Chem* **273**, 32377–32379 (1998).

151 Rosnet, O. *et al.* Close physical linkage of the FLT1 and FLT3 genes on chromosome 13 in man and chormosome 5 in mouse. *Oncogene* **8**, 173-179 (1993).

152 Agnès, F. *et al.* Genomic structure of the downstream part of the human FLT3 gene:exon/intron structure conservation among genes encoding receptor tyrosine kinases (RTK) of subclass III. *Gene* **145**, 283-288 (1994).

153 Lyman, S. D. *et al.* Characterization of the protein encoded by the *flt3 (flk2)* receptor-like tyrosine kinase gene. *Oncogene* **8**, 815-822 (1993).

154 Carow, C. E. *et al.* Expression of the hematopoietic growth factor receptor FLT3 (STK-1/Flk2) in human leukemias. *Blood* **87**, 1089-1096 (1996).

155 el-Shami, K., Stone, R. M. & Smith, B. D. FLT3 Inhibitors in Acute Myeloid Leukemia. *Expert Rev Hematol* **1**, 153-160 (2008).

156 Rosnet, O. *et al.* Human FLT3/FLK2 receptor tyrosine kinase is expressed at the surface of normal and malignant hematopoietic cells. *Leukemia* **10**, 238-248 (1996).

157 Gabbianelli, M. *et al.* Multi-level effects of flt3 ligand on human hematopoiesis; expansion of putative stem cells and proliferation of granulomonocytic progenitors/monocytic precursors. *Blood* **86**, 1661-1670 (1995).

158 Ratajczak, M. Z. *et al.* FLT3/FLK-2 (STK-1) ligand does not stimulate human megakryopoiesis *in vivo*. *Stem Cells* **14**, 146-150 (1996).

159 Hjertson, M., Sundstrom, C., Lyman, S. D., Nilsson, K. & Nilsson, G. Stem cell factor, but not flt3 ligand, induces differentiation and activation of human mast cells. *Exp. Hematol* **24**, 748-754 (1996).

160 Rusten, L. S., Lyman, S. D., Veiby, O. P. & jacobson, S. E. The FLT3 ligand is a direct and potent stimulator of the growth of primitive and committed human $CD34^+$ bone marrow progenitor cells *in vitro*. *Blood* **87**, 1317-1325 (1996).

161 Shah, A. J., Smogorzewska, E. M., Hannum, C. & Crooks, G. M. Flt3 ligand induces proliferative quiescent human bone marrow $CD34^+CD38^-$ cells and maintains progenitor cells *in vitro*. *Blood* **87**, 3563-3570 (1996).

162 Kelly, L. M., Liu, Q., Kutok, J. L. & et al. FLT3 internal tandem duplication mutations associated with human acute myeloid leukemias induce myeloproliferative disease in a murine bone marrow transplant model. *Blood* **99**, 310-318 (2002).

163 Mackarehtschian, K. *et al.* Targeted disruption of the *flk2/flt3* gene leads to deficiencies in primitive hematopoietic progenitors. *Immunity* **3**, 147-161 (1995).

164 Kikushige, Y. *et al.* Human Flt3 is expressed at the Hematopoietic Stem Cell and the Granulocyte/Macrophage Progenitor stages to maintain cell survival. *J Immunol* **180**, 7358-7367 (2008).

165 Carow, C. E. *et al.* Localization of the human stem cell tyrosine kinase-1 gene (FLT3) to 13q12->q13. *Cytogenet Cell Genet.* **70**, 255-257 (1995).

166 Birg, F. *et al.* The expression of FMS/KIT-like gene FLT3 in human acute leukemias of the myeloid and lymphoid lineages. *Blood* **80**, 2584-2593 (1992).

167 Birg, F., Rosnet, O., Carbuccia, N. & Birnbaum, D. The expression of FMS, KIT and FLT3 in hematopoietic malignancies. . *Leuk Lymphoma* **13**, 223-227 (1994).

168 Levis, M. & Small, D. FLT3:ITDoes matter in leukemia. *Leukemia* **17**, 1738-1752 (2003).

169 Meshinchi, S. *et al.* Prevalence and prognostic significance of Flt3 internal tandem duplication in pediatric acute myeloid leukemia. *Blood* **97**, 89-94 (2001).

170 Kottaridis, P. D. *et al.* The presence of a FLT3 internal tandem duplication in patients with acute myeloid leukemia (AML) adds important prognostic information to cytogentic risk group and response to the first cycle of chemotherapy: Analysis of 854 patients from the United Kingdom Medical Research Council AML 10 and 12 trials. *Blood* **98**, 1752-1759 (2001).

171 Moreno, I. *et al.* Incidence and prognostic value of FLT3 internal tandem duplication and D835 mutations in acute myeloid leukemia. *Hematologica* **88**, 19-24 (2003).

172 Schnittger, S. *et al.* Analysis of FLT3 length mutations in 1003 patients with acute myeloid leukemia: Correlation to cytogentics, FAB subtype, and prognosis in the AMLCG study and usefulness as a

marker for early detection of minimal residual disease. *Blood* **100**, 59-66 (2002).

173 Chia, W., Savakis, C., Karp, R., Pelham, H. & Ashburner, M. Mutation of the Adh gene of Drosophila melanogaster containing an internal tandem duplication. *J Mol Biol* **186**, 679-688 (1985).

174 Kiyoi, H. *et al.* Internal tandem duplication of the FLT3 gene is a novel modality of elongation mutation which causes constitutive activation of the product. *Leukemia* **12**, 1333-1337 (1998).

175 Griffith, J. *et al.* The structural basis for autoinhibition of FLT3 by the juxtamembrane domain. *Mol Cell* **13**, 169-178 (2004).

176 Nakao, M. *et al.* Internal tandem duplication of the flt3 gene found in acute myeloid leukemia. *Leukemia* **20**, 1911-1918 (1996).

177 Abu-Duhier, F. M., Goodeve, A. C., Wilson, G. A. & et al. FLT3 internal tandem duplication mutations in adult acute myeloid leukemia define a high risk group. *Br J Hematol* **111**, 190-195 (2000).

178 Iwai, T. *et al.* Internal tandem duplication of the FLT3 gene and clinical evaluation in childhood acute myeloid leukemia. The Children's Cancer and Leukemia Study Group, Japan. *Leukemia* **13**, 38-43 (1999).

179 Kiyoi, H. *et al.* Prognostic implication of FLT3 and N-RAS gene mutations in acute myeloid leukemia. *Blood* **93**, 3074-3080 (1999).

180 Kiyoi, H. *et al.* Internal tandem duplication of FLT3 associated with leukocytosis in acute promyelocytic leukemia. Leukemia Study Group of the Ministry of Health and Welfare (Kohseisho). *Leukemia* **11**, 1447-1452 (1997).

181 Kondo, M. *et al.* Prognostic value of internal tandem duplication of the FLT3 gene in childhood actue myelogenous leukemia. *Med Pediatr Oncol* **33**, 525-529 (1999).

182 Yokota, S. *et al.* Internal tandem duplication of the FLT3 gene is preferrentially seen in acute myeloid leukemia and myelodysplastic syndrome among various hematological malignancies. A study on a large serie of patients and cell lines. *Leukemia* **11**, 1605-1609 (1997).

183 Jiang, J. *et al.* Identifying and characterizing a novel activating mutation of the FLT3 tyrosine kinase in AML. *Blood* **104**, 1855-1858 (2004).

184 Thiede, C. *et al.* Analysis of FLT3-activating mutations in 979 patients with acute myelogenous leukemia: Association with FAB subtypes and identification of subgroups with poor prognosis. *Blood* **99**, 4326-4335 (2002).

185 Yamamoto, Y. *et al.* Activating mutation of D835 within the activation loop of FLT3 in human hematological malignancies. *Blood* **97**, 2434-2439 (2001).

186 Till, J. H. *et al.* Crystallographic and solution studies of an activation loop mutant of the insulin receptor tyrosine kinase: Insights to kinase mechanism. *J Biol Chem* **276**, 10049-10055 (2001).

187 Kelly, L. M., Liu, Q., Kutok, J. L. & et al. FLT3 internal tandem duplication mutations associated with human acute myeloid leukemias induce myeloproliferative disease in murine bone marrow tansplant model. *Blood* **99**, 310-318 (2002).

188 Khan, M. M. *et al.* PML-RARalpha alleviates the transcriptional repression mediated by tumour suppressor Rb. *J Biol Chem* **276**, 43491-43494 (2001).

189 Khan, M. M. *et al.* Role of PML and PML-RARalpha in Mad-mediated transcriptional repression. *Mol Cell* **7**, 1233-1243 (2001).

190 Roca, H., Varsos, Z. & Plenta, K. J. CCL2 Protects Prostate Cancer PC3 Cells from Autophagic Death via Phosphatidylinositol 3-Kinase/AKT-dependent Survivin Up-regulation. . *J Biol Chem* **283**, 25057-25073 (2008).

191 Thimmaiah, K. N. *et al.* Identification of N10-Substituted Phenoxazines as Potent and Specific Inhibitors of Akt Signaling. . *J Biol Chem* **280**, 31924-31935 (2005).

192 Iwasaki, H. *et al.* The order of expression of transcription factors directs hierarchical specification of hematopoietic lineages. *Genes Dev* **20**, 3010-3021 (2006).

193 Yanjun, M. & Hendershot, L. M. The role of the unfolded protein response in tumor development: friend or foe? *Nat Rev Cancer* **4**, 966-977 (2004).

194 Kaufman, R. J. Orchestrating the unfolded protein response in health and diseases. *J Clin Invest* **110**, 1389-1398 (2002).

195 Lane, A. A. & Ley, T. J. Neutrophil elastase cleaves PML-RARα and is important for the development of acute promyelocytic leukemia in mice. *Cell* **115**, 305-318 (2003).

196 Lane, A. A. & Ley, T. J. Neutrophil elastase is important for PML-retinoic acid receptor activities in early myeloid cells. *Mol Cell Biol* **25**, 23-33 (2005).

197 Ng, A. P. P., Chng, W. J. & Khan, M. Curcumin Sensitizes Acute Promyelocytic Leukemia Cells to Unfolded Protein Response-induced Apoptosis by Blocking the Loss of Misfolded N-CoR Protein. *Molecular Cancer Research* **Epub ahead of Print** (2011).

198 Yu, H. *et al.* Relevant mouse model for human monocytic leukemia through Cre/lox-controlled myeloid-specific seletion of PTEN. *Leukemia* **24**, 1077-1080 (2010).

199 Hu, P., Han, Z., Couvillon, A. D. & Exton, J. H. Critical Role of Endogenous Akt/IAPs and MEK1/ERK Pathways in Counteracting Endoplasmic Reticulum Stress-induced Cell Death. *J Biol Chem* **279**, 49420-49429 (2004).

200 Stover, D. R., Becker, M., Liebetanz, J. & Lydon, N. B. Src phosphorylation of the epidermal growth factor receptor at novel sites mediates receptor interaction with Src and P85 alpha. *J Biol Chem* **270**, 15591-15597 (1995).

201 Brandts, C. H. *et al.* Constitutive Activation of Akt by Flt3 Internal Tandem Duplications Is Necessary for Increased Survival, Proliferation, and Myeloid Transformation. *Cancer Research* **65**, 9643-9650 (2005).

202 Jönsson, M., Engström, M. & Jönsson, J. I. FLT3 ligand regulates apoptosis through AKT-dependent inactivation of transcription factor FoxO3. *Biochem Biophys Res Commun.* **318**, 899-903 (2004).

203 Mori, Y., Kiyoi, H., Ishikawa, Y. & Naoe, T. FL-dependent wild-type FLT3 signals reduced the inhibitory effects of FLT3 inhibitors on wild-type and mutant FLT3 co-expressing cells. *Blood* **114**, Abstract 2067 (2009).

204 Wiernik, P. H. FLT3 inhibitors for the treatment of Acute Myeloid Leukemia. *Clinical Advances in Hematology & Oncology* **8**, 429-437 (2010).

205 Vardiman, J.W. *et al.* The 2008 revision of the WHO classification of myeloid neoplasms and acute leukemia: rationale and important changes. *Blood* **114**, 937-951 (2009).

206 Kindler, T., Lipka, D.B., Fischer, T. FLT3 as a therapeutic target in AML: still challenging after all these years. *Blood* **116**, 5089-5102 (2010).

APPENDIX 1

List of kinase and their coordinates on the Human Phospho-Array Blots.

Coordinate	Target	Phospho Site
A1	positive control	
A2	positive control	
A3	p38α	T180/Y182
A4	p38α	T180/Y182
A5	ERK1/2	T202/Y204, T185/Y187
A6	ERK1/2	T202/Y204, T185/Y187
A7	JNK pan	T183/Y185, T221/Y223
A8	JNK pan	T183/Y185, T221/Y223
A9	GSK-3α/β	S21/S9
A10	GSK-3α/β	S21/S9
A13	p53	S392
A14	p53	S392
A17	positive control	
A18	positive control	
B3	MEK1/2	S218/S222, S222/S226
B4	MEK1/2	S218/S222, S222/S226
B5	MSK1/2	S376/S360
B6	MSK1/2	S376/S360
B7	AMPKα1	T174
B8	AMPKα1	T174
B9	Akt1	S473
B10	Akt1	S473
B11	Akt1	T308
B12	Akt1	T308
B13	p53	S46
B14	p53	S46
C1	TOR	S2448
C2	TOR	S2448
C3	CREB	S133
C4	CREB	S133
C5	HSP27	S78/S82
C6	HSP27	S78/S82
C7	AMPKα2	T172
C8	AMPKα2	T172
C9	β-catenin	
C10	β-catenin	
C11	p70 S6 Kinase	T389
C12	p70 S6 Kinase	T389
C13	p53	S15
C14	p53	S15
C15	p27	T198
C16	p27	T198
C17	Paxillin	Y118
C18	Paxillin	Y118
D1	Src	Y419
D2	Src	Y419
D3	Lyn	Y397
D4	Lyn	Y397
D5	Lck	Y394
D6	Lck	Y394
D7	STAT2	Y689

Coordinate	Target	Phospho Site
D8	STAT2	Y689
D9	STAT5a	Y699
D10	STAT5a	Y699
D11	p70 S6 Kinase	T421/S424
D12	p70 S6 Kinase	T421/S424
D13	RSK 1/2/3	S380
D14	RSK 1/2/3	S380
D15	p27	T157
D16	p27	T157
D17	PLCγ-1	Y783
D18	PLCγ-1	Y783
E1	Fyn	Y420
E2	Fyn	Y420
E3	Yes	Y426
E4	Yes	Y426
E5	Fgr	Y412
E6	Fgr	Y412
E7	STAT3	Y705
E8	STAT3	Y705
E9	STAT5b	Y699
E10	STAT5b	Y699
E11	p70 S6 Kinase	T229
E12	p70 S6 Kinase	T229
E13	RSK 1/2	S221
E14	RSK 1/2	S221
E15	c-Jun	S63
E16	c-Jun	S63
E17	Pyk2	Y402
E18	Pyk2	Y402
F1	Hck	Y411
F2	Hck	Y411
F3	Chk-2	T68
F4	Chk-2	T68
F5	FAK	Y397
F6	FAK	Y397
F7	STAT6	Y641
F8	STAT6	Y641
F9	STAY5a/b	Y699
F10	STAY5a/b	Y699
F11	STAT1	Y701
F12	STAT1	Y701
F13	STAT4	Y693
F14	STAT4	Y693
F15	eNOS	S1177
F16	eNOS	S1177
F17	PBS negative	
F18	PBS negative	
G1	positive control	
G2	positive control	
G5	PBS (negative)	
G6	PBS (negative)	